
**Faculty of Science**
**Department of Earth Science**
**Environmental and Water Science**

# APPLICATION OF ENVIRONMENTAL AND HYDROCHEMICAL ANALYSIS TO CHARACTERIZE FLOW DYNAMICS IN THE SAKUMO WETLAND, GHANA

**By**

**CYNTHIA LAAR**



A thesis submitted in fulfilment of the requirements for the degree of Doctor of Philosophy (PhD)

Supervisor
**Professor Yongxin Xu**

Co-supervisor
**Professor Shiloh Osae**

**July, 2018**

# DECLARATION

I, Cynthia Laar declare that **Application of environmental and hydrochemical analysis to characterize flow dynamics in the Sakumo wetland, Ghana** is my own work, that it has not been submitted for any degree or assessment in any other university, and that all the sources I have used or quoted have been indicated and acknowledged by means of complete references.

Full name: Cynthia Laar Date: 16th July, 2018

Signed: C.L

# ABSTRACT

**Application of environmental and hydrochemical analysis to characterize flow dynamics in the Sakumo wetland, Ghana**

**Cynthia Laar**

This research focused on understanding the current hydrogeology of the Sakumo wetland by developing a conceptual flow model and simulating the groundwater flow system. The purpose of the model is to assist in understanding the groundwater flow system and quantify the water fluxes contributing to the wetland water storage. The research adapted quantitative, qualitative and mixed analysis to characterize the water flow in the basin. This involved the use of numerical modelling techniques to determine the zones of groundwater discharge to the wetland and zones of wetland water released for groundwater recharge. Field investigation was carried out to estimate the hydraulic parameters and sample rainwater, wetland water and groundwater.

The Sakumo wetland aquifer is situated in the quaternary unit consisting of sandy clay and weathered quartzite. The average annual precipitation in the study area from 1970 to 2016 was estimated at 760 mm/yr. Groundwater recharge rate was estimated as 5% of the mean annual rainfall which provided inputs into the numerical groundwater flow model. Evaporation from the wetland and evapotranspiration from the basin estimated using the Hargreaves and Samani method were 1341 mm/a and 546 mm/a, respectively. The hydrogeologic conceptual model was developed from the geology, borehole lithology, groundwater and wetland water levels. Groundwater in the basin was found to occur in both the alluvial formation and the underlying weathered rocks. Two major groundwater flow systems were identified: a local (top soil-water) flow in the alluvium and an intermediate flow in the shallow unconfined layer. A simple 2D finite-difference groundwater flow model was used to simulate the groundwater flow system in the wetland basin using ModelMuse. The study area was conceptualized as an unconfined single layered system. The hydraulic conductivity and transmissivity estimated using field methods were 1.58E-6 m/s and 3.05E-4 $m^2/s$ of the study area. The model developed was calibrated with steady state run. The resulting numerical model defined clear groundwater flow paths and showed that, the wetland water fluxes were predominantly local to intermediate flows in the domain. The simulation result

indicates that changes in recharge significantly affect the wetland water balance. Also, the water table declines during the dry season as a result of high evapotranspiration with little rain. This was evident as the wetland water balance components declined in storage (ΔS) with decreased rainfall and recharge. Simulation of increased groundwater flow showed minimal effect on the observed wetland fluxes. Hence, it was concluded that, there was little interaction between the wetland and the underlying aquifer.

pH of the groundwater and wetland waters were generally alkaline which is characteristic of water bodies influenced by seawater under oxygenated conditions. The increasing trends of electrical conductivity, sulphates, phosphates and nitrates point to deteriorating water quality in the wetland. The abundance of cations and anions was in the order, $Na^{+}>Ca^{2+}>Mg^{2+}>K^{+}$ and $Cl^{-}>HCO_3^{-}>SO_4^{2-}>NO_3^{-}>PO_4^{3-}$, respectively. The high concentration of trace elements (e.g., Fe, Mn) was attributed to local dissolution of the trace element bearing minerals in the alluvial sediments. The plot of the major ions of groundwater and wetland water on the Piper, Durov, and Stiff diagrams indicated two hydrochemical facies in the basin: Na-Cl and Na-$HCO_3$. Sea water intrusion and weathering of silicate minerals are the main hydrogeochemical processes controlling the hydrochemical composition of the wetland and groundwater quality.



Environmental isotopes composition of rainwater, groundwater and wetland water showed the mechanism of recharge to the groundwater was direct infiltration of local rainfall of mean isotopic composition $\delta^{18}O$ = -1.40 ‰ V-SMOW and $\delta^{2}H$ = -3.39 ‰ V-SMOW. The $\delta^{18}O$ vs. $\delta^{2}H$ values of the groundwater were mostly scattered close to or slightly to the right of the LWML indicating that modern precipitation is their predominant origin. The hydraulic head distribution, wetland water level, hydrochemical and environmental isotope data showed no direct hydraulic link between the aquifer and the wetland. The major outcome of this study is the development of the conceptual flow and numerical model of the Sakumo basin and laid the foundation for the development of detailed future predictive model. The model developed can be improved and used as a tool for the management of the wetland water resources.

**Keywords:** Hydrogeology, hydrogeochemistry, conceptual model, numerical model, water balance, groundwater-wetland interactions, major ions, multivariate statistics

# DEDICATION

With love and gratitude to the memory of my late father, Mr. Laar Namang and to my family especially, Dr. Engelbert Nonterah and my children. Thank you for your patience and endurance during my studies.

Also to my heroines, my mom and grand mom. All that I am today, I owe it to you and my creator. To my siblings, I appreciate the unconditional love and support. May God Bless us all. Amen!

# ACKNOWLEDGEMENT

Glory be to God Almighty who made this possible. I would like to sincerely thank my supervisors Professor Yongxin Xu, Professor Shiloh Osae and Dr. Thomas Akiti, for their patience, guidance and the many amazing opportunities they allowed me. A special appreciation to Dr. Thokozani Kanyerere; your insight and helpful suggestions throughout the entire process has been invaluable. A big thank you to my employers, Ghana Atomic Energy Commission and to my Director-General Professor B.J.B. Nyarko for granting me permission to undertake this study. Special thanks to Dr. Richard Winston of the United States Geological Agency (USGS) for his patience in taking me through the MdelMuse software. To Prof. Richmond Fianko for his support and valuable assistance on specific aspects of my research. To Dr. Langbong Bimi, Dr. Daniel Achel, Dr. Anthony Duah and Prof. Mary Boadu, thank you for always encouraging and believing in me.

My enormous gratitude goes to the Organization for Women in Science in the Developing World (OWSD) and the Swedish International Development Cooperation Agency (Sida) for the intellectual and material contribution towards this research. The whole experience has been amazing and rewarding. I am also very grateful to the management and staff of the National Nuclear Research institute, for providing logistical support for fieldwork and assistance in analyzing my samples.



I am grateful to the Water Research Institute (WRI) of the Council for Scientific and Industrial Research (CSIR), Ghana Hydrological Services and to Community Water and Sanitation Agency (CWSA) for providing me with the opportunity and access to data. I also grateful to Dr. Samuel Ganyaglo for assisting me obtain data from a private consultancy firm.

To my colleagues and friends at GAEC; Dr. Sheriff Owiredu Gyampo, Mr. John Hanson, Mr. Obeng Agyemang (of blessed memory), Mr. Godfred Ayanu and Mr. David Saka, thank you for supporting me throughout the entire journey. I am very grateful. To my senior, Mr. Samed Aliou, for assisting me during the pumping test. You are dependable. My heartfelt gratitude to Dr. Mrs. Paulina Amponsah. Madam, you showed me so much love and supported me throughout this journey. I am so grateful. To Dr. Juliet Atta, you are an amazing friend. I have benefitted enormously from your wisdom and understanding. To all the friends' l met at UWC, thanks for the moral support and good times during my studies. Special thanks to Onengiye Oranene, Dr. Kobamelo Dikgola, Dr. Xiaobin Sun and Siyamthanda Gxokwe. I appreciate all your friendship and our time outs.

TABLE OF CONTENT

## LIST OF FIGURES

# LIST OF TABLES

# CHAPTER 1: INTRODUCTION

## 1.1 Background

The Sakumo wetland is internationally-recognized as an important wetland, and has unique structural characteristics as it supports fish and aquatic life. It is the third most important site for migratory birds in Ghana (Agyepong *et al.,* 1999). The wetland has economic significance as it has great hydro-structure with freshwater and helps in flood prevention. The previously freshwater wetland discharges into the Gulf of Guinea. However, in the past two decades, nearly half of the total wetland land surface area has been lost due to urbanization, agricultural use, industrial sites and development in the country's largest harbor (Nonterah *et al.,* 2015).

Large scale losses of wetland vegetation cover and the dwindling loss of water from the wetland due to reduced fresh water inflows, clearing of vegetation for land developments and agriculture and high evaporation has increased surface runoff to the wetland and consequently decreased recharge especially during the dry season. Expansion works at the Tema harbor located few meters away from the wetland is postulated to cause hydrological impact on the wetland hydrology. The wetland catchment is also home for a number of companies including food and beverage industries, textiles and chemical manufacturing companies. Domestic and industrial waste are channeled into the wetland whiles fertilizers, agro-chemicals and animal wastes from surrounding farms are washed into the wetland. These contemporary environmental and land use changes impact on the hydrological and ecological function of the wetland and thus, threaten the economic status of the wetland.

Understanding the water flow in a wetland system is critical for understanding the water balance and the groundwater-wetland interaction. This is important in maintaining the quantity and quality of the fresh and saline water inflows. This requires the use of quantitative, qualitative and mixed methods to quantify the water fluxes and determine the hydrogeochemical processes controlling the water chemistry. Groundwater has been recognized as an important component of wetland hydrology for quantitative and qualitative purposes. Studies have been conducted to assess the dependency of ecosystems on groundwater contributions (Rosenberry *et al*., 2015). Although difficult to quantify (Golden *et al*., 2017; Cohen *et al.*, 2016), groundwater input can form a

dominant or small part of the wetland's water balance especially during the dry season when there is little or no rain. Several methods including the use of Darcian estimations, hydrologic models, hydrochemical analysis, environmental isotopes tracers and numerical models have been used to quantify groundwater inputs to wetlands (Liu & Mou 2016; Cartwright & Morgenstern, 2012; Kalbus *et al*., 2006).

Simple numerical models have been used simulate groundwater-wetland interactions and provide an accurate means in understanding the hydrogeological characteristics of wetlands (Ameli & Creed 2017; Golden *et al.,* 2017; Rudnick *et al.,* 2014; Guay *et al*., 2013). Numerical flow models serve as an efficient tool for investigating the response of a wetland's hydrodynamics to historical and future events. Numerical groundwater flow models serve as an efficient tool for investigating the response of a wetland's hydrodynamics to historical and future events (Yihdego *et al.,* (2017).

Hydrochemical analysis have been used to determine the potential sources of minerals, identify the physical and chemical controls of the water chemistry and determine groundwater-wetland water interaction in wetland environments (Mosimane e*t al*., 2017; Shan *et al*., 2017; Taak & Singh 2014; Somay & Filit 2003). Hydrochemical characteristics provides evidence for differentiating between various hydrological units in a system and the groundwater-wetland interaction. Environmental isotopes of water (oxygen-18 and deuterium) have been used to trace water sources and groundwater-surface water interaction in wetlands (e.g. Qian *et al*., 2014; Chen *et al.,* 2014; Turner *et al*., 2010). The use of environmental stable isotope of water ($\delta^{18}O$ and $\delta^{2}H$) are useful tracers for the source of groundwater in alluvial groundwaters, especially because surface water often has an evaporation signal (Clark & Fritz, 1997). Hence, a combination of hydrochemical and environmental isotopes analysis model provides a better understanding of the flow dynamics of the groundwater-wetland system.

In order not to lose the wetland functions and its socio-economic value, there is need to develop practical sustainable wetland protection plans. This requires development of accurate predictive tools for water resources managers in developing effective protection strategies. The present study used hydrogeological conceptual and numerical model to quantify the groundwater contribution to the wetland and characterize the groundwater-wetland interaction. This approach enabled the

description of water flow system and the hydrogeochemical processes controlling the water chemistry. The development of the conceptual and numerical model provides valuable hydrogeological information of the Sakumo wetland basin and lays the foundation for the development of detailed future predictive model.

## 1.2 Research aim and objectives

The aim of the present study is to develop a hydrogeological conceptual and numerical flow model that would be used to predict groundwater contribution to the wetland water budget. Such models will facilitate decision-making that would inform practical strategies for managing coastal wetlands.

More specifically, the research aims to:

1. Develop a conceptual flow model of the Sakumo wetland basin and quantify the water resources using numerical flow models;
2. Characterize the quality of water in the wetland and identify hydrogeochemical processes controlling the water chemistry using hydrochemical and environmental isotopes analyses methods;
3. Assess the occurrence of groundwater-wetland interaction using hydrochemistry and environmental isotopes.

## 1.3 Layout of this thesis

This thesis contains 7 chapters which are discussed below;

Chapter 1, provides a brief background of the study and outlines the structure of the thesis. This chapter describes the problem and outlines the aim and objectives of the current study. It also addresses the methodological approach.

Chapter 2, outlines the literature available and related to wetland and provides a background for the current study. The review explores a wide range of topics related to quantitative approach of measuring water balance using numerical models, qualitatively describe the water resources composition and the groundwater-wetland interaction by means of hydrochemical and stable isotope analysis models.

Chapter 3, provides a brief insight into the climate, topography, geology and land use activities of the study area. The chapter also outlines the methodology used collect, prepare and analyze the data. The applied methods include, quantitative, qualitative and mixed methods.



Chapter 4, a wetland hydrogeological conceptual model is developed to improve understanding of the groundwater flow system and quantify the water fluxes contributing to wetland water storage.

Chapter 5 demonstrates the use of hydrochemical and environmental isotopes analysis model in characterizing the wetland water quality and the major hydrogeochemical processes controlling groundwater and wetland quality in the basin. It also provides explanation on how local hydrogeology affect groundwater quality.

Chapter 6 establish groundwater-wetland interaction and the hydrogeochemical controls on the water quality.

Chapter 7 summarizes the important findings of the study and elucidates on the shortcomings. The chapter also provides recommendation for further research to gain more detailed information on the model development.

# CHAPTER 2: LITERATURE REVIEW

## 2.1 Introduction

The literature review provides a broad coverage of topics related to the thesis topic. The review considers three separate research components each representing an integral part in defining water movement in wetland and water flow exchange between wetland and the underlying groundwater and ways to quantify the interaction if any, between the two. This involves descriptions of the key wetland processes, identification of water flow controls in wetlands, understanding the role of groundwater to wetland and a review of groundwater flow modelling processes for quantifying groundwater-wetland interactions. An overview on the techniques that can be used for measuring groundwater-wetland interaction is provided. Groundwater flow properties and groundwater-wetland interaction in fractured rock aquifers that can occur in a coastal system are discussed. Groundwater flow properties in a coastal wetland is greatly influenced by the nature of the underlying groundwater. Calculating wetland water balance is necessary to determine the losing or gaining status of the wetland in order to ensure sustainable wetland protection for water resources management. This chapter also reviews some of the methods for assessing groundwater-wetland interaction.



## 2.2 Wetland hydrogeology

Wetlands are the interface for the major water reservoirs in the hydrologic cycle: surface water, ground water, atmospheric water, and, in some places, seawater. Water fluxes in a wetland includes, precipitation, transpiration and exchange of water. Understanding a wetland's water balances depends in part, to measuring the interaction between wetland and groundwater (Choi & Harvey, 2000) and by extension, the water cycle. In Figure 2.1, the sources of water to the wetland are shown as rainfall, groundwater recharge and surface water runoff shows the water cycle of a wetland occurring simultaneously in the water cycle. When sea water evaporates forming clouds that are blown into the continent, where they gradually are condensed and fall as rain. On hitting the ground, part of the rain is turned into surface runoff which flows into the wetland or back into the ocean whiles part is returned to the atmosphere by evapotranspiration. The rest of the water

infiltrates and joins groundwater reservoirs, ultimately returning to the wetland or ocean through groundwater discharge (Mazor, 2004).

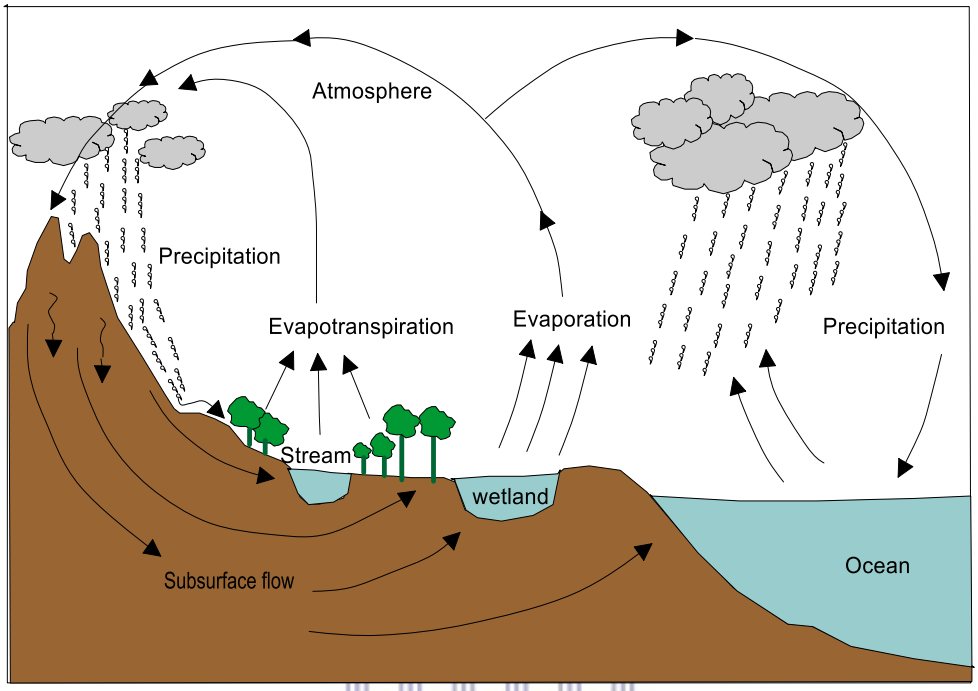


**Figure 2.1: The hydrological cycle**



Water in wetlands is either the result of surface flooding or outcropping of the water table, which is the top of the saturated zone where pore pressure equals atmospheric pressure (Freeze and Cherry, 1979). Wetlands can exist where the surface is flooded for extended periods or where there is saturation because ground water moves or stands close to the land surface.

## 2.3 Classification of wetlands

Classification is the process of systematic arrangement of objects or phenomena into classes according to criteria and the schemes developed, which can be used to provide a common framework for implementation or studying a phenomenon. A number of wetland classification systems have been developed to classify wetlands, include hydrogeomorphic, hydrogeology and landscape systems. One commonly used classification system for wetlands is the Cowardin system (Cowardin *et al.,* 1979). The Cowardin system classifies wetlands by their landscape position,

vegetation cover and hydrologic regime. The Cowardin system includes five major wetland types: marine, tidal, lacustrine, palustrine and riverine.

Williams (1990) classified wetlands based on the following definitions for the various types of wetlands: Marine wetlands such as coastal wetlands including coastal lagoons, rocky shores and coral reefs. Estuarine wetlands to include for example deltas, tidal marshes and mangrove swamps. The third type are riverine wetlands which occurs along rivers and streams. The fourth types of wetlands, known as lacustrine includes marshes, swamps and bogs. Last but not the least are human-made wetlands such as reservoirs, fish pond, flooded mineral workings, salt pans, sewage farms and canals (Levin, 2001). The first four systems include wetland, land deep-water habitats but the palustrine includes only wetlands. According to William (1990), estuarine and palustrine wetlands are the most familiar and popularly known types of marshes and fens/swamps and account for the bulk of the world's wetlands.

Another classification method is the hydrogeomorphic classification system based on the structure and functions of wetland as an expression of the geomorphic setting, water source and hydrodynamics. The hydrogeomorphic classification describes the pattern of functional diversity of wetland in a region, which can be used as a standard to make and assess management decisions (Gwin *et al.*, 1999; Bedford 1996). Gwin *et al.*, (1999) defined four classifications of wetlands for naturally occurring wetlands. These are depression, lacustrine fringe, riverine, and slope. Brinson (1993) classified wetlands using the hydrogeomorphic system based on distinguishable content as shown in Table 2.1.

Hydrogeomorphic classification has become an appropriate approach for wetland landscape scale analysis, because it has an intrinsic link between hydrology and geomorphic setting and could also augment other wetland classification systems (Brinson, 1993). The method uses readily available existing mapped data in addition to rapid non-destructive field verification. Bedford (1996) proposed the use of landscape profiles to describe the number and kind of wetlands in the landscape using classes defined in terms of hydro-geomorphic factors that cause a specific type of wetland to form and support their functions.

**Table 2.1: Hydrogeomorphic classification of wetlands**

| Class | Definition |
|---|---|
| Depression | Occur in topographic low areas that allow accumulation of surface water. Potential water sources are precipitation, overland flow, streams, or groundwater/interflow from adjacent uplands. The direction of flow is from the higher elevations towards the centre of the depression. |
| Lacustrine fringe | Occur adjacent to lakes where the water elevation of the lake maintains the water table in the wetland. In some cases, the wetlands consist of a floating mat attached to the land. Additional sources of water include precipitation and groundwater discharge. |
| Riverine wetlands | Occur in floodplains and riparian corridors in association with stream channels. Dominant water sources are overbank flow from the channel or subsurface hydraulic connections between the stream channel and wetlands. Additional sources may be interflow, overland flow from adjacent uplands, tributary inflow, and precipitation. |
| Slope wetlands | Found in association with groundwater discharge point to the land surface or at sites with saturated overflow with no channel formation. They occur on sloping land ranging from slight to steep. The source of water is mostly groundwater or interflow discharging at the land surface. Precipitation is often a secondary contributing source of water. Hydrodynamics are dominated by downslope unidirectional water flow. Slope wetlands can occur in nearly flat landscapes if groundwater discharge is a dominant source to the wetland surface. |
| Tidal fringe | Occur along the coasts and estuaries and are under the influence of sea level. They intergrade landward with riverine wetlands where tidal current diminishes and river flow becomes the dominant water source. Additional water sources may include groundwater discharge and precipitation. |
| Mineral soil flats | These are most common on interfluves, extensive relic lake bottoms, or large floodplain terraces where the main source of water is precipitation. They receive virtually no groundwater discharge, which distinguishes them from depressions and slopes. |
| Organic soil flats | Organic soil flats, or extensive peatlands, differ from mineral soil flats in part because their elevation and topography are controlled by vertical accretion of organic matter. They occur commonly on flat interfluves but may also be located where depressions have become filled with peat to form a relatively large flat surface. Water source is dominated by precipitation, while water loss is by overland flow and seepage to underlying aquifer. |

Source: Brinson (1993) as provided in Nyarko (2007)

Tiner (2003) also proposed a classification based on the hydrogeology (Figure 2.2). Many wetlands develop in shallow waters or floodplains associated with rivers, lake streams and estuaries. Some other wetlands develop in poorly drained depressions, partly surrounded by upland, known as isolated wetlands. Isolated wetlands are defined by the geographic, hydrologic and ecological perspective. In addition, four commonly occurring wetland systems have been identified. These are surface water depression wetlands, groundwater slope wetlands, groundwater depression wetlands and surface water slope wetlands (Brinson, 1993).

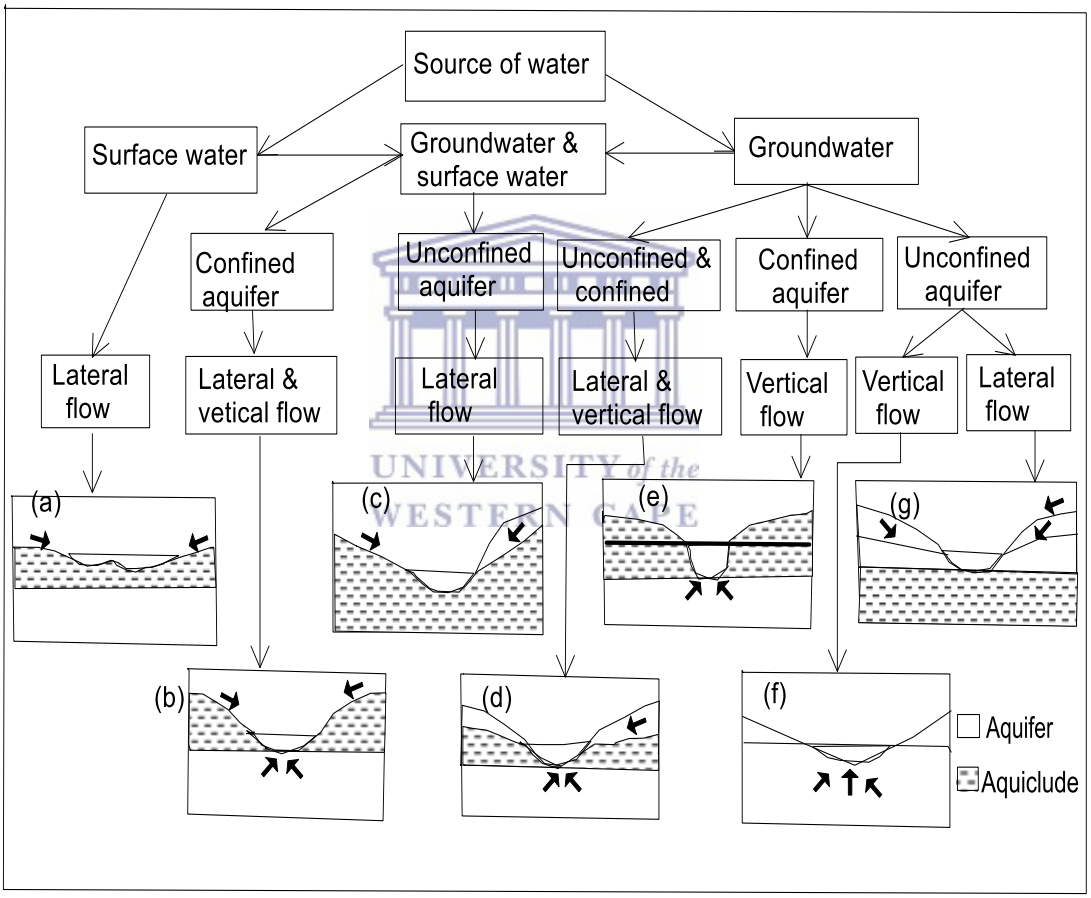


**Figure 2.2: Hydrogeologic classification of wetlands (adapted from Nyarko, 2007)**

Surface water depressional wetlands receive water primarily from rainfall whilst groundwater slope or groundwater depressional wetlands receive water predominately from groundwater. Wetlands dependent on surface water inflow are classified as riverine or fringe wetlands along existing bodies of open water. Andriesse (1986) identified four categories of wetland occurring in Africa: coastal wetlands, inland basins, inland valleys, and river floodplains.

### 2.3.1 Wetlands in Ghana

Wetlands cover nearly ten percent of Ghana's land surface. Ghana's coastal wetlands are important for water birds and serve as economic purposes for the local people. Based on the criteria of the Ramsar convention, three major types of wetlands are identified in Ghana (MLF, 1999); (i) rocky marine shores (Senya Bereku, Cape Three Points beaches), (ii) estuarine waters (Volta Delta, Pra and Ankobra Rivers), (iii) mangrove/tidal forests (lower reaches of Volta), brackish/ saline wetlands (open lagoons such as Korle and Amisa, and closed wetlands such as Muni and Songor). Table 2.1 is a summary of major coastal wetlands in Ghana.

Inland wetlands in Ghana are mainly freshwater ecosystems which occur when streams, springs, run-off or even groundwater causes flooding and saturated soils and create temporal and/or permanent shallow water. Examples of these include perennial rivers and streams such as the Densu and Afram, permanent freshwater lakes such as Lake Bosumtwi and fresh water marshes such as, the Red, Black and White Volta floodplains. Man-made or artificial wetlands are ponds constructed for water storage, salt mining, agriculture, aquaculture, and urban/industrial purposes. Examples are (i) the salt pans of Elmina, Songor, Muni and Densu Delta), (iii) water reservoirs (Volta Lake, Kpong Head Pond) and (iii), irrigated lands (Dawhenya) (Ministry of Lands and Forestry, 1999).



### 2.3.2 Coastal wetlands in Ghana

More than 90 wetlands of various sizes are found along the nearly 550 $km^2$ coastline of Ghana (Koranteng *et al*., 1998). The wetlands form important ecosystems, housing a wide variety of fish, shrimps, crabs, mollusc and polychaete species. Some of the wetlands have been recognized both nationally and internationally as migratory water bird habitats (Ntiamoa-Baidu, 1991b). The coastal wetlands of Ghana have been categorized into open and closed. Open wetlands have sufficient volumes of water at all seasons to maintain a permanent outflow from their mouths into the sea. They have a permanent opening to the sea and are normally fed by rivers that flow all-year-round. They occur mostly on the central and western parts of the coastline where higher rainfall results in a more continuous flow of the rivers and streams (Armah, 1991). The closed wetlands are separated from the sea by sand barriers and are common on the eastern segments of the coastline of Ghana where rainfall is low and seasonal. Some closed wetlands open to the sea

in the rainy season when floodwaters break the sand barrier (Kwei, 1977). Storm surges may also erode sandbars and open up closed wetlands to the sea (Armah, 1991). Under other circumstances, the sandbar may be manually breached during the rainy season to reduce the risk of flooding adjacent settlements where this is considered a threat.

Coastal wetlands have been found to be extremely vulnerable to the buildup of contaminants from the terrestrial, freshwater and marine environment. According to EPA/World Bank report (1997), 25% of the population in Ghana lived in coastal areas. This has resulted in increased amount of untreated domestic waste discharged into the coastal environment. The dumping of refuse, discharge of industrial and domestic sewerage, as well as agricultural run-off into the coastal environment, has increased the nutrient and organic loading of the coastal wetlands. This may seriously contaminate the water, endangering the plants, animals and people living in or near to the water.



**Table 2.2: Examples of coastal wetlands in Ghana**

| Marine/Coastal Ecosystems | Location/Examples |
|---|---|
| Rocky Marine Shores | Senya Bereku, Cape Three Points etc. |
| Estuarine Waters | Mouths of Volta, Pra, Butre, Ankobra |
| Mangrove/Tidal forest | Lower reaches of Volta, Kakum, Ankobra |
| Brackish/Saline wetlands | Sakumo, Muni, Densu, Songor, Amisa |

### 2.3.3 Sources of water to wetland

The availability and sustainability of wetland require a persistent, long term inflow of water. The sources of water in a wetland may be direct rainfall, runoff from storm water, floods caused by elevated water levels in nearby surface water bodies, groundwater and a combination of any, or all, of these sources. Rain-fed wetlands are known as surface water depressional wetlands whiles

groundwater-fed wetlands are referred to as groundwater slope/discharge areas. Riverine or fringe wetlands are wetlands receiving inflow from surface water or storm water.

#### 2.3.3.1 Rain-fed wetlands

Rainfall is the commonest driver of wetland hydrological processes. It provides direct water input into wetlands and generates runoff on the uplands. Rainfall also recharges groundwater, sustains groundwater discharge to wetlands during rainy and dry seasons. The distribution of rainfall across the world is affected by major climatic patterns. Tropical areas such as Ghana receive large amounts of rainfall in the rainy season and very minimal rains during the dry season when the atmosphere is dry.

#### 2.3.3.2 Runoff

Surface runoff to wetlands may be permanent, seasonal or temporarily present in a wetland. Runoff normally occurs as a result of floods from rivers, lakes and overland flow, through stream flow, groundwater discharge and tides. Where groundwater is discharged into wetlands it becomes runoff. Water outflow from wetlands occurs in channels or across the wetland and is normally high during the raining season and periods of floods. Runoff from wetlands that are groundwater discharge are often more evenly distributed than runoff from rain-fed wetlands (Ramsar Convention, 1971), because the quantity of groundwater discharge are relatively constant compared to rainfall which is seasonal. Coastal wetlands often receive water during high tides which serves as a major source of water into wetlands.



#### 2.3.3.3 Groundwater

Groundwater originates from the infiltration of meteoric waters or rainfall or as areas from seepage of surface water bodies. When rain falls, it moves through the unsaturated zone to the saturated zone where it recharges the water table (Mazor, 2004). Groundwater discharge occurs as a result of difference in hydraulic heads which causes water to move to the land surface or into nearby surface water bodies.

Most wetlands are commonly groundwater discharge areas however, ground water recharge also occurs in wetlands depending on the topography, soil characteristics, climate and season. Groundwater reaches coastal wetlands by direct discharge or as baseflow in the streams and rivers that drain into the wetland environment. It is evident that direct groundwater discharge can be a

substantial contributor of freshwater and dissolved constituents, particularly in coastal wetlands consisting of highly permeable soils with high rates of groundwater recharge and low rates of surface runoff. Recharge in wetlands is normally slow compared to adjacent uplands. Groundwater discharge areas in a wetland environment changes the water chemistry of the receiving wetland whereas groundwater recharge areas change the water chemistry of the underlying groundwater. Groundwater input contributes to the wetland water volume and maintains the balance between the fresh and brackish water which is important in species composition and production.

#### 2.3.3.4 Infiltration

Infiltration occurs when surface water moves through the subsurface under the influence of suction and gravity. Infiltration is highest in porous and permeable media, flat topography, and in dry conditions settings (Fitts, 2002). Infiltrating water moving through the soil zone becomes loaded with $CO_2$ which is formed in the biogenic processes. This makes the water slightly acidic which dissolves some soil and rocks components. The nature of these dissolution processes varies with soil and rock types, climate, and drainage conditions. Infiltrating water plays an important role during nutrient and contaminant transport, groundwater recharge, runoff and evapotranspiration.



#### 2.3.3.5 Evapotranspiration

Evapotranspiration (ET) is the loss of water in surface water attributable to direct evaporation from bare surfaces (including exposed soil surfaces and water intercepted by plants during precipitation) and transpiration by plants. ET occurs as a result of an energy and water exchange in the root zone and near the earth's surface. Water loss is, therefore, a function of several parameters including atmospheric and climatic conditions and land surface characteristics such as topography and vegetative cover. Land surfaces and slopes affect fluxes of moisture and heat attributable to differences in water availability, variability of precipitation, surface temperature, and plant and soil parameters (Molders & Raabe, 1996). The influence of so many parameters renders direct measurement complex and expensive. A direct measurement device such as the use of a lysimeter requires careful installation and calibration to simulate natural conditions in a spatially limited environment.

## 2.4 Use of groundwater flow models in wetland studies

Groundwater modelling involves the quantification of groundwater-surface water interaction using mathematical equations built within software packages such as an excel spread sheet, MODFLOW and FEFLOW. The values for the parameters for these mathematical equations are based on field measured parameters. These models mathematically simulate the water flow regime around the streams and also generate simulated hydraulic heads. The process of modelling groundwater flows is governed by the Darcy's law based on the results of his laboratory experiment of water flow in a sand column. Darcy concluded that, flow through a porous medium is proportional to the hydraulic gradient and hydraulic conductivity of the fluid. Given a representative volume of any porous medium, the general equation of conservation of mass for a volume may be expressed as given in Eq. 2.1:

(rate of mass inflow) - (rate of mass outflow) + (rate of mass production/consumption) = (rate of mass accumulation) (2.1)

This statement of conservation of mass (or continuity equation) may be combined with a mathematical expression of the relevant process to obtain a differential equation describing flow or transport (Bear, 1997; Freeze & Cherry 1979). Groundwater flows can be calculated using Darcy's law written as given in Eq. 2.2:



$$qi = -Kij\frac{\partial h}{\partial xj} \quad (2.2)$$

Where

$q_i$ = specific discharge, $LT^{-1}$

$K_{ij}$ = hydraulic conductivity of the porous medium (a second-order tensor), $LT^{-1}$

h = hydraulic head, L.

The simulated hydraulic heads are then used to simulate groundwater flow directions and calculate groundwater discharge to the particular surface water body (Brodie *et al.*, 2007). Groundwater models are mostly applied at the intermediate to regional scale over a duration of time. The advantage of using a model in quantifying groundwater surface-water interaction is that changes in seepages can be estimated through time and space and also modelling helps in defining the gaps

in information. The disadvantage with groundwater models like any other modelling technique has to do with the amount of data and time required to run and can calibrate the model.

In wetland studies, model applications are considered to be an option to understand the role the wetlands play and ascribe the appropriate management procedure or application. An example of a physical model is sand-tank experiment to define flow rates. Mathematical models are either empirical probabilistic or deterministic (Bear & Verruijt 1987) whiles empirical models are derived from experimental data fitted in a mathematical function. Probabilistic models use the laws of probability and statistics (Anderson & Woessner 2002). Deterministic models are based on the law of conservation of mass, momentum, and energy and describe relationship between them (El-Kadi, 1995). There are two groups of deterministic models depending on the type of mathematical equations involved; analytical and numerical models.

### 2.4.1 Analytical models

Analytical models use differential equations of exact solutions. Analytical models are applied to simple groundwater flow and contaminants transport systems. They are also used when establishing hydrogeological conditions. Analytical Models include Theis, Cooper-Jacob, Neuman's and Bower-rice analytical solutions. The advantages of using the analytical models in groundwater flow and contaminants transport system is because one solution can be used in different numerical values of coefficients and parameters. However, the solutions are not applicable in all systems due to groundwater heterogeneity of the modelled area, irregularity in shapes of the boundary conditions and non-analytic forms of various functions.



### 2.4.2 Numerical solutions

Numerical models are mostly applied to complex groundwater flow and contaminants transport systems. They are often applied in spatial and temporal groundwater flow systems, hydrogeological characteristics and hydraulic or chemical sources and sinks. Numerical models provide discrete solutions over the whole modelled area and uses direct methods to perform approximations. There are two types of numerical models depending on the equation used; Finite Difference method (FDM) and Finite Element Method (FEM). The equations used can be one, two or three dimensional depending on the conditions of the groundwater being modelled.

FDM is more widely used in hydrogeology as they allow a higher level of user intuition. It uses rectangles or quadrilateral grids to discretize the area being modelled. Within the finite difference model, each rectangle grid cell used has an X, Y and Z co-ordinates and the hydraulic head is calculated within the center of the cell (Spitz & Moreno 1996). For each grid cell, a hydraulic head is computed as the average of the adjacent cells and no assumption is made about the form of variation of the head from one center of the cell to the next (Anderson & Woessner 2002). Flows in and out from a cell is calculated based on the equation being solved by the model. The advantages of the FDM are that the method has the intuitive basis, easy data input, efficient matrix techniques and programme changes easy (Faust & Mercer 1980). The method, however, has low accuracy in some problems and regular grid.

Bradley (2002) simulated the water table variations in a British floodplain wetland that is the Naborough Bog using MODFLOW. The model results defused the water fluxes exchange through river seepage. Analysis of the model results indicated the effects of individual precipitation and evapotranspiration events on the water table variations. The water budget indicates the quantities of water that are estimated to flow from the wetland to the river. Bradford & Acreman (2003) applied a 3D groundwater flow model to simulate the groundwater system in the wet coastal grassland in the central part of Pevensey Levels in Sussex, UK. At the field-scale, it was considered necessary only to model the surface clay layer as vertical groundwater leakage to or from the deeper, more permeable part of the sequence and the regional groundwater flow within this part of the sequence can generally be neglected. Rainfall and evaporation were identified to have the most influence on water table fluctuations and in-field wetness in coastal grassland.



Nyarko (2007) established the interaction that between the main river and two floodplain wetlands within the White Volta Basin in Ghana. HYDRUS-ID and PM-WIN (MODFLOW) was used as simulate groundwater recharge. The simulation results indicated variations in water levels of the wetlands to changes in rainfall pattern. The interaction between the wetlands and the river was bi-directional in terms of horizontal direction with most of the flow coming out of the river. FEM are based on dividing the domain area into finite elements equations and using the equations as one, such that they represent the original system (Smith, 1985). It is the recently developed model with respect to FDM and uses integration instead of differentiation.

FEM mostly uses triangles to discretize the area being modelled and variation in the head in each

element is defined by interpolation. Hydraulic heads are calculated at the nodes and defined by basis function (Anderson & Woessner 2002). FEM produces large linear or non-linear systems equations which can be solved by computer programmes. FEM allows better description of the geometry, description of thin sections and complex shape, detailed description of fluid flows and allows for stress calculation. The method, however, requires advanced mathematical calculations and large data inputs and programming. Schot *et al*., (2004) applied a numerical finite element code that solves the Richards' equation for water flow in a saturated-unsaturated domain to a fen drained by ditches to simulate the formation of rainwater lenses on top of the groundwater system. The model simulations identified factors important for the dynamics of rainwater lens formation without field verification.

### 2.4.3 The modelling process

Steps taken towards developing a groundwater model is summarized from (Anderson & Woessner 2002) and is shown in Figure 2.3. These steps have been categorized into three sub processes that is; setting up the model, calibration process and prediction. These processes are discussed below.



First, the purpose of the model must be established in order to guide the user in identifying the relevant data needed to perform the task. The purpose of groundwater model includes the synthesis of hydrogeological data, evaluation of groundwater behavior under stress periods and assisting in decision making regarding water resource management (Faust & Mercer 1980). The next step involves characterization of hydrogeological data assembling the collected data to describe the groundwater flow condition of the modelled area. This process gives a further understanding of the groundwater behaviour within the specified boundary (Anderson & Woessner 2002). This step also aids the user to determine the modelling approach to be use either analytical or numerical model.

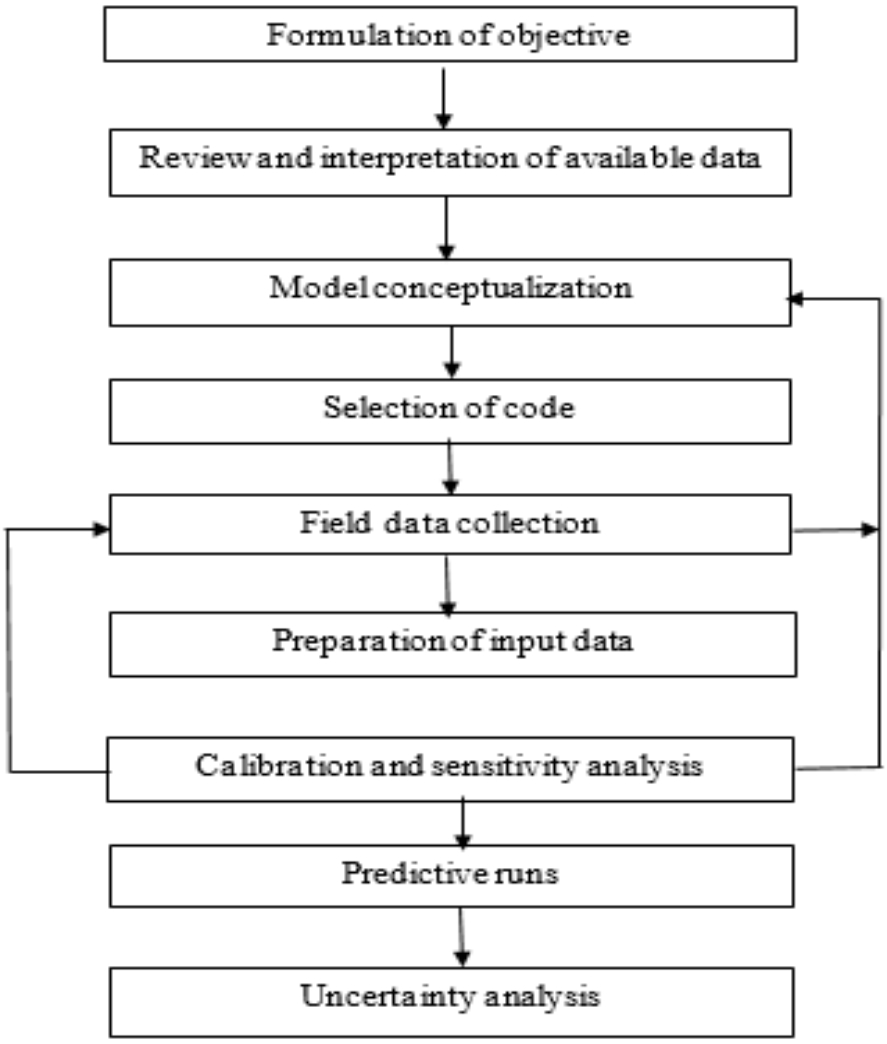


**Figure 2.3: Chart showing the groundwater flow modelling steps**

The next step involves the selection of a suitable code based on the hydrogeological conditions, conceptual model and a nature of the problem being addressed. The selected code should be able to simulate the specified model conditions. A suitable code is one that has been verified against analytical solutions, includes a water budget calculation and has been tested in similar/other field studies. Commonly used codes include PLASM, MODFLOW and AQUIFEM-1 (Anderson & Woessner 2002).

The next step involves specifying and assigning specific hydraulic parameters such as, topographic elevation, defining the grids, hydraulic conductivity, storage coefficient, recharge, evapotranspiration, constant heads, drains using the required packages. After running the model,

the model needs to be calibrated to minimize errors (Anderson & Woessner 2002).

Calibration can be achieved in two ways, through trial and error and automated calibration. Trial and error involve manually adjusting some parameters through and a number of sequential runs to match the simulated parameters and field parameters. Trial and error is influenced by the user knowledge and bias. Automated calibration model can be achieved through the use of automated parameter estimation codes such as PEST, MODINV and INVERT-3.

The next is to test the calibrated model's sensitive to uncertainty by varying some of the model inputs parameters and observing the change in heads or fluxes. The final step in the modelling process involves the use of predictive scenarios to test the model responds. The last step of the modelling process is to test the model results by setting and predicting scenarios.



## 2.5 Quantitative assessment of wetland water fluxes

Groundwater-wetland interactions constitute a hydrological link between wetlands and the surrounding aquifer and may serve as a channel through which water is exchanged in those environments. Hence, groundwater-wetland interactions thus play an important role with respect to spatial and temporal availability of both surface water and groundwater in a wetland ecosystem. Understanding the natural flow relationship between the groundwater and wetland may help wetland managers to deal with issues such as flood mitigation, groundwater exploitation and biodiversity conservation, in a more integrated and sustainable manner. Studies by researchers such as Rosenberry *et al.,* (2015); Bertrand *et al*., (2013) and Jolly *et al*., (2008) have confirmed the importance of groundwater contribution in wetlands.

Groundwater-wetland interaction is necessary for effective management of the wetland water resources. The degree of quantifying this interaction depends on various factors such as topography, underlying geology, hydraulic properties, temporal variation in precipitation and local groundwater flow pattern. In quantifying groundwater-wetland interaction various methods can be used. The most common methods used are, hydrochemistry and isotope tracers, water balance analysis, temperature monitoring, hydrogeological mapping, hydrometric analysis, geophysical tracers and modelling. Matos *et al*., (2002) examined groundwater heterogeneity and channel

pattern on flow interactions between stream and groundwater systems. MODFLOW was used to simulate the, direction and magnitude of the spatial distribution of subsurface flows exchange. After intense runoff-producing rainfall events, the soil textural composition enhances infiltration of the surface runoff waters.

Extensive review of the different methods available for assessing groundwater-wetland interactions is provided by Liu & Mou (2016) and Kalbus *et al.,* (2006). The authors summarized the different available methods in four categories namely: the direct estimation method, the mass balance approaches, Darcy's Law, and heat tracer method. Direct estimation method involves the direct measurement of water flux across the groundwater-surface water interface by using seepage meters. The mass balance approach for groundwater surface water interactions is further classified as incremental streamflow method, hydrograph separation method and environmental tracer method (Kalbus *et al.,* 2006). The incremental streamflow method is based on the concept of the difference in streamflow measured at two successive cross-sections. Hydrograph separation method is the most widely used standard method in hydrology for estimating the base flow component of the hydrograph. The method involves separating the hydrograph measured at a gauging station in different hydrograph components such as base flow and quick flow. Base flow is then assumed to represent the groundwater discharge.



### 2.5.1 Wetland water balance

A water budget is a "black box" calculation balancing all inputs and outputs of water with the change in volume of water stored in the system. For a given period of time, $\Delta t$, discrete determination of storage change yields as given in Eq. 2.3:

$$\frac{\Delta s}{\Delta t} = P + Qsi + Qgwi - Qso - Qgwo - ET \quad (2.3)$$

Where:

P = precipitation,

*Qsi* = surface inflow (including runoff and channel flow),

*Qgwi* = groundwater inflow,

*Qso* = surface outflow,

*Qgwo* = groundwater seepage,

*ET* = evapotranspiration, and

*S* = water storage of system.

The terms are defined as volume per time.

For wetland conditions to exist, the sum of the inputs must be greater than the sum of the losses for most periods, thereby maintaining a positive value for the storage term. Consistent positive values for the storage term indicates potential for development of hydric soil conditions. In permanently flooded wetlands, $\Delta S/\Delta t = 0$ or is greater than zero for almost the entire growing season (Garbisch, 1994).

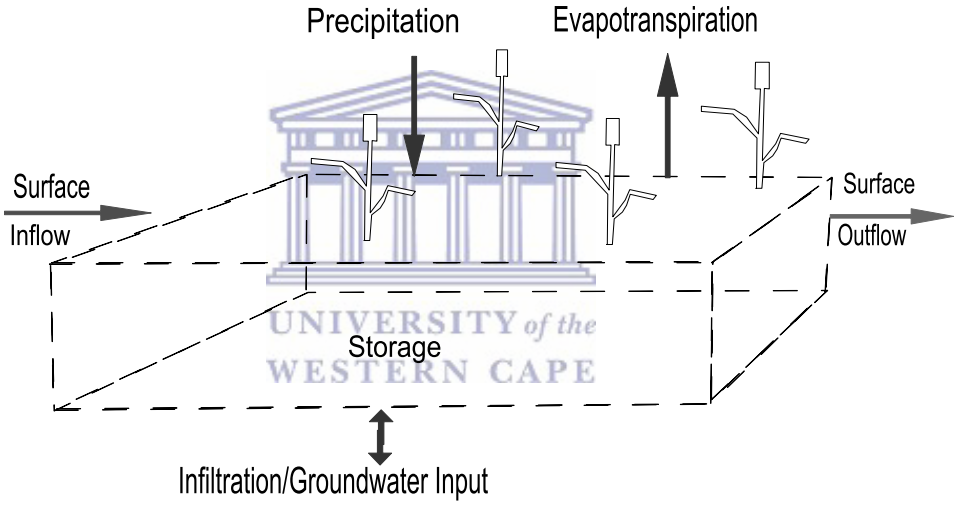


**Figure 2.4: Schematic diagram showing wetland water balance**

Precipitation can be the significant contributor to a wetlands water budget in situation where inputs are dominated by surface runoff. However, not all precipitation falling on the surface is available for use. Approximately 10 to 20 percent of the precipitation is lost through interception by the vegetation and some goes back into the atmosphere through direct evaporation. Where precipitation, P < 0.025 cm, interception losses may be as high as 100 percent, and even when *P* ~ 1 cm, losses can still be as high as 40 percent (Viessman & Lewis, 1996).

Surface water inflows and outflows ($Q_{si}$, $Q_{so}$) account for water flowing into and out of the wetland via open channels or overland flow. Common forms of surface flow include streams, rivers and highway drainage systems that convey storm water as runoff. The frequency, intensity and duration

of storms and the characteristics of the drainage area influences how much water a wetland receives as runoff. (Garbisch, 1994). Groundwater inflows and outflows ($Q_{gwi}$, $Q_{gwo}$) can be significant sources or losses in the natural wetlands. In general, subsurface contributions are often negligible (<0.01%) when there is above-ground flow.

### 2.5.2 Application of numerical model

Where groundwater and surface water occur in close association, it is the elevation of the groundwater table relative to the surface water level that controls the direction and quantity of flow in or out of the surface water system. The relation between these two systems is in part influenced by climate (discharge volumes and patterns), geology, (aquifer properties and changes in topography), and human activity such as land-use, damming of rivers, groundwater abstraction (Xu *et al*., 2002).

Groundwater-wetland interaction are characterized by different climatic zones. Tropical regions for instance are characterized by low water tables and perennial rivers. Seasonal changes in the water table often result in perennial rivers being seasonal especially in the upper reaches of a catchment. Hydraulic gradient between wetland and groundwater often determines the water flow direction. Variations in hydraulic conductivity also influences the rate and location of groundwater discharge or recharge. Even in a homogenous system, the hydraulic conductivity determines the location of the interface where the interaction is occurring. For example, in the numerical model presented by the U. S. Army Corps of Engineers (1999) of groundwater discharge to a seepage lake. The model showed that high hydraulic conductivity of the underlying aquifer caused a reversal of inflow through the bottom of the lake.

Human activities such as increased agriculture and industrial waste waters in a catchment often affect the quantity, and chemical quality of water resources. Such activities, tend to decrease groundwater flow to wetlands that are hydraulically connected to the underlying aquifers (U. S. Army Corps of Engineers, 1999). Altered hydrology of rivers and streams also has the ability to induce surface water recharge to aquifer thereby limiting groundwater discharge to wetland. Agriculture activities in results in modified landscape and impact on the water fluxes and quality. This results in a modification of the infiltration and runoff characteristics of the land, which affects recharge to groundwater, the water exchange to wetlands and evapotranspiration (Winter, 1998).

Changes in these factors in a wetland environment influences the water table of the aquifer and the wetland and also determines the type and extent of the groundwater-wetland interaction.

Groundwater-wetland interaction has been most commonly quantified using Darcy Law where hydraulic head gradients are measured in the wetland and the soil hydraulic conductivity (K) determined (Hayashi and Van der Kamp, 2009). Shaw *et al.*, (2017) integrated physical flux measurements with environmental isotopes ($\delta^{18}O$ and $\delta^{2}H$) of groundwater, lake water, streams and rain to investigate groundwater–wetland interactions in Georgetown Lake, Montana, USA. The annual water balance and the environmental isotope mass balance were used to calculate the annual groundwater inflows to the lake. The isotope mass balance showed that groundwater contributes 57% of the total inflow into the Georgetown wetland. The wetland was categorized as a medium-high to a high groundwater inflow lake.

Yihdego *et al.*, (2017) studied the interaction between the groundwater system and wetland in the Lake Linlithgow in Australia using a water budget computation approach. The method is based on a simple concept of the bucket-model. A simple spreadsheet model was developed and used to calculate the water balance and the effect of groundwater on the water level over a specified time. A node was selected on the spreadsheet to represent the groundwater component. The model was run based on the surface water components by switching the node off, in the absence of groundwater and on when groundwater is discharged and the simulated and observed lake levels compared. The water balance showed a progressive separation between observed and calculated lake levels. Where the calculated levels implied that the lake accumulate more storage than is actually observed. The separation was attributed to the groundwater fluxes. The model showed that, the lake water budget computation approach was a convenient approach in providing valuable information on the effect of groundwater on wetland or lake levels. The method reflects the contemporary understanding of the local groundwater system in a wetland. The researchers argued that the method is the model is efficient in data-scarce environments and is convenient for getting first-hand information on groundwater-wetland interaction. The model was however unable to properly define the water table hence the groundwater system regardless of the number and position of wells in the setting. This led to uncertainties in the groundwater component of the lake water budget. However, the objective of the current study was to define the groundwater flow

system and the quantify the water fluxes hence the method by Yihdego *et al.,* (2017) was not used in the current study.

Ameli & Creed (2017) developed a physically based hydrologic model used to characterize subsurface-surface connectivity of wetlands in the Prairie Pothole Region in Canada.The researchers used a 3-D groundwater–surface water interaction model to simulate subsurface flow in the watershed. The model was set to steady state and calibrated with velocity fields and the infiltration rate. The results showed slow subsurface connection between wetlands and the downstream river originating from the wetland whiles a fast surface connection was limited to large events and originated from wetlands located near the river. The model was used to assess and quantify the hydrologic connectivity between the isolated wetland. The developed model was used to establish subsurface-surface connectivity between individual wetlands. This current study hydrologic connectivity between the wetland and the underlying groundwater hence, the method by Ameli *et al*., (2017) was not used in the current study.

Beretta & Terrenghi (2016) studied groundwater flow in Venice lagoon in Italy using numerical groundwater flow models. The numerical groundwater flow code MODFLOW 2000, was used to simulate the fluxes of water from industrial area towards the lagoon. The simulated model showed that isolated inflows contribution from the industrial area resulted in significant low level of contaminated groundwater in the lagoon. The results also contributed to the reuse of the industrial area for other sustainable environmental activities. The model was able to predict the exact value of infiltration within the lagoon however, the model could not estimate the order of magnitude for the groundwater recharge.

Kelbe *et al.,* (2016) predicted the water-table profile in the Maputaland Coastal Plain using a numerical groundwater model. The 3 D groundwater model (MODFLOW) was used to simulate the water-table fluctuations in the Coastal plain under wet and dry conditions. Remote sensing imagery was used to map the permanent and temporary wetlands in dry and wet years. The model was used to show the extent and distribution of water table variation between wet and dry conditions. The model revealed that, areas with shallow water table (below 2 m) showed strong correlation with permanent wetlands dry climatic conditions. The results showed the importance of topography on wetland formation in the Plain as groundwater discharge zones in the lowland

supported permanent wetlands. The only concern with the predicted water table profile had to do with the accuracy and suitability of selected parameter set as other parameters could equally provide good results. The developed model by Keelbe *et al.,* (2016) used remote sensing imagery to map out potential hydrogeomorphic changes in the wetland hence this method was not used in the current study.

Jaros *et al*., (2016) quantified the wetland-groundwater interactions in the Kälväsvaara esker groundwater in Northern Finland using a physically-based groundwater-surface water code, HydroGeoSphere. The HydroGeoSphere model was used to simulate surface and subsurface flow in the groundwater and the adjacent areas and calibrated to steady-state. The model results were evaluated by comparing the simulated output with the observed average groundwater and lake levels and spring discharge data. The model produced spatially distributed hydrological variables such as water depths and groundwater-surface water exchange fluxes in the wetland area. The model also showed strong wetland-groundwater interactions in some areas. The model however, failed to capture small-scale groundwater discharge points such as springs. The model demonstrated the use of an integrated physical-based groundwater-surface water model in studying wetland-groundwater interactions. The current study aims to characterize the groundwater flow system and quantify the groundwater contribution to the wetland using limited data. Hence this method by (Jaros *et al.,* 2016) was not used in the current study.

Brannen *et al*., (2015) examined connectivity between wetland storage and stream flow response in a Canadian prairie wetland using changes in stream level and water budget analysis. Spatial and temporal subsurface connectivity was established through a transmission zone along the flow pathways. The transmission zone was found to be very heterogeneous and focused around the riparian areas of the wetland when activated. The authors found that, wetland topology and storage conditions control the movement of water out of the basin. The results indicated that shallow groundwater flow from beneath the hillslopes to the wetlands and that groundwater contributed significantly to the wetland surface storage. The model results suggested that, groundwater input to the wetland played a role in sustaining the surface connections between wetland and streamflow. The researchers recommended that, improvement of the model may be used to explore greater estimates capabilities of flood risk and water resources models in the area.

Turnadge & Lamontagne (2015) developed steps to assess wetland–groundwater interaction in the Lower Limestone Coast Prescribed Wells Area, Australia. The groundwater flow simulation code MODFLOW was used to simulate groundwater flow system in the catchment. Precipitation, evapotranspiration, surface water and groundwater flows represented significant components of the wetland water mass balances. Lateral flows, including vertical leakage, evapotranspiration from shallow water tables, wetland–groundwater interactions and changes in groundwater storage volumes were used to represent the groundwater domains. These components were characterized as temporal fluxes. Results of the simulated model indicated that, the duration of inundation was positively correlated with the magnitude of surface water addition (Turnadge & Lamontagne 2015). The use of developed steps to identify changes in wetland hydrological conditions such as long-term variations in climate, land use and/or water allocation policy was recommended by the researchers for further research.

Weitz & Demlie (2014, 2015) developed a hydrogeological conceptual model for the Lake Sibayi catchment located adjacent to the Kosi Bay area using hydrological, hydrochemical and environmental isotope data. The conceptual model together with the water balance revealed that the groundwater and surface water were highly interconnected, and that groundwater and surface water abstraction will eventually have a negative impact on the environment.

Ferrarin *et al*., (2013) analysed the spatio-temporal dynamics of the water residence time in the Venice lagoon in predicting current and future changes in the lagoon using numerical models. A 3-D hydrodynamic model SHYFEM was applied. The model used a semi-implicit algorithm for integrating time, which made the system environmental with respect to gravity waves and bottom friction and solved for the transport variables. The model served as a management tool used to describe the spatial heterogeneity and lagoon response to inputs of pollutants and increased population. The authors also predicted the effects of future scenarios of Sea Level Rise and climate change on the lagoon. The analysis showed that, sea level rise increased the lagoon volume and periodic closure of lagoon which reduced the lagoon interaction with the sea. This resulted in a decrease in the lagoon purification capacity.

Kyei-Baffour *et al.*, (2013) simulated the groundwater flow system in the Besease wetland in Ghana. The study determined the adequate irrigation depth for maximum crop yield and quantified the water balance in the area. The groundwater was modelled using a 3D groundwater flow model, PM-WIN MODFLOW. The authors estimated groundwater recharge in the area using the water table fluctuation method which served as the model input parameter and the model was assumed to be in steady and transient state conditions. The simulated model indicated that water levels varied from 259.10 to 259.97 m in the wet season and 258.19-258.86 m in the dry season (Kyei-Baffour *et al.*, 2013). The model also established interaction between the underlying groundwater and the bordering river particularly during flood periods. The model results showed substantial changes in wetland water storage which was attributed to spatial and temporal variability in water table heights. The model predicted marginal groundwater heights in the dry season when there is little or no rain. The model results were used as a management tool for crop production in the area.

Yuan *et al*., (2011) developed a coupled 3D groundwater-surface water model that was used to simulate interaction between surface water and groundwater flow and solute transport in coastal wetlands. The coupled model was modified from two existing sub models; a 3D finite-difference model for simulating shallow water flow and solute transport in surface waters known as ELCIRC and a 3D finite-difference groundwater model for simulating fluid flow and solute transport in porous media known as SUTRA. Surface water level and solute concentrations were computed in the ELCIRC model and used to determine the boundary conditions of the SUTRA-based groundwater model. The groundwater model provided water and solute fluxes as inputs for the continuity equations of surface water flow and solute transport to account for the mass exchange across the interface. The two models were coupled spatially at an interface through a local boundary condition that ensured mass and pressure continuity in the system. The coupled model simulated groundwater flow and solute transport in the lagoon and groundwater and incorporated the influence of the sea and landward surface water using the boundary conditions (Yuan *et al*., 2011). Flux from the seepage face was routed to the nearest surface water cell according to the local sediment surface slope. With the external coupling approach, the two sub-models were made to run parallel at time steps of different sizes. The model showed the interaction between the lagoon and groundwater flow and solute transport processes in the lagoons. However, many aspects of the model were yet to be validated. The coupled model to study the groundwater-surface water

interaction in coastal wetlands incorporated complex modifications to the codes which required high computational demand and hence was not used in the current study.

Nyarko (2007) established the interaction between the main river and floodplain wetlands within the White Volta Basin in Ghana. A HYDRUS-ID model was used to determine groundwater recharge which served as input into the PM-WIN (MODFLOW) model. The simulated model showed variation in hydraulic head of the wetland to changes in rainfall pattern. For instance, the initial measured depth of 0.65 m in the Pwalugu wetland was due to a combination of groundwater upwelling and accumulated rainfall on the saturated surface (Nyarko 2007). The results also indicated a bi-directional interaction between floodplain wetlands and the river with most of the flow coming out of the river in a horizontal direction.

In this current study, groundwater flow system was characterized and water fluxes quantified using the method by Grygoruk *et al.*, (2011) and Yuan *et al*., (2011). The numerical groundwater flow model ModelMuse (Winston 2009) was used to quantify the water storage in the wetland and hydrogeochemical tools were used to characterize the water flow system and groundwater-wetland interaction.



## 2.6 Characterizing wetland water quality

Hydrogeochemical assessments improves understanding of possible causes or changes in the water chemistry (Glynn & Plumber 2005). As water moves from the surface of the groundwater into the ground, it reacts with various components of the rock materials. Hence, the use of hydrogeochemical analysis requires assessment of the physicochemical parameters of the water in relation to the surrounding geology and land uses activities in the catchment. Ganyaglo (2014) studied the hydrogeochemical evolution of groundwater in central Region of Ghana and concluded that, high salinity in the coastal groundwater which was due to the slow movement of groundwater in the saturated zones. Hydrogeochemical studies on groundwater in the Accra plains have showed poor water quality due to high salinity (Glover et al., 2012; Kortatsi & Jorgensen 2001; Darko *et al.*, 1995; Akiti, 1980). Very few studies have explored the use of hydrogeochemical tools in the Sakumo basin.

### 2.6.1 Hydrochemical analysis

Analyzing and interpreting hydrochemical data of wetland water provides insights into chemistry of the water and the possible areas where groundwater-wetland interactions occurs. Dissolved ion in water can be used as a target tracer to trace the source of water, calculate mixing ratios of groundwater and wetland exchange, estimate the residence time and determine average rates of chemical reactions taking place during nutrient transport (Winter *et al*., 1998; Cook *et al.,* 2003).

In order to explain the mechanisms of the hydrochemical evolution of groundwater in saline wetlands in Murray basin in south eastern Australia, Herczeg *et al.,* (2001) analyzed major ions and stable isotopes of pore water and groundwater. The results indicated that major ions indicated that evapotranspiration increased with increasing $Na^+$ and $Cl^-$ concentrations whilst changes in ratios and concentrations of other ions were largely due to cation exchange, reverse weathering, carbonate dissolution and precipitation. A catchment scale salt balance and Cl/Br ratios discounted the weathering of minerals sources of salts and the contribution of halite dissolution. Stable isotopes signatures of $\delta^{18}O$ and $\delta^{2}H$ were typical of mean rainfall therefore indicating meteoric sources of salt rather than a dilution of remnant sea water. This approach suggested that, the source of salts in the wetland was due to the long-term deposition of airborne oceanic aerosols transported inland by precipitation, combined with evapotranspiration and long periods of relative aridity.



Hayashi *et al*., (2016) showed that, wetland water chemistry influenced the adjacent groundwater system. Négrel *et al.,* (2003) revealed that the oxbow wetlands in Mississippi alluvial plain have different major ions compositions, which is suggestive of a time-delayed water input by the rivers. Studies by Phillips & Shedlock (1993) showed that pH, bicarbonate and aluminum ion concentration in small ponds are influenced by mixing with groundwater. However, hydrochemistry alone is not enough indicator for analyzing the hydro-environmental aspects of wetlands because several chemical (and biologically mediated) reactions with groundwater material alter the chemical compositions of the water. Hence, environmental tracers occurring naturally and those released into water by human activities are often used as field tracers. The commonly used tracers include field parameters such as, electrical conductivity EC, DO, ORP and pH; water chemistry such as major ions ($Na^+$, $K^+$, $Ca^{2+}$, $Mg^{2+}$, $F^-$, $Cl^-$, $SO_4^{2-}$, $NO_3^-$, $HCO_3^-$ and

$PO_4^{3-}$) and other ions e.g. $Fe^{2+}$, $Cu^{2+}$, $Al^{3+}$ and $Pb^{2+}$. Environmental stable isotopes commonly used tracers include $^{18}O$ and $^{2}H$, Nitrogen-15 ($^{15}N$) and radioisotopes such as tritium ($^{3}H$).

#### 2.6.1.1 Major ions chemistry

Major ions chemistry of water are the natural constituents that forms the chemical composition of the water. The occurrence of dissolved ions in water is due to the different chemical reactions taking place in the subsurface. Hence, the detection of the ions in measurable amounts in the water can be used to identify the physical and chemical processes in the water (Carol & Kruse 2012). Hydrogen-bicarbonate or bicarbonate ions ($HCO_3^-$) occur in natural waters in equilibrium with carbonic acid and forms a carbonate system of chemical equilibrium connected with the pH of water (Equation 2.11). The sources of $HCO_3^-$ is from the dissolution of carbonate rocks such as limestones, dolomites, magnesites. Bicarbonate ions are high in low and moderately mineralized water. The presence of $HCO_3^-$ in water suggests either silicate or carbonate weathering or a combination of both processes (Elango & Kannan 2007).

The presence of chloride ($Cl^-$) in water is naturally associated with processes such as leaching from minerals, rocks and from saline deposits in coastal areas. Chloride is also associated with anthropogenic activities industrial and domestic wastes and can be detected in rai as acid precipitation. Naturally occurring $Na^+$ in waters are as a silicate weathering (Eq. 2.10), ion exchange and halite dissolution. Other sources of sodium in water includes weathering of sodium bearing rocks, sea water intrusion, return flows from agricultural farms and industrial and domestic effluent (Dinka *et al*., 2015). Potassium ($K^+$), is very similar to sodium in terms of its magnitude and solubility. Potassium occurs in low concentrations in surface waters than sodium due to the active participation of potassium in biological processes, such as, absorption by living plants and micro-organisms hence, its weak migratory ability in water. The weathering of feldspar and potash feldspars contribute to $Na^+$ and $K^+$ ions in groundwater (as presented in Eq. 2.4). High potassium in water is indicative of contamination as potassium is a major constituent of chemical fertilizers used in agricultural activities (Dinka *et al*., 2015)

$$2NaAlSi_3O_8 + 2H_2CO_3 + 9H_2O = Al_3Si_2O_5(OH)_4 + 2Na^+ + 4H_4SiO_4 + 2HCO_3$$

(silicate weathering) (2.4)

Calcium and Magnesium are normally present in natural waters and constitute 48% of cations in groundwater (Nur *et al*., 2012). Natural sources of calcium and magnesium ions in water are as a result of weathering of Ca and Mg rich rocks such as limestone and dolomite. Magnesium seldom dominate calcium ions in water due to the weaker biological activity of magnesium high solubility of magnesium sulphate and bicarbonate.

During infiltration, saturated rainwater (carbonic acid) dissolves calcium carbonate ($CaCO_3$) or Calcium Magnesium Carbonate ($CaMg(CO_3)_2$) rocks which increases the concentration of $Ca^{2+}$ and $Mg^{2+}$ ions present in the water (Eq. 2.5).

$$CO_2+H_2O \rightleftharpoons H_2CO_3 \text{ (Formation of carbonic acid)} \quad (2.5)$$

The acidic water influences the dissolution of carbonate minerals (calcite and dolomite) in the groundwater system (Eq. 2.6 and 2.7):

$$CaMg(CO_3)_2 + 2H_2CO_3 \rightleftharpoons Ca^{2+} + Mg^{2+} \text{ (Dolomite dissolution)} \quad (2.6)$$

$$CaCO_3+H_2CO_3 \rightleftharpoons Ca^{2+}+2HCO_3 \text{ (Calcite Dissolution)} \quad (2.7)$$

High $Ca^{2+}$ and $Mg^{2+}$ in groundwater is indicative of dissolution of carbonate minerals (Zabala *et al*., 2015). $Ca^{2+}$ ions in groundwater could also be an indication of other sources such as weathering of plagioclase and the dissolution of gypsum. Naturally occurring sulphates ($SO_4^{2-}$) are dissolved in wetland waters and their presence is associated with rocks containing gypsum, anhydride and other sulphur containing compounds. The occurrence of sulphate in natural waters is limited by the presence of calcium ions as they form a slightly soluble $CaSO_4$.

### 2.6.2 Environmental isotopes

Environmental isotopes of oxygen-18 and deuterium ($^{18}O$ and $^{2}H$) are widely used environmental isotopes in defining the origin of water and recharge characteristics in wetland hydrological studies. These isotopes, $^{18}O$ and $^{2}H$ forms part of the water molecule, $H_2O$ as $H_2{}^{18}O$ or $H^{16}O$, and exhibit variations during fractionation. Hence, the use of $^{18}O$ and $^{2}H$ in natural waters acts as effective tracers in the terrestrial water cycle (Aggarwal *et al*., 2005) thus provide insights into the ecological, climatic and hydrological processes at the local, regional and continental scale of a body of water. Isotopic abundance is typically described in terms of its isotopic ratios. For example, for the deuterated water

R = [$^2$H]/[H] (or R=½[$^2$HO]/[$H_2O$])

These isotopic ratios are themselves typically reported as per mil deviations from a standard:

$$\delta = 1000(\frac{R}{R_0} - 1) \quad (2.8)$$

where $R_o$ is the isotopic ratio of the standard

(the symbols $\delta^{18}O$ and $\delta^2H$ are used for the isotopic abundances of deuterium and oxygen-18 in water vapour, respectively).

The isotopic composition of water is expressed in per mil (‰) deviations from the VSMOW standard. For this purpose, an internationally agreed sample of ocean water has been determined and used, called Vienna Standard Mean Ocean Water (VSMOW) (IAEA, 2010). These deviations are written as $\delta^{18}O$ for Oxygen-18 and $\delta^2H$ for deuterium:

$$\delta^{18}O‰ = \frac{\left(\frac{^{18}O}{^{16}O}\right)\text{sample} - \left(\frac{^{18}O}{^{16}O}\right)\text{VSMOW}}{\left(\frac{^{18}O}{^{16}O}\right)\text{VSMOW}} \text{x}1000 \quad (2.9)$$

and

$$\delta^2H‰ = \frac{\left(\frac{^{2}H}{H}\right)\text{sample} - \left(\frac{^{2}H}{H}\right)\text{VSMOW}}{\left(\frac{^{2}H}{H}\right)\text{VSMOW}} \text{x}1000 \quad (2.10)$$



Water with less deuterium than VSMOW has a negative $\delta^2H$ whiles water with more deuterium than VSMOW has a positive $\delta^2H$. The same is true for $\delta^{18}O$ (Mazor, 2004).

Changes in the isotopic relationships between $^{18}O$ and $^2H$ during the evaporation and condensation of water (fractionation), allows defining its origin (Craig, 1961). This is because as the water evaporates, the lighter molecules are preferentially enhanced in the vapor and evaporated whiles during condensation of vapor to liquid, the reverse is true. The unique signature of environmental isotopes as tracers is the fact that their concentrations usually does not change by interaction with groundwater material or interaction with other elements in the water cycle. This study aims to use field parameters and major ion analyses to qualitatively describe the water exchange and assess the extent of the interaction between the wetland and the underlying groundwater.

### 2.6.2.1 Variations of $^{18}O$ and $^{2}H$ in the water cycle

Variations in the environmental isotope composition of natural waters occur in the atmospheric part of the water cycle and surface waters which are exposed to the atmosphere. Soil and subsurface waters have isotopic signatures similar to atmospheric and surface water inputs. While individual rainfall events may have little impression on a hydrological system, long term average data of the isotopic composition of the precipitation should be used as the input to the system. A global IAEA/WMO (International Atomic Energy Agency/World Meteorological Organization) network was established to conduct a worldwide survey of $\delta^{18}O$ and $\delta^{2}H$ in the precipitation since 1961. According to Craig (1961), the following observations were made:

1) Latitude effect: A decrease in $\delta^{18}O$ and $\delta^{2}H$ content moving from lower to higher latitude. Stations located in the northern and southern hemisphere are depleted in isotopic values compared to those located near the equator. The depletion in the isotopic values towards the poles is related to decrease in temperature.

2) Continental effect: A decrease in $\delta^{18}O$ and $\delta^{2}H$ values moving from the coast inland. The moist air masses from the ocean condenses near the coast. The first condensation will have heavy isotopic content similar to the ocean water. As the moist air masses moves inland the vapour gets continually decrease in the heavy isotopes since the precipitation leaving, the system is enriched in $\delta^{18}O$ and $\delta^{2}H$.



3) Altitude effect: A decrease in the $\delta^{18}O$ and $\delta^{2}H$ content with increase in altitude. The magnitude of the altitude effect depends on local climate and topography. Typical gradients in $\delta^{2}H$ observed is 1.5 to 4 ‰ per 100 m and in $\delta^{18}O$ is 0.2 to 0.5‰. One reason for the altitude effect is the progressive rainout of heavy isotopes during upward movement of moist air masses (which occurs in the windward side of the mountain range). The depletion in the isotopic composition with altitude is also related to decrease of temperature.

4) Seasonal effect**:** Seasonal variation of $\delta^{18}O$ and $\delta^{2}H$ is related to seasonal variation of temperature. Seasonal fluctuations are more predominant in places far from the coastal stations, whereas in coastal stations seasonal variation is relatively small.

5) Amount effect: For some tropical stations a strong negative correlation between $\delta^{18}O$ and $\delta^{2}H$ and rainfall amount is observed. The amount effect results in average depletion of -1.5 ‰ in $\delta^{18}O$ per 100 mm of rainfall in these stations. This has been partly explained as being due to evaporation of the falling raindrops and also due to exchange with the atmospheric water vapor which occurs

during light rains periods. The relation between the $\delta^{18}O$ and $\delta^{2}H$ values of natural waters is determined by equilibrium fractionations $\delta^{2}H$ v/l and $\delta^{18}O$ v/l.

Craig (1961) and Dansgaard (1964) found a relation between the $\delta^{18}O$ and $\delta^{2}H$ values of precipitation from various stations in the world as given in Eq 2.11:

$$\delta\ ^{2}H = 8\ \delta^{18}O + 10\ ‰ \quad (2.11)$$

This relation is known as the Global Meteoric Water Line (GMWL) is shown in Figure 2.4.

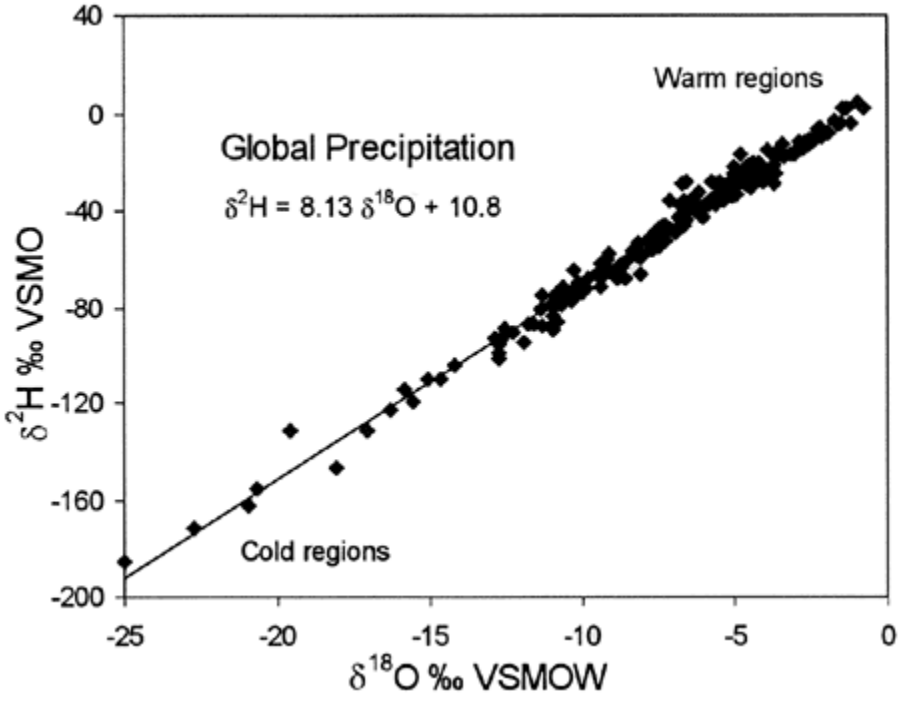


**Figure 2.5: Global meteoric water line (modified after Clark & Fritz 1997)**

#### 2.5.2.2 Deuterium excess

The International Atomic Energy Agency (IAEA) measured the global isotopic composition of rainwater. The results showed similar trends as Craig's work (Dansgaard, 1964) in Eq. 2.12:

$$\delta^{2}H = (8.17 \pm 0.08)\ \delta^{18}O + (10.56 \pm 0.64) \quad (2.12)$$

Where the gradient is the temperature relationship between $\delta^{18}O$ and $\delta^{2}H$ during condensation and the intercept is as a result of the evaporative conditions in region. The intercept is also called deuterium excess or d-excess and is given as in Eq 2.13:

$$d = \delta^{2}H - 8\delta^{18}O \quad (2.13)$$

The intercepts in most places around the world are about 10‰. However, some areas may have slightly different slopes and intercepts due to different and rainfall evaporation conditions. Generally, intercepts are higher in areas where evaporation is faster or rainfall evaporation occurs. For example,

North America: $\delta^2H = 7.95\ \delta^{18}O + 6.03$ (Dansgaard, 1964);

Tropical Island area: $\delta^2H = 6.17\ \delta^{18}O + 3.97$ (Dansgaard, 1964);

Japan: $\delta^2H = 8\ \delta^{18}O + 17.5$ (Sakai & Matsubaya 1977).

Some works have used d-excess to trace the source and movement of air mass source of meteoric water which have also been used identify seasonal groundwater recharge zones (Gibson *et al*., 2006). Stable isotopes have also been applied to quantify water fluxes within wetlands. Hunt *et al*., (1996) proposed the use of stable isotope mass balance method in estimating groundwater inflow to a wetland. Chapman *et al*., (2003) estimated the groundwater contribution to a wetland based on their results of stable isotopic compositions of the groundwater and surface water.

### 2.6.3 Application of hydrochemical and environmental isotopes in wetland studies



The use of environmental tracers such as water quality field parameters (Woldemariyam & Ayenew, 2016; Lessels *et al*., 2015; McCallum *et al.,* 2014) dissolved ions in water (Soulsby *et al*., 2007), temperature monitoring (Moseki, 2013; Butler, 2009; Constantz, 2008) environmental isotopes of water (Yang *et al*., 2012) and radioactive isotopes (Banks *et al.,* 2011) have been used to studied groundwater-wetland interaction. Hydrochemical and environmental isotopes data can be integrated into existing sampling programs to understand the hydrogeological processes in wetland studies. Conceptually, groundwater outflow from a wetland influenced by evaporation represents a solute and isotopically enriched plume analogous to a mobile contaminant. Evaporation of water from a wetland results in increased $Na^+$ and $Cl^-$ concentration and enrichment of $\delta^{18}O$ and $\delta^2H$ isotopes.

Smith *et al.,* (2015) used environmental tracers to conceptualize the groundwater–surface water interactions in Bool lagoon and Lake Robe in the lower limestone coast prescribed wells area, Australia. Measured environmental tracers included major ions chemistry, environmental isotopes of water, tritium, radon and noble gases. The results of major ion chemistry, environmental

isotopes of water and tritium showed that surface water recharged occurred at the Bool Lagoon. Groundwater salinity had also increased over the past decades which indicated that discharge was the dominant surface water – groundwater process. This study also showed that, Bool lagoon had separate periods of recharge and discharge, whilst the surface water coupled with low recharge rates resulted in salinization of the wetland. Lake Robe was found to be discharge zone but appeared as a local discharge feature in the regional discharge setting. There was evidence of local discharge of fresh water coming from the adjacent dune system.

Sola *et al*., (2014) carried out a study to determine the hydrogeochemical characteristics of the Cabo deGata coastal groundwater in Spain using hydrogeochemical and isotope analysis method. A cluster of piezometers was set up and used to monitor the groundwater quality. Water was sampled at different intervals from the top to the bottom. Seawater was sampled was near the coast, as well as fresh-water sample from the groundwater. Multivariate analysis was used to classify the water types into two groups. One group represented water from the upper part of the groundwater with 10 to 60% proportion of seawater. The other group taken from the lower part of the groundwater, contained 60−70% seawater. Hydrogeochemical model was applied, which showed that the waters as highly evaporated. The results proved that evaporated waters occurred during the Holocene, in the coastal lagoon environment; hence brines that were formed infiltrated into the groundwater due to the high density of the waters. This hydrogeochemical information was used to identify the prevailing environmental conditions and the groundwater-lagoon interaction reconstructed. The current study is not focused on the sea water intrusion or contribution to groundwater hence this method was not used.

Liu *et al*., (2014) provided quantitative and qualitative insight into the hydrological and geochemical process between wetland and the coast in the Yellow River Delta in China, using hydrochemical and environmental isotope data. Groundwater salinity at the Coast reflected the presence of seawater trapped in the clay sediments This was confirmed through groundwater levels measurements, environmental isotopes and major ion signatures. The $\delta^{18}O$ and $\delta^{2}H$ results indicated that, the groundwater in the Farmland and Wetland exhibited more depleted isotopic signatures compared to groundwater from the Coast. The depleted groundwater resulted from the diversion of water whiles the less depleted groundwater at the Coast was due to minimal

fluctuations in the water table along the Coast. Piper diagram was used to identify trends in the water composition. The chemical characteristics of the groundwater in Farmland did not exhibit the possibility of seawater intrusion. The hydrochemical facies evolution diagram (HFE-D) indicated that, freshening was taking place in most parts of the groundwaters. The isotopic mass balance was used to calculate the surface water contributions to groundwater in the Wetland. Surface water accounted for 50–70% of Wetland and Farmland groundwater composition after water diversion. Hence, the researchers concluded that, the quality of waters in coastal groundwaters in the Yellow River Delta were influenced by water diversion, land use practices and lithological properties of the drainage landscape (Liu *et al*., 2014).

Taak & Singh (2014) investigated the hydrochemical dynamics of Sukhna wetland and the adjoining groundwater using major ion chemistry. Seasonal surface water and groundwater samples were collected from the wetland and borewells in the catchment and analysed for the chemical composition. Major ions were plotted on a piper diagram to identify the water types. $Ca^{2+}$, $Mg^{2+}$, $CO_3^{2-}$, and $HCO_3^-$ were the dominant hydrochemical facie in the water chemistry in the catchment. Irrigation parameters such as, sodium adsorption ratio (SAR), percent sodium, magnesium ratio and RCS were calculated and used to show the suitability of the waters for irrigation. The Wilcox diagram was used to classify the waters for irrigation purposes, based on electrical conductivity and percent sodium. The water samples fell in the excellent to good water classification which indicated the suitability of the waters in the Sukhna catchment irrigation (Taak & Singh 2014). Sodium adsorption ratio (SAR) was calculated and based on the USSL classification, the wetland waters fell in the S1– C1 class which indicated low to medium sodium and salinity hazards whilst the groundwater fell in S1–C2 class which indicated low sodium hazard and high salinity hazard Taak & Singh 2014). Residual Sodium Carbonate (RSC) was calculated and used to determine the suitability of water for irrigation purpose and based on the alkalinity hazard in the wetland soil. The RSC values ranged from 0.1 to 3 meq/l which indicated that, wetland and groundwater in the Sukhna wetland were suitable for irrigation.

Bocanegra *et al*., (2013) assessed and quantified the water balance and the hydrogeological processes related to wetland–groundwater interaction in the Pampa Plain using hydrogeochemical, isotopic and numerical modelling techniques. Water table depths were measured in wells located

in the vicinity of the wetland. Water samples were analysed for physicochemical and environmental isotope composition. Hydrogeochemical inverse mass balance models were numerically tested by using NETPATH software. Recharge was estimated at 14% using the soil–water-balance and water table fluctuation method and used as input data for the model. Integrated analysis of hydrochemical and isotopic information was used to calibrate the groundwater flow model. The model was validated using hydrochemical and isotopic data and the water balance calculated using hydrologic information and a combination of mathematical and hydrogeochemical models. Similar volumes were obtained for both methods. The calculated water balance showed an increase of 0.09 m in the wetland level for the simulated year.

Skrzypek *et al*., (2013) developed geochemical models and a salt inventory for estimating duration of salt accumulation and decouple geochemical characteristics of salt from modern groundwater in the Fortescue Marsh catchment, Northwest Australia. The conventional mass balance model based on major ions, geochemical modelling as well as water environmental isotopes ($\delta^{18}O$ and $\delta^{2}H$) were used to carry out the study. The researchers applied geochemical models and stable isotopes to characterize the groundwater flow and hydraulic connections, and identified interactions between groundwaters. Groundwater in the catchment were characterised by their environmental isotope compositions into two distinct groups; i) fresh and brackish groundwater and ii) saline and brine groundwater. Brackish water indicated modern recharge whilst saline and brine groundwater indicated mixing between modern rainfall, brackish water and relatively old groundwater. The environmental isotope composition of the brine groundwater also suggested evolution which could not be explained by evaporation only. The Cl mass balance calculations suggested between 40,000 and 700,000 years was required to accumulate the observed salt load in the Fortescue Marsh.

Sánchez-Martos *et al*., (2013) studied the groundwater-surface water interaction in the coastal wetlands of Campo de Dalías in Spain using simple hydrogeochemical tools. The ionic ratios of the waters were calculated and used to analyse the evolution of surface waters in the area. Box-plot and Piper diagrams were used to show the variability of ion content in the wetland waters. Results of the study showed high concentration of dissolved salts in some parts of the wetland which was attributed to impact of salt extraction works. Hydrogeochemical tools were used to

characterize the water types and the main processes that controlled the water type diversity were described.

Cartwright *et al*., (2009) used hydrochemical and environmental isotopes data in the absence of detailed hydrological data to understand groundwater and surface water interactions in wetlands in the Willaura region in South eastern Australia. Major ions and environmental isotopes of water were sampled from groundwater and wetland. The "salt effect" was applied to environmental isotopes data to account for the high solute concentration in the waters. The use of ionic ratios particularly $Cl/Br^-$ provided insight into the role of halite precipitation and dissolution and the influence of high evaporation on the saline groundwater. The data gained from the study enabled a rapid and qualitative assessment of wetland type (that is groundwater recharge, discharge or flow through) and hydrological function. Cl/Br ratio were used in differentiating evapotranspiration losses and discharge to the underlying shallow groundwater. Despite the wetland volume appearing relatively static, trends in the environmental isotopes and hydrochemical data of the wetland were dynamic highlighting a short coming of basin water balance on physical hydrology alone.



Reynolds & Marimuthu (2007) used the physical hydrological parameters of the Lake Warden in addition to hydrochemical and environmental isotopes data to characterize groundwater flow in the Lake Warden coastal wetland. Groundwater, surface water and rainfall data were compiled to solve annual water cycle problem. They used a theoretical single-batch evaporation model to measure the residual isotopic signature of the wetland water using Craig & Gordon (1965) "Salt effect". stable isotopic mixing models was used to determine the relative contribution from surface water, groundwater and precipitation to wetland water balance. The outcome from the study of the lake Warden wetland resolved the hydrological uncertainties relating to the wetland hydrology. Previous interpretation of bathymetry survey data indicated that the wetland operated as a single water body however, the combined use of hydrochemical analysis and environmental isotopes showed the wetland as geologically separate entities.

### 2.6.4 Geographic Information System (GIS)

Geographic information System (GIS) is used in understanding the spatial distribution and temporal variation of parameter distribution with land use or land cover changes for water resources management. The use of GIS enables generation of information for developing solutions

for water resources problems such as understanding flows in the natural environment, assessment of water quality, determination of water availability and managing water resource (Johnson, 2008). For example, Nur *et al*., (2012) characterized the flow dynamics and the chemical evolution of groundwater in Damaturu, Northeast Nigeria using GIS. Nur *et al*., (2012) used GIS to mapped out the different hydrochemical facies and the water-rock interaction in the catchment. GIS's uses geographically referenced layers and registers them to a known projection system. The layers contain information related to the location of the selected parameter. The layers are laid over each other in order to match each location with the corresponding locations on the other maps for proper correlation (Johnson, 2008). This enables the determination of the influence of one layer over the others.

### 2.6.5 Multivariate statistical analysis

Multivariate statistical methods such as cluster analysis (CA), principal component analysis (PCA) and correlation analysis have been used in characterize water quality and to source identification (Barakat *et al*., 2016; Belkhiri *et al*., 2010; Yidana *et al*., 2010). Multivariate statistical tools are used to identify possible factors and or sources influencing the water chemistry and provides first hand solution to pollution problems (Bhuiyan *et al*., 2015; Molla *et al*., 2015). They provide a better understanding of the water quality and the interrelationships between variables and sampling sites.



The use of multivariate statistical techniques to assess and characterize water from groundwater inflow and wetland has been carried out (Bhat *et al*., 2014; Sarkar & Bhattacharya 2010; Sundaray, 2010; Kim *et al*., 2005). Cluster analysis is based on similarities or dissimilarities in variables in such a way that each cluster represents a different process (Yidana *et al*., 2010). Cluster analysis is used to observe the inter-relationships between variables by first reducing the number of observations or cases into groups of smaller cluster sets. The smaller sets are represented by identifiable processes common to the group.

Principal component analysis (PCA) is a used to identify patterns in a large data with many parameters. Principal component analysis can be used with cluster analysis to reduce the number of dimensions in a data set without losing much information. Correlation analysis is used in water

quality studies to measure the strength or dominance of ions based on their linear relationship (Zeng *et al.*, 2012). Factor analysis (FA) is used to generate an unobserved or latent variable which compiles variations in three or more observed variables. Is used to identify the relationship among a number of observable quantitative variables and compiles the variations into factors. Factor analysis in hydrogeochemical studies to identify similarity in variables with respect to a particular environment and serve as an indicator for parameter associations (Odokuma-Alonge & Adekoya, 2013). These associations are used to identify the hydrogeochemical or environmental processes responsible for them.

Yang *et al*., (2015) integrated multivariate statistical techniques, principal component analysis (PCA) and hierarchical cluster analysis (HCA) with graphical methods (Piper diagram) to identify the groundwater quality in a coastal groundwater, Fujian province, South China. With the use of multivariate analysis, they were able to conclude that salinization, water-rock interaction and anthropogenic pollution influenced the ground water quality in the catchment.

Sheela *et al*., 2012 used multivariate analysis cluster analysis (CA) and factor analysis (FA), to analyze variations in the freshwater and saline water quality of the Akkulam-Veli coastal lake in Kerala, India. The study indicated the organic pollution factor played a dominant role in the lake water quality. Medina-Gómez & Herrera-Silveira (2003) used Principal Component Analysis (PCA), in characterizing water quality and nutrient dynamics in Dzilam lagoon, Yucatan, Gulf of Mexico. The multivariate analysis showed salinity gradient and nutrient concentration as the dominant variables controlling lagoon hydrologic heterogeneity.

## 2.7 Theoretical and conceptual framework for wetlands

This study applied Darcy's law of flow in a porous medium and the theory of infiltration to conceptualize the water flow dynamics and quantify the groundwater -wetland interaction using the Sakumo wetland as a proxy. These theories were used to interpret the results. The Sakumo wetland was selected for this study because of the increasing environmental pressure and also it is well demarcated and more information was available hence the choice of the Sakumo wetland as a case study.

The theory of water flow has been studied in lakes, streams and wetlands (Toth, 1963; Freeze & Witherspoon 1968; Gusvey & Haitjema, 2011; Wang *et al.,* 2014; and Zech *et al.,* 2016). The Darcy law is governed by flow through the porous medium. The Darcy law states that the fluid flow through the porous bed medium shows direct proportionality to the differences in heights of fluid between the two ends of the filter bed, and inversely proportional to the length of flow path. In the Darcy experiment, water was applied at a known pressure to a horizontal pipe fitted with sand and flows from one end to the end. Darcy found that, discharge was directly proportional to the difference in heads and inversely proportional to the flow length. Groundwater flow models based on the Darcy Law have been developed and used to determine flow pattern in groundwaters. This theory was used to explain the modelling results of the Sakumo wetland basin, which is a fractured rocker with a porous medium.

The theory of infiltration involves the movement of water from precipitation or surface water, through the soil profile and into groundwater recharge. Factors such as, hydraulic conductivity, saturation, soil type and porosity affect how much water moves from the surface to the ground. Beekman & Xu (2003) proposed methods of quantifying groundwater recharge in South African. Sun *et al*., (2013) reviewed methods of groundwater recharge, which included vertical or lateral inter-groundwater flow, induced recharge from the nearby surface water bodies as a result of groundwater abstraction, artificial recharge as a result of injection of water into wells and the flow of water through the unsaturated zone reaching the water table. The theory of natural groundwater recharge was applied in this study to characterize the water flow and assess the groundwater-wetland interaction.



The thermodynamic principles which determine the chemical composition of natural waters was applied to characterize the water resources in the study area. The concept was first put forward by Chevoratev (1955) and later developed by Garrels & Christ (1965). Glynn & Plummer (2005) in their review of the application of geochemistry to understanding groundwater flow systems, points the advantages in terms of the relative ease and independence from hydrodynamic methods. The present study explores the application of hydrogeochemical models in characterizing the water types, identifying correlations, flow lines, mixing or evaporative processes and quantifying the interaction between different water sources in the Sakumo wetland basin.

# CHAPTER 3: RESEARCH DESIGN AND METHODOLOGY

## 3.1 Introduction

Chapter one has provided the situational analysis that informed the problem statement, research question, the main thesis statement, aim, scope, rationale and objectives of the current study whereas chapter 2 has presented the reviewed literature on the what is known and not known with regards to the current study topic in addition to the theoretical and conceptual framework that inform the present study. The current chapter describes the research design, research methodology and research methods that were used to collect and analyze the needed data to answer the research question set in chapter one thereby fulfilling the objectives for present study. In this chapter, the argument is that detailed description on i) research design; ii) research methodology; iii) research methods for data collection and analysis and iv) statements on research integrity are important because they provide the basis for the results of the present study to be considered adequate, objective and appropriate evidence for answering the research question of the current study.



## 3.2 Study area description

### 3.2.1 General description of the study region

Ghana lies between longitudes 3° 15' W and 1° 12' E, and latitude 4° 44'and 11° 15' N. It is bordered to the East by the Republic of Togo, the West by Cote d'Ivoire, the North by Burkina Faso and the South by the ocean. The coastline of Ghana forms part of the Gulf of Guinea and extends between latitudes 4" 30' N and 6" N. The coast line of Ghana stretches for a distance of 550 km between 3' W and l° E.

The climate of Ghana is influenced by Tropical Continental Air Mass and the Equatorial Easterly Winds (ITCZ) (Figure 3.1). The rainfall pattern is related to the movement of the ITCZ (Dickson & Benneh, 1995). The ITCZ crosses Ghana twice in a year giving rise to two main rainfall regimes that occur from April to July and from September to November (Dickson & Benneh, 1995). The relatively dry coastal climate of the southeast is believed to be caused by the south-southwest winds blowing parallel to the coast. The mean minimum rainfall is 900 mm/a occurring around the

South-eastern part of Ghana (Accra-Aflao) while the mean maximum rainfall is about 2000 mm/annum occurring in the South-western precisely at Axim. Mean minimum temperature ranges from 21°C – 23°C and mean maximum temperature is from 30°C – 35°C. The mean annual evapotranspiration rate is low in southern Ghana (80 mm) and higher in northern Ghana (190 mm).

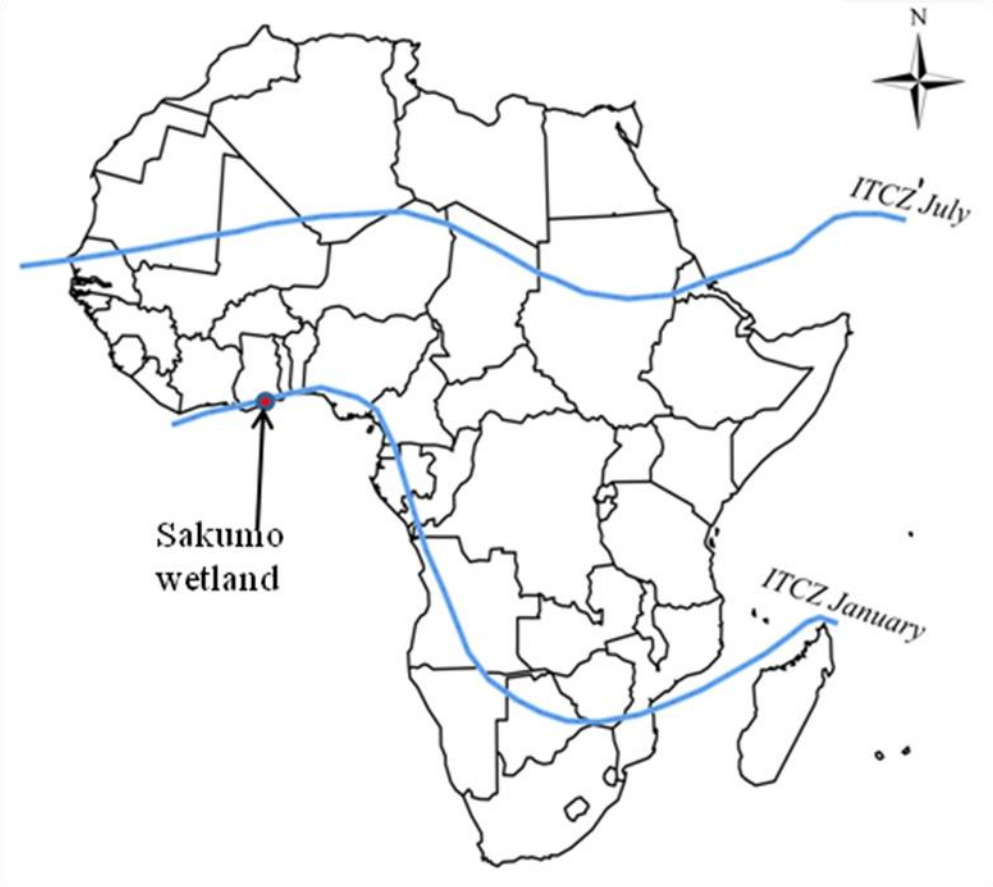


**Figure 3.1: Map showing the position of the ITCZ over Ghana, Africa**

### 3.2.2 Location of the Sakumo wetland basin

The Sakumo basin has a total drainage area of 276 km$^2$ at the point of outfall into the sea but the effective catchment area is 127 km$^2$ because of dams that are placed in the streams leading towards the wetland. The Sakumo wetland has a surface area of 1.08 km$^2$. The basin is comprised of a coastal brackish-saline wetland whose main habitats are open wetland, surrounding flood plains, freshwater marsh and coastal savanna grassland. The Sakumo wetland is the main water body within the Sakumo Ramsar site and is 4.42 km long with a surface area of 0.53 km$^2$. The wetland is separated from the sea by a narrow sand dune on which the Accra-Tema beach road is built and

is connected to the sea by two small channels, constructed to prevent flooding. Hence the wetland is a semi-closed system whose functions are much more unpredictable with abiotic conditions changing very rapidly from time to time. The wetland is normally full during the raining season where the entire basin becomes inundated with flood water and covers a surface area of approximately 10 $km^2$. The wetland reaches its lowest in the dry season and the water levels drop due to high evaporation rates and the surface area of the wetland shrinks to about 1 $km^2$. During high tides where there is complete reversal of flows, sea water flows into the wetland. And the wetland reaches a maximum depth of 0.9.m (Kwei, 1976).

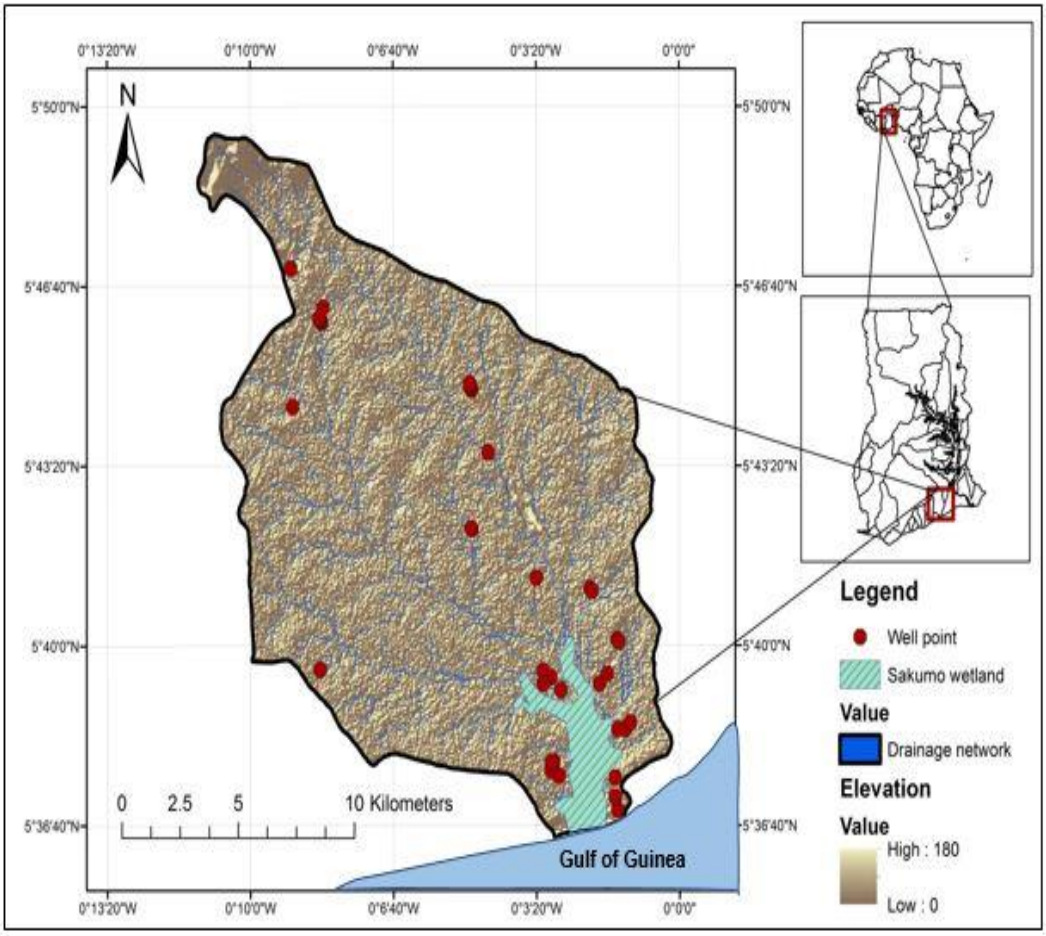


**Figure 3.2: Location map of the Sakumo wetland basin showing the well points**

The basin generally has a flat topography with few braided channels running through the swamp into the wetland before it discharges into the sea. Farming in the basin occurs mainly in the upper part of the basin but recently, farms are springing up within the immediate environs of the wetland.

Pollution in the basin is mainly from industrial, domestic and agricultural sources (Nonterah *et al*., 2015). Domestic and industrial pollution from untreated sewage from households are channeled into the wetland. Pollution from agricultural farms onto the wetland is from fertilizer use and farm animal wastes. During dry the season, significant drop in the wetland water levels occurs.

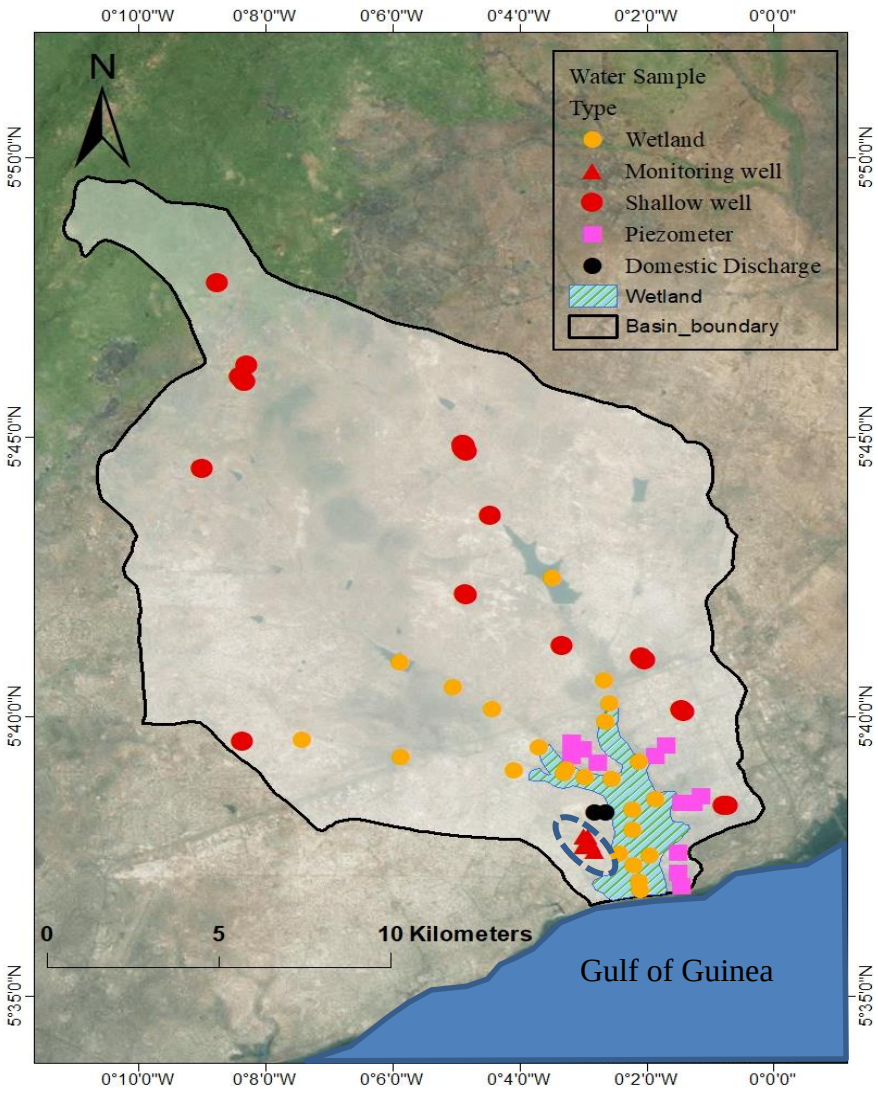


**Figure 3.3: Location map of the Sakumo Basin**

### 3.2.3 Climate of the study area

The Sakumo wetland basin is situated in the coastal savannah zone of Ghana. Annual rainfall ranges from 630 mm to 1000 mm and averages 760 mm. Peak rainfall is in June and the lowest rainfall is measured in January. There is a double maxima annual distribution of rainfall in the

Ghanaian coastal zone, with the high maximum occurring during May–June and the low maximum in September–October. Minimum temperatures occur in August and the maximum in February. Pan evaporation data from Tema meteorological agency indicates high evaporation rates between March–April and October–November with an estimated annual evaporation value of 1,400 mm. Relative humidity varies from 60%–80% during the raining season to less than 30% in the dry season. Relative humidity is generally high in the afternoon varying from 65% in the afternoon to about 95% at night. Water levels in the wetland varies throughout the year with the highest level occurring in the raining season and the lowest in the dry season due to evaporation.

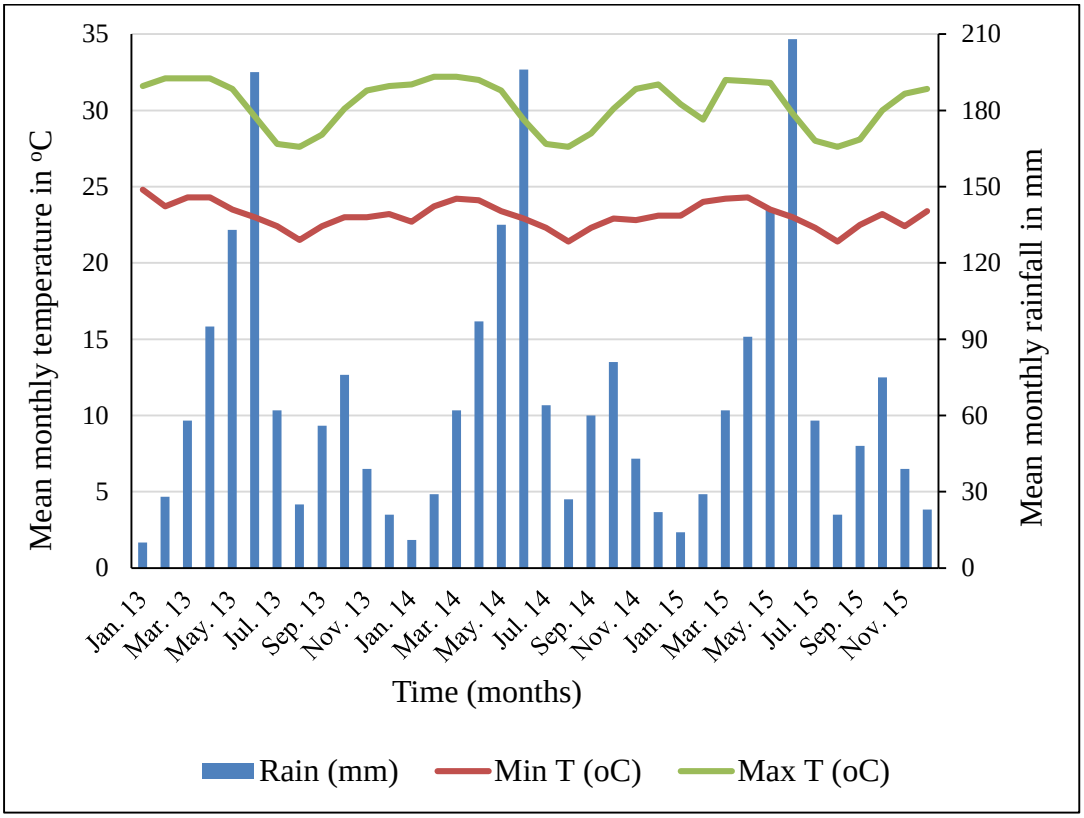


**Figure 3.4: Monthly mean rainfall and temperatures at the Sakumo wetland based on measurements from Tema meteorological station from 2013-2015**

### 3.2.4 The role of geology and soils on the wetland hydrogeology

The geology of the Sakumo wetland basin is underlain by Dahomeyan (Pre-Cambrian) rocks. The Dahomeyan rocks occurs as alternating belts of acid and basic gneisses. They consist mainly of crystalline gneisses and migmatites, with subordinate quartz schist, biotite schist, and other

sedimentary remnants. The rock types occur as persistent parallel belts several 1niles wide that strike north-northeast and dip about 25 ° towards the southeast. Rocks of the acid Dahomeyan consist generally of muscovite-biotitic gneiss, quartz-feldspar gneiss, augen gneiss and minor amphiboles. These rocks decompose to slightly permeable calcareous clay. The basic Dahomeyan rocks consist of two groups - the metabasics and the basic intrusive. The metabasics are very uniform, coarse- grain and usually well foliated of garnet hornblende gneiss and granules with minor layers of hornblende and biotitic schist and pyroxene gneiss at the base (Junner & Bates 1945). The wetland is situated in the recent alluvium and marine sands are deposited in the narrow strip along the coast.

The soils in the Sakumo wetland are mainly vertisol normally referred to as Tropical Black Earth, and are classified as Calcic vertisol (FAO/UNESCO, 1990). The vertisols are characterized by their low water infiltration (saturated hydraulic conductivity) hence they are susceptible to water logging during the raining season.

### 3.2.5 The role of hydrology on the wetland



The Sakumo basin is drained by a number of streams which flows into the brackish wetland. There are three sub-basin within the Sakumo basin which discharges into the wetland namely; the upper sub-basin (Dzorwulu river), western sub-basin (Onukpawahe-Mamahuma stream) and the Eastern sub-basin. The south of the Sakumo basin is bounded by the Gulf of Guinea. The Dzorwulu river flows through Ashaiman whiles Mamahuma stream flows from Adenta and Frafraha, the Onukpawahe stream flows from Madina and as well as Tema SOS, Communities 12, 6, 5 and 3. The Dzorwulu River joins Gbemi River in Ashaiman and runs a distance of 7.0 km before discharging into the weland. The Mamahuma and the Onukpawahe joins and run a distance of 3 km before discharging into the wetland. These drains run through very densely built up and heavily populated communities. The Dzorwulu and Mamahuma, have been re-channeled and dammed for irrigation. This has resulted in reduced flows into the wetland especially during the dry season as most of the streams are perennial (Amatekpor, 1998). Presently, there is no monitoring system to check the water levels in the wetland.

### 3.2.6 The impact of land use and urbanization on the Sakumo wetland

The Sakumo wetland lies between two rapidly growing cities of Accra and Tema with the highest urban growth-rates in Ghana. Nearly, 60% of industries in Ghana can be found in this area (GCLME, 2007). The Sakumono village is on the immediate west of the wetland and stretches from Madina to Oyarifa on the west and to the Aburi highlands in the north. The wetland is bordered to the east by the Terna municipality and northeast by Ashiaman township.

The main occupation of the people in the Sakumono and the surrounding communities is fishing. The catch comprises tilapias, *Sarotherodon melanothero,* the horse mackerel *Caranax hippopo*, the blue legged lagoon swimming crab *Calliectes latimaus* and other species (Amatekpor, 1998). The continuous fishing in the wetland and the exploitation of popular species has resulted in extinction of certain fish species. The major activities in the Sakumo basin are shown in Figure 3.6 (GSS, 2010).

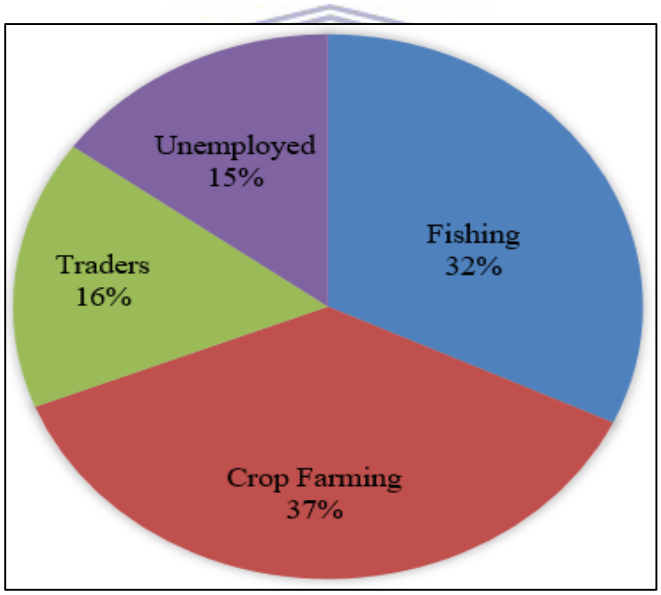


**Figure 3.5: Major activities in the Sakumono area**

Total agricultural land which comprises cultivated and fallow areas in the wetland area were estimated at 13,562.3ha, which account for 49.1% of the area (Amatekpor, 1998). This has decreased to 37% (Figure 3.6) as built up developments comprising residential, industrial and other construction activities are on the increase. Arable agriculture includes the cultivation of rice, cassava and vegetables occur on the northern parts of the wetland, along the banks of the

Dzorwulu, Onukpawahe and Mamahuma streams which flow into the wetland (Amatekpor, 1998). Figure 3.6 shows different activities within the Sakumo basin.

**Figure 3.6: Some farms and human settlements in the vicinity of the Sakumo wetland**

The farmers apply pesticides, fertilizers and other agro-chemicals in the cultivation process in order to increase their yield (Dadson, 1995). Pesticide residues, nitrate from fertilizers and microorganisms from animal waste are sometimes found in the water bodies located near the farms

(Williams & Langely, 2001). The semi-nomadic grazing of cattle competes with arable agriculture in the area. Increase in urban expansion has decreased available pasture for cattle grazing. The intensity of fishing and cattle grazing also varies with the pattern of rising and falling water levels.

Industrial activities dominate the western part of the basin. Other land use activities include developments of residential and tourism facilities around the wetland. The current land use activities provided insight into the water use system in the basin and the possible areas were groundwater-wetland interaction could be occurring. These activities have greatly changed the land use and landcover structure of the basin which if not controlled can pose major threat to the existence of the wetland.

## 3.3 Research design



Different studies apply different philosophical assumptions in addressing a research problem depending on the nature or type of the study that is, whether the study is quantitative or qualitative and whether the problem to be addressed is a scientific, social or economic. The three main methodological approaches used in the current study involve quantitative, qualitative and mixed methods. The principles or philosophies underpinning the use of these methods in the study are different but compatible. quantitative approach that allows predicting and explaining causal relationships among variables. For example, the current study measured the elevation of the wetland topography to characterize the groundwater flow system in the area. Wetland and groundwater water levels were also measured and used to estimate the groundwater contribution to the wetland and the wetland water balance.

Qualitative method provides alternative theoretical and practical approach to research, which involves describing using experimental methods. Qualitative methods were applied to achieve the second objective by analyzing field and chemical parameters to establish the water type and processes controlling the water composition. Mixed methods involved the use of more than one method to determine a trend. The use of physical, hydrological, GIS analyses, hydrochemical and environmental isotopes were used to determine groundwater-wetland interaction.

### 3.3.1 Study design

The general approach to this study was a case study approach where the Sakumo wetland was used as a case study. A comprehensive approach to quantifying the water balance and understanding the groundwater-wetland interaction was adopted. The focus was to determine the groundwater flow in the Sakumo basin and quantify the groundwater contribution to the wetland. The study approach involved desk study, data collection and laboratory work. The desk study comprised review of literature, compilation of existing borehole data, topographical and geological maps. The data collection involved collection of rainwater, wetland water and groundwater from the underlying groundwater.

First, a desktop study was conducted on wetland hydrogeology and water flow system. Hydrogeological data of the study area were obtained from government agencies such as the Water Research Institute (WRI) section of the Council for Scientific and Industrial Research (CSIR) and the Community Water and Sanitation Agency (CWSA). Topographic, land based maps and geographical information on the study area were obtained from the Geological Survey Department (GSD) of Ghana. Data was also obtained from the private sector including consultancy firms in order to supplement the available literature sources. However, there was not much information on well construction profile especially on the thickness of weathered zone or depth to bedrock screen length and saturation thickness, extent of gravel packing if any, and depth to which top of well was sealed. The most reliable and readily available data were those on depth, yield, static and dynamic water level. This information was however adequate in as much as specific capacity estimates were concerned. Data gathered from the monitoring wells was used to observe water table gradients and fluctuations. All the data collected during the desktop study was used to compliment the field data collected throughout the duration of the study. Table 3.1 is a summary of the research objectives, hypotheses and methods used address the current research study.

**Table 3.1: Research design table showing the study approach**

| Research objective | Research hypothesis and research question | Materials and methods |
|---|---|---|
| 1) Develop a hydrogeological conceptual flow and numerical model to quantify the wetland water fluxes | RH: the use of numerical flow model improves knowledge of the hydrogeological system<br><br>RH: calibrated model can provide a basis for predicting groundwater and wetland storage<br><br>RQ: what is the present flow pattern in the wetland?<br><br>RQ: What is the water balance under natural and stress conditions (low recharge) | - Review historic data<br>-Field survey<br>- Delineation of study area/ identification of physical boundaries Borehole location<br>-Well completion/pumping test data<br><br>-DEM, Land use/landcover maps<br>-Meteorological data (available/measured)<br>-GW levels monitoring<br>-SW level monitoring<br>-Pumping test<br>-Soil hydraulic properties<br>Simulation of steady state flow model<br>-Calibration of model<br>-Sensitivity of model<br>-Setting scenarios |
| 2) Identify sources and quality of water in the wetland | RH: Characterizing water quality helps in identifying the hydrochemical processes controlling the water chemistry<br><br>RQ: what is the present composition of groundwater underlying the wetland | - Review historic data<br>- Field observations<br>- Field measurements<br><br>-water samples<br>-water chemistry<br>-environmental isotopes<br>-geochemical analysis<br>-water classification<br>-hydrogeologic analysis |
| 3) Occurrence of groundwater-wetland interaction | RH: possible groundwater-wetland interaction aid water resources to design appropriate monitoring plan<br><br>RQ: to what extent does the wetland interacts with the underlying aquifer? | -Geological data<br>-Groundwater levels<br>- temperature and EC profiles<br>- hydrochemical data<br><br>-Simulation of steady state GW flow model<br>-Calibration of model<br>-Sensitivity of model<br>-Prediction of scenarios |

### 3.3.2 Sampling design method

In order to define all the required parameters suitable to aide this study and achieve representativeness of the sites, some criteria were outlined. The selection of monitoring and sampling sites was based on the availability of monitoring wells and perennial streams, good database and land use impact on the wetland hydrology. The availability of the monitoring wells is key in carrying out groundwater resources monitoring and assessment studies. The monitoring wells were preferred due to cost involved in drilling new wells. The monitoring wells are located on a golf course within the corridors of the wetland. Sampling sites for surface water bodies in the basin were chosen based on land used activities around the water bodies and the anticipated water flow direction in relation to the wetland. Historic data on monitoring wells was collated from the database of Water Resources Commission (WRC) and Water Research Institute of the Council for Scientific and Industrial Research (CSIR) to establish the historic trends and properly evaluate the outcome of the present study. The following point were considered in selecting the sampling sites; All direct contributing flows to the catchment were considered. Flows localized along major drainage axis of the catchment. Accessibility of sites at any time or at least most times of the year to enable sampling and monitoring. Areas with dominant agricultural land uses. Industrial areas. Residential /built-up areas. Based on the above criteria, eight sampling sites were selected with 80 sampling points as shown in Figure 3.7 as follows:



Sakumo wetland: The wetland receives water from the Onukpawahe, Mamahuma and Dzorwulu streams. These streams run through a per-urban agriculture belt before discharging into the wetland. The wetland was sampled and monitored for water quality and Temperature profile data was obtained by measuring temperatures at different depths of the wetland to identify points of interaction.

Onukpawahe stream: The Onukpawahe sub-basin has a drainage area of 30 $km^2$ but the stream stretches about 12.5 $km^2$ long to the wetland. The Onukpawahe stream takes its source upstream of the wetland and flows through the dense areas of Ashaley Botwe, Trasacco Estates and then links the Mamahuma stream in the vicinity of the Accra abattoir before flowing into the wetland. The stream is a major source of water for agriculture activities around the mid-western section of the catchment.

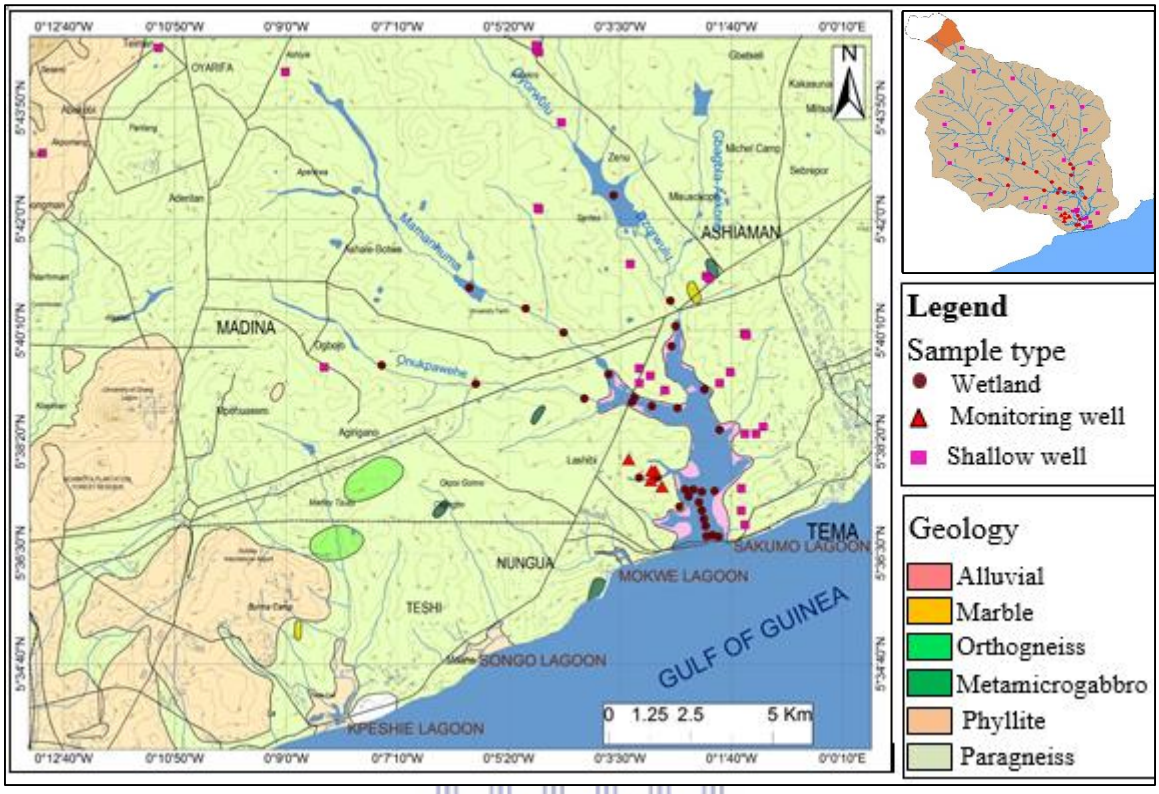


**Figure 3.7: Water sampling sites, lithology and topography of the Sakumo catchment**



Mamahuma stream: The stream originally runs through the community 19 to link the Mamahuma stream. A new channel diversion has been constructed after the 1995 floods to link it with a new confluence with the Mamahuma stream about 1.0 km upstream of the original confluence. The combined stream flows through the RSS housing estates and through Lashibi community and finally discharges into the Sakumo wetland.

Dzorwulu river: The river is located upstream in the upper part of the basin and runs through Ashiaman and drains in the wetland. The Dzorwulu river was dammed upstream for irrigation.

Lebanon dam: The dam was originally built to supply water for irrigation for rice farming. However, due to the activities of encroachers, most of the farmers have shifter to vegetable and maize farming I order to avoid lost. University dam: This site is used for Crops and Animal Research largely for irrigation and as a livestock farming.

Monitoring wells: The five monitoring wells (MW2, MW4, MW6, MW8 and MW 15) were drilled in the 1970's as part of the monitoring work in the Accra plains. The wells are used in this study to monitor groundwater levels in the basin. The monitoring wells were selected based on their availability, accessibility and close proximity to the wetland. Data on the groundwater levels and water quality were used to characterize the groundwater quality within the wetland environment and also to identify possible areas of groundwater-wetland interaction. Shallow Piezometers: Sub-surface water levels were measured at each of the selected sites and groundwater elevation was obtained by calculating the difference between groundwater level and surface elevation. Piezometers were installed closed to the wetland to monitor the shallow ground within the vicinity of the wetland.

### 3.3.3 Study population

To describe the flow dynamics, there is a need to include boreholes from high, medium and low areas of the groundwater. This study uses wells located in the upper and middle part of the basin and shallow piezometers installed on the lower parts of the basin as the study population. All wells penetrate through the fractured rock groundwater in the Dahomeyan whiles the piezometers are shallow (>5 m deep) and only used to measure subsurface flow. The study followed purposive sampling design for two reasons. First, because normally groundwater flows from areas of high altitude to areas of low altitude, it is important to include monitoring sites from these areas in order to properly monitor the water movement. Secondly, the basin is overlain by different activities on the surface which in turn influences the groundwater in different ways hence the need to sample within each of the areas where these activities are taking place.

## 3.4 Research methodology used in the current study

The section describes the research design and methods used for collection and data analysis. This section also covers data validation methods used to ensure data reliability and reproducibility. Last but not the least, discussions on the limitations of the study.

### 3.4.1 Collection of hydrogeological data

#### 3.4.1.1 Meteorological data

Daily rainfall data were collected from the Ghana Meteorological Agency (GMA) in Tema. Rainfall data were collected at a daily time step therefore it is expected that the model will perform better in predicting runoff volumes. Preliminary results indicate that the overall runoff pattern is well described. The monthly averages of the three years' data recorded and monthly were plotted to analyse the pattern of monthly rainfall amounts in the basin (Figure 3.3).

#### 3.4.1.2 Groundwater monitoring network

Existing groundwater data on the monitoring wells were used as baseline information for the groundwater monitoring study (Figure 3.9). The wells were drilled to a depth of 60 m below the water table at a diameter of 250 mm and fitted with 125 mm / 144 mm PVC screen and casing. The screen extended from 6 m above the water table to the bottom of the borehole and the annulus was backfilled with sand. Water table fluctuations were measured using the monitoring wells and shallow piezometers drilled within the vicinity of the wetland.

Groundwater data were obtained from pumping tests carried out on monitoring wells. Data gathered from the monitoring wells was used to observe water table gradients and fluctuations. Other private boreholes drilled in the vicinity of the wetland had been mechanized for the purpose of water supply. However, there was not much information on well construction profile on these wells especially on the thickness of weathered zone or depth to bedrock screen length and saturation thickness, extent of gravel packing if any, and depth to which top of well was sealed. The readily available data were those on depth, yield, static and dynamic water level.

A monitoring network consisting of 12 shallow manually drilled piezometers approximately 20 feet (2-6 m) was set up for this study. The holes were drilled using a hand auger with a diameter of 10 cm and installed with PVC pipes of the same diameter. The end of the PVC pipes was capped and perforated to allow the flow of water from the ground into the pipes. The other end of the piezometer was covered with nets to prevent insects and flying objects from falling inside and clogging the pipes. Upon completion of piezometer construction, relative elevation from the top of each casing was measured to the nearest centimeter. All piezometers were constructed using

standard installation procedure from Sprecher (2008). The piezometers correspond to three rows perpendicular to the coastline; the first row (SP-1, SP-2 and SP-3) located at the south of the wetland, two rows (SP-4, SP-5, SP-6) and (SP7 and SP8) at the middle of the wetland and a third row (SP-9, SP-10, SP-11 and SP-12) at the north of the wetland.

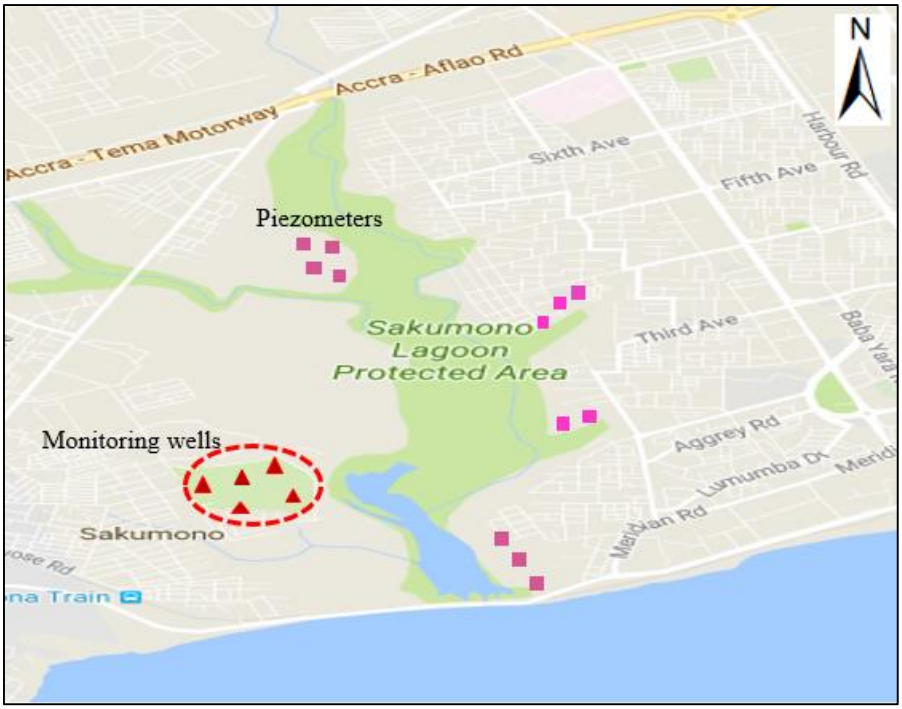


**Figure 3.8: Location of the monitoring wells in the study area**

The piezometers were installed 6 m apart according to the terrain of the site (Figure 3.8). The distance of the first piezometer from the wetland varied from each sampling point due to the landscape of the area. Static water level of the monitoring wells and piezometers were monitored using an electronic dip meter. The electronic dip meter consists of an LED located in the hub of the cable reel illuminates and a beeper sounds as soon as the probe gets in contacts the surface of the water in the wells. A 12 VDC peristaltic pump was used to pump water out from the piezometers for analysis.

#### 3.4.1.3 Land survey

Land survey was carried out to establish the topography of the basin. The survey was carried out from the Golf course where the monitoring wells are located relative to the elevation of the wetland. The land survey was performed for the five (5) monitoring well locations (MW 2, 4, 6, 8 and 15) in the straight line to the wetland. A theodolite was fastened to a tripod at the first monitoring well. The tripod was aligned with the wetland level and the theodolite was levelled using levelling screws. The levelling rod was positioned vertically to the wetland water level until the theodolite could be sighted and then the reading was recorded. The process was repeated at the other four monitoring wells in order to determine their elevations. The elevation at each monitoring site was determined relative to the wetland level reading.

Cross-sectional survey of the wetland was also done to describe the shape of the wetland. Cross-section measurements was done using a levelling instrument mounted on a tripod. Readings were taken at bench mark points by placing the levelling staff at selected points of the wetland. Distances were measured along the wetland at required intervals for the longitudinal section. Measurements were taken at five different points across the wetland.



#### 3.4.1.4 Aquifer hydraulic testing

A step-down and constant-rate test was conducted to obtain initial estimates of hydraulic parameters. The step-down test was first carried out to determine the optimum pumping rate at which the wells can be pumped and used in the constant rate test. The step-down test was to improve the reliability of the data collected.

A 6-hour constant rate test was conducted at a rate of 3 l/s after the step-down test. The constant rate test conducted for the current study followed the principle of hydraulic testing given by Freeze & Cherry (1979). Stress was applied to the groundwater by pumping water at the constant rate from the pumping well, and the groundwater response measured in observation wells. The wells were pumped for 3 hours and water level depth measured at intervals as the groundwater recovers for another 3 hours. Results from the pumping test were analyzed using time-drawdown curves based on the Cooper-Jacob approximation method.

#### 3.4.1.4.1 Estimation of soil hydraulic conductivity

Soil hydraulic conductivity was determined using the auger-hole method. The method was originally developed by Diserens (1934) and was modified by Kirkham (1955). The method involves boring a hole in the soil below the water table until equilibrium is reached with the surrounding groundwater. As water is removed from the hole, water seeps back into the hole again. The rate at which water rises in the hole is then measured and the hydraulic conductivity (K) of the soil calculated. The following steps were distinguished in using the auger-hole method:

1. Drilling of the holes – This has to be done with the minimum disturbance to the soil.
2. Taking water out from the holes – This start when equilibrium is reached with the surrounding groundwater and the depth of the water table is recorded.
3. Measuring the rate of water rise in the holes – The measurement consists of the rate at which the water rises in the hole. The observations are made either with a constant time interval (Δt) or with fixed intervals for the rise of the water (Δy), depending on the equipment available.
4. Estimation of the soil hydraulic conductivity – The equation by Ernst & Westerhof (1950) is applied to homogeneous soil as given in Eq. 3.1:

$$K = \frac{4000 \times r \times \Delta y}{\left(\frac{H}{r} + 20\right)\left(2 - \frac{y}{H}\right) y \times \Delta t} \qquad (3.1)$$



Where:

K= Hydraulic conductivity (m/day)

H= Depth of hole below the water table (cm)

y= Distance (cm) between the water level in the hole and the surrounding groundwater level for a time interval Δt(s)

the water in the hole for the time interval

S= Depth (cm) of the impermeable layer below the bottom of the hole or

the layer

### 3.4.1.5 Hydrological measurements

A dysfunctional river gauging system at the Dzorwulu river was re-established in the basin to improve upon the hydrological data situation of the basin. Stage and discharge measurements were taken and used to calculate mean flows. The river flow measurements were taken through depth sounding with a meter and rod assembly. The number of revolution measurements was also recorded. The mean velocity at each of the measuring points in a vertical line was determined with the current meter using the two-point method.

### 3.4.1.6 Discharge computations

The velocity-area principle was used to compute discharge from current-meter data. Total discharge was determined by summation of partial discharges. A partial discharge is the product of an average point or vertical line velocity and its associated partial area as shown in Figure 3.9 a,b and expressed as in Eq. 3.2 and 3.3 (Alfa, 2010):

$$q_n = \bar{V}_n a_n \quad (3.2)$$

$$Q = \sum_1^n q_n \quad (3.3)$$



Where:

q = discharge ($m^3/s$) for a partial area

Q = total discharge ($m^3/s$)

$\bar{V}$ = mean velocity associated with the partial area

a = partial area of total cross section

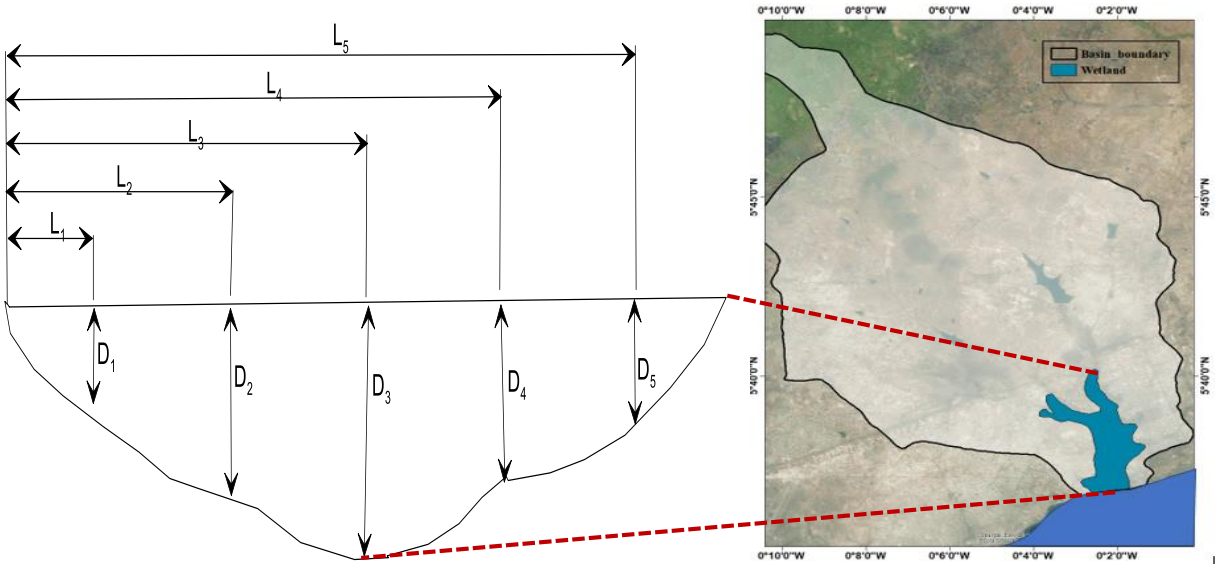


**Figure 3.9a: Calculation of discharge using simple average method using cross-section**

Where: $L_1$, $L_{2...}$ Ln= distance to vertical measurement locations in feet from an initial point to vertical station; $D_1$, $D_{...}$ Dn = the water depths in feet at verticals and n = the number of verticals related to the partial area



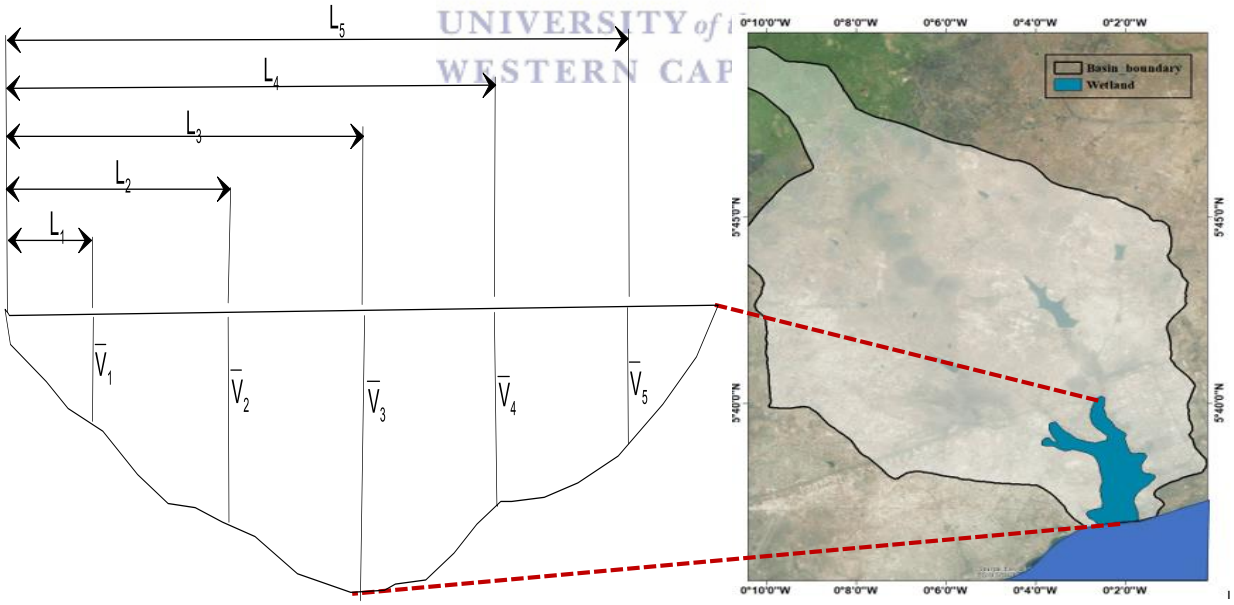


**Figure 3.9b: Calculation of discharge using the simple average method by horizontal velocity profile.** Where: $L_1$, $L_{2...}$ Ln= distance to vertical measurement locations in feet from an initial point to vertical station; $\bar{V}_1$ $\bar{V}_2 \ldots \bar{V}_n$ =the respective mean velocities in feet per second at vertical measurement stations.

#### 3.4.1.7 Outflow to the Atlantic Ocean

Seepage along the two narrow culverts of the Sakumo wetland was calculated using the Dupuit's equation (Fetter, 2001). Assuming a horizontal flow of water from the wetland to the Atlantic Ocean is given by Eq. 3.4:

$$q = \frac{K(h_0^2 - h_1^2)}{2x} \quad (3.4)$$

Where:

q= discharge rate along the narrow culverts per unit width of coastline ($m^2$/day)

K= mean hydraulic conductivity of the underlying groundwater (m/day)

ho = hydraulic head elevation of the wetland water

h1 = hydraulic head at the coastline

The discharge face was estimated along the coastline as straight-line distance from the mouth of the wetland using ArcMap 10.2. The product of the length of the seepage face and the seepage rate was used to quantify the volume of water that seeps across the culverts to the Ocean.



### 3.4.2 Surface Water Network

Surface water bodies in the Sakumo basin were identified and sampled. These included, the Sakumo wetland, Mamahuma and Onukpawahe streams, the Dzorwulu River, the University Farms Dam and the Lebanon Dam. The sampling points were selected based on the criteria that, they were near urban, domestic and/or industrial discharge points, agricultural areas, places of tourism activities and estuarine region.

#### 3.4.2.1 Sampling groundwater and wetland for water quality analysis

Prior to well water sampling, the monitoring wells and piezometers were pumped for five minutes to purge them of stagnant water so that fresh water was sampled for the analysis. The wells and piezometers were considered purged once key water quality parameters (pH±0.1, EC ±5 % and temperature ±0.2 $^oC$) was stabilized.

The wetland and stream water samples were collected from 0.5 m below the surface of the water using a manual collector mounted on a pole. At each sampling point, two samples were collected for anion and cation analysis. The samples were collected into 500 mL pre-conditioned high-

density linear polyethylene (HPDE) bottles to avoid unpredictable changes in sample characteristic (APHA, 2008). Each sample bottle was rinsed with the sampling water before finally taking the samples. Samples for anion analysis were field filtered using 0.45 µm filter paper whiles samples for cation analysis were unfiltered and acidified with 65 % trace metal-grade nitric acid solution to a pH <2 to preserve the metals until chemical analysis was performed. All field equipment were decontaminated using 0.3% Decon-90 solution and deionized water and calibrated when appropriate to manufacturer's specifications prior to the start of the sampling campaign. Temperature, pH, EC, DO and alkalinity were measured in-situ.

Water samples for environmental isotopes analysis of oxygen–18 and deuterium were collected directly from the wetland and streams using a water grab sampler. Water from the piezometers and wells were first purged to get rid of stagnant water and to ensure that, the sampled water had minimal contact with the atmosphere. The water was pumped into a bucket and collected into 60 mL polyethylene bottles and tightly sealed devoid of air to prevent fractionation of samples. Rain water was sampled on an event-based from a rain gauge installed in the vicinity of the wetland. The rain gauge was made of a large Teflon funnel attached to a sterile 500 mL HDPE bottle.



#### 3.4.2.2 Measurement of field parameters

Air and water temperatures were measured using a mercury-in-glass thermometer. For air temperature, the thermometer was held up right in the air with the lower part exposed to the air for about four to five minutes. For water temperature, the thermometer was immersed below the water surface and left to stabilize for about five minutes. The average values for air and water temperatures were recorded in degrees centigrade (°C). Prior to the measurement, the instrument was calibrated using a standardized temperature 0.0–60 °C.

pH of water samples was measured using HANNA digital pH meter. The pH meter measurements range from 0.00 to 14.00, resolution 0.01 pH, accuracy ±0.05. The pH meter was standardized using pH 4.0, 7.0 and 9.0 buffer solutions. Once standardized, the combination sample/reference pH probe is stored in a receptacle of deionized water. After use, the probe is rinsed with distilled water dipped in pH 4.0 buffer and replaced in its protective cover

Electrical conductivity and salinity was measured using HANNA Combo handheld tester. The instrument was standardized against standard conductivity solution of conductivity 0-3999 µS/cm, resolution 1 µS/cm, accuracy ±2% F.S. The results EC are reported in micro-Seimens/cm.

Dissolved oxygen was determined volumetrically. Oxygen present in the water sample was made to react with Mn(OH) and precipitated as hydrated oxide after adding NaOH and KI as indicators. Manganese reverts to the divalent state and liberates iodine from added KI which is equivalent to the original DO present as given in Eq 3.5 and 3.6.

$$Mn^{2+}{}_{(aq)} \rightarrow Mn(OH)_2O \quad (3.5)$$

$$4Mn(OH)_2 + O_2 \rightarrow 4MnO(OH) + 2H_2O \quad (3.6)$$

The liberated iodine was titrated against sodium thiosulphate solution ($Na_2S_2O_3$) using starch as indicator as shown in Eq 3.7:

$$2S2O_3^{2-} + 3I^- \quad (3.7)$$

From equation 3.6, 3.7, and 3.8 the mole ratio of $O_2$ to $S_2O_3^{2-}$ (1:4) is determined and the mg/L of dissolved oxygen in the water samples is calculated.

Alkalinity was measured as bicarbonate ($HCO_3^-$) in the field using a digital micro titrator. The water sample was titrated against standardized hydrochloric acid (HCl) (0.02N) using methyl orange as the indicator. The alkalinity results were expressed as mg/L as $CaCO_3$.



### 3.4.2.3 Laboratory Analysis of major ions and trace metals

#### 3.4.2.3.1 Calcium and Magnesium

For calcium determination, 1 ml of the water sample was added to 99 ml of distilled water. 2 ml of NaOH was added to the resultant solution and a drop of murexide indicator added. The solution was titrated against EDTA and the calcium and magnesium concentrations were estimated using Eq. 3.8 to 3.10:

Calcium in mg/L = Calcium hardness x 0.4 (3.8)

Magnesium in mg/L = Magnesium hardness x 0.243 (3.9)

Magnesium hardness = Total hardness-Calcium hardness (3.10)

#### 3.4.2.3.2 Sodium and Potassium

Sodium and potassium were measured using a flame photometer. A photocell and the corresponding wavelength were chosen and the lit width adjusted. Blank solution and standard sodium and potassium calibration solutions were prepared and the instrument re-set for analysis.

#### 3.4.2.3.3 Chloride

Argentometric titration was used to measure the chloride ions in the water samples. A volume of water sample was measured and one drop of potassium chromate was added as an indicator. The solution was titrated against standardized $AgNO_3$ solution (0.0282N) as shown in Eq. 3.11.

$$Cl^-_{(aq)} + AgNO_{3(aq)} \rightarrow AgCl_{(s)} + NO_3^-{}_{(aq)} \quad (3.11)$$

#### 3.4.2.3.4 Sulphate

Sulphate concentrations in the water samples was measured using Nephelometric method. The method uses barium chloride in an acid medium to precipitate the sulphate ions. The absorbance of the sulphate ions was measured with UV–spectrophotometer and the sulphate concentration calculated as in Eq.3.12 and 3.13:



$$mg/L\ SO_4^{2-} = mg\ SO_4^{2-} X\ 1000 / mL \quad (3.12)$$

$$SO_4^{2-}{}_{(aq)} + BaCl_2 \rightarrow BaSO_{4(s)} + 2Cl^-_{(aq)} \quad (3.13)$$

#### 3.4.2.3.5 Phosphate-phosphorous

Phosphate-$PO_4^{3-}$ was measured using Ammonium molybdate method. $PO_4^{3-}$ in the water samples is made to react with ammonium molybdate to form molybdophosphoric acid. The acid is reduced to molybdenum blue by the addition of stannous chloride. The absorbance of the solution was measured using the UV-spectrophotometer at a selected wavelength and reported as mg/L of $PO_4^{3-}$

#### 3.4.2.3.6 Nitrate-nitrogen

Nitrate, $NO_3^-$ in the water samples was measured using cadmium reduction method. The water samples were passed through a column containing amalgamated cadmium fillings. The cadmium fillings reduce nitrate in the water to nitrite. The nitrite produced was measured by diazotizing

with sulphanilamide and coupling with N (1-Naphthy1) ethyl diamine to form a highly colored azo dye which was measured colorimetrically using UV-Visible spectrophotometer at a selected wavelength.

#### 3.4.2.3.7 Trace metals

Water samples were analyzed for trace metal concentration using VARIAN AA 240FS Flame Atomic Absorption Spectrometer. To ensure the reliability of the analytical method, standard reference solutions were used to calibrate the equipment. Sample blanks were prepared and digested along with each set of samples and analysed for trace metals using the same procedure.

### 3.4.2.4 Laboratory analysis of environmental isotopes

Environmental isotopes of water, $^{18}O$ and $^{2}H$ were measured using a DLT–100 Liquid water Isotope Analyzer (Los Gatos research Inc. Mountain View, CA, USA) at the national Nuclear Research Institute in Ghana. Each sample was analysed six times with the first two being discarded and the last four (4) averaged. Working standard waters calibrated against IAEA reference waters (Vienna Standard Mean Ocean water-2 (VSMOW2), Greenland Ice Sheet precipitation (GISP) and Standard light Antarctic precitation-2 (SLAP2) were interspaced with the samples for calibration. Data were normalized following Copen (1988) and expressed as $\delta^{18}O$ and $\delta^{2}H$ per mil (‰) relative to V-SMOW. The analytical precision was 0.04 ‰ for $\delta\,^{18}O$ and 0.3‰ $\delta^{2}H$ as was given in equation 2.9 and 2.10 respectively. Event based rainfall environmental isotopes values were converted to monthly and annual rainfall weighted delta-values (delta p) using (Guan *et al.*, 2013) (Eq. 3.14)

$$\delta p = \frac{\sum_{i=1}^{n} \delta \text{ X P}i}{\sum_{i=1}^{n} Pi} \qquad (3.14)$$

## 3.5 Data Analysis methods

Historic and field data collected such as water level, physiochemical parameters, pumping test data and flow measurement was first processed in Microsoft Excel. The processed data in excel was applied to the selected tools and software for analysis. Jacob (1944) and the Neuman's curve fitting analytical flow model were used to estimate the aquifer parameters of the pumping test results.

Theis (1935) solution was applied in some cases because the aquifer is assumed to be homogeneous, isotropic, uniformly thick and of infinite areal extent.

The Aqua-test and AQUTESOLV software packages were applied in estimating the aquifer parameters. Aqua-test software package provides a comprehensive set of solutions such as Theis analytical flow model, Stallman's and Strelsova's curve fitting method for the analysis of different types of hydraulic tests such as step-down pumping and the constant rate test. AQUTESOLV also provide comprehensive sets of solutions such as Neuman's curve fitting for unconfined aquifers, Huntush method for leaky aquifers, and Theis for confined aquifers for the analysis of different types of hydraulic tests such single well tests, constant rate test, step-down tests and variable rate tests.

For each well, displacement-time graph was drawn and Cooper and Jacob's method employed to determine aquifer transmissivity (T) and storativity (S) using the Eq. 3.15 in the AQTESOLV software.

$$T = \frac{2.303Q}{4\pi\Delta s} \quad (3.15)$$



Where:

T = Transmissivity

Q = discharge and

Δs= Change in drawdown taken over one log cycle

The aquifer thickness b was estimated from the well construction borehole logs and water level data for the five wells reported to be successful by deducting the aquifer top screen level from the bottom level of the well. The only exceptions to this aquifer thickness determination were the three wells reported to be marginal as the screen locations were not indicated on the borehole logs. Knowing the thickness of the aquifer, the hydraulic conductivity (K) was calculated as given in Eq. 3.16.

$$K = \frac{T}{b} \quad (3.16)$$

Where, b = aquifer thickness

The water table depth in the basin was interpolated using the kriging tool in Surfer 11 (Golden Software, Golden, Co. USA). Groundwater levels including monitoring well, boreholes and piezometers, and wetland water level data were used to map the water table elevation and determine the direction of hydraulic gradients. The water table elevation was then subtracted from the elevation to give the water table depth below ground surface. These maps were used to interpret where the water table resided in soil layer.

The physicochemical (e.g. pH, EC, $Cl^-$, $NO_2^-$, $SO_4^{2-}$, $HCO_3^-$, $Na^+$, $K^+$, $Ca^{2+}$ and $Mg^{2+}$) and environmental isotopes data were first analyzed in Microsoft excel using the data analyst tool. Descriptive statistics (minimum, maximum, median, mean, standard deviation) was used to characterise the groundwater and surface water composition for the study duration for the water chemical and isotope data. Frequency distributions and deviation from normal distribution were analysed through a Kolmogorov–Smirnov Test (IBM SPSS Statistics 23). A Levene's Test was applied on untransformed data to determine the homogeneity of variance. The results showed that, the data were not normally distributed which is common for groundwater data (Helsel & Hirsch, 1992) and no general homogeneity of variance was observed. Hence, non-parametric tests were applied for further statistical analysis. The analyzed data was plotted using various graphical tools such as bivariate plots, hierarchical cluster analysis (HCA) and principal components analysis (PCA). A mass balance method was used to determine the water balance.



### 3.5.1 Water fluxes estimation

Water fluxes was quantified using Darcy's Law which involves determination of hydraulic gradient and hydraulic conductivity. Darcy flux also known as Darcy velocity is computed by multiplying hydraulic gradient with hydraulic conductivity. Darcy Law is the standard way of formulating groundwater-surface water fluxes exchange mechanisms in most standard groundwater models. The actual water velocity between any two points is computed by dividing the Darcy velocity by porosity. The rate of groundwater discharged into a surface water body that is, the wetland can be calculated using Darcy's Law as given in Eq. 3.17:

$$Q = T\ i\ 2L \quad (3.17)$$

Where:

Q = rate at which water flows from stream to groundwater ($L^3/T$)

T = transmissivity ($L^2/T$)

i = hydraulic gradient between groundwater and wetland

L = length over which discharge is calculated (L)

In a similar way, the rate of surface water discharged into the underlying groundwater can be calculated using Darcy's Law as given in Eq 3.18:

$$Q = K\ L\ W\ I \tag{3.18}$$

Where:

Q = rate at which water flows from wetland to the aquifer ($L^3/T$)

K = vertical hydraulic conductivity of stream bed (L/T)

L = length over which discharge is calculated (L)

W = width of wetland over which discharge is calculated

i = hydraulic gradient between the wetland and the aquifer

The hydraulic gradient (i) between the wetland and the underlying aquifer can be determined as in Eq. 3.19:

$$i = \frac{(h_{aquifer} - h_{wetland})}{M} \tag{3.19}$$

Where:

h*groundwater* = hydraulic head of the underlying aquifer (mamsl)

h*wetland* = hydraulic head of wetland (mamsl)

M = thickness of stream bed (L)

#### 3.5.1.1 Estimation of wetland water balance

Application of the water balance approach included quantifying the inputs and outputs of water and storage in the wetland. A steady state equation was applied to calculate the water balance of the wetland. The major input and output of water in the wetland are rainfall and evaporation respectively. Water balance for the wetland was estimated using a simplified open-lake water-balance model (Kedebe *et al.*, 2006) as given in Eq. 3.20 to 3.22:

Storage = Inputs – Outputs (3.20)

$$\Delta H = P(t) + E(t) + \left[\frac{R_{in}(t) + R_{out}(t) + G_{net}(t)}{A(h)}\right] + \varepsilon_t \quad (3.21)$$

Where:

H = water level of the wetland (mm),

A = surface area of the wetland (mm),

P =rate of rainfall over the basin (mm/day),

E = evaporation (mm/day),

t = time,

R*in* and R*out*=surface water inflow and outflow (mm/day),

G*net* =net groundwater flux (mm/day) and Hence,

$$\frac{\Delta_v}{\Delta_t} = G_i + S_i + P - G_o - S_o - ET = 0 \quad (3.22)$$

Where:

$\frac{\Delta_v}{\Delta_t}$ = Change in wetland volume over time (t)

P = Precipitation inflow volume

Gi and Si= volume of groundwater and surface water inflow

Go and So = volume of groundwater and surface water outflow

ET= Evapotranspiration



### 3.5.1.2 Estimation of recharge

Groundwater recharge is an important hydrological parameter that is normally estimated at a variety of spatial and temporal scales (Sophocleous & Perry, 1985). Recharge was estimated using a modified version of Chaturvedi (1973) for tropical regions based on the water level fluctuation and rainfall depth (Misstear *et al.,* 2009; Allen *et al*., 1998). The equation is given in Eq. 3.23:

$$R = 1.35(P - 14)^{0.5} \quad (3.23)$$

Where:

R= net recharge due to precipitation in (mm), and

P = precipitation in millimeters (mm).

The recharge coefficient is defined as the ratio of recharge to effective rainfall and is expressed as a percentage (Muteraja 1986) and given as in Eq 3.24:

$$\text{Rcoefficient} = \frac{\text{R}}{\text{Pe}}\% \quad (3.24)$$

Where:

R= recharge

Pe= effective rainfall

### 3.5.1.3 Estimation of evapotranspiration

Reference evapotranspiration (ET) is an important parameter that needs to be estimated accurately to enhance its utilization in numerous applications. Although the widely-recommended procedure for calculating ET involves using the FAO Penman-Monteith equation (ETo). The latter's effectiveness is constrained by its considerable large data requirements. To overcome this constraint, alternative methods using limited available data have been explored.

The Hargreaves method (Hargreaves & Samani, 1985) was used to estimate potential evapotranspiration for the study area. The method uses daily weather minimum and maximum air temperature for the estimation. The Hargreaves and method is given as in Eq. 3.25:



$$\text{E} = 0.0135.\,\text{K}_{\text{Rs}}.\,\text{R}_{\text{a}}\sqrt{\text{T}_{\text{Max}} - \text{T}_{\text{Min}}}.\,(\text{T}_{\text{a}} + 17.8) \quad (3.25)$$

Where:

Ra = Extra-terrestrial radiation ($mmd^{-1}$)

0.0135 = Conversion factor,

$K_{RS}$ =Radiation adjustment coefficient.

In the modified version of Hargreaves and Samani equation the value $K_{RS}$ = 0.17 is used.

### 3.5.2 Hydrochemical data analysis

Water samples were taken to water research institute (WRI) of the Council for Scientific and Industrial Research (CSIR). Preservation of samples and estimation of various water quality parameters were done as per standard procedures reported in APHA (APHA, 2012). Water samples were analyzed at Water Research Institute of CSIR in Ghana. All samples were analyzed in accordance with standard procedures for analyzing water and wastewaters and are ISO/IEC 17025

certified. Major cations analysis was done using Inductive Coupled Plasma Optic Emission Spectroscopy and anions using Ion Chromatography.

### 3.5.2.1 Major ions chemistry

The major ion chemistry of the groundwater and wetland water was used to provide a proper description of the hydrochemical characteristics of the water in the Sakumo basin. The major ions chemistry was also used to determine the physical and chemical processes resulting in the current ionic composition of the water (Jessen *et al.*, 2014). Hence major ions were used to define the characteristics of the water and determine the hydrogeochemical process that influenced the water chemistry. To understand and differentiate the influences of precipitation, evaporation and water-soil (water-rock) interaction on the water chemistry, scatter diagrams of EC against the major ions such as EC vs. Cl, EC vs. $Cl^{-}$/ ($Cl^{-}$ +$HCO_3$), $Na^{+}$–$Cl^{-}$ and ($Ca^{2+}$+$Mg^{2+}$)–($HCO_3^{-}$ + $SO_4^{2-}$) as suggested by Gibbs (1970). The dissolution of halite (NaCl) as a possible contributing factor to $Na^{+}$ and $Cl^{-}$ ions in the water samples was determined using the $Na^{+}$ vs. $Cl^{-}$, Na/Cl vs Cl scatter diagrams. Furthermore, probable influence from anthropogenic activities on the water chemistry can be determined using the $Cl^{-}$ vs. $SO_4^{2-}$ scatter diagram.



To further understand reverse ion exchange as the possible reason for the calcium dominance in some of the groundwater samples, Na/Cl ration can be used. The $Ca^{2+}$ vs. $SO_4^{2-}$ scatter plots can also be used to determine the possible contribution of gypsum and/or anhydrite in the $SO_4^{2-}$ and $Ca^{2+}$ concentrations (Glover *et al*., 2012). ($Ca^{2+}$ + $Mg^{2+}$) vs. ($HCO_3^{-}$ +$SO_4^{2-}$) can be used to deduce influence of silicate weathering process. The influence of silicate weathering on the groundwater samples can be deduced using the relationships between $Na^{+}$+$K^{+}$, $Ca^{2+}$+$Mg^{2+}$ and Total Cations (TZ) and the meq/L ratios of these cations to the total cations (Carol *et al*., 2010). To further understand the type of ion exchange taking place, $Ca^{2+}$ +$Mg^{2+}$ vs. $SO_4^{2-}$ + $HCO_3^{-}$ and $Ca^{2+}$+$Mg^{2+}$ vs. $Na^{+}$ scatter diagrams can be used.

### 3.5.2.2 Hydrochemical facies

Graphical methods such as the piper, stiff and expanded durov diagrams were used to determine the major water types and the hydrochemical and environmental processes controlling the water chemistry. In the piper diagram, cations and anions for each sample are first plotted separately in

the ternary plots and both projected onto the diamond shape. The diamond shape plot has six main water types each describing the composition of the water type. The interpretation of the water type is based on the area the water falls on the diamond shape. Water samples with similar chemical composition projects to the same area of the diamond shape whiles water with different chemical composition would lie in different areas of the diamond (Figure 3.10). Hydrochemical parameters and environmental isotope data were also used to infer the origin and movement of the water in the basin. Interpretation of the graphical diagrams relied on a simple mass balance approach based on reaction stoichiometry.

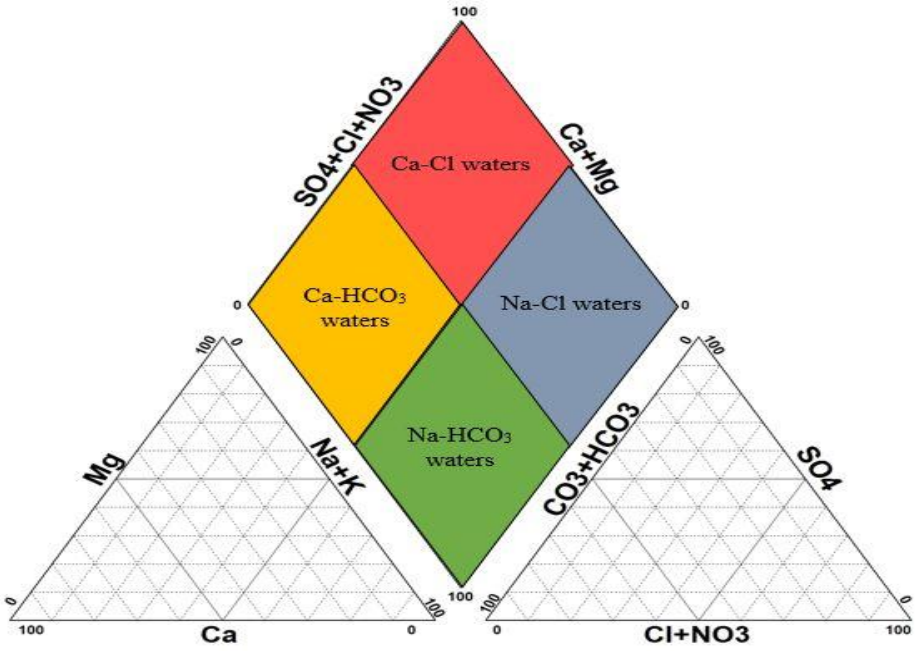


**Figure 3.10: Characterizing water type using the Piper diagram**

The expanded Durov diagram is used to analyze hydrochemical data. The Durov diagram consists of two ternary diagrams each representing a plot of the anions against cations. The results are the total of the cations and anions concentrations on the two ternary sides. In order to give more detailed comparison, the ternary diagrams were modified to include pH and EC hence the name expanded Durov diagram. In the expanded Durov diagram, similar ratio techniques are used to plot major ions concentrations. The diagram has a total of six triangular diagrams: three each for cations and anions. The sum of the ions on each diagram add ups to 50% and the ions combined differently.

Stiff diagrams provide a visual summary of ionic composition of each water sample at one location. Stiff diagrams plot the major-ion composition of a water to produce a figure with a shape representative of the relative proportions of the different ions and a size indicative of total ion concentration. The stiff diagram is a polygon created from three parallel horizontal axes extending on either side of a vertical zero axis. Cations are plotted to the left of the axis and anions to the right, in units of milliequivalents per litre (meq/L) (Guler *et al.*, 2002). The Stiff diagram allows a visual comparison of waters with different characteristics. Since the pattern tends to maintain its shape upon concentration or dilution and also allows the tracing of flow paths. The Stiff diagram is particularly useful for comparing results from many samples in combination with a multivariate statistical analysis. In the current study, piper, expanded durov and stiff diagrams were used to characterize the water types in the Sakumo basin.

#### 3.5.2.3 Multivariate analysis



Multivariate statistical techniques such as correlation coefficient, cluster analysis (CA) and principal component analysis (PCA) were used for further classification and characterization of the water types based on a wide variety of measured parameters. Correlation analysis was used to describe the relationship between two measured variables based on their quantitative strength. (Venkatramanan *et al*., 2013). This relation or association of the variables is represented by the correlation coefficient (r). A correlation coefficient of or near 1 or -1 showed strong relationship between the two variables, whiles a correlation coefficient of or near zero suggests that, there is no relationship between the variables (Ha & Ha, 2011). A positive r value, indicates a direct relationship between variables and a negative r value indicates an inverse relationship (Salvendy, 2012). Parameters with correlation coefficient showing r $\geq$0.7 were considered as strongly correlated and *r* ranging between 0.5 and 0.7, were considered as moderately correlated (Venkatramanan *et al*., 2013). The measured physico chemical parameters such as Temperature, EC, pH, $Ca^{2+}$, $Mg^{2+}$, $Na^{+}$, $K^{+}$, $Cl^{-}$, $SO_4^{2-}$, $HCO_3^{-}$, $NO_3^{-}$ and the trace metals of the groundwater and wetland water samples were analyzed using the Pearson correlation coefficient using a two-tailed test of significance in IBM SPSS Statistics 23.

Principal component analysis was achieved by transforming the data set to a new set of variables which are uncorrelated but ordered so that, the first few variables maintain the original variables.

Hence, to eliminate biasness by any parameter of different units with high concentration and renders the data dimensionless, standardization (*z* scale) was made on each physicochemical parameter prior to the analysis. The principal components loadings were generated in a sequentially manner with decreasing contributions to the variance, that is, the first principal component (PC1) explains most of the variations present in the original data, and subsequent principal components accounted for decreased proportions of the variance (Vieira *et al.*, 2012). The classification by Liu *et al*., (2003) was applied to principal components corresponding to absolute loading values >0.75, 0.75–0.50 and 0.50–0.30 as strong, moderate and weak loadings respectively.

Cluster analysis (CA) was used to group the measured physicochemical parameters into clusters based on their similarity or dissimilarities on the measured field. Cluster analysis was performed in IBM SPSS Statistics 23 and the agglomerate algorithm method was used. At each step, clustering was formed and merged to reduce the number of clusters by grouping the most similar parameters until only one cluster is left containing all the clusters (Templ *et al*., 2008). The Wards method was selected for the clustering. The Ward's method uses the variance approach to evaluate the distances between clusters (Krishna *et al*., 2012). The constituents of each cluster were assessed by calculating the sum of squared deviations from the mean of the cluster. The common approach used during clustering is Hierarchical Agglomerative Clustering Analysis (HACA), which provides intuitive similarity relationships between one sample and the entire data set and is illustrated by a dendrogram (Ketchen & Shook, 1996). In the current study, HACA was performed on the normalized dataset by means of the Ward's method, using Euclidean distances as a measure of similarity. Sampling sites with similar physicochemical characteristics and relationships were clustered together at low linkage distances, whilst samples with varied characteristics were linked at higher distances.

In the current study, correlation coefficient, principal component and cluster analysis were used to understand the factors that dominate the control of groundwater and wetland water chemistry in the Sakumo basin. In addition, since clustering groups similar data together, the use of cluster analysis is expected to indicate possible interaction between the wetland and the underlying groundwater.

#### 3.5.2.4 Spatial distribution maps

Spatial distribution maps were used to show the distribution of the major ions and trace metals in the basin. Spatial data were prepared in ArcMap using the Spatial Analyst extension of ArcGIS 10.2 from ESRI. All the sampling points coordinates were imported into ArcMap using the latitude and longitude coordinates and projected using the WGS_1984_UTM_Zone_34S projected coordinate system. The spatial distribution of measured physicochemical parameters such as EC, $Ca^{2+}$, $Mg^{2+}$, $Na^{+}$, $K^{+}$, Cl, $SO_4^{2-}$, $HCO_3^{-}$, $NO_3^{-}$ and trace metals were displayed using Inverse Distance Weighted (IDW) interpolation method. The IDW Interpolation method was used to extrapolate concentrations in areas where no measurements were available. This method of extrapolation is based on Tobler's First Law of Geography which states that, "Everything is related to everything else, but near things are more related than distant things" (Tobler, 1969). The concentrations of the measured parameters were displayed using the reclassification method of the interpolated parameters.


## 3.6 Reliability and validity of data

The aim of this section is to provide the steps taken during data collection and analysis in order to ensure that, the data produced representative, complete, accurate, reliable and relevant to the objectives of the present study. Duplicate groundwater level measurements were taken from monitoring wells and boreholes to ensure difference between measurements were less than 0.01. Clean, sterile sampling high-density polyethylene (HDPE) bottles were used to collect ground and surface water samples and powdered free nitrile hand gloves were worn during sampling, sample preparation and sample analysis to prevent contamination. To minimize the introduction of contaminants during sample collection, preparation, storage and analysis, field and procedural blanks were collected. Field blank is deionized filled in a sampling bottle under field conditions sealed, stored, transported with the other samples and analyzed along with the other field samples. Quality control measures in the collected water samples also included the use of duplicate samples and spiked samples. Duplicate and spiked water samples were collected randomly from selected sampling sites for all chemical parameters during sampling. A water sample is spiked with known concentrations of selected parameters and submitted together with other water samples for

analysis. Corrective action procedures were applied where the field blanks and spiked samples exceed the set quality control limit.

The chemical quality of the groundwater data analysis in the present study was verified by applying the principle of electroneutrality (Younger, 2007). The principle states that, the sum of positive and negative charges within the water must balance to zero. In accordance with Güler (2010), a limit of ±5% charge balance was used in the current study in order to obtain a good spatial coverage and data reliability of the groundwater samples. Water samples with negative charge balance error indicated higher proportions of anions than cations and vice versa The charge balance error was calculated based on the mathematical equation by Freeze & Cherry (1979) as stated in Eq. 3.26:

$$\%\text{Charge Balance Error (CBE)} = \frac{\sum \text{Z}\, x\, \text{M}c - \sum \text{Z}\, x\, \text{M}a}{\sum \text{Z}\, x\, \text{M}c + \sum \text{Z}\, x\, \text{M}a}\ X\ 100 \qquad (3.26)$$

Where:

Z = absolute value of the ionic valence

$M_c$ = molarity of the cations

$M_a$ = molarity of the anions

No data was rejected as the deviations were within ±5%, range.



## 3.7 Statements on research integrity

For the current study, there were no data collected and analyzed that required technical, legal and ethical consideration.

## 3.8 Study limitations

The study experienced some challenges in carrying out the research. Firstly, resources were inadequate. For example, the research required drilling of atleast two deep piezometers at approximately 60 m depth within the brackish wetland and six shallow piezometers at 10 m depth within the floodplain. This was not possible due to inadequate funds. This challenge was resolved by using existing monitoring wells drilled in the study area by the Council for Scientific and Industrial Research (CSIR). This study drilled 12 piezometers in the floodplain at approximately

2 m deep to compensate for the shallow unsaturated zone and also record the stratigraphic logs. Secondly, there was little literature with similar focus to the current study in the study area. Hence it was difficult to identify gaps and establish trend analysis. This study provided valuable hydrogeological information and laid the foundation for the detailed model development for the Sakumo wetland basin.

The third challenge encountered during numerical modelling, was data limitation in some areas of the basin for model prediction. The study relied on five previously drilled monitoring wells for the model prediction. This limitation was resolved by field estimation of the aquifer properties and the predictions were presented as the system's response to a fairly realistic model input parameter. An associated limitation rose from the use of the field estimated parameters. Numerous methods are available for estimating aquifer properties which the current study did not explore extensively. This study employed two methods of aquifer estimation to resolve this limitation: Theis's method and the Cooper-Jacob's method.

The fourth limitation was the inability to account for the unsaturated zone processes using the mixing calculator in estimating the groundwater–wetland interaction. Due to the very shallow nature of the installed piezometer, wetland water and ground water mixed in the alluvial aquifer, which resulted in similar chemical and isotopic characteristics of the wetland water and subsurface water in the piezometers. This resulted in underestimation of the groundwater component in the mixing equation. Last but not least, was the inability to account for unsaturated zone processes during numerical simulation of groundwater–wetland interaction. A fall in the wetland water level below the base gave a negative hydraulic head due to the negative pressure head at the base of the wetland. For example, when the wetland water level was its minimum, elevation at the bottom of the wetland was used to set the pressure head of the wetland. This underestimates the simulated hydraulic heads and the rate of flow in the wetland. Since the characteristics of clogging layer in the Sakumo wetland is not well known, the method used was considered sufficient at present. A correct representation of the physics of unsaturated subsurface water flow was used to address this challenge.

# CHAPTER 4: CONCEPTUAL FLOW AND NUMERICAL MODEL

## 4.1 Introduction

This chapter focuses on the simulation of water flow system in the Sakumo basin using groundwater flow modelling. The chapter provides details on the aquifer characteristics and input data for groundwater model (hydraulic parameter, transmissivity, storativity, porosity, flow path, flow rate); conceptual model; physical domain; groundwater flow; and numerical model (Modflow 2005), boundary and initial conditions, and model validation. Conceptualization of the hydrostratigraphy and simulation of groundwater flow in the study area is presented. The wetland and aquifer system was modelled using ModelMuse assuming steady. Groundwater recharge was estimated as a percentage of annual recharge. A trial and error was used to calibrate the model using the observed hydraulic heads and fluxes in the wetland.



## 4.2 Groundwater characteristics and their hydraulic properties

Available drilling records, geology, soil and the knowledge gain from the field studies were integrated to demarcate the hydrostratigraphic units of the study area. Water level data were used to construct a water level contour map of the study area, allowing for determination of the direction of groundwater flow and hydraulic gradients. Groundwater levels were measured manually in the monitoring wells (MW2, MW4, MW6, MW8 and MW15) from February 2014 to January 2015.

**Table 4.1: Field data of the monitoring wells located in the vicinity of the wetland**

| Well ID | Longitude | Latitude | Elevation (m) | Depth to water (m) | Well Depth (m) | Water level (m) |
|---|---|---|---|---|---|---|
| MW 2 | -0.048760 | 5.630810 | 22 | 12.19 | 61 | 9.81 |
| MW 6 | -0.049860 | 5.628220 | 27 | 12.19 | 61 | 14.81 |
| MW 15 | -0.046830 | 5.626530 | 28 | 12.4 | 61 | 15.6 |
| MW 8 | -0.049730 | 5.630810 | 22 | 6.2 | 49 | 15.8 |
| MW 4 | 0.047835 | 5.628698 | 22 | 6.2 | 42 | 15.8 |

The water level elevation ranged from less than 0.5 m near the wetland and the coast to over 3 m in the inland area. At depths between 5.5-10 m, alluvial deposits are found. The alluvium comprises of interbedded sands, silts and gravels which host the freshwater groundwater zones of wetland area. Underneath the alluvium, is a layer of weathered quartzites overlaying the quartz-schist rock. Its thickness varies from 25 to 35 m. A simplified cross-section of the stratigraphic units of basin is provided in Figure 4.1.

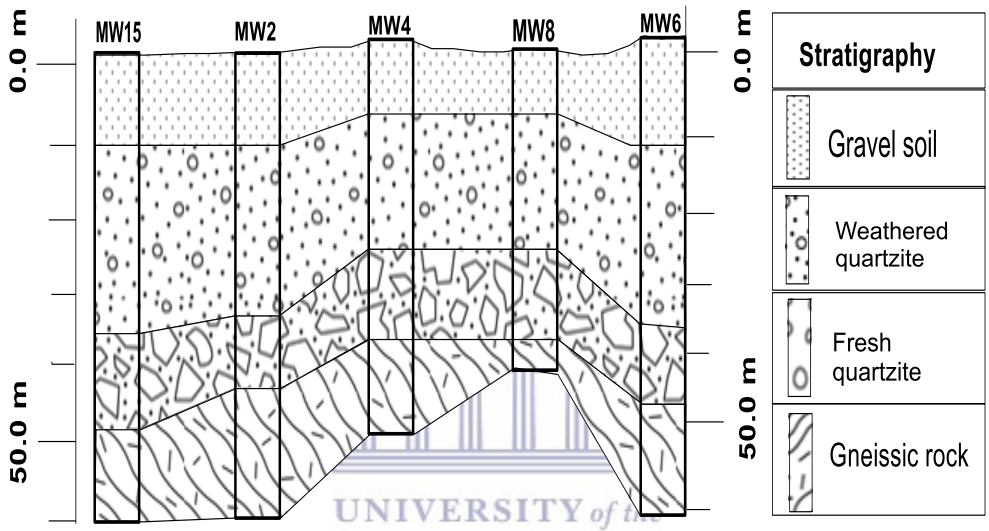




**Figure 4.1: Stratigraphy correlation in cross-section of the study area based on the lithology**

The main water bearing of the aquifer is held within porous media. The porosity and permeability of the rocks are very low (0.1 to 3%). Borehole depths ranges from 12 to 60 m with an average borehole depth of 48 m below ground level. Groundwater regimes encountered at a mean depth of 31.6 m within a range of 5.5 to 60 m. The thickness of the aquifer varied from 0.2 m to 12.5 m with a mean thickness of 3.2 m. Borehole yield varied considerably from 1.4 $m^3$/h to 2.7 $m^3$/h. Mean transmissivity is 1.8 $m^2$/day and the magnitude of the hydraulic conductivity is 0.2 m/day and the storage coefficient of the order of $10^{-5}$ (Table 4.2). The specific capacity determined from the transmissivity estimates ranged from 0.5 to 21.1 $m^3$/day/m with an average value of 5.0 m/day/m. Mean potential yield of the aquifer was estimated to be 59.5 $m^3$/day.

**Table 4.2: Hydrogeological data of the underlying aquifer in the Sakumo basin**

| Aquifer characteristics | | Dahomeyan |
|---|---|---|
| Borehole depth (m) | Range | 11.1-60.4 |
| | Mean | 37.8 |
| Depth to aquifer (m) | Range | 4.6-50 |
| | Mean | 31.6 |
| Aquifer thickness (m) | Range | 0.2-12.5 |
| | Mean | 3.2 |
| Static water level (m) | Range | 0.2-20.3 |
| | Mean | 2.4 |
| Transmissivity ($m^2$/day) | Range | 0.2-5.5 |
| | Mean | 1.8 |
| Hydraulic conductivity (m/dayx$10^{-3}$) | Range | 0.05-21.3 |
| | Mean | 5.0 |
| Specific capacity ($m^3$/day/m) | Range | 0.5-59.5 |
| | Mean | 5.0 |



The semi-log graphs in Figures 4.2 (A-D) show the residual drawdown versus time ratio plotted for recovery test data of borehole used in the research. The graphs in Figure 4.2 were used in estimating the transmissivities using the Theis method in Equation (3.16) for the individual boreholes. The aquifer thickness b was obtained through analyses of borehole logs data and the hydraulic conductivity calculated using Equation (3.17). The drawdown-time graphs show that the wells were drilled in consolidated, confined and fractured rock aquifers of the study area.

Figure 4.2 a, d (MW8 and MW15) show smooth curves which suggest that, at early times, the flow towards the well is completely through the fractures which are heavily blocked. Throughout pumping, the flow comes almost entirely from fractured storage as the contributions from micro fractures are highly negligible. The low yields encountered in Figure 4.2 d (MW15) was due to fractures that may have been blocked by clayey materials hence the domain is a heterogeneous fractured aquifer system.

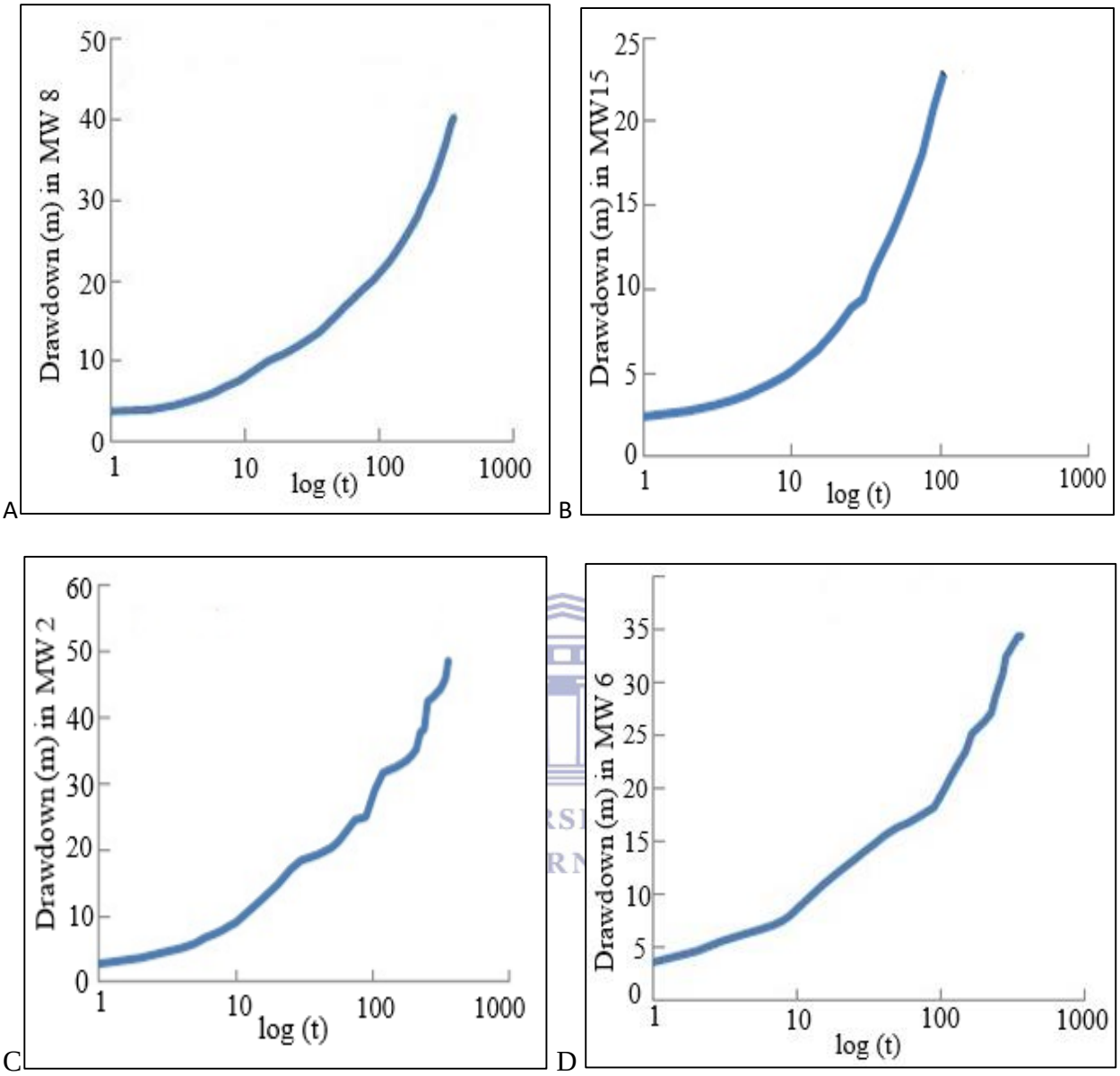


**Figure 4.2: Semi-log plots of constant-rate test data of 4 monitoring wells located in the vicinity of the Sakumo wetland**

The graphs in Figure 4.2 c, d (MW2 and MW6) showed similar trend but wavy in nature. These graphs show wells whose fracture were not blocked and the fracture density increases from MW6 and MW2. Therefore, groundwater flow also increases in that order. At early pumping times, the flow is entirely from fractured storage. The flow is then supplied minimally intermittently from micro fractures of matrix block mainly from the storage in the fracture until late time of pumping.

These are pumped wells whose fractures were not blocked and the aquifer system can be described as purely fractured with varying degrees.

## 4.3 Groundwater occurrence and flow direction

The mode of groundwater occurrence and hydraulic-head data were used to evaluate the groundwater flow direction in the catchment. Groundwater occurrence is mainly due to the existence of linear features as a result of faulting and weathering of the impermeable rocks. The hydrogeological setting the Sakumo wetland as described in Chapter 3, is composed of fractured rocks. The rocks are mainly granitic gneiss and schistose lithologies which are impermeable and have limited capacity within their matrix.

Groundwater flow is towards coast and can be understood better from the groundwater contour map. The groundwater flow direction follows the topography of the area. The river and streams carries domestic and industrial wastewater into the wetland and discharges into the sea. Average groundwater levels from the monitoring wells were used to derive the piezometric map as shown in Figure 4.3.



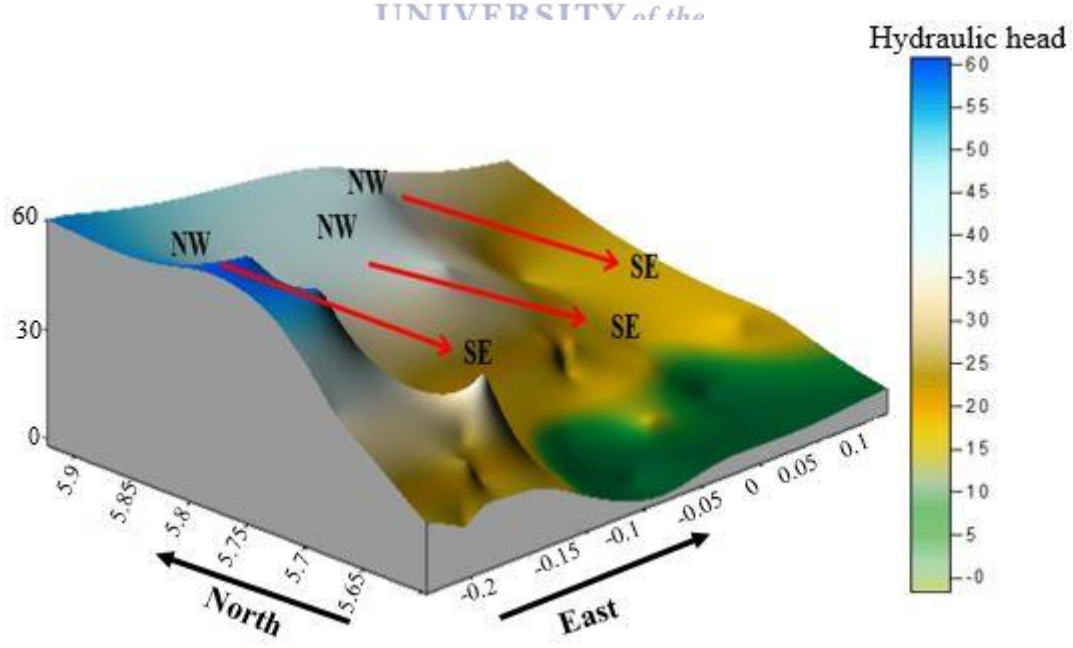


**Figure 4.3: Regional water table map of the study area**

Figure 4.3 shows that the wetland is a discharge area as groundwater converges towards the topography low point of the basin. It is demonstrated that regional groundwater flow of the groundwater is towards Northeast to southwest. Overall the hydraulic gradient is small, indicating that the regional groundwater flow is slow.

Three groundwater flow types occur in the rock formation. The groundwater regimes are unconfined, semi-confined and confined conditions. The first is the alluvial aquifer and this occur under the water table in the recent sand with depths between 2 and 4 m deep and contains meteoric water. The semi-confined aquifer occurs mainly in the red continental deposits of sand clay and gravel. The depth of this aquifer varies from 6 m to 60 m. The confined aquifer occurs in the impermeable fractured rocks. A correlation of the drill logs indicates that the main water-bearing zone of the rock has a thickness of 3 m occurring at depths between 20-25 m below ground level.

Direct precipitation falls on the surface of the aquifer over the unconsolidated soil which overlies the sandy weathered zone. The sandy soils provide the storage and permeability for rain water to percolate through the unsaturated zone to the water table. Precipitation amount and intensity is spatially uniform over the basin. Once the rainfall reaches the ground, it infiltrates through the soil and fractures on rock outcrops. Runoff from the upper (highly) catchment of the basin start immediately. The rate and amount of infiltration depends on the amount and intensity of the rainfall, the local topography and the infiltration capacity of the soil. In the basin, groundwater recharge is assumed to occur almost immediately after rainfall through fractures on rock outcrops. Delayed recharge which is the most likely and dominant system occurs when infiltration through the soil is required. In these areas recharge occurs only when the soil is completely saturated. The infiltration capacities of soils are exceeded easily in areas where the soil permeabilities are lowest or where initial water contents are high. Once groundwater recharge occurs, a corresponding rise in wetland water levels also occurs.



Groundwater flow paths through the basin generally trend northwest-southeast towards the coastline, except for saline waters that permeate landward from the sea shoreline (Figure 4.4). Two major flow systems exist in the catchment. The first, a local (water table) flow occurs within the alluvial deposits with an average thickness of 5.5 m. The hydraulic conductivity derived from this zone is 0.03 m/day and the groundwater seepage velocity is 0.01 m/day. Flows within this layer

are relatively fast and are controlled by horizontal faults which defines the nature of groundwater movement in the basin. The second known as intermediate flow, occurs in the semi-unconfined aquifer and is separated from the first by successive deposits of sandy clay to silty clay to clay layer. The semi-unconfined layer varies in thickness between 10 -25 m. The layer has a seepage velocity of 1.45 m/day and hydraulic conductivity of 0.2 m/day. A third flow, a regional flow may occur in the deep fractured rock. The confined layer is the saturated zone and occurs at a depth of between 25 and 35 m below sea level. However, there has been doubts as to whether any regional groundwater flow or movement exist within the area (Darko *et al*., 1995) and this study could not confirm this.

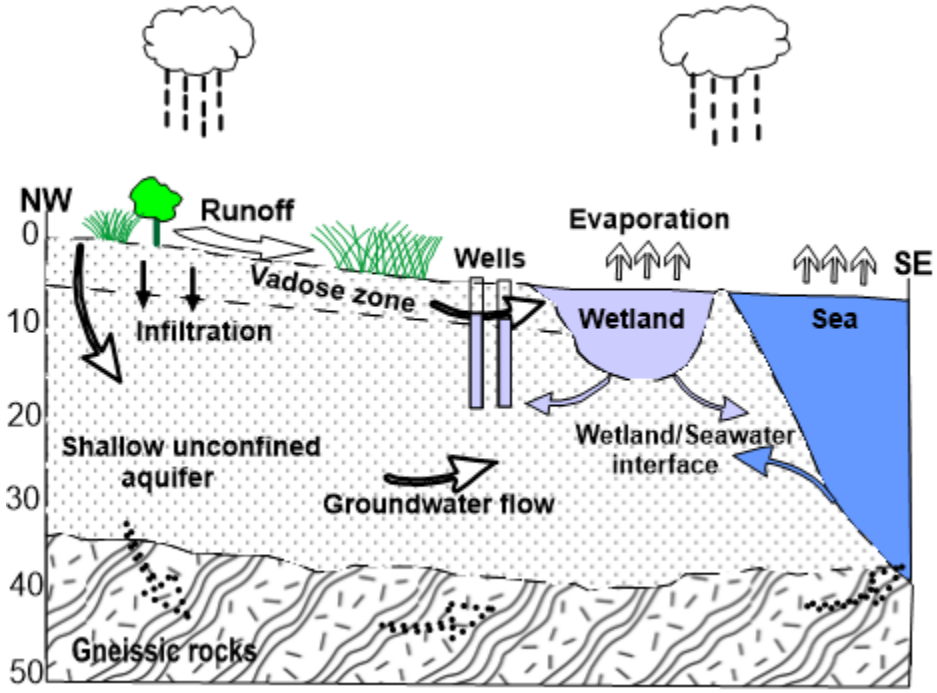


**Figure 4.4: Schematic cross-section of the groundwater flow system in the basin**

The unconfined aquifer model was run with steady state conditions and December-2008 was chosen as initial aquifer head. The output results show the groundwater flow was found to follow topography; the groundwater flow direction is predominantly from the upper sub-basin through the wetland to the coast.

## 4.4 Hydrogeological conceptual model

The conceptual framework of the wetland model is based on findings from geochemical data for the wetland and aquifer system. The thickness of the Quaternary sediments varies from several meters to less than 70 m (Atobra, 1983). The sediments generally consist of a unit of silt and clay marine sediments called the alluvium which overlays the wetland channel (Figure 4.4). The upper part of rocks is largely weathered when the sea level is low and forms a layer of weathered clay. Both the weathered clay and alluvial form the aquitard and the alluvial sediments of sand and gravel at the bottom of the Quaternary form the major confined aquifer. A simple hydrogeological section depicting the groundwater-wetland system is illustrated in Figure 4.5.

The general groundwater flow for the study area as established in section 4.2 is predominantly Northwest-Southeast. The water table elevation in the catchment changes continually in response to precipitation (P) and evapotranspiration (ET). Three main processes influences the water table depth in the aquifer system, namely recharge of groundwater from the unsaturated zone, subsurface flow that feeds the wetland and local (top-soil) flow from the lower reaches of the wetland.



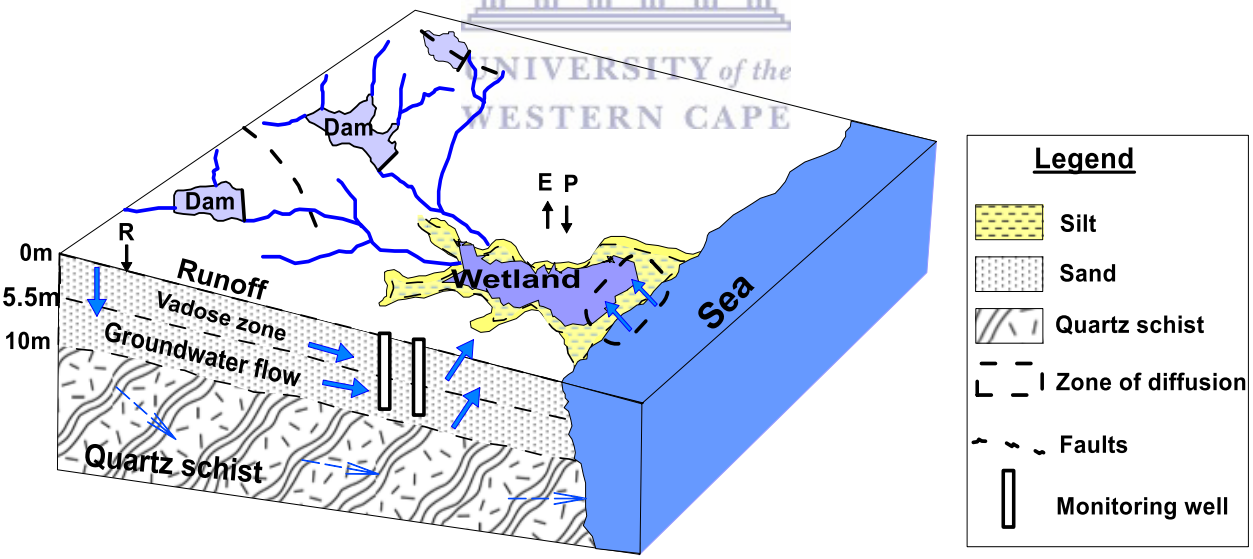


**Figure 4.5: Sketch of the hydrogeological conceptual model of the groundwater-wetland system** P: precipitation, E: evaporation, R: recharge. **Not drawn to scale**

Chemical analysis of the waters discussed in Chapter 5 indicates that, at least two major groundwater flow systems based on the measured electrical conductivities of the water. A shallow flow system located in the recent sand unit that is locally recharged at the lower reaches (top soil

layer) of the wetland and intermediate flow in the unsaturated zone recharged in the upper-middle reaches of the wetland (Figure 4.5). Electrical conductivity of groundwater from monitoring wells located within the vicinity of the wetland showed mean measured concentration of > 5000 µS/cm. The high EC of the waters which has been attributed to sea water intrusion is prove that, groundwater in the catchment has longer flow paths and travel times of the waters in the wells. EC of streams showed values lower (>1500 µS/cm) than samples from the wetland with EC values (>20,000 µS/cm). However, EC values of the Dzorwulu River and Mamahuma were consistently high (mean value of 2000 µS/cm). This may be due to anthropogenic sources given the vicinity of the township and activities of agricultural farms.

## 4.5 Numerical groundwater flow modelling

Modelling water flow is a way of evaluating groundwater resources to understand why a flow system behaves in a particular manner and used to predict flow system under different stress scenarios. Groundwater models simulate the hydraulic head and flows in a groundwater environment. There are several ways of classifying groundwater flow models, and these can either be steady state or transient and with one, two or three spatial dimensions. The steady state represents conditions where the inflows and outflows to the model are constant with time (Anderson & Woessner, 2002). Groundwater flow models have been used to solve practical problems in a wide variety of hydrogeological environments in different parts of the world (Mahmoodinobar *et al.,* 2013; Grygoruk *et al*., 2011; Ayenew *et al*., 2007; Guiguer & Molson 1996). Groundwater flow in the Sakumo wetland basin was simulated using ModelMuse (Winston, 2009), a graphical user interface for United States Geological Survey MODFLOW-2005 (Harbaugh, 2005) under steady-state conditions. The steps taken towards developing the model are presented in the flow chart in Figure 4. 6.

The MODFLOW-2005 code was selected as is been proved to be useful for solving partial differential equations of similar nature. The programme is based on finite differential method which allows the simulation in steady-state and transient flow in an a confined, unconfined or combination of both. The finite-difference code numerically solves the three-dimensional (3D) groundwater-flow equation under steady or transient flow conditions in a heterogeneous and anisotropic medium (Harbaugh *et al*., 2000). Although the system and the involved flow processes

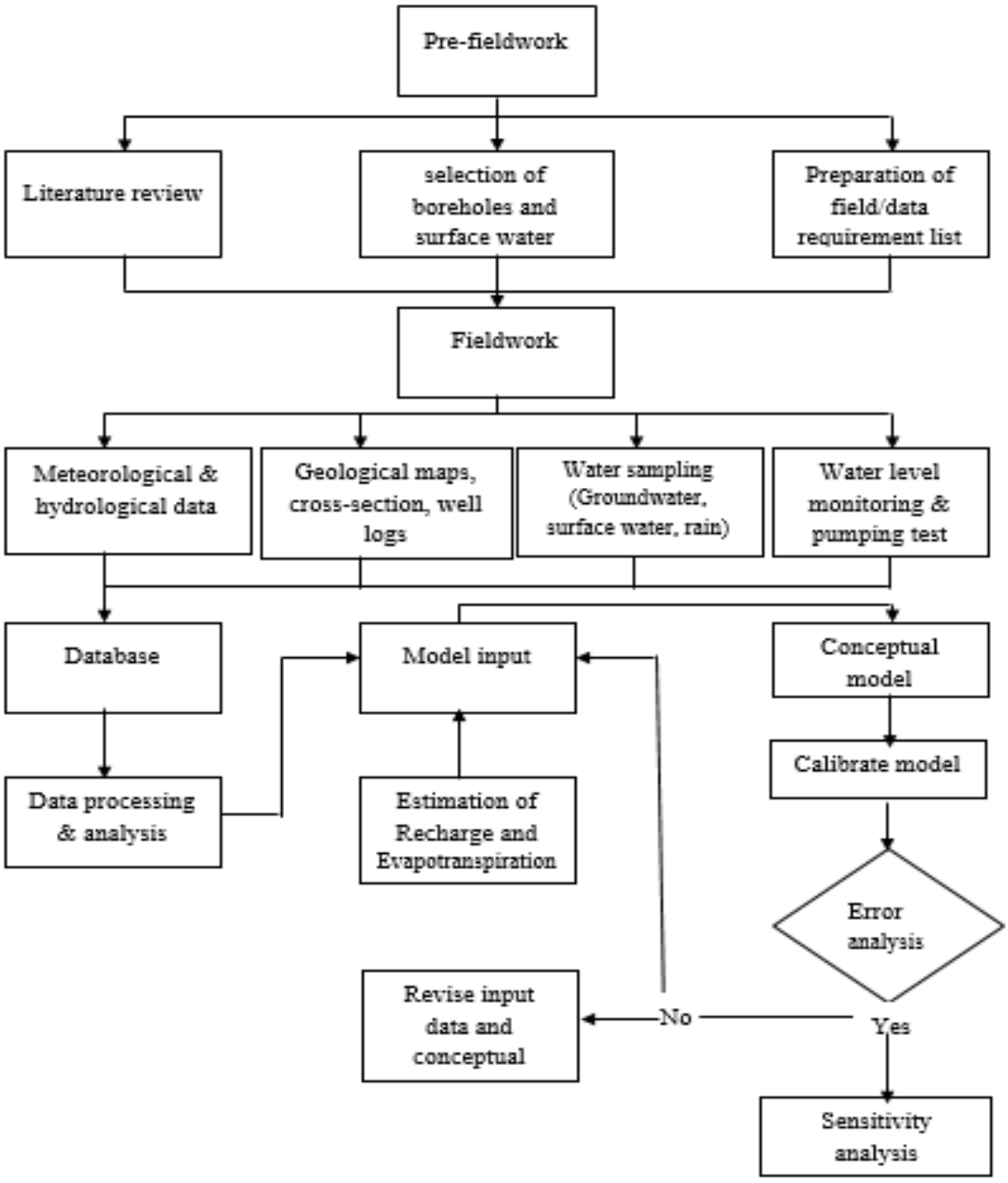


**Figure 4.6: Groundwater flow chart for the numerical model**

were essentially two-dimensional (2D), the model was set up in three dimensions with uniformity in the y-direction. 2D means the flow into the groundwater is from the x and y directions. Homogeneous means that the geological formation is uniform throughout the groundwater. Isotropic means hydraulic conductivity is independent of position within the groundwater. Steady

state means that inflow to the aquifer and outflow from the aquifer are equal hence there is no change in storage.

The 2D steady state numerical was simulated based on the governing differential equation given in Eq. 4.1 (Anderson & Woessner 1992).

$$\frac{\partial}{\partial x}\left(Tx\frac{\partial h}{\partial x}\right)+\left(\frac{\partial}{\partial y}Ty\frac{\partial h}{\partial y}\right)\pm R=0 \quad (4.1)$$

Where:

h= hydraulic head

R = source or sink

$T_x$ and $T_y$ = Transmissivity in the x and y directions

The programme was chosen because it can be used to simulate flow to wells, recharge, evapotranspiration, flows to drains and through river beds. ESRI ArcGIS 10.2 was used for the generation of maps and processing of the model input data (Figure 4.7).



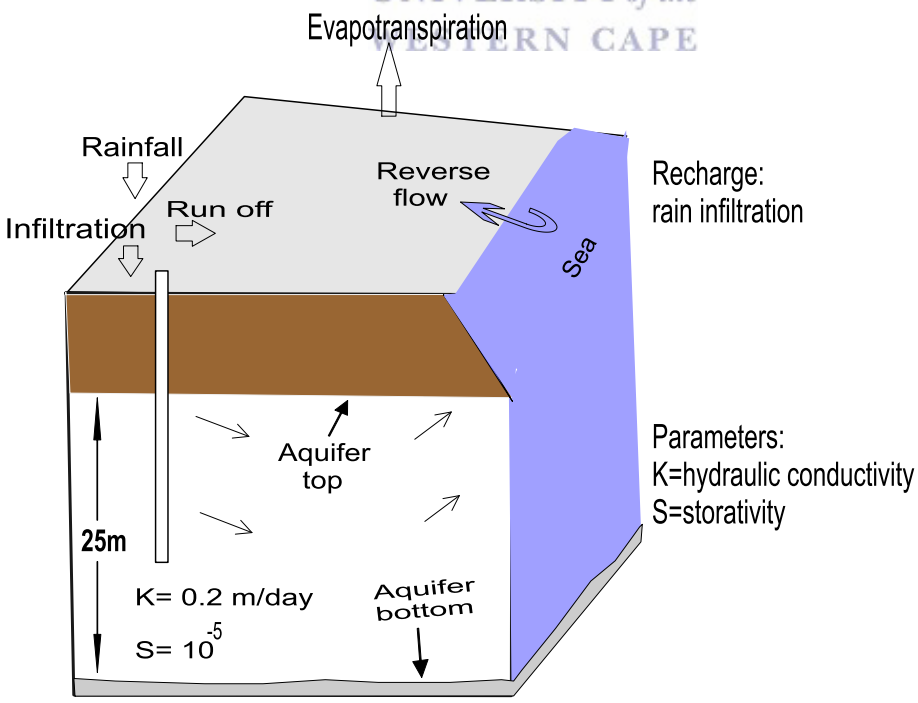


**Figure 4.7: Conceptual box model showing the model input parameters**

### 4.5.1 Selection of the code

The numerical model code to simulate Sakumo wetland basin is based on the U.S. Geological Survey ModelMuse. ModelMuse is a Graphical User Interface (GUI) for MODFLOW-2005 (Winston, 2009) based on a two-dimensional finite-difference groundwater. The selection of this code is justifiable in that:

1) It simulates steady and no steady flow in an irregularly shaped flow system in which aquifer layers can be confined, unconfined, or a combination.

2) It allows the user to define the spatial input for the model by drawing points, lines, or polygons on top, front, and side views of the model domain.

3) The points, lines, and polygons can be used to assign data set properties at locations that are enclosed or intersected by them or by interpolation among objects.

4) The program (ModelMuse) is relatively easy to understand and open source from the USGS web at: http://water.usgs.gov/software

5) ModelMuse can be applied to realistic conditions and it can be used for future developments of the model.



### 4.5.2 Defining the model extension

The first step in developing a model after selecting the numerical code for the model is to define the study area known as the Model Domain in ModelMuse. The GIS map tools (ARCMAP) was used to create boundary shapefile of the study area and imported to ModelMuse to set the grid area and also define the areas of active and inactive cells. From the conceptual model in Figure 4.4, groundwater in the basin was found to occur in both the alluvial aquifer and in the underlying weathered rocks. The measured heads in the monitoring wells, screened in the alluvial and weathered formation, was about the same. Based on these findings, the alluvial and the weathered fractured rocks were considered as a single unconfined layered system.

The model consists of one layer with constant layer thickness of 25 m. The layer simulated the top soil and upper weathered part of the rocks and is defined by the formula [Model top=model_aquifer_upper_top as 0 m and model_ aquifer_upper_bottom as-25 m] (Figure 4.6. The layer together with bedrock was modelled as unconfined/confined (convertible) type, however, the bedrock is considered inactive in order to simplify the model.

### 4.5.3 Defining model grids

The model domain was divided into 400 rows and 338 columns of finite difference grids of 0.001×0.001m in size. In the vertical direction, the model is single layered and the top elevation surface of the model represents the land surface of the study area. Elevations of the top grid cells were assigned using 30 m resolution DEM obtained from the USGS earth explorer. Elevation of the bottom cells were determined using the aquifer thickness within the study area.

### 4.5.4 Topography

The topographic map of the area was used to define the topography of the model domain. Values of contour maps were set by interpolation for the layer with digital topographic map prepared in Arc Map v 10.2 in determining the cell elevations. The altitude of the ground surface in the study area was adapted from Digital Elevation Map (DEM) surveys from ASTRM. A detailed 90 m x 90 m Digital Elevation Map (DEM) was obtained from Shuttle Radar Topography Mission (SRTM) and converted to the resolution of the model grid to allow detailed assessment of the groundwater-surface water exchange at reasonable computation time. The extracted DEM was used to define the top elevation of the aquifer.



### 4.5.5 Hydraulic conductivity (K)

The area has uniform hydraulic conductivity. The hydraulic conductivity was estimated from the aquifer pumping test data conducted in the five monitoring wells located within the study area. Estimated hydraulic conductivity values are presented in Table 4.3. The value of the hydraulic conductivity, K was obtained using the relation,

$$K = \frac{T}{b} \quad (4.2)$$

Where:
K= Hydraulic conductivity (m/d)
T=Transmissivity ($m^2$/day)
b= saturated thickness of the aquifer (m)

**Table 4.3: Estimated hydraulic conductivities of the wells located in the vicinity of the Sakumo wetland**

| Well ID | b (m) | Q (l/min) | ΔS' (m) | T ($m^2$/day) | K (m/day) |
|---|---|---|---|---|---|
| MW 2 | 61 | 10 | 13.90 | 0.18 | 0.0063 |
| MW 6 | 61 | 12 | 10.30 | 0.31 | 0.0099 |
| MW 15 | 61 | 12 | 16.40 | 0.19 | 0.0092 |
| MW 8 | 49 | 10 | 5.20 | 0.50 | 0.0175 |
| MW 4 | 42 | 60 | - | - | |

### 4.5.6 Recharge

Water enters the wetland system in the form of the precipitation which can be modelled using the Recharge Package. The Recharge Package (RCH) in ModelMuse was used to specify the recharge rate. Recharge was estimated as a fraction of precipitation and set at 38 mm/a, calculated based on a 5% value of the total seasonal precipitation the mean annual precipitation value of 760 mm. Recharge in the study area is assumed to be uniform hence, a uniform recharge boundary condition was assigned on top of the model cells.

Evapotranspiration in this model refers to reference crop evapotranspiration ETo. Reference crop evapotranspiration is a key component of hydrological studies which is incorporated in water balance studies. Reference evapotranspiration was used was calculated based on the Hagreaves and Samani formula given in Eq. 4.3. The Hagreaves and Samani method uses minimum and maximum temperature together with meteorological data to calculate reference evapotranspiration. Figure 4. 8 shows the calculated evapotranspiration for the hydrological year under study.

$$ET_0 = 1.25 \times 0.0023 \times R_a T_r^{0.5} (T_a + 17.8) \quad (4.3)$$

Where:

$ET_0$ = Reference evapotranspiration (mm/a)

$R_a$ = Extra-terrestrial radiation (mm)

$T_r$ = Temperature (°C)

$T_a$ = Average temperature °C

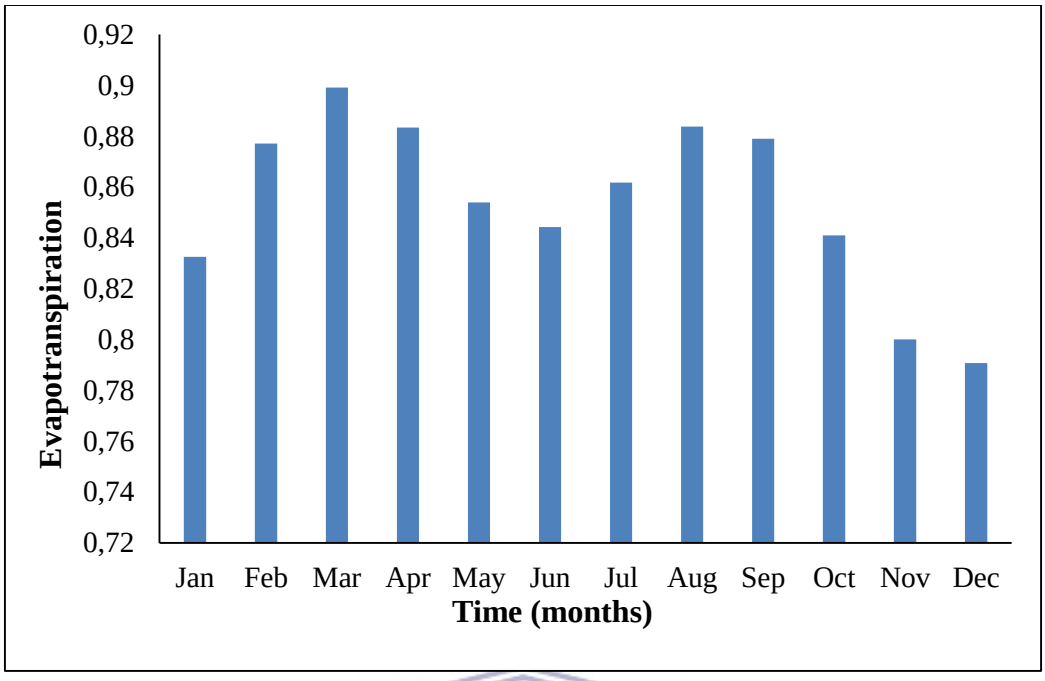


**Figure 4.8: Monthly mean evaporation rated calculated for the one hydrological year using Hargreaves and Samani method**



### 4.5.7 Assigning the boundary conditions

Boundary conditions in the study area were defined as hydrogeological features which significantly impact the groundwater flow pattern such as the catchment boundaries and surface water features within the basin. Figure 4.9 shows the boundary conditions identified in this study. No flow boundaries form the physical or hydrogeological barriers which prevents water from flowing in and out of the model domain. These boundaries are normally assigned when defining the boundary of a model grid or by setting the grid blocks as inactive. A no flow boundary condition was assigned for the wetland basin although there was flow observed in field.

Constant head boundaries are water source(s) that have invariant water level at the model boundaries. They are used to model an aquifer in good communication with the other source of water. In this study, the wetland and two dams in the catchment were identified as constant head boundaries and were specified using the CHD package in ModelMuse. A polygon was used to assign 0.7 m deep layer confining the wetland base.

Head dependent boundaries boundary conditions where flow of water into and out of the wetland is a function of the elevation of the wetland bed. These conditions are mostly used to model rivers

with poor connection with the wetland. In this study the three streams namely, Dzorwulu, Mamahuma and Onukpawahe streams which runs from the northern part through the central portion to the south of the domain were identified as the head dependent boundaries. The head dependent was simulated using the DRAINS package in ModelMuse.

### 4.5.8 The flow rate

In order to calculate the flow rate, an equivalent conductance was determined. As defined in MODFLOW-2005, conductance (C) has units of $L^2/t$ and is a function of hydraulic conductivity (K), cell length (L), cell width (W) and cell thickness (M). By substituting the calculated hydraulic conductivity with the drain dimensions, an equivalent conductance was determined. MODFLOW Drain Package (DRN) in ModelMuse was used to simulate the southern border of the wetland (Anderson & Woessner 2002). The unconfined aquifer model was run with steady state conditions and December-2015 was chosen as the initial aquifer head. The domain area, spatial discretization and grid lines, head observations and drain is presented in Figure 4.9.

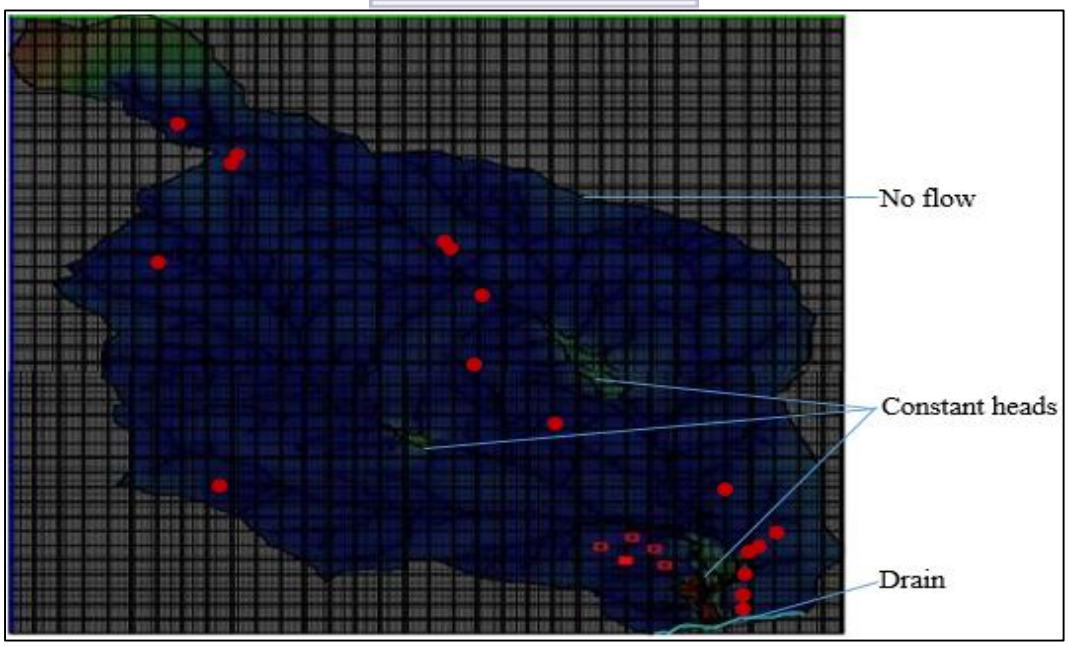


**Figure 4.9: Spatial discretization of the domain area**

## 4.6 Results

Table 4.3 shows the water budget of the model based on the uncalibrated model. From Table 4.4, it is evident that major contributors to the water budget of the domain area are recharge and constant heads. Drains and Evapotranspiration are major depressions in the catchment.

Table 4.5a shows the comparison of observed heads with the simulated heads of five the monitoring wells within the domain area. Assessment of error criterion was done using Mean Error (ME), Root Mean Square Error (RMSE) and Mean Absolute Error (MAE). In general, RMSE values are larger than MAE values, and the degree to which RMSE exceeds MAE is an indicator of the extent to which large outliers (variance between the observed and the simulated values) exist in the model performance (Karunanithi *et al*., 1994). Each technique revealed an error less than 10. These parameters are defined by Eqs 4.4, 4.5 and 4.6 as:

**Table 4.4: Water budget for the uncalibrated model**

| Cumulative volumes | In, $m^3/s$ | Out, $m^3/s$ |
|---|---|---|
| Storage | 0.000 | 0.000 |
| Constant Head | 17.66 | 0.000 |
| Drains | 0.000 | 55.5305 |
| ET | 0.000 | 8.37E-02 |
| Recharge | 38.00 | 0.000 |
| Total | 55.66 | 55.6142 |
| IN-OUT | | 4.58E-02 |
| % Discrepancy | | 0.000 |



$$ME \frac{1}{N}\sum_{i=1}^{N}(h_{obs} - h_{sim}) \quad (4.4)$$

$$RMSE=\sqrt{\frac{1}{N}\sum_{i=1}^{N}(h_{obs} - h_{sim})^2} \quad (4.5)$$

$$MAE=\frac{1}{N}\sum_{i=1}^{N}|h_{obs} - h_{sim}| \quad (4.6)$$

Where:

ME= Mean error

RMSE=Root mean squared error

MAE= Mean absolute error

N= number of observations

$h_{sim}$= simulated head

$h_{obs}$= observed head

The simulated heads were found to be higher than the observed heads except for wetland. Quantitively, RMSE reflect the discrepancy between the observed and calculated values. The lower the value of RMSE, the more accurate the prediction is. RMSE value of 2.22 was calculated for the groundwater and 2.41 for the wetland, respectively. Mean absolute error (MAE) was calculated to be 1.98 and 5.82 for the groundwater and wetland respectively. RMSE and MAE values were consistent with the percent errors calculated for the groundwater and wetland which indicates an accurate simulation results.



**Table 4.5a: Comparison between the observed and simulated heads of the uncalibrated model**

| Well ID | Observed heads (m) | Simulated heads (m) | Residuals (m) | Residual$^2$ (m) | Absolute residuals (m) |
|---|---|---|---|---|---|
| MW2 | 9.81 | 11.82 | -2.01 | 4.04 | 2.01 |
| MW6 | 14.81 | 13.78 | 1.03 | 1.06 | 1.03 |
| MW15 | 15.60 | 14.67 | 0.93 | 0.86 | 0.93 |
| MW8 | 15.80 | 17.99 | -2.19 | 4.80 | 2.19 |
| MW4 | 15.80 | 12.07 | 3.73 | 13.90 | 3.73 |
| RMSE | | | | **2.22** | |
| ME | | | | **0.30** | |
| MAE | | | | 1.98 | |

Table 4.5b shows the comparison between the observed and simulated fluxes of the Sakumo wetland and the dams based on the uncalibrated model. The observations were made during the start of simulation process using DROB package. The simulation is within the expectable error margin of less than 10 based on RMSE, ME and MAE. The differences in fluxes are shown as residuals and based on these residuals, the differences between fluxes observed and simulated is slightly bigger.

**Table 4.5b: Comparison between the observed and simulated water fluxes of the uncalibrated model**

| Fluxes | Observed heads (m) | Simulated Heads (m) | Residuals (m) | Residual$^2$ (m) | Absolute residuals (m)_ |
|---|---|---|---|---|---|
| S. Wetland | 0.70 | -1.04 | 1.74 | 3.03 | 3.03 |
| Uni. Dam | 6.26 | 7.50 | -1.24 | 1.54 | 1.54 |
| L. Dam | 10.70 | 14.30 | -3.59 | 12.9 | 12.9 |
| ME | | | | **1.03** | |
| RMSE | | | | **2.41** | |
| MAE | | | | 5.82 | |

### 4.6.1 Calibration

Calibration according to Anderson & Woessner (2002) refers to the process of demonstrating the capability of a model to produce the field measured heads and flows. This can be achieved through finding input parameters, stresses or boundary conditions which produces simulated values similar to the observed heads or fluxes. Calibration can be done in two ways, through forward modelling and inverse problem solution. In the current study, forward modelling was applied using conventional trial and error technique. In order to achieve the best overall agreement between the simulated and the observed data, the calibration strategy was initially done by varying the best-known parameters as little as possible and the poorly known or unknown values the most. In this case, aquifer thickness and recharge were adjusted within the reasonable range.

Table 4.6 shows the initial and calibrated hydraulic parameters of the simulated heads. Hydraulic parameters and recharge was adjusted during model calibration. Initial parameter of K used in the calibration was set 1.58E-06 m/s as given in literature (Agbevanu, 2015) and recharge at 140.4 mm/a (Adomako *et al*., 2010).

**Table 4.6: Initial and calibrated parameters used in the model calibration**

| Parameter | Unit | Initial value | Calibrated value |
|---|---|---|---|
| Aquifer thickness, b | m | 25 | 5.5 |
| Recharge, Re | mm/a | 38 | 124.8 |

### 4.6.2 Simulation results of the calibrated model

The calibrated model was used to simulate the local groundwater head and this was compared to the observed data of the monitoring wells and the wetland water fluxes. Table 4.7 shows the water budget of the model domain based on the calibrated model. There is good agreement between the simulated and observed heads. The results of the numerical simulation indicate that there is a decline in the wetland fluxes. Generally, there is a very minimum decline in wetland water level over the simulated period.



**Table 4.7: Water budget of the calibrated model of the Sakumo wetland**

| Cumulative volumes | Flows in, $m^3/s$ | Flows out, $m^3/s$ |
|---|---|---|
| Storage | 0.00 | 0.00 |
| Constant Head | 10.60 | 2.60 |
| Drains | 0.000 | 132.72 |
| ET | 0.000 | 8.37E-02 |
| Recharge | 124.8 | 0.000 |
| Total | 135.40 | 135.4037 |
| IN-OUT | | -3.7E-03 |
| % Discrepancy | | 0.000 |

Table 4.8a shows the comparison of observed heads with the simulated heads of the wells within the domain area. Assessment of error criterion was done using Root Mean Square Error (RMSE), Mean Error (ME) and Mean Absolute Error (MAE). A perfect fit between the observed and simulated values occur at $R^2$ =1, RMSE=0 and ME= 1.

**Table 4.8a: Comparison between the observed and simulated heads of the calibrated model**

| Well ID | Observed (m) | Simulated (m) | Residuals (m) | Residual$^2$ (m) | Absolute residuals (m) |
|---|---|---|---|---|---|
| MW2 | 9.81 | 10.80 | -0.01 | 1.02 | 0.01 |
| MW6 | 14.81 | 15.78 | -0.97 | 0.94 | 0.97 |
| MW15 | 15.60 | 16.67 | -1.07 | 1.14 | 1.07 |
| MW8 | 15.80 | 16.00 | -0.20 | 0.04 | 0.20 |
| MW4 | 15.80 | 16.01 | -0.27 | 0.07 | 0.27 |
| ME | | | | **-0.70** | |
| RMSE | | | | **0.80** | |
| MAE | | | | 0.70 | |

Table 4.8b shows the comparison between the observed and simulated fluxes of the Sakumo wetland and the two dams (Lebanon and University dam) in the model domain area based on the calibrated model. The observations were made during the start of simulation process using DROB package. The simulation is within the expectable error margin of less than 10 based on RMSE, ME and MAE. The differences in stages are shown as residuals and based on these residuals, the differences between fluxes observed and simulated is slightly bigger.



**Table 4.8b: Comparison between the observed and simulated water fluxes of the Sakumo wetland based on the calibrated model**

| Fluxes | Observed (m) | Simulated (m) | Residuals (m) | Residual$^2$ (m) | Absolute residuals (m)_ |
|---|---|---|---|---|---|
| S. Wetland | 0.70 | 0.30 | 0.04 | 0.16 | 0.16 |
| U. Dam | 6.26 | 5.03 | 1.23 | 1.51 | 1.51 |
| L. Dam | 10.70 | 11.50 | 0.8 | 0.64 | 0.64 |
| ME | | | | **0.28** | |
| RMSE | | | | **0.88** | |
| MAE | | | | 0.77 | |

Figure 4.11 shows a relationship between simulated heads and observed heads based on the calibrated model. The hydraulic heads were monitored in 37 wells within the domain area during the start of the simulation and at the end of the simulation using head observation package (HOB).

Figure 4.10 shows an $R^2$ determinant of 0.942 shows a strong correlation between simulated and observed heads and therefore proving that calibration had been achieved.

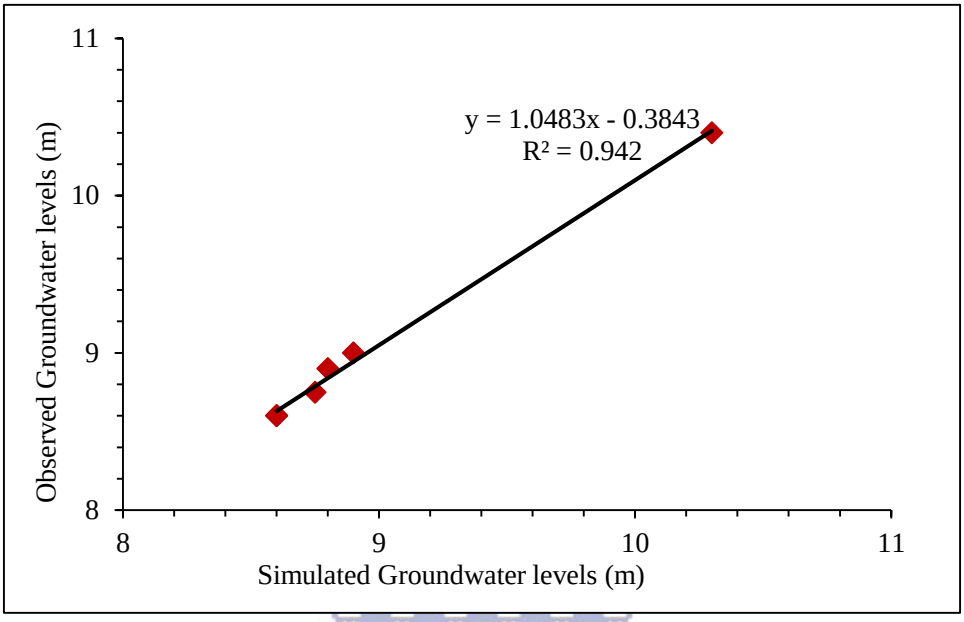


**Figure 4.10: Comparison of the simulated and observed groundwater levels**



The output results shows that, groundwater flow follows the natural topography; that is, groundwater flow direction is predominantly from the upper sub-basin towards the wetland to the sea as shown in Figure 4.11.

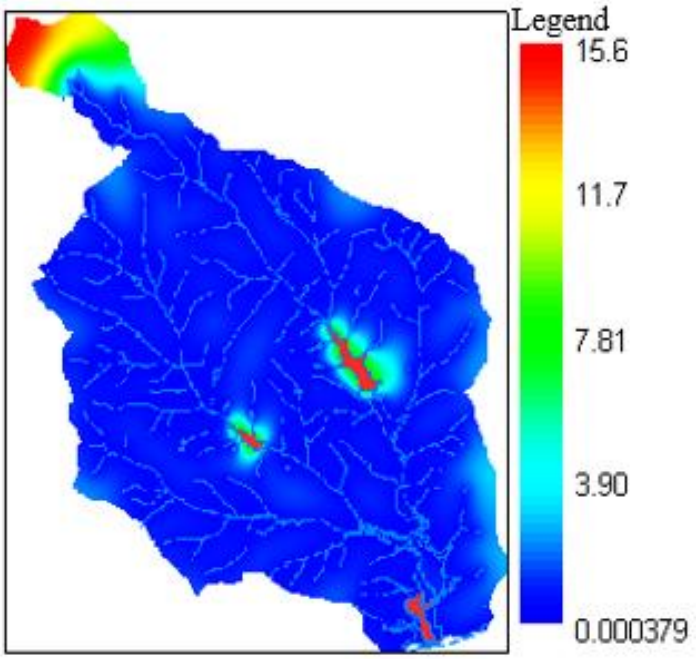


**Figure 4.11: Calibrated head distribution in the Sakumo wetland basin**



## 4.7 Discussion

### 4.7.1 Setting scenarios and predictions

The calibrated steady state flow model was used to assess the effects of varied groundwater recharge rates on the wetland water balance components, head distribution, fluxes and groundwater flow directions. The changes in the hydraulic head were noted throughout the scenario analyses. The purpose for the scenario analysis was to predict the possible impacts of reduced rainfall and the corresponding effects on groundwater recharge in the basin, following climate variability. For each of the monitoring wells used in this study, the abstraction rate was estimated from the transmissivities values as given by (Krasny, 1993) and used as the initial abstraction rates. The tested scenarios are presented in Tables 4.7 and 4.8.

#### 4.7.1.1 Varying recharge rates

This section presents results obtained from varying recharge based on the calibrated model. The aim was to test how varying groundwater recharge rates influences the wetland water balance components. The results from the varying recharge are presented in Table 4.8. Table 4.8 shows water budget components and predicted recharge influence on these components based on the

calibrated model. The aim was to assess the behavior of the water balance component under hydrological stresses. Simulations were made based on three scenarios using a recharge value of 124.8 mm/a as scenario 1. Increasing the recharge value by 10% was used as scenario 2. Decreasing the recharge value by 10% was used to simulate scenario 3. The recharge value was doubled and simulated as scenario 4. The results of the various scenarios are presented in Figure 4.12. The water budget results from the various simulated recharge scenarios are presented in Table 4.9. The Table shows that, varying recharge rates impacts the wetland water budget components. This in evidence in the percentage differences change in recharge rates with respect to the calibrated value. An increase in recharge rate by 50% shows a difference of outflow with respect to the calibrated values increases. The similar pattern was observed when recharge rate was decreased by 50%.

**Table 4.9: Effects of varying recharge on the wetland water balance components**

| Scenarios | Water balance components | Inflow ($m^3/s$) | Outflow ($m^3/s$) | Change with respect to the calibrated value (%) |
|---|---|---|---|---|
| Scenario 1: Calibrated value | Constant head | 17.66 | 2.6 | |
| | Drains | 0 | 446.44 | |
| | ET | 0 | 8.31E-02 | |
| | Recharge | 124.8 | 0 | |
| Scenario 2: Increasing by 10% | Constant head | 17.12 | 0 | -100 |
| | Drains | 0 | 30.35 | -93.202 |
| | ET | 0 | 8.31E-02 | 0 |
| | Recharge | 137.28 | 0 | 0 |
| Scenario 3: Decreasing by 10% | Constant head | 17.17 | 0 | 0 |
| | Drains | 0 | 27.93 | -7.97 |
| | ET | 0 | 8.32E-02 | 0.12 |
| | Recharge | 112.32 | 0 | 0 |
| Scenario 4: Increasing by 25% | Constant head | 17.02 | 0 | 0 |
| | Drains | 0 | 35.05 | 25.49 |
| | ET | 0 | 8.32E-02 | 0 |
| | Recharge | 156 | 0 | 0 |
| Scenario 5: Decreasing by 25% | Constant head | 17.27 | 0 | 0 |
| | Drains | 0 | 23.23 | -33.72 |
| | ET | 0 | 8.35E-02 | 0.36 |
| | Recharge | 93.6 | 0 | 0 |
| Scenario 6: Increasing by 50% | Constant head | 16.94 | 0 | 0 |
| | Drains | 0 | 38.6 | 66.16 |
| | ET | 0 | 8.31E-02 | -0.479 |
| | Recharge | 187.20 | 0 | 0 |
| Scenario 7: Decreasing by 50% | Constant head | 17.35 | 0 | 0 |
| | Drains | 0 | 19.68 | -49.02 |
| | ET | 0 | 8.31E-02 | 0 |
| | Recharge | 62.4 | 0 | 0 |

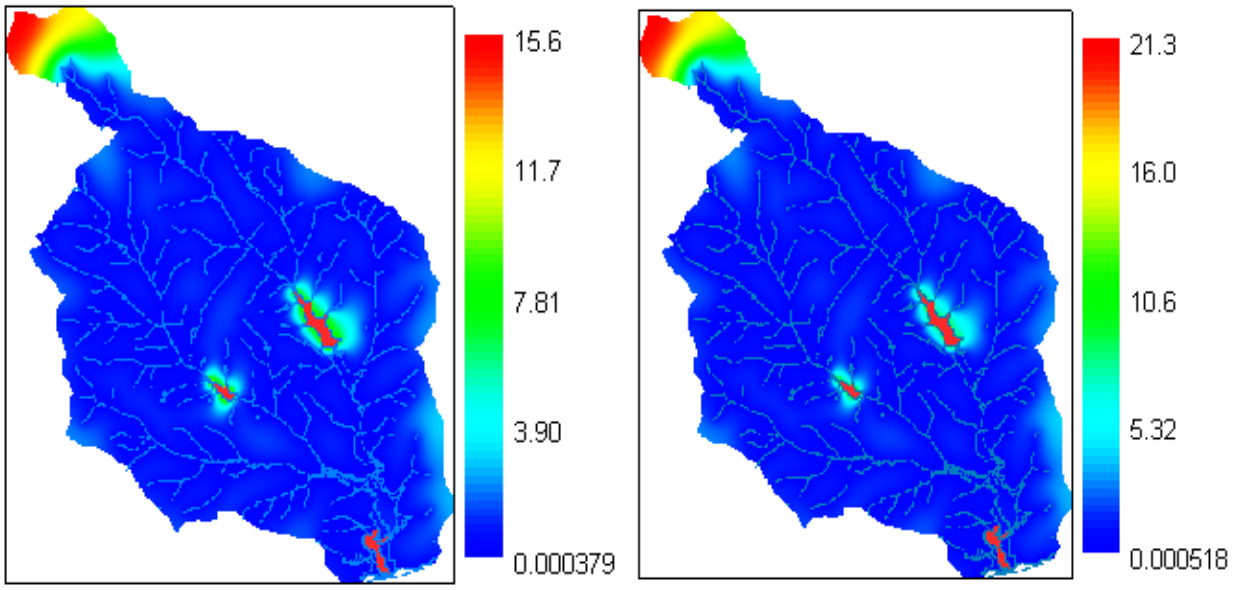


A) Calibrated recharge value B) 10% increase in calibrated recharge value

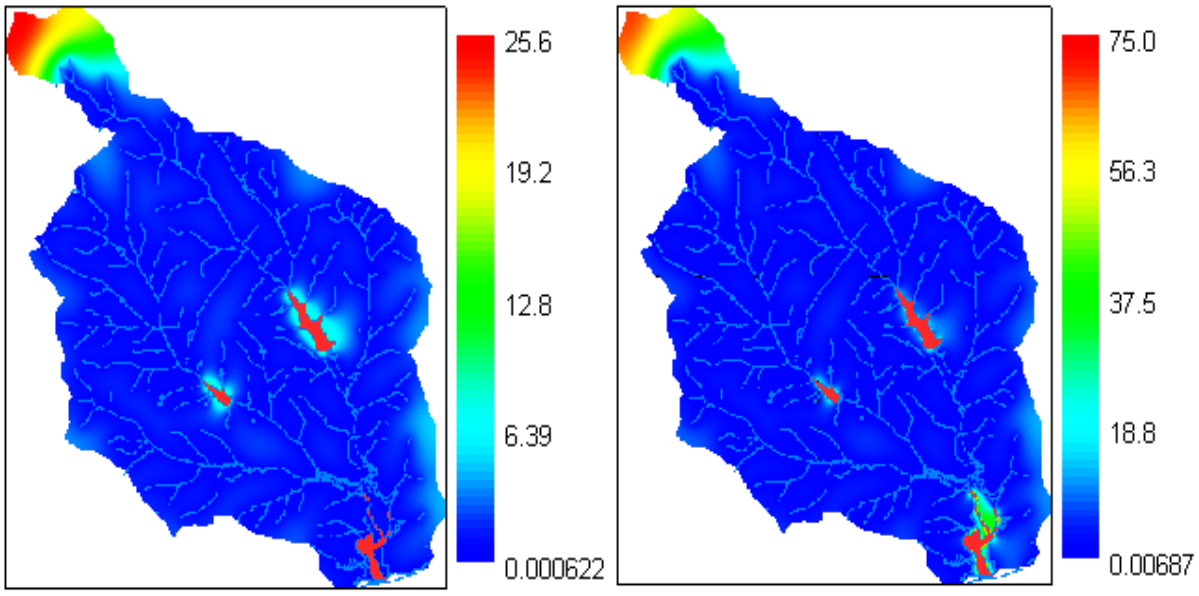


C) 25% increase in calibrated recharge value D) 50% Increase in calibrated recharge

**Figure 4.12: Groundwater levels distribution based on varying recharge rates scenarios**

#### 4.7.1.2 Varying pumping scenarios

The aim was to assess the behavior of the water balance components and the wetland fluxes response under variable water withdrawal rates. This section presents results obtained from variable withdrawal rates simulation. The aim was to test the effect of varying groundwater withdrawal rates on the wetland water balance components, groundwater levels distribution and flow direction. The assumption of steady state conditions in the current study was based on the fact that the current abstraction rates are considered very minimal and insignificant. This was confirmed in the simulation of the various groundwater abstraction scenarios in the study area.

The simulations were set based on groundwater withdrawal at a rate of 5l/s (reference abstraction rate based on the average transmissivity range <1 $m^2$/d to 10 $m^2$/d in Kránsý, 1993). This was set as Scenario 1. Scenario 2 involved doubling the groundwater withdrawal rate to 10 l/s and Scenario 3, increasing the withdrawal rate four times that is, withdrawal at 20 l/s. Table 4.9 shows the influence of varying pumping rates on water balance components of the Sakumo basin based on the calibrated model. The water budget results presented in Table 4.10 shows that, varying abstraction rates does not overly influence the wetland water balance components of the area. This suggests that, there is no hydraulic link between the wetland and the underlying groundwater. Even with an increased in abstraction by up to 80%, does not significantly change the wetland water storage significantly. Figure 4.13 shows the results of the various scenarios of groundwater abstraction simulated in the study area.

**Table 4.10: Effects of varying abstraction on the wetland water balance**

| Scenarios | Water balance components | Inflow ($m^3/s$) | Outflow ($m^3/s$) | Change with respect to 5 l/s based on T value (%) |
|---|---|---|---|---|
| Scenario1: Pumping at 5l/s | Constant head | 17.66 | 0 | |
| | Wells | 0 | 0.2 | |
| | Drains | 0 | 28.94 | |
| | ET | 0 | 8.25E-02 | |
| | Recharge | 124.8 | 0 | |
| Scenario 2: Increasing pumping by 10% | Constant head | 17.15 | 0 | 0 |
| | Wells | 0 | 0.19 | -5 |
| | Drains | 0 | 28.95 | 0.03 |
| | ET | 0 | 8.26E-02 | 0.12 |
| | Recharge | 124.8 | 0 | 0 |
| Scenario 3: Decreasing pumping by 10% | Constant head | 17.14 | 0.3658 | 0 |
| | Wells | 0 | 0.175 | -7.89 |
| | Drains | 0 | 28.97 | 0.07 |
| | ET | 0 | 8.27E-02 | 0.12 |
| | Recharge | 124.8 | 0 | 0 |
| Scenario 4: Increasing pumping by 50% | Constant head | 17.15 | 0 | -100 |
| | Wells | 0 | 0.21 | 20 |
| | Drains | 0 | 28.93 | -0.14 |
| | ET | 0 | 8.25E-02 | -0.24 |
| | Recharge | 124.8 | 0 | 0 |
| Scenario 5: Decreasing pumping by 50% | Constant head | 17.15 | 0 | 0 |
| | Wells | 0 | 0.145 | -30.95 |
| | Drains | 0 | 28.998 | 0.24 |
| | ET | 0 | 8.29E-02 | 0.485 |
| | Recharge | 124.8 | 0 | 0 |
| Scenario 6: Increasing pumping by 80% | Constant head | 17.15 | 0 | 0 |
| | Wells | 0 | 0.225 | 55.17 |
| | Drains | 0 | 22.9191 | -20.96 |
| | ET | 0 | 8.24E-02 | -0.60 |
| | Recharge | 124.8 | 0 | 0 |
| Scenario 7: Decreasing pumping by 80% | Constant head | 17.15 | 0 | 0 |
| | Wells | 0 | 0.11 | -51.11 |
| | Drains | 0 | 29.03 | 26.66 |
| | ET | 0 | 8.30E-02 | 0.73 |
| | Recharge | 124.8 | 0 | 0 |

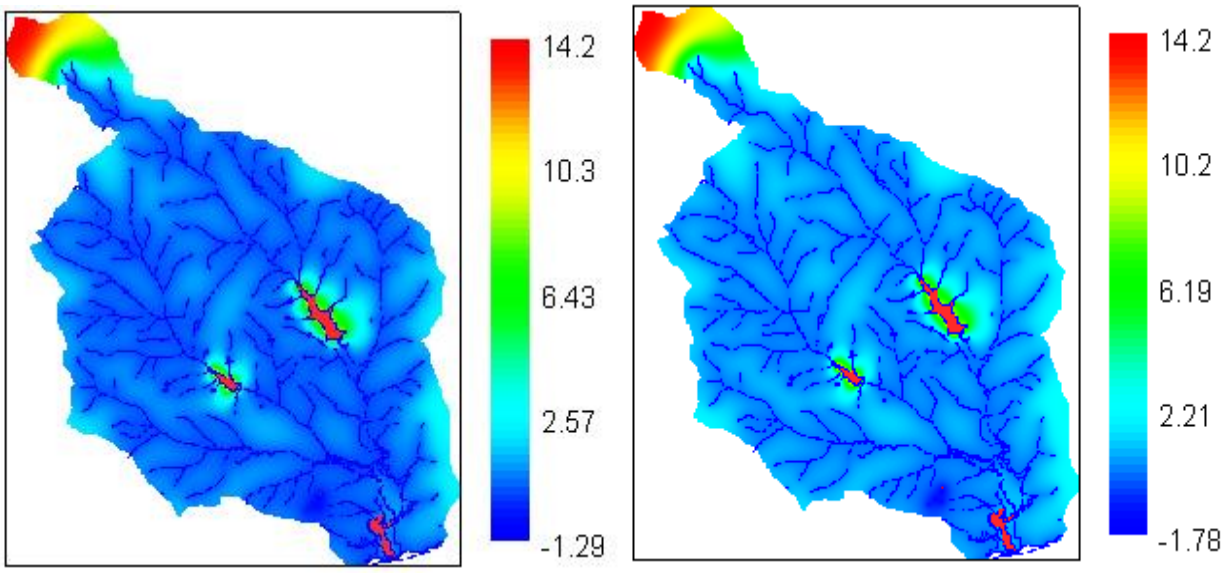


A) Groundwater abstraction at 5 l/s B) Groundwater abstraction at 10 l/s

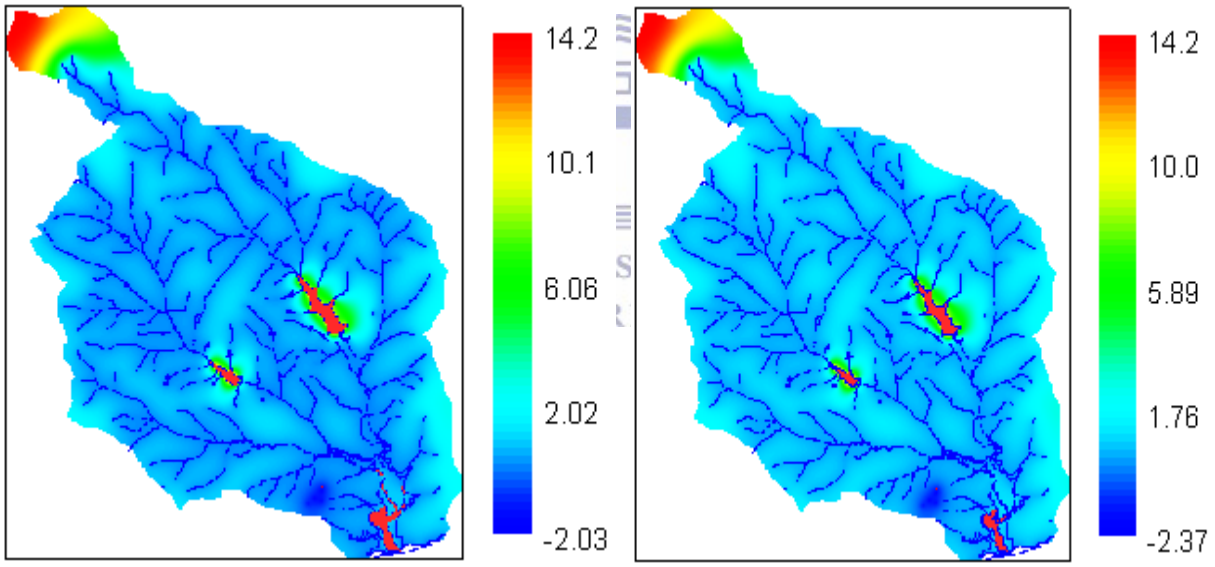


C) Groundwater abstraction at 20 l/s D) Groundwater abstraction at 40 l/s

**Figure 4.13: Groundwater levels distribution based on varying abstraction rates**

### 4.7.2 Sensitivity analysis

Parameter sensitivity tests were conducted iteratively using forward simulation to test the influence of change in magnitude of input parameters on the simulation results of the groundwater model (Gedeon & Mallants 2012). A change in the parameter results in significant difference between the simulated and observed head and fluxes (Zhou & Li 2011). In order to test the sensitivity of

the model, hydraulic conductivity was varied by several magnitudes of 10%, 50% and 80% increases and decreases in each run. Hydraulic conductivity value was changed uniformly of the entire area whiles other parameters were kept constant to the steady state calibrated values. The magnitude of change in heads and fluxes from the calibrated solution were used to measure the sensitivity of the model to the particular parameter.

Results of the sensitivity analysis presented in Table 4.11 is shown as differences in groundwater levels and wetland fluxes. Large differences between simulated heads and observed heads were recorded for the wells at higher hydraulic conductivity values which shows that, the model is sensitive to changes in hydraulic conductivity values.

**Table 4.11: Results of sensitivity analysis on the water fluxes**

| Parameter | Heads/ Fluxes | Increasing | | | Decreasing | | |
|---|---|---|---|---|---|---|---|
| | | 10% | 50% | 80% | -10% | -50% | -80% |
| | | m | m | m | m | m | m |
| Hydraulic conductivity K | MW2 | 9.48 | 9.52 | 9.53 | 5.45 | 9.30 | 8.73 |
| | MW4 | 15.78 | 14.51 | 14.52 | 15.75 | 14.24 | 13.61 |
| | MW6 | 14.46 | 15.47 | 15.48 | 14.42 | 15.41 | 15.26 |
| | MW8 | 15.90 | 15.86 | 15.84 | 15.95 | 16.12 | 16.70 |
| | MW15 | 15.46 | 15.82 | 15.83 | 15.45 | 15.62 | 15.20 |
| | S.wetland | -0.45 | -0.71 | -0.87 | -0.31 | 6.47E-02 | 0.50 |
| | U. Dam | 6.52 | 5.43 | 4.70 | 7.17 | 8.75 | 6.72 |
| | L. Dam | 0.94 | -0.51 | -1.44 | 1.80 | 4.01 | 10.54 |



## 4.8 Summary

This chapter conceptualized the local flow system in the Sakumo wetland catchment in Ghana by developing a conceptual flow model and simulating the groundwater flow system. This is significant in quantifying the water fluxes contributing to the wetland water storage. Two major groundwater flow systems were identified: a local (top soil-water) flow in the alluvium and an intermediate flow in the shallow unconfined unit. A simple 2D finite-difference numerical model was applied to analyse the groundwater flow system in the Sakumo wetland catchment using ModelMuse. The purpose of the model was to explain the groundwater flow system and quantify the water fluxes contributing to the wetland water storage. The source of groundwater in the

catchment is mostly from the shallow unconfined aquifer situated in the quaternary sediment. The modelling result indicates that changes in recharge significantly affect the wetland water balance. The water table declines during the dry season as there is high evapotranspiration with little rain. The modelling results confined that the Sakumo wetland water fluxes are predominately local to intermediate flows. The simulation of the calibrated model showed no hydraulic link between the wetland and the underlying groundwater. This study thus provides valuable hydrogeological information of the Sakumo wetland basin and laids the foundation for the development of detailed future predictive model.

# CHAPTER 5: HYDROCHEMICAL AND ENVIRONMENTAL ISOTOPE CHARACTERISATION OF THE FLOW SYSTEM

## 5.1 Introduction

In this chapter, the physicochemical and isotopic compositions of the water resources (the wetland, groundwater, piezometers and rain water) sampled in the Sakumo basin during the research period are presented and discussed. The results of the field investigations will be presented. Water levels, elevations, soil classification and hydraulic conductivity results will be implemented in the developed model. Water level measurements in the monitoring wells will be used to validate the developed model which will be discussed further in the next chapter.

The chemical properties of water are very important in determining its suitability for domestic, industries, agriculture and other uses. When groundwater moves through subsurface geological materials, its chemistry changes as water mixes and react along its path (Mazor, 1991). Water chemistry also gives indications of the rock types through which the water has come in contact with and can give clues about the residence time and flow velocity (Mazor, 1991). The amount of chemicals dissolved in water is attributed to the type of mineral that the water comes in contact with, the temperature, the pH and the environmental conditions. In order to understand the hydrochemistry, water quality and the interaction of groundwater and surface water within the catchment, major ions, trace elements and environmental isotopes data were analyzed.



## 5.2 Results and Discussion

## 5.2.1 Hydrochemical measurements

#### 5.2.1.1 Physical parameter

The physical and chemical properties of the groundwater and wetland water in the Sakumo basin are presented in Table 5.1 Water temperature controls the habitat of species in environment as temperatures affects feeding, reproduction and metabolism of almost all aquatic animals. Changes in water temperature affects the solubility of dissolved oxygen and calcium carbonate in water and also influences the extent metal uptake (Luoma, 1983) in the wetland. Water temperatures measured in the Sakumo basin ranged from 23.0℃ to 32℃. Temperatures measured in the wetland

**Table 5.1: Statistical summary of the physicochemical parameters of all the water types in the Sakumo Basin (units in mg/L except Temp [ºC], EC [µS/cm] and pH [no units]**

| Parameter | Units | Min. | Max. | Mean | Std. dev. |
|---|---|---|---|---|---|
| T | ºC | 22.7 | 31.5 | 26.43 | 2.95 |
| pH | pH units | 6.0 | 8.6 | 8.33 | 1.22 |
| EC | µS/cm | 186.70 | 42800 | 19801.11 | 5222.22 |
| Ca | mg/L | 5.22 | 415 | 97.44 | 93.88 |
| Mg | mg/L | 0.330 | 350 | 78.21 | 53.90 |
| Na | mg/L | 47.80 | 5840 | 1205.68 | 1584.09 |
| K | mg/L | 10.0 | 316 | 47.80 | 41.33 |
| $HCO_3^-$ | mg/L | 45.0 | 1850 | 350.37 | 243.54 |
| $Cl^-$ | mg/L | 30.0 | 8185 | 1939.30 | 1313.30 |
| $SO_4^{2-}$ | mg/L | 1.80 | 510 | 178.96 | 150.23 |
| $PO_4^{3-}$ | mg/L | 0.11 | 3.40 | 1.08 | 0.95 |
| $NO_3^-$ | mg/L | <0.001 | 42.0 | 2.92 | 0.20 |
| Fe | mg/L | 0.02 | 8.94 | 1.77 | 1.24 |
| Cu | mg/L | 0.08 | 0.28 | 0.40 | 0.29 |
| Zn | mg/L | <0.001 | 0.08 | 0.01 | 0.02 |
| Mn | mg/L | 0.05 | 0.86 | 0.21 | 0.21 |

water ranged from 23.4 to 32.3℃ and 23.4 to 26℃ in the piezometric waters. Measured temperatures in the groundwater ranged from 26.4 to 31.5℃. Measured temperature in the streams varied between 23. 0 to 27.5℃ whiles rainwater temperatures varied between 23.5 to 27.3℃. Wetland and stream water samples indicate higher equilibrium with temperature at 23 to 32°C (Table 5.2). These temperatures are reasonable due to the shallow water temperatures and air temperatures measured as high as 35°C. Temperatures recorded in the basin were not above the recommended values for fish farming and crop cultivation. The physicochemical parameters of the major ions measured in the study area is presented in Figure 5.1.

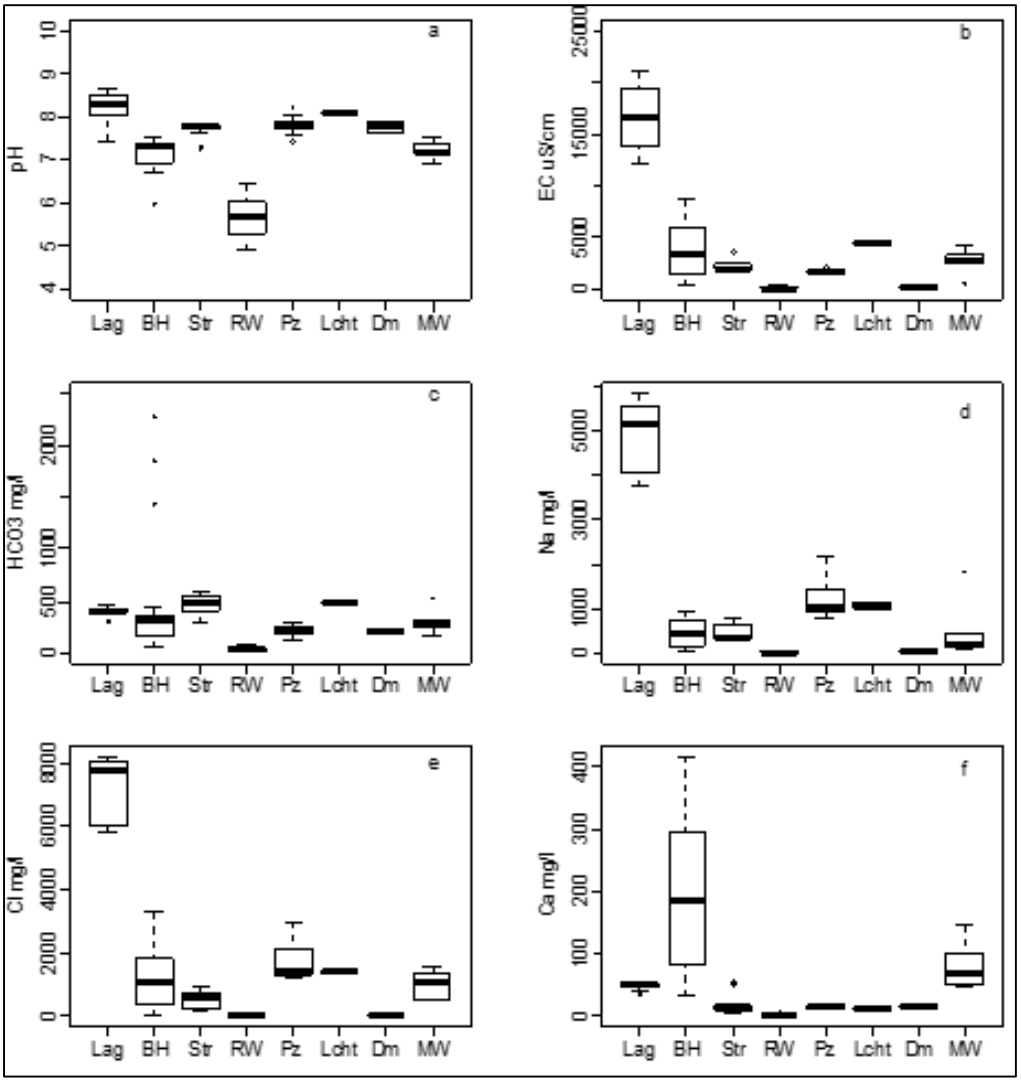


**Figure 5.1: Box plots of major ions in the sampled groundwater and wetland water samples in the Sakumo basin**

The concentrations of most physicochemical parameters increased at relatively higher temperatures. For example, electrical conductivity values were observed to be high (41050 µS/cm) when the water temperature increased (32°C) during sampling of the wetland waters. Groundwater normally maintains a constant temperature which is normally close to the mean annual air temperature. The mean groundwater temperature of 29.6°C was slightly higher than the mean

**Table 5.2: Descriptive statistical summary of measured wetland water samples**

| Variable | Units | Min. | Max. | Mean | Std. dev. |
|---|---|---|---|---|---|
| pH | pH units | 7.42 | 8.66 | 8.03 | 0.35 |
| EC | µS/cm | 1458 | 49900 | 9137.29 | 7876.48 |
| Temp | $^{o}$C | 24.7 | 32.2 | 30.62 | 0.67 |
| $HCO_3^-$ | mg/L | 110 | 43000 | 2078.33 | 1716.92 |
| $Cl^-$ | mg/L | 1195.5 | 8185.93 | 4472.64 | 2918.30 |
| $Na^+$ | mg/L | 806 | 5840 | 3048.15 | 1980.09 |
| $K^+$ | mg/L | 41.6 | 120 | 78.85 | 27.14 |
| $Ca^{2+}$ | mg/L | 11.74 | 53.98 | 31.65 | 17.13 |
| $Mg^{2+}$ | mg/L | 10.33 | 61.13 | 39.18 | 17.58 |
| $SO_4^{2-}$ | mg/L | 155.3 | 490 | 309.27 | 134.05 |

atmospheric temperature of 28°C. The high-water temperatures in the groundwater could accelerate the rate of chemical reactions. The difference in temperature was attributed to the variation in sampling time of the day and the season.

The pH of water sample is an important parameter in that it contributes in the determination of the species, mobility, accumulation and toxicity of elements present in a water. The pH of coastal waters is close to 8.2 due to ocean acidification whereas most natural freshwaters have pH values ranging from 6.5 to 8.0 (Hinga, 2002). Most aquatic organisms such as fish, require pH of a specific range. For example, physical damage to the gills, skin and eyes can also occur when pH is sub-optimal for fish. Changes in pH can alter the biological availability of trace metals and speciation of nutrients (Hinga, 2002). The waters in the Sakumo catchment analysed were slightly acidic to basic, with pH ranging from 6.0 to 8.6. pH of the wetland water was basic with pH between 7.27−8.8. Generally, sampling points closest to the mouth of the wetland that is, the upper section were slightly basic (pH of 7.86) whereas the middle portions of the wetland were basic (pH of 8.05). The southern part of the wetland which connects to the sea was slightly acidic (pH of 6.93). Groundwater from the domestic wells were slightly acidic to basic (pH ranging from 6.5 and 8.5) whereas pH of the monitoring wells was neutral to slightly basic (pH of 7.24 and 8.05) (Table 5.3).

**Table 5.3: Descriptive statistical summary of measured groundwater samples**

| Variable | units | Min. | Max. | Mean | Std. dev. |
|---|---|---|---|---|---|
| pH | pH units | 6.4 | 7.5 | 7.10 | 0.29 |
| EC | µS/cm | 480 | 9370 | 3626.97 | 2359.39 |
| Temp | °C | 25.1 | 31.5 | 28.99 | 1.38 |
| $HCO_3^-$ | mg/L | 56.15 | 1850 | 337.72 | 317.78 |
| $Cl^-$ | mg/L | 178.15 | 4232 | 1312.39 | 927.22 |
| $Na^+$ | mg/L | 89.5 | 1850 | 450.55 | 357.39 |
| $K^+$ | mg/L | 10.3 | 316 | 35.22 | 15.88 |
| $Ca^{2+}$ | mg/L | 30.09 | 495 | 181.03 | 125.86 |
| $Mg^{2+}$ | mg/L | 21.7 | 380.07 | 115.46 | 85.94 |
| $SO_4^{2-}$ | mg/L | 12.85 | 586 | 142.40 | 138.38 |
| $NO_3^-$ | mg/L | 1.01 | 16.5 | 4.86 | 3.73 |

Water from the shallow piezometers were slightly basic (pH of 7.86). The surface waters from the streams (Onukpawahe, Mamahuma and Dzorwulu) were slightly basic (pH of 7.79, 7.73 and 7.77 respectively). pH of the sewage flowing from settlements within the catchment was basic (pH of 8.1). pH of the dams measured 7.65 whiles rainwater collected during the study period measured the lowest pH with values ranging from 5.1 to 7.0 (Table 5.4). The alkaline nature of the wetland water may be due to the presence of dissolved bicarbonates (as carbonates were not measured) in the water which are known to affect pH of wetland waters (Davidson, 1995). This is due to the decomposition of vegetation within the wetland environment results in organic acids which remove $CO_2$ hence lowering the pH of the water (Appelo & Postma, 2005). Additionally, sewage flowing from settlements in the area coupled with sea water intrusion into the wetland may account for the acidic nature of the wetland water (Cai *et al.*, 2011). Wotany *et al*., (2013) confirmed that, such processes lead to reactions with lateritic soils and humic acids from the decomposition of organic matter in the infiltration zones leading to acidification from dissolved carbon dioxide. The slightly acidic nature of the lower part of the wetland is indicative of the pollution status in the wetland. Water with a pH value of more than 9 or less than 4.5 becomes unsuitable for most life forms and also for most other uses (Chapman, 1992). In the present study, the measured pH values were within the permissible limit for water and wastewater (WRC, 2003).

**Table 5.4: Descriptive statistical summary of measured rainwater samples**

| Variable | Units | Min. | Max. | Mean | Std. dev. |
|---|---|---|---|---|---|
| Rainfall Amount | mm | 3.40 | 81.6 | 21.57 | 18.24 |
| pH | pH units | 4.53 | 7.47 | 5.95 | 0.62 |
| EC | µS/cm | 5.74 | 370.0 | 63.01 | 74.88 |
| Temp | $^{o}C$ | 17.58 | 123.6 | 30.83 | 17.55 |
| $HCO_3^-$ | mg/L | 1.09 | 126.79 | 28.89 | 24.32 |
| $Cl^-$ | mg/L | 6.9 | 95.97 | 20.46 | 14.05 |
| $Na^+$ | mg/L | 2.3 | 44.23 | 10.69 | 8.03 |
| $K^+$ | mg/L | 0.18 | 25.5 | 5.48 | 2.06 |
| $Ca^{2+}$ | mg/L | 0.64 | 19.84 | 2.19 | 0.51 |
| $Mg^{2+}$ | mg/L | 0.06 | 1.8 | 0.55 | 0.38 |
| $SO_4^{2-}$ | mg/L | 0.46 | 73.1 | 14.54 | 10.94 |
| $NO_3^-$ | mg/L | 0.0009 | 17.68 | 1.32 | 1.19 |

Electrical conductivity (EC) is a measure of total dissolved solids and ionized species in water and it has a direct correlation with salinity. Variation of EC in groundwater has been used to identify recharge areas and flow paths as EC increases according to flow direction under natural conditions. Also, freshwater fish generally thrive over a wide range of EC. High conductivity often results from high nitrate, phosphate and sodium in polluted waters. Measured EC values in the Sakumo basin ranged from 25.7 µS/cm to 49900 µS/cm. The highest EC was measured in the wetland and ranged from 42200 to 49900 µS/cm (Table 5.2). Measured EC in groundwater from the monitoring wells ranged from 1420 µS/cm to 5000 µS/cm whereas EC in the domestic wells ranged from 1550 µS/cm to 4390 µS/cm. EC of water from the shallow piezometers varied between 15450 µS/cm and 20050 µS/cm. Mean EC values in the streams Onukpawahe, Mamahuma and Dzorwulu measured 1850 µS/cm, 1950 µS/cm and 2020 µS/cm respectively. Mean conductivity of sewage was 4570 µS/cm whiles mean conductivity in rainwater samples recorded 63 µS/cm (Table 5.4). Lowest EC was measured in the dam (mean of 185 µS/cm). The maximum EC value was measured in the wetland during the dry season which was expected due to high evaporation leaving behind salts. The spatial distribution of EC within the study area is given in Figure 5.2.

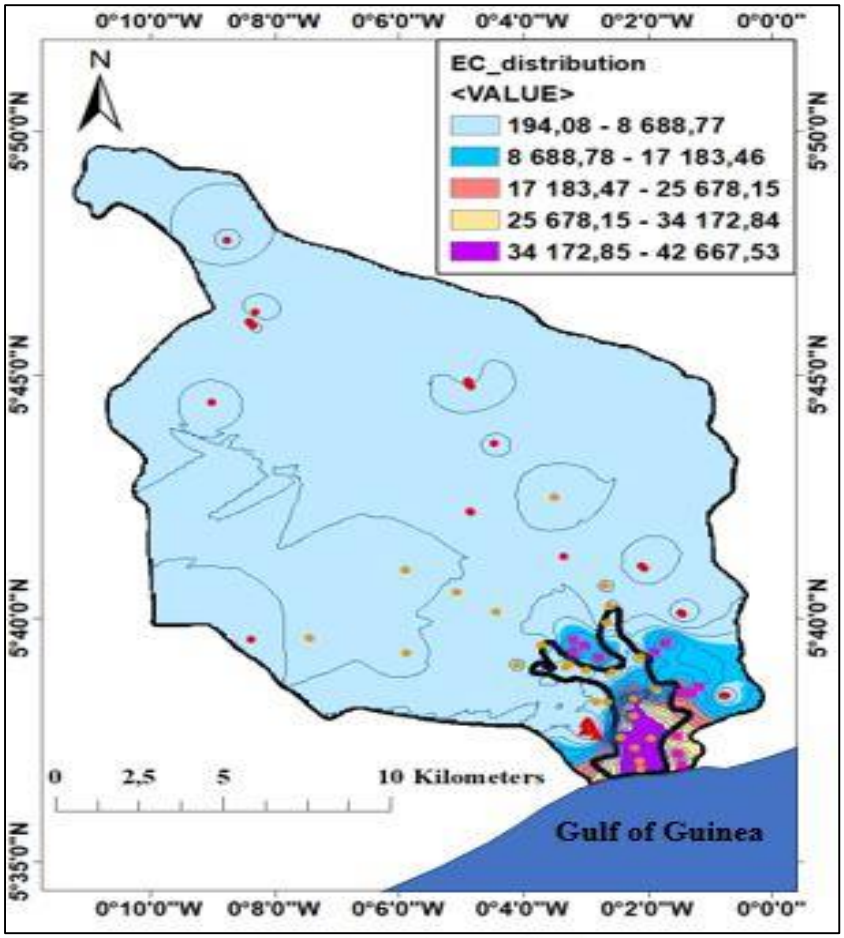




**Figure 5.2: Spatial distribution of EC in the study area**

The relationship between electrical conductivity and the major ions in the Sakumo basin are presented in Figure 5.3 a, b. Three major groups of waters can be identified according to the electrical conductivity measurements. The first are the wetland with mean EC higher than 20000 µS/cm. The second are the groundwater samples with mean EC lower than 5000 µS/cm. The third group are the streams with mean EC lower than 2000 µS/cm. The high concentrations of EC in the wetland (42,800 µS/cm) indicate high ionic concentration and can be attributed to high mineralization. The high EC in the water resources indicate high ionic concentration and can be attributed to high mineralization. The overall mineralization of wetland water is mainly controlled by Cl and Na, which account for 10.4−46.9% and 22.1−39.7% of the relative major ion content. For the groundwater group with EC lower than 5000 µS/cm, the relative Cl and Na contribution is in the range of 30.7−46.9% and 24.8−37.2% and respectively for 14.2−49.3% and 16.2−40.8% in the stream samples.

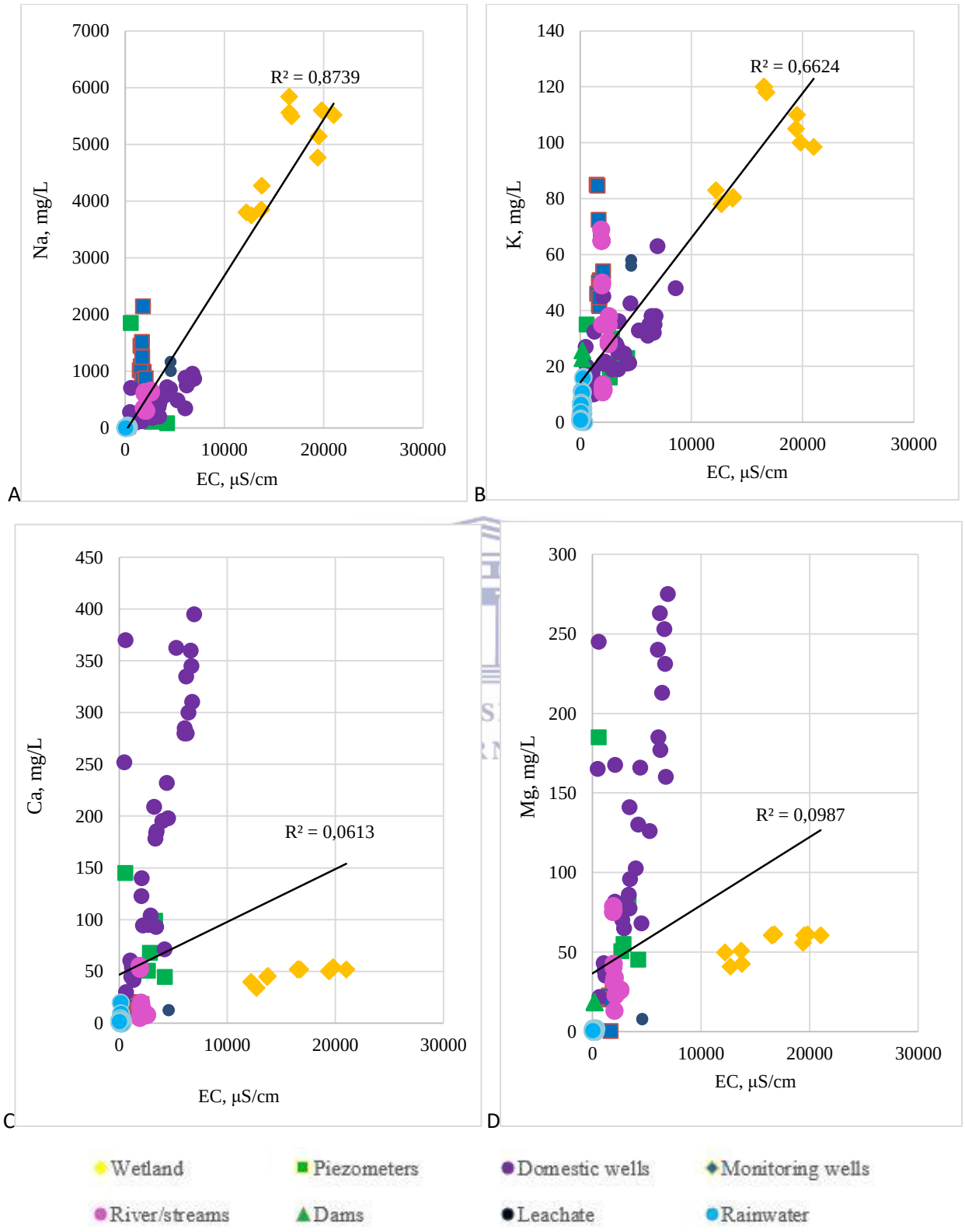


**Figure 5.3a: Relationship between electrical conductivity (µS/cm) and the major ions (mg/L) of the groundwater and wetland water samples**

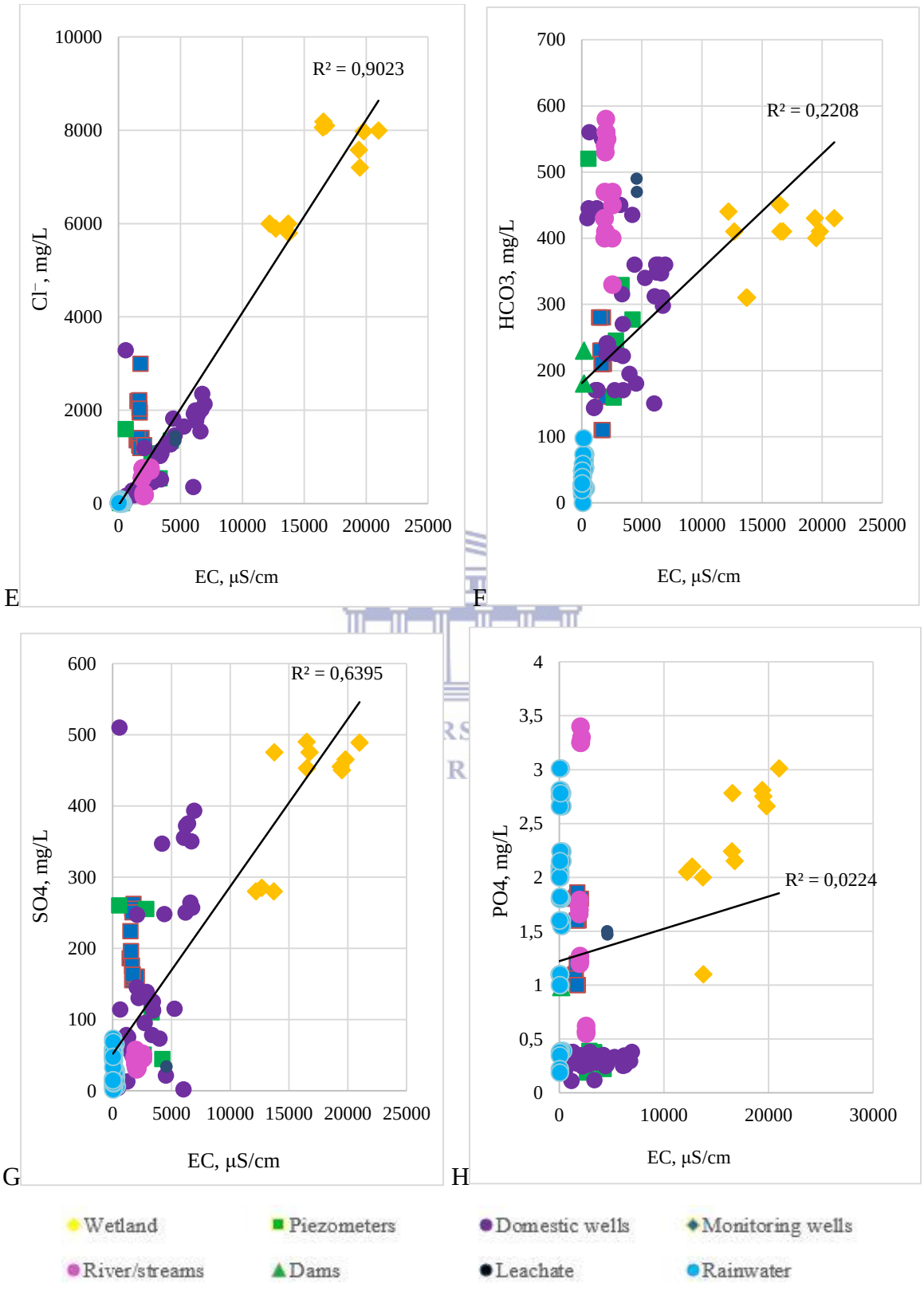


**Figure 5.3b: Relationship between electrical conductivity (µS/cm) and major ions (mg/L) in the groundwater and wetland water samples**

The highest correlation coefficients between EC and the major ion composition is computed for $Cl^-$ (r = 0.9023; Figure 5.2b, E), $Na^+$ (r = 0.874; Figure 5.2b, A), $K^+$ (r = 0.662; Figure 5.2a, B) and $SO_4^{2-}$ (r = 0.640; Figure 5.2b, G). Both $Na^+$ (R=0.87) and $Cl^-$ (R=0.90) were linearly correlated with EC indicating primary salinity contributors in the waters (Mazor, 1991). Consequently, the waters are mostly classified as Na–Cl facies (Section 5.2). $K^+$ (R=0.66) and $SO_4^{2-}$ (R=64) shows a moderate correlation with EC and this could be attributed anthropogenic sources such as fertilizer input and sewage. The remaining ions having correlation coefficient of $HCO_3^-$ (R=0.22), $Mg^{2+}$ (R=0.10), $Ca^{2+}$ (R=0.06) and $PO_4^{3-}$ (R=0.02) with EC shows a lesser contributor towards salinity in the catchment.

The high EC values in the wetland could be due to many factors including sea water intrusion, discharge of industrial effluents, sewage from the urbanized area and run-off from agricultural farms. High EC in water may produce unpleasant taste, odour and colour and causes physiological reactions in the consumer as in (Spellman & Drinan 2000). This could account for the bad odour and taste of the water in the Sakumo basin as confirmed by some residents in the study area. Minimum salt content (150 to 500 µS/cm) is desirable to support diverse aquatic life hence, the high conductivity in the wetland will cause a reduction in fish species population. The high electrical conductivity measured is an indication of the anthropogenic activities in the basin.



#### 5.2.1.2 Major ions chemistry in water

The amount and nature of the major ions concentration in the wetland and groundwater samples depend on the underlying geology in the basin. The Sakumo wetland is dominated by readily soluble carbonate and sulphate rocks from the Dahomeyan formation which undergoes partial dissolution under favourable conditions. Alkalinity of water is the amount of buffering material in the water. Alkalinity may be due to carbonate ($CO_3^-$), bicarbonate ($HCO_3^-$) or hydroxide ion concentration. A water body with high bicarbonate is more stable and resistant to changes in pH and vice visa. Coastal systems tend to reflect high bicarbonate ($HCO_3^-$) and other ions relatively consistent with ionic composition of seawater. $HCO_3^-$ in coastal wetlands results from the carbonation of carbonates, aluminosilicates, and silicates minerals (Hodson *et al*., 2002). Anthropogenic sources of bicarbonate concentrations in wetland waters include land-use activities such as application of chemical fertilizers (Stets *et al*., 2014).

Measured alkalinity ($HCO_3^-$) in the sampled waters ranged from 45.0 mg/L to 560 mg/L. $HCO_3^-$ concentration measured in the wetland ranged between 280 mg/L to 560 mg/L. Mean $HCO_3^-$ concentrations of 330 mg/L, 550 mg/L and 280 mg/L was measured in the monitoring wells, domestic wells and shallow piezometers respectively. Mean $HCO_3^-$ concentration of the streams (Onukpawahe, Mamahuma and Dzorwulu) measured 430 mg/L, 470 mg/L and 550 mg/L respectively whiles that for the sewage measured 480 mg/L. Lowest $HCO_3^-$ concentration was measured in rainwater (between 14.65 to 72.50 mg/L) whiles mean $HCO_3^-$ in the dams measured 180 mg/L. The highest $HCO_3^-$ was measured in the wetland and streams particularly the Dzorwulu river. The high $HCO_3^-$ concentration in the streams particularly the Dzorwulu stream was attributed to the presence of carbonates minerals in the rocks and the oxidation of organic matter from domestic sewage and run-off from agricultural farms. Aufdenkampe *et al*., (2011) found that, the total alkalinity (bicarbonate and carbonate ions) increased over time and space in the Mississippi River watershed due to agricultural practices. Alkalinity is important for fish and other aquatic life because it keeps the pH of the water fairly constant and makes the water less vulnerable to acid rain that may cause these changes. The spatial distribution of total alkalinity within the study area is given in Figure 5.4.

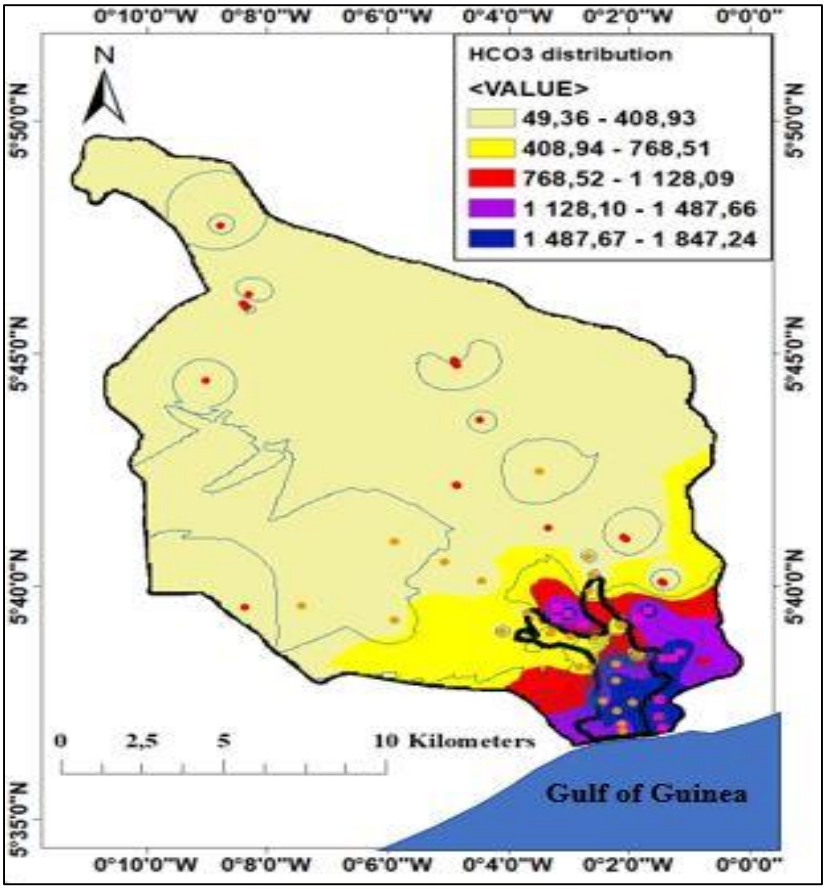




**Figure 5.4: Spatial distribution of EC in the study area**

Concentrations of chloride ion ($Cl^-$) measured within the catchment and over the study period ranged from 9.5 mg/L to 14095 mg/L with the wetland recording the highest $Cl^-$ concentration. Mean $Cl^-$ concentration of 11540 mg/L, 8095 mg/L and 11405 mg/L was measured in the monitoring wells, domestic wells and shallow piezometers respectively. Mean $Cl^-$ concentrations of the stream waters (Onukpawahe, Mamahuma and Dzorwulu) measured 550 mg/L, 560 mg/L and 430 mg/L respectively. Mean $Cl^-$ concentration measured in the sewage recorded 1350 mg/L was and 40 mg/L in the dam. The lowest $Cl^-$ concentration was rainwater (mean of 24.99 mg/L). The common sources of chlorides in the Sakumo basin are halite (NaCl), sea spray, brines and sewage outlet. The high $Cl^-$ concentration in the wetland was attributed to seawater encroachment, halite dissolution and sewage discharge into the wetland (Figure 5.3). High chloride ion causes severe problem in the crops at concentration >350 mg/L (Hopkins *et al.*, 2007). High chloride ions in the wetland is mainly due to the effect of sea water intrusion. The spatial distribution of chloride within the study area is given in Figure 5.5.

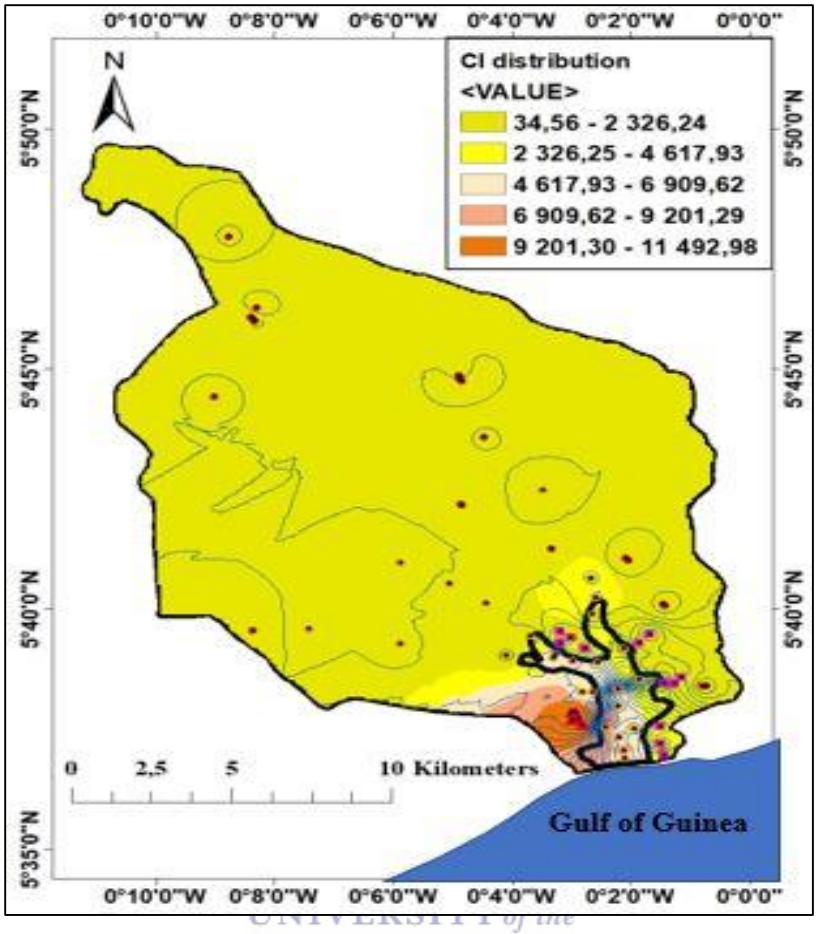




**Figure 5.5: Spatial distribution of Chloride in the study area**

Sodium is of great importance as an essential nutrient in wetland ecosystems. Sodium ion ($Na^+$) concentrations varied between 4.4 mg/L to 5840 mg/L with the highest $Na^+$ concentration measured in the wetland. Mean $Na^+$ concentrations of 2730 mg/L, 1880 mg/L and 4560 mg/L was measured in the monitoring wells, in the stream (Onukpawahe, Mamahuma and Dzorwulu) recorded mean values of domestic wells and shallow piezometers respectively. $Na^+$ concentrations measured 340 mg/L, 410 mg/L and 385 mg/L respectively. Mean $Na^+$ concentration measured in sewage recorded 950 mg/L. A mean $Na^+$ concentration of 50 mg/L was measured in the dam whiles the lowest $Na^+$ values of 17.5 mg/L was measured in rainwater. The high $Na^+$ and $Cl^-$ were attributed to sea water encroachment leading to the washing of solute evaporite as a result of the complete reversal of flow direction as high tide seawater enters the wetland. The high levels of Na and Cl ions in the study may indicate a significant effect of seawater mixing (Mondal *et al.*, 2010).

Another source of high $Na^+$ is industrial waste waters due to salts used in the chemical processes. The spatial distribution of sodium within the study area is given in Figure 5.6.

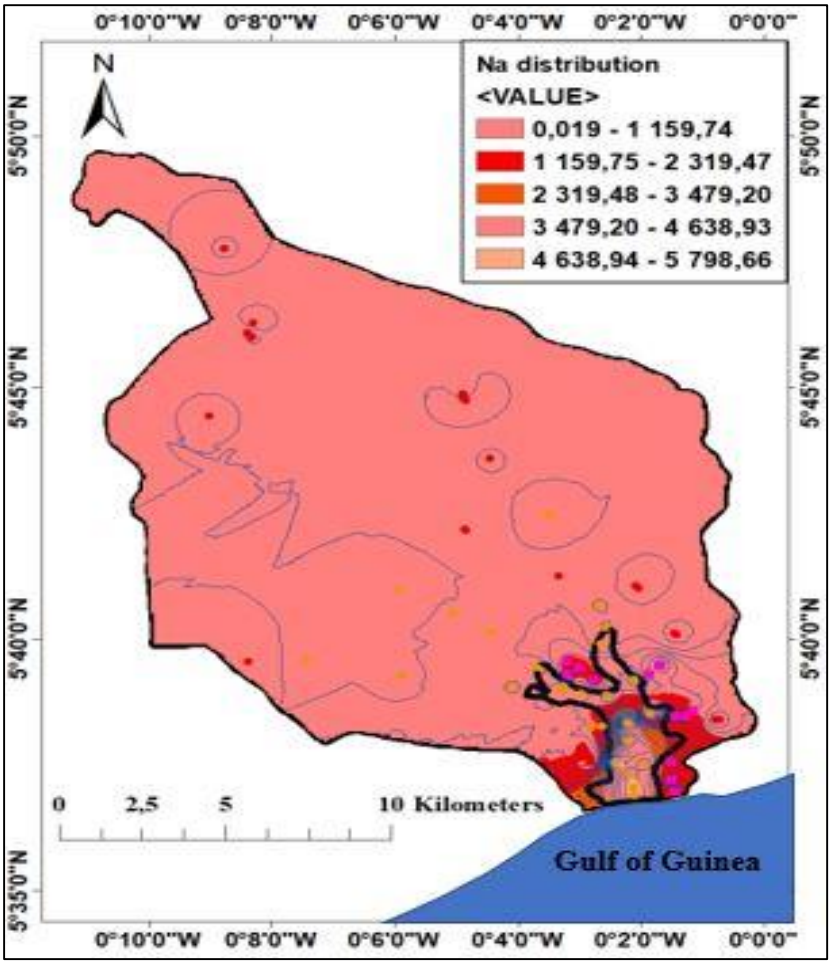


**Figure 5.6: Spatial distribution of Chloride in the study area**

Potassium (K) is an intracellular cation found mostly bound to protein in the body along with sodium where they influence osmotic pressure and contribute to normal pH equilibrium. $K^+$ concentration ranged between 0.5 to 120 mg/L with the highest concentrations measured in the wetland. Relatively high $K^+$ concentrations were also measured in the Dzorwulu and Onupkawahe streams (mean values of 65 and 58 mg/L respectively). $K^+$ concentration measured in the monitoring wells and domestic wells recorded mean concentrations of 60 and 70 mg/L respectively and 50 mg/L for the shallow piezometers. Mean $K^+$ values of the streams Onukpawahe,

Mamahuma and Dzorwulu measured 36, 65 and 12 mg/L respectively whereas $K^+$ concentration in domestic sewage measured 55 mg/L. Dam water measured mean $K^+$ concentration of 22.5 mg/L whiles the lowest $K^+$ concentration was measured in rainwater (mean value of 13.5 mg/L). The high $K^+$ values measured in the wetland and the streams was attributed to runoff from the use of fertilizers on agricultural lands along the banks of the streams and the upstream of the catchment. High potassium levels in the basin could also be attributed to the release of the metal in solution by the dissolution of K−feldspar from the rock minerals. The spatial distribution of potassium within the study area is given in Figure 5.7.

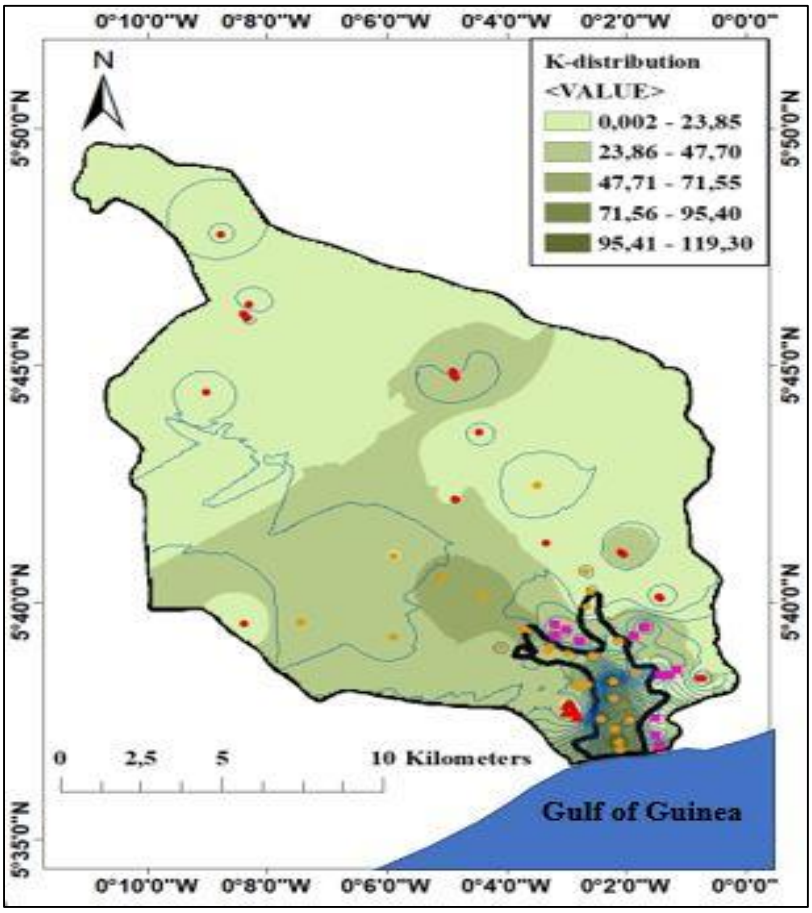


**Figure 5.7: Spatial distribution of potassium in the study area**

Concentrations of calcium ($Ca^{2+}$) varied from 0.52 to 61.15 mg/L within the catchment with the highest concentrations measured in groundwater and wetland. $Ca^{2+}$ concentration measured in the wetland ranged from 40 to 61 mg/L with a mean of 58 mg/L. A mean $Ca^{2+}$ concentration of 52.88

mg/L was measured in the monitoring wells and 160 mg/L in the domestic wells. Mean $Ca^{2+}$ concentration of water from the shallow piezometers measured was 25 mg/L. Mean $Ca^{2+}$ values of the streams Onukpawahe, Mamahuma and Dzorwulu measured 50, 28 and 34.20 mg/L respectively. Mean $Ca^{2+}$ concentration in domestic sewage measured was 12.5 mg/L. The concentration of $Ca^{2+}$ in the dam measured a mean 18.3 mg/L whiles $Ca^{2+}$ concentration measured in rainwater recorded mean value of 7.85 mg/L. The maximum allowable limit of calcium ion concentration in groundwater is 200 mg/L as per WHO 2004 classification. Figure 5.8 shows the spatial distribution of calcium in the study area.

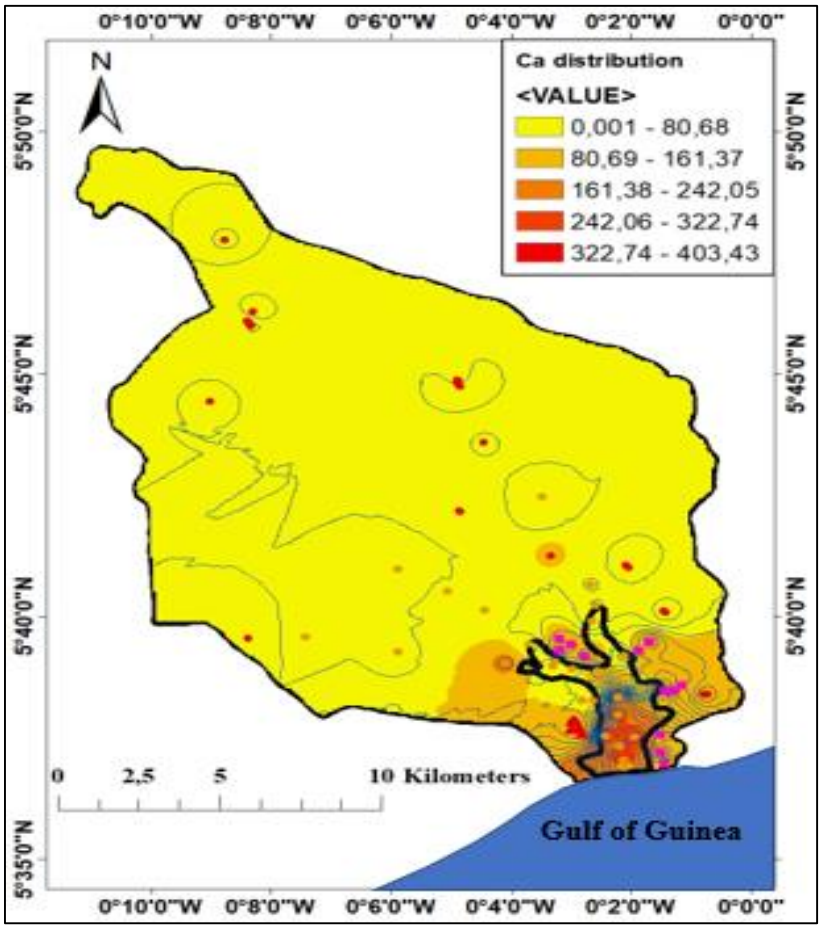


**Figure 5.8: Spatial distribution of calcium in the study area**

The high $Ca^{2+}$concentration in the groundwater could be due to the dissolution and precipitation of the calcite (Figure 5.9). The calcium-sulphate deposits dissolves as infiltrating water moves

through the soil (Schot *et al.*, 2004) changing the groundwater chemistry. The calcium-sulphate deposits dissolves when there is rain or freshwater inflow into the wetland which then influences the water chemistry of the wetland resulting in the high levels of calcium and sulphate ions in the water.

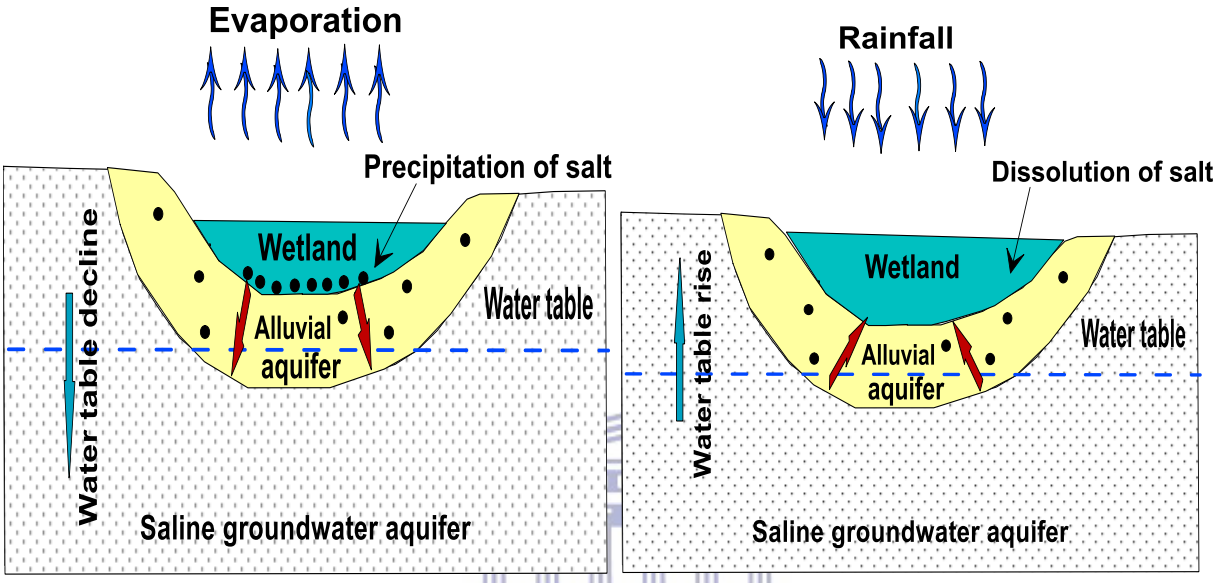


**Figure 5.9: Conceptual diagram of the precipitation and dissolution of salt in the groundwater-wetland system**



Magnesium ($Mg^{2+}$) is an essential element for living organisms hence occurs in organic matter and in many organometallic compounds. Groundwater from areas rich in magnesium containing rocks such as dolomite; $CaMg(CO_3)_2$ and magnesite ($MgCO_3$) may contain high concentrations of magnesium. Sulphate and chloride ions of magnesium are normally very soluble in water and this may contribute to the high concentrations of the ions in water. $Mg^{2+}$ concentrations in the catchment varied from 0.15 to 55 mg/L. $Mg^{2+}$ concentration measured in the wetland ranged from 34 to 55 mg/L with a mean of 52.40 mg/L. A mean $Mg^{2+}$ concentration of 50.10 mg/L was measured in the monitoring wells and 53 mg/L in the domestic wells and 32.45 mg/L the shallow piezometers. Water samples from the streams (Onupkawahe, Mamahuma and Dzorwulu) measured mean $Mg^{2+}$ concentrations of 14, 8.05 and 18 mg/L respectively. Mean $Mg^{2+}$ concentration in domestic sewage measured was 7.85 mg/L. $Mg^{2+}$ in the dam measured a mean 15.9 mg/L whiles $Mg^{2+}$ concentration measured in rainwater recorded mean value of 1.62 mg/L. Magnesium concentration in the water bodies was attributed to presence of mica from the

underlying geological material. $Mg^{2+}$ is liberated through weathering of biotite and amphiboles in the rock minerals. The spatial distribution of magnesium within the study area is given in Figure 5.10.

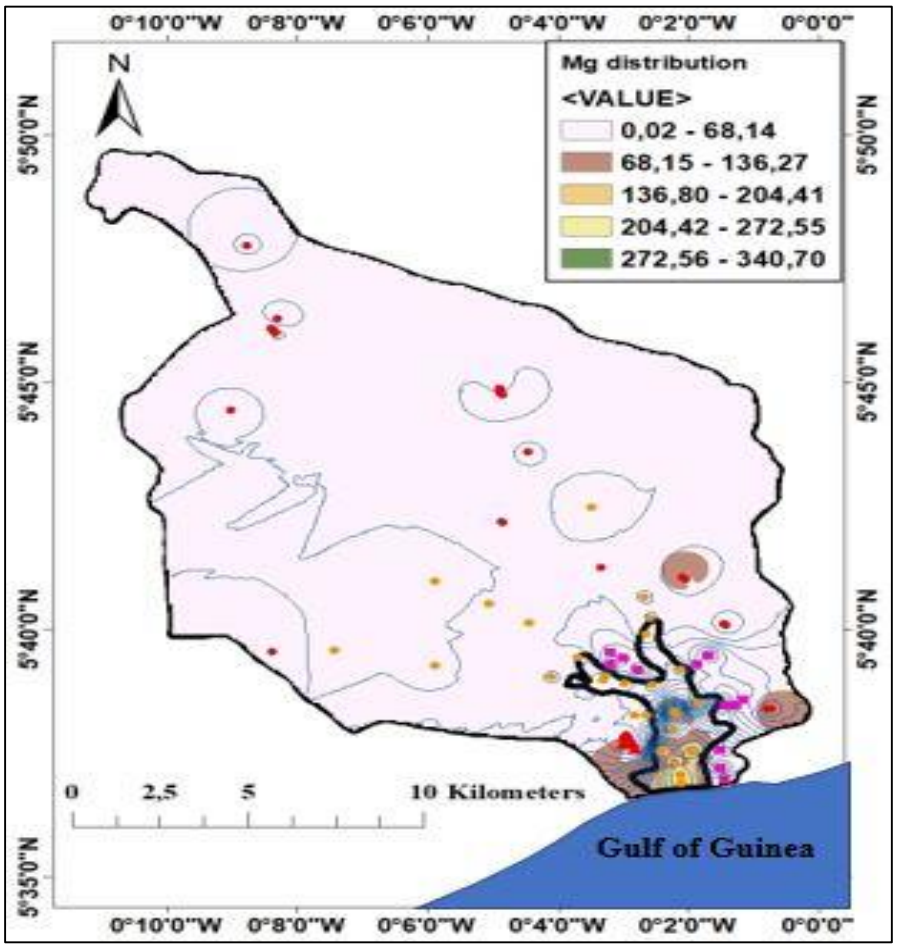


**Figure 5.10: Spatial distribution of magnesium in the study area**

Sulphates ($SO_4^{2-}$) concentrations are normally high in natural waters receiving waste waters from industries and runoff from agricultural lands where fertilizers have been used. $SO_4^{2-}$concentrations in the catchment varied from 4.65 to 585.90 mg/L with the highest concentration measured in the wetland. $SO_4^{2-}$ concentration measured in the wetland ranged from 280 to 585 mg/L with a mean of 425.40 mg/L. A mean $SO_4^{2-}$ concentration of 255.87 mg/L was measured in the monitoring wells and 375 mg/L in the domestic wells and 195.45 mg/L in the shallow piezometers. Water samples from the streams (Onukpawahe, Mamahuma and Dzorwulu) measured mean $SO_4^{2-}$ concentrations of 32, 48 and 57 mg/L respectively. Mean $SO_4^{2-}$

concentrations measured 34 mg/Lin the sewage, 45.7 mg/Lin the dam and 54.10 mg/L in rain water.

The major source of $SO_4^{2-}$ in the Sakumo basin could be attributed to sea water intrusion and the oxidation of pyrite. The other sources of sulphate is from dissolution of the small amounts of gypsum scattered through the groundwater, present in the catchment and the evaporation of the excess irrigation water. The dissolution of anhydrite and gypsum in the rock minerals which is evident by the high $Ca^{2+}$ and $SO_4^{2-}$ concentrations in the wetland waters. The presence of anaerobic sulphate-reducing bacteria (such as *Desulfovibrio)* in the wetland acts on the bacteria which is characteristic of the hydrogen sulphide ($H_2S$) odour of the wetland water. Studies by Readon & Harrell (1990) reported sulphate toxicity in some aquatic organisms including some fishes of concentrations at or below 100 mg/L sulphate. Sulphate especially $H_2S$ are quite soluble in water and are toxic to humans and fish. The high sulphate concentrations in the wetland could be toxic to the fishes and the foul smell repels fishes most fish species. The spatial distribution of sulphate within the study area is given in Figure 5.11.

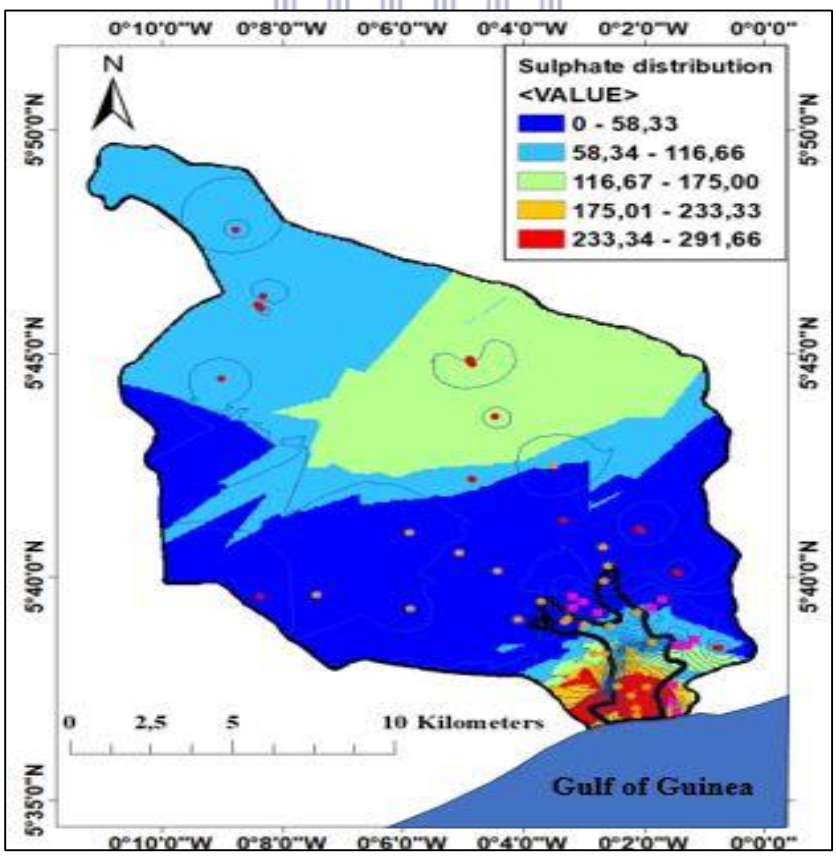


**Figure 5.11: Spatial distribution of sulphate ions in the study area**

The wide ranges in concentrations of $Na^+$ and $Cl^-$ (4.4–5840 mg/L and 9.5–14095 mg/L respectively) showed wide ranges whiles the concentrations of Ca, Mg and $SO_4^{2-}$ showed lower variations with ranges of 0.52–61.15, 0.15–359 and 1.8–50 mg/L, respectively. These distributions indicate that chemical composition is affected by multiple processes, including seawater mixing (Park *et al.*, 2005). The surplus concentrations of $SO_4^{2-}$ and $Cl^-$ in the basin is indicative of pollution aside seawater intrusion. Partial dissolution of the hornblende minerals in the underlying rocks increases the major ion concentration of the groundwater. The high sodium and calcium ions is as a result of the high mobility of the ions during weathering of granitic rocks due to their high concentration in plagioclase feldspar and mafic minerals and their high solubility in natural waters (Nesbitt *et al*., 1980). The high concentrations of $HCO_3^-$, $Ca^{2+}$ and $Mg^{2+}$ in the rock minerals and the wetland water resources reflect water–rock interaction. The order of relative abundance of cations in the wetland water was $Na^+ > Ca^{2+} > Mg^{2+} > K^+$ (on mg/L basis) with $Na^+$ ion constituting 86% of the total cation concentration, while the order of anions was $Cl^- > SO_4^{2-} > HCO_3^-$ with chloride concentration constituting 88% of the total anions concentration. The order of cations in the groundwater was in the order, $Na^+ > Ca^{2+} > Mg^{2+} > K^+$ (on mg/L basis), with $Na^+$ ion constituting 50% of the total cation concentration while the order of anions was $Cl^- > HCO_3^- > SO_4^{2-}$ with chloride concentration constituting 76% of the total anions concentration.



#### 5.2.1.3 Nutrient load in the water

Nitrogen (N) in the form of dissolved nitrate ($NO_3^-$) is an important nutrient for vegetation and is an essential element for all life. Nitrogen is originally fixed from the atmosphere and then mineralized by soil bacteria into ammonium. $NO_3^-$ in soil that is utilised by plants partly returns to the soil when the plants die. The nitrate in the soil however is artificially increased when nitrate fertilisers are used. Farm animals also produce considerable amounts of nitrogenous organic waste. High nitrate concentrations in groundwater under cultivated areas, intensive horticulture areas and on animal farms, results from direct leaching of nitrate from fertilisers and reduced nitrogen compounds. The $NO_3^-$ ions concentrations of all the groundwater samples are within the desirable limit of 45 mg/L as per WHO 2004 standard.

High concentration of nitrate ($NO_3^-$) and phosphate ($PO_4^{3-}$) speeds up the growth of algae in water. This algae take-up oxygen hence reducing oxygen levels in water (anaerobic) which affects the

quality of water (Akpabli & Drah, 2001). Nitrates of potassium and ammonium ($KNO_3$ and $NH_4(NO_3)$ are an important source of nitrogen in chemical fertilizers. Measured $NO_3^-$ concentrations in the basin ranged from 0.38 to 42 mg/L with the highest concentration measured in the wetland. Mean $NO_3^-$ concentrations of 1.05, 4.0 and 1.23 mg/L was measured in the monitoring wells, domestic wells and shallow piezometers respectively. $NO_3^-$ concentrations measured in the stream (Onukpawahe, Mamahuma and Dzorwulu) recorded mean values of 0.49, 1.20 and 0.85 mg/L respectively. Mean $NO_3^-$ concentration measured in sewage recorded 0.40 and 17.5 mg/L in rain water. The highest $NO_3^-$ concentration of 42.0 mg/L was measured in the dam. The areas around the dams are places of intensive farming and cattle grazing. The sources of nitrates in the basin is from the use of fertilizers, livestock waste and domestic and industrial wastewater. The high $NO_3^-$ concentrations in the dam was attributed to runoff from the use of fertilizers on farms. The low $NO_3^-$ concentrations in the wetland could be attributed to the uptake of nitrate by plants and algae. The spatial distribution of Nitrate within the study area is given in Figure 5.12.

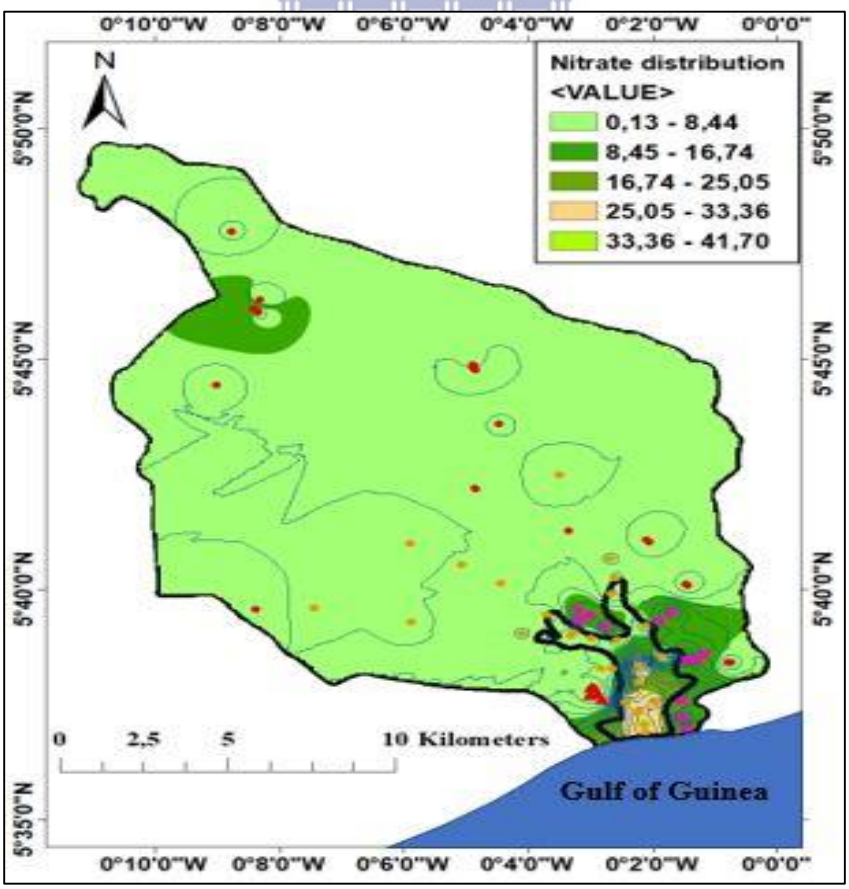


**Figure 5.12: Spatial distribution of Nitrate in the study area**

Phosphorus in the form of phosphate, is an important essential nutrient in wetland ecosystems and can exist in water in both dissolved and particulate forms (Baird, 2000). Phosphate in most natural surface waters ranges from 0.005 to 0.020 mg/L (Chapman, 1992). Measured $PO_4^{3-}$ concentrations values were generally high (more than the WHO limit of < 0.3 mg/L). Measured $PO_4^{3-}$ concentrations in the catchment ranged from 0.04 mg/L to 14.78 mg/L with the highest concentration measured in the wetland. Mean $PO_4^{3-}$concentrations of 0.37, 0.25 and 1.82 mg/L were measured in the monitoring wells, domestic wells and shallow piezometers respectively. The concentrations of $PO_4^{3-}$ measured in the streams (Onukpawahe, Mamahuma and Dzorwulu) recorded mean values of 3.30, 1.70 and 1.55 mg/L respectively. Mean $PO_4^{3-}$ concentration measured in sewage measured 1.50 and 1.6 mg/L in the dam.

The high phosphate value recorded around the wetland could be attributed to the application of phosphate containing inorganic fertilizer to rice farms. The high $PO_4^{3-}$ concentration in the wetland resulted in the observed eutrophic condition of the wetland. The effect of high $PO_4^{3-}$ concentration in water causes a reduction in fish production as a result of depleted oxygen in the water.

#### 5.2.1.4 Trace metals in the water



Trace metals have serious implications in the natural environment due to their toxicity, persistence and ability to be incorporated into food chains. Living organisms require trace amounts of some trace metals such as, iron, cobalt, manganese, copper, molybdenum, strontium, vanadium and zinc. However, high levels of these metal can be toxic to organisms. Non-essential heavy metals such as cadmium, chromium, mercury, lead, arsenic, are of concern when found in groundwater and surface water systems even in low concentrations due to their toxicity, persistence and ability to be incorporated into food chains. Hence their presence in the natural waters is normally undesirable. Wetlands especially, acts as sinks as they are able to filter pollutants from water before discharging hence retaining most metals in the wetland sediments.

Low levels of trace metals Iron (Fe), Manganese (Mn), Copper (Cu) and Zinc (Zn) were measured during the duration of the study. Other potentially toxic elements such as lead, (Pb), arsenic (As), mercury (Hg), Chromium (Cr), Cadmium (Cd) and Cobalt (Co) were, however, below detection of the instrument used. The low levels of the measured metals could be due to the fact that the, metals form insoluble precipitates in solution under some specific physical and chemical

conditions in the water and this may control the solubility of these metals. For instance, the solubility of Cd, Pb, Cu, Hg, As and Cr increases with the decreased pH thus, in alkaline waters, these metals form insoluble precipitates in solution (Li *et al*., 2013). Sources of trace metals in the environment include atmospheric deposition, erosion of the geological matrix or from anthropogenic sources such as, industrial and domestic waste and runoff from agricultural lands. Domestic waste from settlements can also introduce metals into the solid waste stream in the form of batteries, used engine oils, paint chips, ceramics, consumer electronics, electric light bulbs, and plastics.

Ferrous iron ($Fe^{2+}$) is a common constituent of anoxic groundwater. Its origin may be the partial oxidation of pyrite (FeS), the dissolution of $Fe^{2+}$ containing minerals, or reductive dissolution of iron oxides. Appelo & Postma (2005) suggest $Fe^{2+}$ to be the dominant form of dissolved iron in the pH range of most groundwater (pH of 5 to 8), since under this condition $Fe^{3+}$ is insoluble. Fe concentrations ranged from 1.47 to 8.99 mg/L with the highest concentration measured in the wetland water. Fe is abundant in the earth crust. The presence of iron in the wetland may be derived from the reductive dissolution of iron species present in the area in the presence of organic matter which is catalysed by micro-bacteria's (Appelo & Postma, 1999). The relatively high (above the EPA criteria for freshwater aquatic life of 1.0 mg/L) iron concentration in the wetland does not pose danger to wetland aquatic life due to high oxygen levels in the water. The spatial distribution of iron within the study area is given in Figure 5.13.

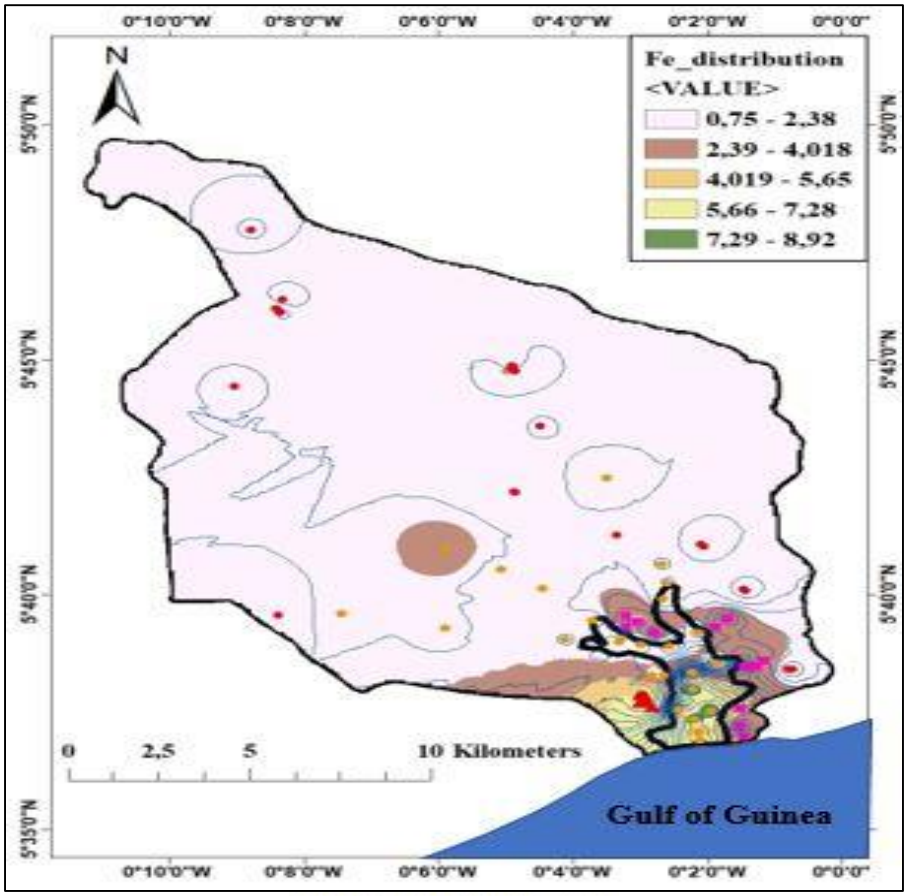




**Figure 5.13: Spatial distribution of iron in the study area**

Manganese (Mn) is an essential element which has biological significance in fishes when in low concentrations. Mn often occurs in association with Fe compounds and is found in waters low with oxygen (WRC, 2003). Manganese normally also occurs in rocks however, humans enhance manganese concentrations in the environment by industrial activities and through the burning of fossil fuels (Nayaka *et al*., 2009). Manganese derived from human sources such as through the application of manganese pesticides, can also enter surface water, groundwater, sewage water and into soils (Nayaka *et al*., 2009). Measured concentration of manganese in the wetland water varied from < 0.001 to 0.78 mg/L. The high Mn concentration in the wetland was attributed to weathering of the rock mineral garnet found in the rock formation. The spatial distribution of manganese within the study area is given in Figure 5.14.

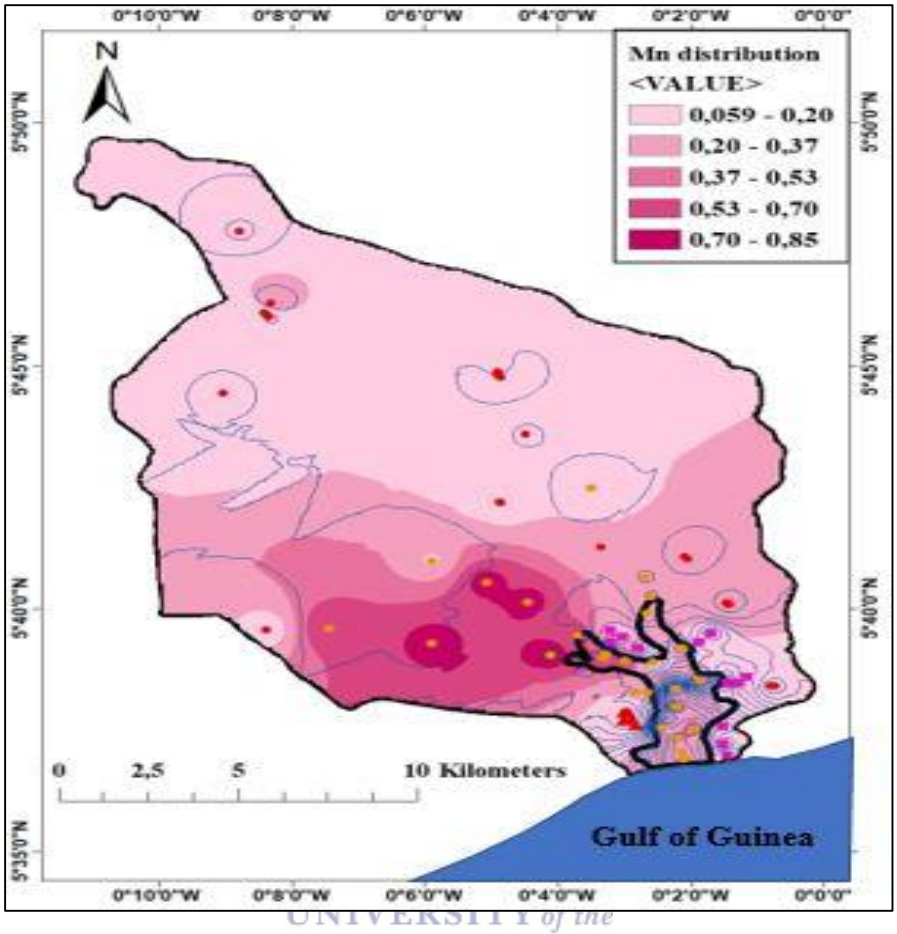




**Figure 5.14: Spatial distribution of manganese in the study area**

Copper (Cu) occurs naturally in the environment and spreads through natural and artificial phenomena. Examples of natural sources of the metal are wind-blown dust, decaying vegetation, potash from ashes and sea spray. The production of phosphate fertilizer and Cu-based fungicides used in agriculture is another means by which Cu is introduced into the environment (Nayaka *et al*., 2009). Copper bioaccumulates in tissues and organs, hence even low concentrations of the metal in the water is undesirable. The concentration of Cu in the wetland water varied from 0.08 to 0.28 mg/L with a mean concentration of 0.19 mg/L. The source of the metal was traced to run-off from agricultural land polluted with cu-based fungicides. The spatial distribution of copper within the study area is given in Figure 5.15.

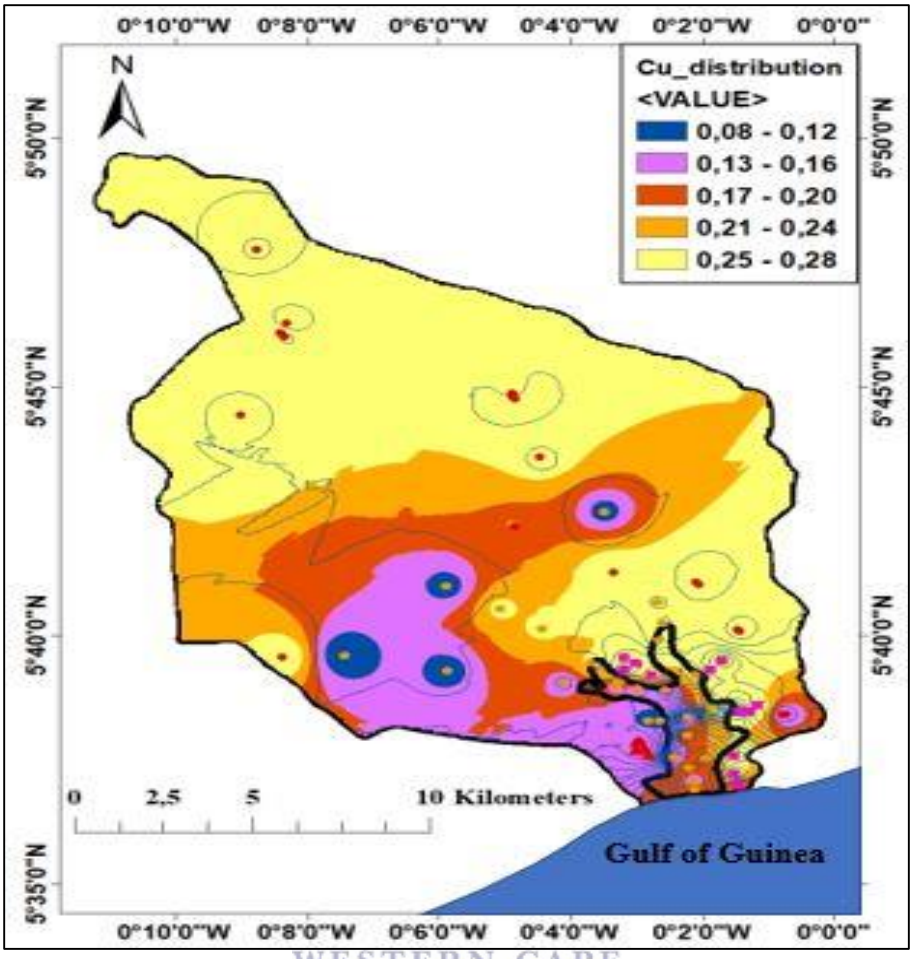




**Figure 5.15: Spatial distribution of copper in the study area**

High concentrations of zinc (Zn) in aquatic environment is normally toxic to some aquatic organisms such as fish. The mean Zn concentrations in the wetland water varied from <0.01 to 0.08 mg/L. These values were within the WHO (2011) standard levels for water and wastewater. The presence of Zn in the wetland water was attributed to natural sources resulting from the weathering of minerals and forms a number of soluble or insoluble salts. The spatial distribution of the zinc measured in the study area are presented in Figure 5.16. All the metals, Fe, Mn, Cu and Zn exhibited low concentrations in the basin. The metals were mostly concentrated in the areas with farming activities especially around the wetland and the dams.

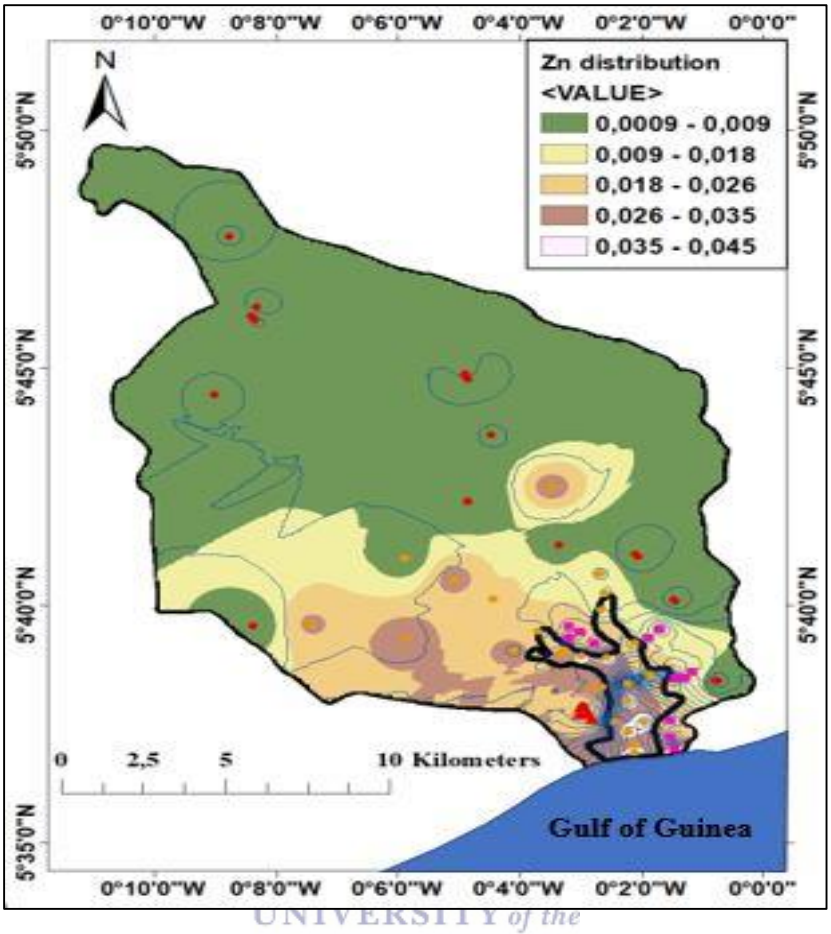




**Figure 5.16: Spatial distribution of zinc in the study area**

### 5.2.2 Hydrogeochemical processes controlling the water chemistry

Bivariate plots can be used to identify the major geochemical processes controlling the chemical composition of groundwater and wetland water in the study area. Scatter plots of selected physicochemical parameters from rainfall, groundwater, river, wetland and seawater sample, expressed in meq/L, are presented in Figure 5.17. Generally, rainwater, river and streams samples are less saline whiles the groundwater are moderately and the wetland waters the most saline. In the bivariate diagram in Figure 5.17 a of Na versus Cl, sodium increases linearly with respect to chloride, showing a high correlation index ($R^2$=0.997). The increase in $Na^+$ and $Cl^-$ content indicates seawater intrusion (Lee & Song 2007), high evaporitic levels of sea water and the halite content in sea aerosols which may cause rain water with a water composition of the sodium chloride type.

Na/Cl ratio is one of the good indicative factors of evaporation process in groundwater. Evaporation will increase the concentration of total dissolved solids in groundwater whiles the Na/Cl ratio remains the same. If evaporation is the dominant process, Na/Cl ratio should be constant when EC increases (Jankowski & Acworth 1997). The Na/Cl vs EC scatter diagram of the groundwater samples in the basin in Figure 5.17 b shows that, the trend line is slightly inclined and Na/Cl ratio decreases with increasing salinity (EC) which seems to be removal of sodium by ion exchange reaction. This indicates that, evaporation may not be the major geochemical process controlling the chemistry of groundwater in this study area. In the saline groundwaters, Na/Cl ratios are nearly constant and are mostly between the seawater value of ~0.86 and observed brine water value of ~0.71.

A plot of $SO_4^{2-}$ against $Cl^-$ showed a moderate positive correlation of 0.67 (Figure 5.17, c). This implies the effect of contamination especially irrigation return flow since the application of gypsum fertilizer is very common in the rice fields in the study area. The saline groundwater is characterized by low ratios of Na/Cl and $SO_4^{2-}$/ $Cl^-$ compared to the fresh and brackish water (Figure 5.17 a, c); indicating a contribution of mineral weathering to the overall solute load at low salinities of the groundwater which becomes overwhelmed at high salinity.

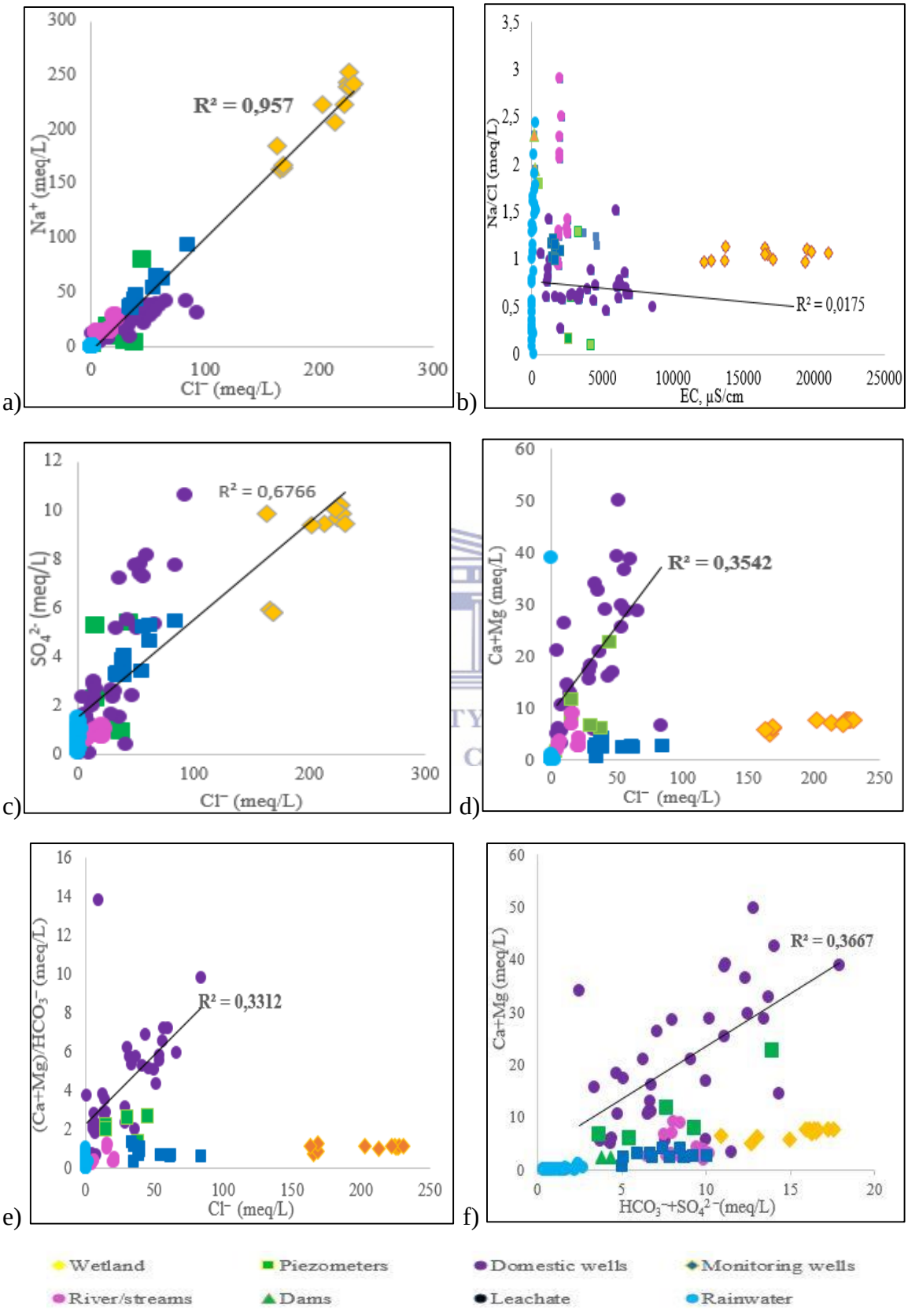


**Figure 5.17: Scatter plot of selected parameters expressed in meq/L**

The plot of (Ca+Mg) versus ($Cl^-$) (Figure 5.17, d) indicates that Ca and Mg increase with increasing salinity. The plot of (Ca+Mg) versus ($Cl^-$) shows that, salinity increases with the decrease in Na/Cl and increase in Ca+Mg, which may be due to reverse ion exchange in the clay/weathered layer. During this process, the groundwater materials may adsorb dissolved sodium in exchange for Ca and Mg. The rock of the Sakumo basin consists of mainly of alumino−silicate minerals and weathering of the alumino−silicate minerals particularly plagioclase (albite), hornblende, micas and pyroxenes will increase the concentration of $Na^+$, $Ca^{2+}$, $Mg^{2+}$, $K^+$ and $HCO_3^-$ in the groundwater. The source of Ca and Mg in groundwater is further deduced from the (Mg+Ca)/$HCO_3^-$ ratio with Cl (Figure 5.17, e). As the (Ca+Mg)/$HCO_3^-$ ratio increases with salinity, Ca and Mg are added in solution at a greater rate than $HCO_3^-$. If Ca and Mg originate solely from the dissolution of carbonates in the groundwater materials and from the weathering of pyroxene or amphibole minerals, the (Ca+Mg)/$HCO_3^-$ ratio would be about 0.5 (Sami, 1992), as the governing weathering equations would be as presented in Eqs. 5.1, 5.2 and 5.3:

For calcite:

$$CaCO_3 + H_2O+CO_2 <-> Ca +2HCO_3 \quad (5.1)$$

For pyroxene:

$$Ca_2Mg_5(SiO_6) + 4CO_2+ 6H_2O <-> Ca+Mg+4HCO_3+Si(OH)_4 \quad (5.2)$$

For amphiboles:

$$Ca2Mg5Si8O_{22}(OH)_2 + 14CO_2+22H_2O <-> 2Ca+\%Mg+14HCO_3+8Si(OH)_4 \quad (5.3)$$

The scatter plot of (Ca+Mg) versus ($HCO_3^-$+$SO_4^{2-}$) in Figure 5.17 f, is used as an indicator of the geochemical processes occurring in the groundwater. According to Elango & Kannan (2007), the samples falling above the 1:1 line indicate dissolution of carbonate minerals, whereas samples below the 1:1 line are characterized by dissolution of silicate minerals. The plot of (Ca+Mg) versus ($HCO_3^-$+ $SO_4^{2-}$) in Figure 5.17 f shows that, most of the groundwater samples are clustered around the 1:1 line. This may be attributed to the composition of the alluvial groundwater in the basin. An excess of calcium and magnesium in the groundwater of may be due to the exchange of sodium in the water by calcium and magnesium in clay material.

### 5.2.3 Environmental stable isotopes of the wetland water resources

Over the past three decades, environmental isotopes of water have been used as tracers in understanding the source and flow paths of various elements of the hydrological cycle (Kendall & McDonnell 2012). Environmental stable isotopes have been used to evaluate hydrogeochemical processes such as defining groundwater flow, groundwater recharge, groundwater–surface water interaction and catchment hydrology (Gat, 1996; Gibson *et al.*, 2005). Environmental isotopes of oxygen-18 and deuterium for example, have been used to determine seasonal contributions of precipitations to groundwater, rivers and lakes in some parts of the Ghana (Akiti, 1980). Recent investigations by Glover *et al*., (2013) focused on the description of the regional isotopic composition of groundwater in the Accra plains. The analysis of environmental isotopes in groundwater, rainwater and wetland has not been studied in details within the Sakumo basin (Nonterah *et al.,* 2015). Hence, this study presents findings of the relationship between the isotopic variation in all three components.

#### 5.2.3.1 Origin and recharge of the groundwater

The oxygen-18 and deuterium signatures of the rainwater, groundwater and wetland water are presented in Appendix 5.2 a, b. The environmental isotope data are expressed as per mil deviations from VSMOW standard. From the analysis, $\delta^{18}O$ and $\delta^{2}H$ values ranged from -35.21 to 10.29‰ and -5.33 to 1.60‰ for rainwater with mean values of -3.39 and -1.40 respectively. The statistical summary of $\delta^{18}O$ and $\delta^{2}H$ signatures in the rainwater are presented in Table 5.5.

**Table 5.5: Statistical summary of environmental isotopes of rainwater samples in the Sakumo basin**

| | $\delta^{18}O$‰ | $\delta^{2}H$‰ | d-excess |
|---|---|---|---|
| Minimum | -5.33 | -35.21 | -19.04 |
| Maximum | 1.60 | 10.29 | 14.71 |
| Mean | -1.40 | -3.39 | 6.36 |

$\delta^{18}O$ and $\delta^{2}H$ values of the groundwater samples ranged from -3.80 to -2.01‰ and 17.00 to -10.32 ‰ with mean values of -3.01 and -13.58 respectively. The statistical summary of $\delta^{18}O$ and $\delta^{2}H$ signatures in the groundwater samples are presented in Table 5.6.

**Table 5.6: Statistical summary of environmental isotopes data of the groundwater in the Sakumo basin**

| | $\delta^{18}O$‰ | $\delta^{2}H$‰ | d-excess |
|---|---|---|---|
| Minimum | -3.80 | -17.00 | 4.73 |
| Maximum | -2.01 | -10.32 | 13.50 |
| Mean | -3.01 | -13.58 | 10.60 |

The wetland and the dams recorded $\delta^{18}O$ values ranging between -1.25‰ to -10.60‰ and deuterium values of 4.10 to 13.38 ‰ with mean values of -8.07 ad 9.3 ‰ respectively. The dams recorded mean isotopic values of 19.12 ‰ and 2.73‰ for $\delta^{18}O$ and $\delta^{2}H$ respectively; the highest values recorded during the present study. The statistical summary of $\delta^{18}O$ and $\delta^{2}H$ signatures in the wetland are presented in Table 5.7.



**Table 5.7: Statistical summary of the environmental isotopes of the Sakumo wetland water**

| | $\delta^{18}O$‰ | $\delta^{2}H$‰ | d-excess |
|---|---|---|---|
| Minimum | -1.25 | 4.10 | -6.00 |
| Maximum | -10.60 | 13.38 | -5.07 |
| Mean | -8.07 | 9.3 | -3.56 |

A plot of the $\delta^{18}O$ and $\delta^{2}H$ data of all the sampled waters in the Sakumo basin is presented in Figure 5.18. GMWL is the Global Meteoric Water Line and LMWL is the Local Meteoric Water Line. The plot shows four Groups (Gr: A, B, C and D. Group A, consisting of the groundwater samples and showed a meteoric origin, as their isotopic composition is similar to that of rainfall. The groundwater samples grouped on a narrow range, around the LMWL and GMWL (Figure 5.18). This indicates a relatively well mixed system which also reflects the average rain water isotopic values in the basin. The depleted nature of the environmental isotope composition of the

groundwater suggests a meteoric origin. This is indicative of rainwater contribution (recharge) which may have undergone slight evaporation during the fall. The $\delta^{18}O$ and $\delta^{2}H$ plot in Figure 5.8 suggests that there is little or no seawater infiltration into the groundwater. Hence, the source of salinity in the groundwater may be due to sea sprays and the ions in the rainwater.

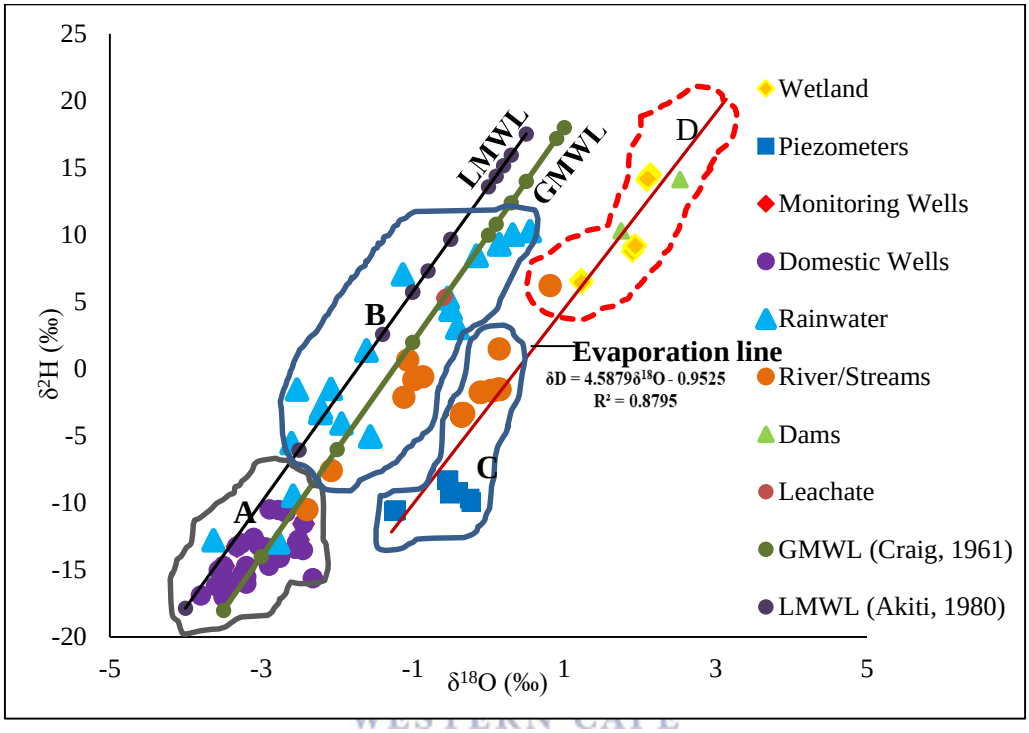


**Figure 5.18: $\delta^{2}H$ (‰) vs $\delta^{18}O$ (‰) plot with GWML and LMWL**

Group B, consisting of rain water shows slightly evaporated waters with enriched isotopic signatures. The isotopic signatures of the rain water samples overlay the global meteoric water line (GMWL), defined by Craig (1961) as the average relationship between $\delta^{18}O$ and $\delta^{2}H$ in natural terrestrial (Figure 5.18). This could be due to effect of rainfall that derives from weather fronts coming from the Atlantic Ocean. The rainwater and the groundwater samples have almost the same isotopic compositions which suggest that the source of water to the groundwater is mainly from rainfall.

Group C, consist of the streams and shallow piezometers samples. The isotopic signatures of the streams fall directly below the LMWL (the same as some rainwater signatures). The isotopic composition of this group presents mixed waters of various composition of rainwater and wetland

waters. The $\delta^{18}O$ and $\delta^{2}H$ isotopic composition of the streams ranged from -2.01 to 0.81‰ and -6.53‰ to 6.25‰, with mean values of -1.19 and 0.76‰ respectively. Enriched $\delta^{18}O$ isotopic values were measured in the dry season, whiles comparatively depleted $\delta^{18}O$ values were measured in the rainy season. The measured stream samples showed more enriched isotopic data than the rainwater.

Group D consist of mainly the wetland and dam samples. This group shows highly evaporated waters with enriched isotopic values. The relationships between $\delta^{18}O$ and $\delta^{2}H$ in wetland and dam waters diverge from the GMWL that forms a semi-linear trend of evaporated waters (Figure 5.9). This indicates that the wetland and dam waters are affected by direct evaporation of raindrops and dam water in the wetland. The evaporated waters of the wetland are parallel to that of the groundwater which suggests that there is no significant contribution of groundwater to the wetland water. Hence, giving the groundwater and wetland water different distinct isotopic signatures, which shows no interaction between the wetland and groundwater samples.



#### 5.2.3.2 Deuterium excess

The deuterium excess (d-excess) defined by Dansgaard (1964) as the intercept of the GMWL is expressed in Eq. 5.4 as:

$$d = \delta^{2}H - 8\delta^{18}O \quad (5.4)$$

The d-value is close to 10 for meteoric waters on the global scale. This is due to slower diffusion of $H_2{}^{18}O$ relative to $H_2{}^{16}O$ ($^{2}H(H_2{}^{18}O)/^{2}H(H_2{}^{16}O) = 0.9691$) than $H^{2}H^{16}O$ relative to $H_2{}^{16}O$ ($^{2}H(H^{2}/H^{16}O)/ {}^{2}H(H_2{}^{16}O)=0.9839$) during evaporation occurring at the air–sea interface (Cappa *et al*., 2003). The mean d-excess obtained for the groundwater samples in the Sakumo basin during this study is 10.60‰ with a range from 4.73 to 13.50‰. The wetland water and rainwater d-excess value had maximum values of -5.07 and 14.71‰ and minimum values of -6.0 and -19.04‰, respectively. The respective mean values are -3.56 and 6.36‰. The wide variation in the rain water d-excess value suggests a contribution of local isolated moist air masses resulting in uncharacteristic low d-excess values. Figure 5.19 shows the relationship between $\delta^{18}O$ and d-excess.

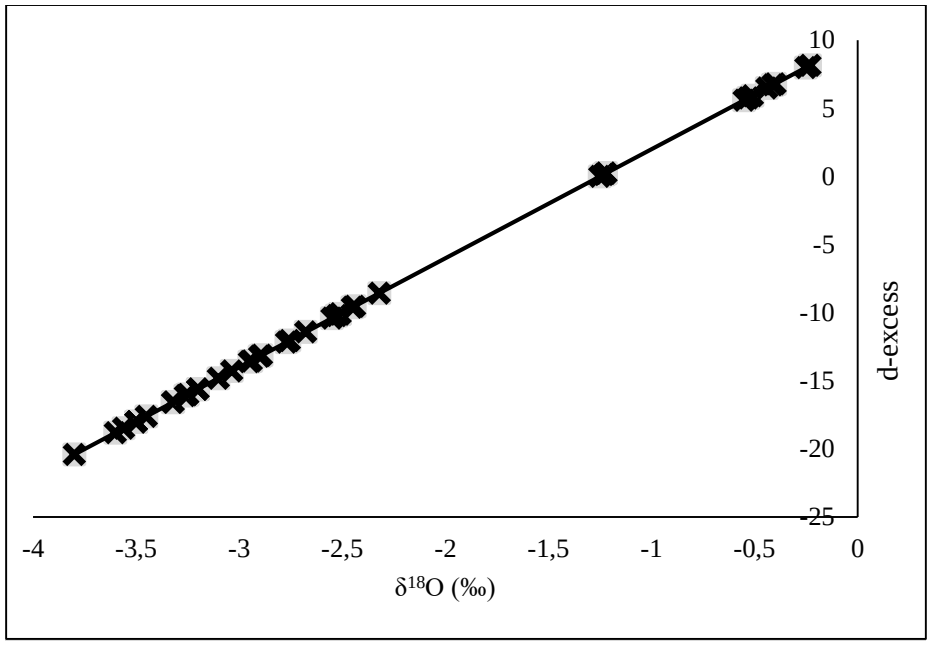


**Figure 5.19: Cross-plot of d-excess verses $\delta^{18}O$‰ of the groundwater samples in the study area**



Most of the groundwater samples had d-excess above 10‰ (Appendix 5.1d). The high d-excess in the basin could be could be due to two possibilities: One is the variation within rain events which is likely due to bimodal rainfall in the area. The other possibility could be as a result of fractionation process which affects deuterium signature. This results to addition of kinetically controlled reevaporated component from the wetland and dam waters to the oceanic vapour. This process is defined by Coplen & Hanshaw (1973) as ultrafiltration. Hoefs (2004) showed that the hydrogen isotopes fractionation is affected by the absorption of water on mineral surfaces due to the tendency for clay minerals to act as semi permeable membranes. This results in the fractionation of hydrogen isotopes such that, the residual water will become enriched in deuterium due to the preferential adsorption of lighter hydrogen isotopes.

The relatively low d-excess (≤6) of some of the groundwater samples in Appendix 5.1 suggests evaporation from source more humid than the global ocean average. This is indicative of significant evaporation of rainwater leaving the residual groundwater water with lower d-excess. This is possible because, the climate of the study area is influenced by the Atlantic Ocean with a high and uniform relative humidity.

### 5.2.3.3 Relationship between EC and environmental isotopes

The relationship between electrical conductivity (EC) and environmental isotopes can be used to further identify the nature of flows, discharge areas and preferential recharge areas within a catchment. The variation of EC and environmental isotopes compositions are consequently an important in the assessment of the flow path in groundwater systems. EC normally increases along flow paths while the isotopic composition remains constant or changes slightly due to local recharge. Hence, the use of EC and $\delta^{18}O$ values can be used to further interpret the factors controlling hydrogeological processes.

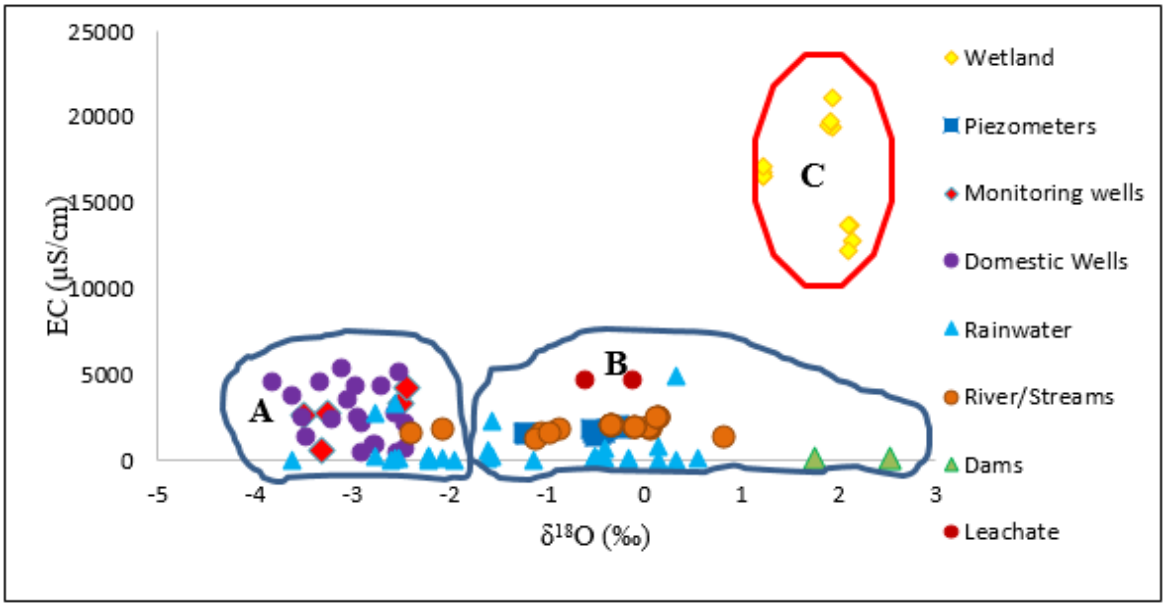


**Figure 5.20: EC vs. $\delta^{18}O$‰ from the groundwater and wetland water samples in the basin**

Relatively high $\delta^{18}O$ and $\delta^{2}H$ values (0‰) along with high concentrations of EC and $Cl^-$ are indicators of the seawater, whereas low $\delta^{18}O$ and $\delta^{2}H$ values and low EC and $Cl^-$ concentrations are characteristics of fresh groundwater derived from local rainfall. To verify the relationships between groundwater salinity and seawater influence, variation of $\delta^{18}O$ values versus concentrations of EC is provided in Figure 5.20. Group A is made up of groundwater and rainwater samples. The waters in group A are relatively fresh and saline with depleted isotopic composition. Group B shows the effect of evaporated water in the dam on the river and streams revealing high enriched waters in the dam. These variations in EC and $\delta^{18}O$ isotope are attributable to evaporation

at the surface of the wetland. Group C consist of mainly wetland waters. These are brackish waters with highly enriched isotopic composition. The heavier (less negative) isotopic signature of waters in the wetland shows a high EC content, whereas the groundwater samples of less saline wells shows more depleted signatures. Figure 5.20 shows no interconnection between the wetland and underlying groundwater.

## 5.3 Summary

Chapter 5 evaluated the hydrochemical and environmental isotopes characteristics of groundwater and wetland water quality in order to determine the hydrogeochemical factors controlling the water chemistry in the Sakumo basin. GIS was applied to visualize the spatial distribution of groundwater and wetland quality in the study area. A total of 86 groundwater samples were collected and analyzed for various physico-chemical parameters. Very wide ranges and high standard deviations of hydrochemical parameters such as EC, $Cl^-$, K, $SO_4^{2-}$, Mg suggest the groundwater in the study area showed anthropogenic contamination. Most of the water samples exceeded the maximum permissible limit of WHO standards. The abundance of cations and anions were in the order, $Na^+ > Ca^{2+} > Mg^{2+} > K^+$ and $Cl^- > HCO_3^- > SO_4^{2-} > NO_3^- > PO_4^{3-}$ respectively. The results showed that, groundwater in the study area was very hard and alkaline in nature. Further evaluation of groundwater and wetland hydrochemical data showed silicate weathering, calcium carbonate dissolution and ion exchange processes as the main factors controlling the water chemistry in the basin.



Environmental isotopes of $\delta^{18}O$ and $\delta^2H$ analyses were used to evaluate the hydrogeological characteristics of the aquifer and wetland system in the basin. The relation between $\delta^{18}O$ and $\delta^2H$ with respect to the global meteoric water (GMWL) line and the local meteoric water line (LMWL) showed the mechanism of recharge to the aquifer was direct infiltration of local rainfall. This suggested that, meteoric water as the main source of recharge to the aquifer. Environmental isotopes also showed seawater intrusion as not the predominant process contributing to high salinity aquifers in the study area. Rather, the dissolution of salts in the soil zone and minerals in rocks was responsible for the groundwater salinity in the study area. Thus, knowledge of hydrogeochemical control of the groundwater and wetland system, formed an important part of

the characterisation of the water regime in the basin, which will contribute to effective management of the wetland water resources.

# CHAPTER 6: ASSESSING THE OCCURRENCE OF GROUNDWATER-WETLAND INTERACTION

## 6.1 Introduction

This chapter presents and discusses results on the use water chemistry characterization methods, temperature and conductivity profile determination method to determine the occurrence of groundwater-wetland interaction in the Sakumo wetland basin. The aim was to characterize the cation and anion parameters and environmental isotopes of wetland and groundwater samples to establish whether or not, groundwater-wetland interaction occurs in the Sakumo wetland basin. The chapter addresses the third objective, which is to use hydrochemistry and temperature profile to establish the occurrence of groundwater-wetland interaction within the Sakumo wetland basin. The methods used in this chapter does not quantify the amount of water exchange between groundwater and wetland. However, it provides an indication of the similarities between wetland and groundwater chemistries. Therefore, the chapter provides evidence of the use of hydrochemistry and temperature profile as a practical qualitative method for determining the occurrence of groundwater-wetland interaction in the catchment.



## 6.2 Results and Discussion

Graphical and statistical methods were used to classify the wetland and groundwater samples into homogeneous groups. Water type characterization was done using Piper diagrams, Expanded Durov diagram and Stiff diagram adopted from Fonteh *et al*., (2017); Amiri *et al.,* (2016); Nyende *et al*., (2014); and Zghibi *et al*., (2014); Carol & Kruse (2012). The diagrams provided insight into the chemical water type sampled from the sampled wetland and groundwater in the catchment.

### 6.2.1 Use of the Piper diagram

Piper (1944) proposed a trilinear diagram that permits the classification of waters. The piper plot is used to characterize the type of water in terms of proportions of major anions and cations composition. It is also used to ascertain the possible origins of the water in terms of mixing between other members. The diagramme software, was used to plot the piper diagram based on the four

main cations (calcium, magnesium, and sodium and potassium) and anions (bicarbonate, sulphate, chloride and nitrate).

The Piper diagram in Figure 6.1 shows the chemical composition of all the sampled water, groundwater, lagoon (wetland), rainwater, stream waters and dam in terms of percentages of milliequivalents per litre. From the analysis of the Piper diagram, $Cl^-$ and $HCO_3^-$ are the dominant anions whereas $Na^+$ and $Ca^{2+}$ are the most dominant cations. According to the piper classification in Figure 3.8, three water types were obtained which conforms to the three groups of water obtained from the cluster analysis in section 6.3. The sampled wetland and groundwater in the catchment are predominantly Na–Cl type during the rainy and dry season with few traces of Na–$HCO_3$ water type in the dry season. Groundwater from the monitoring wells and domestic boreholes are predominately Na–Cl type for the rainy and dry season. However, 9% of the groundwater samples in the upper sub-basin showed Ca–Cl water type during the dry season. The $Ca^{2+}$ could be attributed to the displacement of $Na^+$ by $Ca^{2+}$ in cation exchange as $Na^+$ is preferentially adsorbed on the clay minerals releasing $Ca^{2+}$ into the water and, consequently forming $CaCl_2$ water type (Appelo & Postma 2005). The relative abundance of $Na^+$ and $Cl^-$ in the groundwater is used to indicate zones of groundwater recharge in the area. Where groundwater reflects low $Na^+$ and $Cl^-$ concentration suggest a major rainfall influence on groundwater recharge.

The wetland water shows evidence of seawater intrusion as it is dominated by $Na^+$ and $Cl^-$ and having much higher concentration of all components than the other sampled waters in the catchment. The wetland and shallow piezometers are primarily sodium-chloride type during both seasons. The wetland and piezometer water plot in the same area on the Piper plot which indicates that they have similar origin. It can be deduced that the wetland water and piezometer water are in hydraulic continuity. The same conclusion can be drawn from the observation that water levels in the piezometers are relatively higher than the water levels of the wetland. This shows that the water in the piezometers are a result of surface infiltrations mostly from rainfall which results in subsurface water flow to the wetland (Maclear, 1994). This was further confirmed by drying up of the piezometers during the dry season and filling up during the raining seasons. The water levels in the piezometers were high (7ft -11.3ft which is a depth of 3-5ft of water) during the raining season. Because the water in the piezometers are from sub-surface infiltration, there is little or no

interaction with the underlying geology. This leaves the chemistry of the water then behaves like wetland water than groundwater.

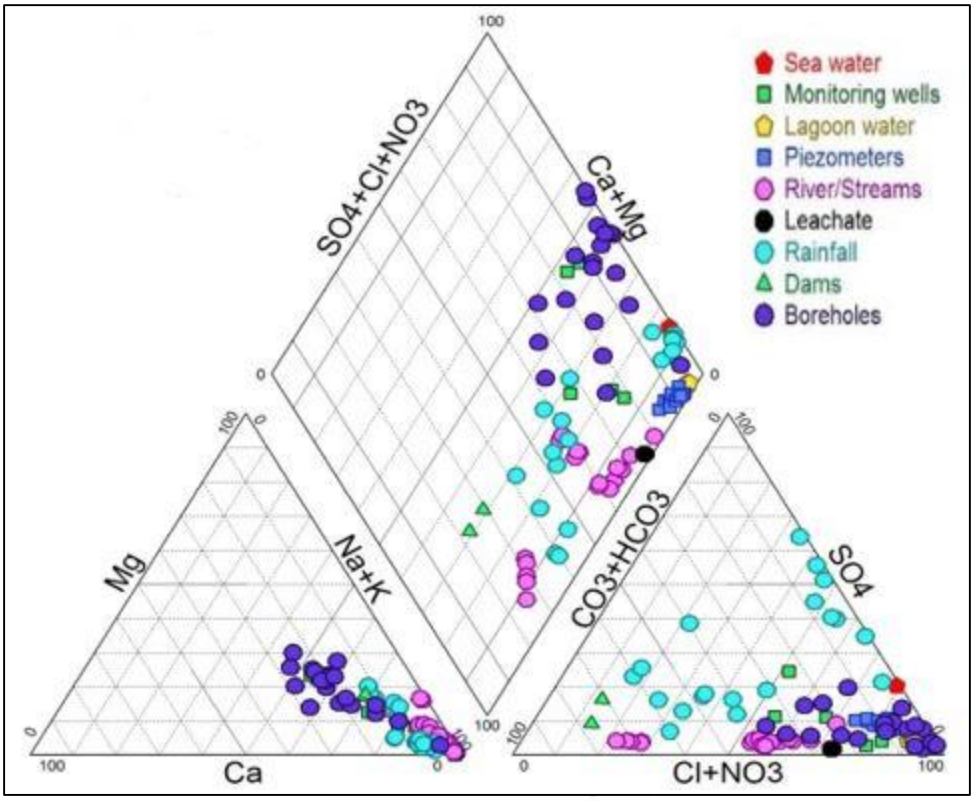




**Figure 6.1: Piper diagram showing the water types in the Sakumo basin. Source of seawater data (Hem, 1970)**

The wetland and groundwater type is attributed to preferential leaching of high soluble NaCl salts, which are completely dissolved during dissolution (Akiti, 1980). Subsequent evaporative concentration may also cause the less soluble salts to precipitate out of solution resulting in the percolating water becoming enriched with NaCl (Drever & Smith, 1978). This could be the result of seawater intrusion in the wetland waters. The similarities in water type between wetland and groundwater in the catchment, indicates water originating from the same source. Hence, the results showed that there was groundwater-wetland interaction as a result of mixing (dilution) by sea water discharging into the wetland. The wetland and groundwater type generally represents mixed waters.

Rainwater was mostly Na-Cl with few traces of Na-$HCO_3$ water types whiles the dams were Na-$HCO_3$ water type during the dry and rainy season. The streams were Na-Cl water type during the

dry season and $NaHCO_3$ type during the rainy season. The enriched $Na^+$ and $HCO_3^-$ in the stream waters could be attributed to weathering of plagioclase (albite) in the rock formation releasing $Na^+$, $HCO_3^-$ and kaolinite in the stream water as given in Eq. 6.1. The use of chemical fertilizers on farm lands along the banks of the streams could also be the source of the high $HCO_3^-$ concentration of the stream waters.

$$2NaAlSi_3O_8 + 2H_2CO_3 = Al_2Si_2O_5(OH)_4 + 2Na^+ + 2HCO_3 + 4H_2SiO_2 \quad (6.1)$$

### 6.2.2 Use of the expanded Durov diagram

Durov (1948) introduced the Durov diagram which provides more information on the hydrochemical facies by identifying the water types and displays some possible geochemical processes that could help in understanding quality of groundwater and its evaluation. The diagram is a composite plot consisting of two ternary diagrams where the cations of interest are plotted against the anions of interest; sides form a binary plot of total cation versus total anion concentrations. The expanded durov diagram incorporates total dissolved salts (µS/cm) and pH data is added to the sides of the binary plot to allow detailed comparisons. The expanded durov diagram (Durov, 1948) for the water resources in the Sakumo basin was plotted to characterize the water type and identify possible groundwater-wetland interaction using GWB 11.0.6 software presented in Figure 6.2. The results from the Expanded Durov diagram showed that there were similarities in water type between wetland water and groundwater samples. Figure 6.2 indicates that the wetland and ground waters are mainly sodium chloride (NaCl) water type which is often associated with sea water intrusion and silicate mineral rocks. The $Na^+$ and $Cl^-$ behave as conservative chemical parameters in the groundwater system and can therefore be used as such. The expanded durov diagram (Figure 6.2) reveals minor occurrence of calcium chloride ($CaCl_2$) and sodium bicarbonate ($NaHCO_3$) waters.

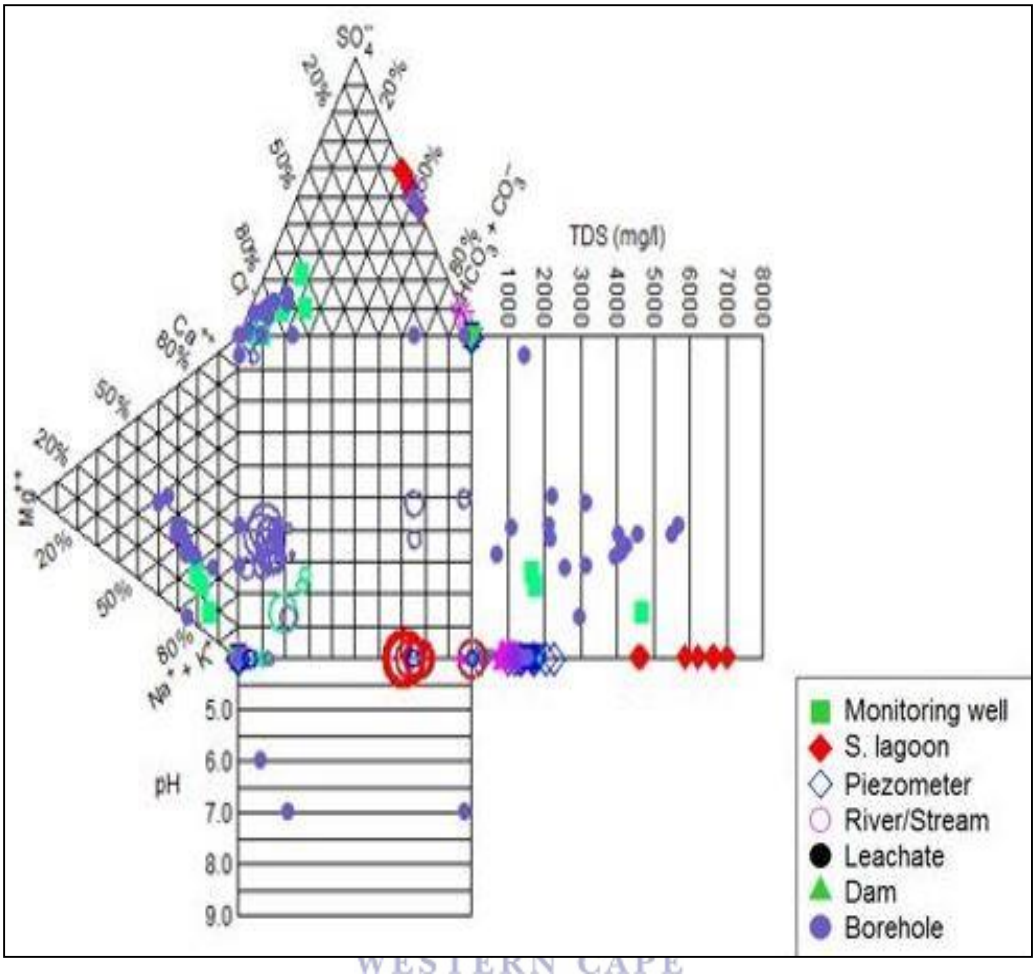




**Figure 6.2: The Durov diagram used to classify the water composition in the basin**

### 6.2.3 Use of the Stiff diagrams

The Stiff diagram is used to deduce the hydrochemical controls by comparing the ionic composition of water samples. The cation and anion concentrations are plotted and connected to form an asymmetric polygon known as the stiff diagram. The Stiff diagram's shapes and sizes are used to determine the water types and the distribution of the major ion composition in the catchment. The stiff diagrams presented in Figure 6.3, gives an overview of the dominant water types in the catchment. From the Stiff diagram data, the anion abundance relates and agrees well with the Piper diagram. Three major water groups were identified.

Group one is Na–Cl water type and brackish characterized by a high $Cl^-$ and $Na^+$ concentration. The group represents mainly wetland water, shallow water from the piezometers and groundwater

from the monitoring and domestic wells. However, three of the groundwater from the domestic boreholes (0.1%) were characterized as Na-$HCO_3$ water type. The spatial distribution of the group one water type varied in the catchment but are generally located in upper sub-basin and lower southern part of the basin. The high concentration of Na and Cl- in the wetland and groundwater samples located close to the coast could be attributed to sea water intrusion into the groundwater.

Group two are Na–Ca-Mg–Cl, Ca–Na-Cl, Na–Ca–Cl, water types characterized by high $Cl^-$ and moderate $Na^+$ concentration. These samples were mainly stream water and shallow piezometers waters. Group three are Na–Mg-Cl-$HCO_3$, Na–Ca-Mg–Cl, Na–Ca–Cl-$HCO_3$ and Na–Ca–Cl water types characterized by low ion concentration. These were mostly stream waters and shallow piezometers forming 25% of the total sampled waters. It is clear that the wetland and groundwater in the Sakumo basin are rich in $Na^+$ and $Cl^-$. The shape of the diagrams suggests that wetland water resources are rich in the cations $Na^+$ and $K^+$ and in the anions $Cl^-$ and $HCO_3^-$. The size of the diagrams also depicts that water in the shallow wells is more mineralized than water in the boreholes. The variation in the shapes and sizes of the stiff diagrams (Figure 6.3) depicts the water-rock interaction processes and the effect of pollution on the chemical composition of the water.

a) Wetland

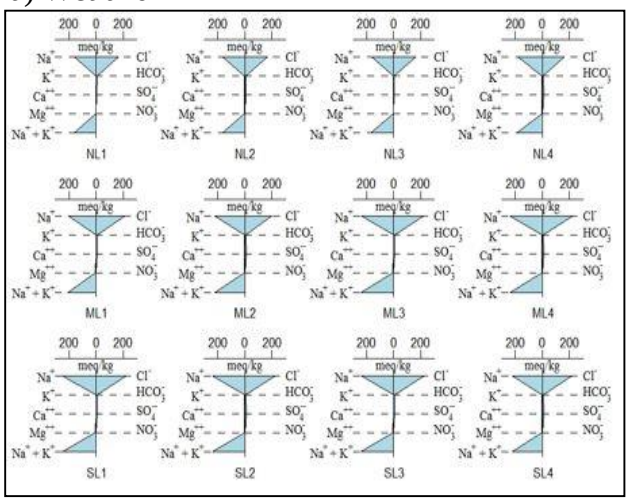


b) Monitoring wells

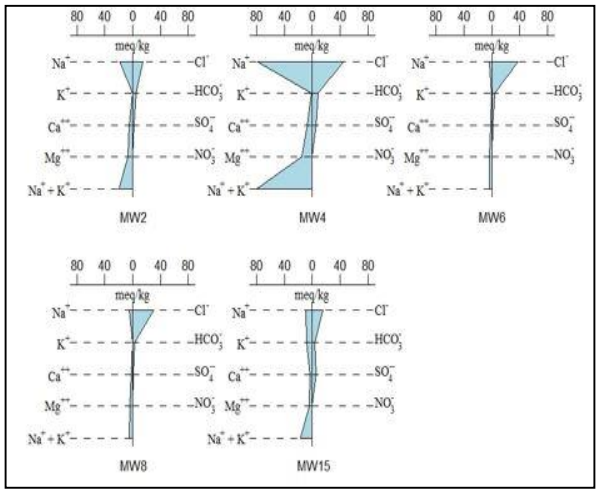


c) Streams

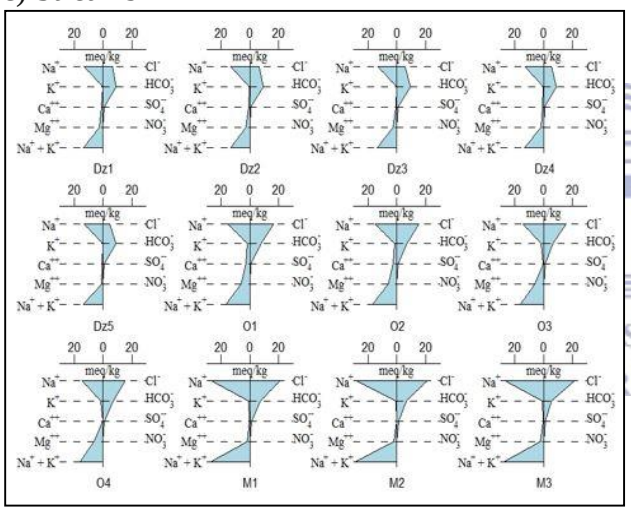


d) Piezometers

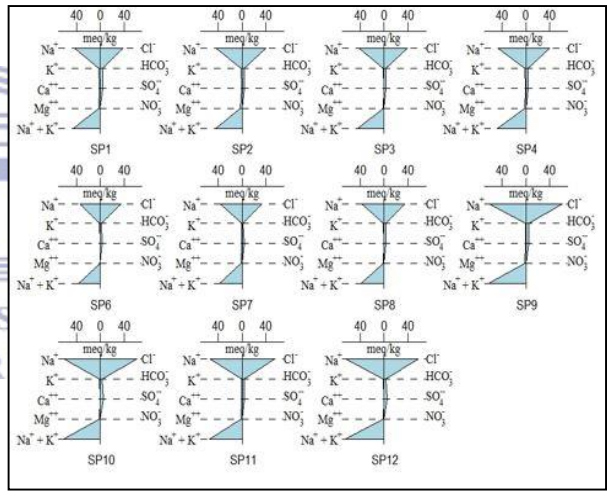


e) Domestic wells

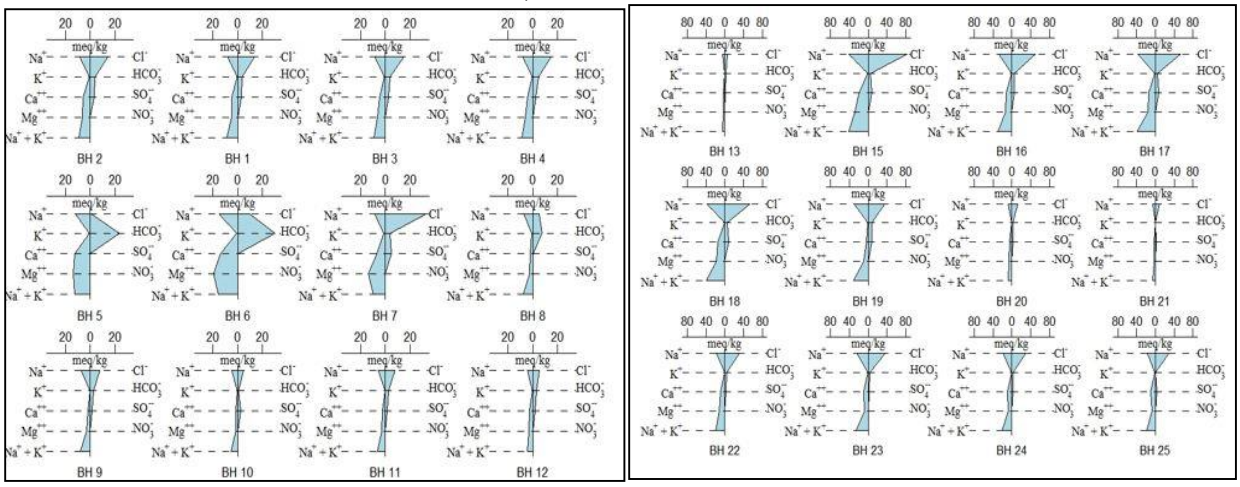


**Figure 6.3: Stiff diagram showing the major ion constituents in the groundwater and wetland**

## 6.3 Multivariate statistical analysis

Multivariate statistical analysis was used as a quantitative tool to group the groundwater and wetland water samples based on their physicochemical parameters. In the current study, three multivariate methods were applied using the computer program IBM SPSS Statistics 23 and Sigma Plot 13.0. Correlation coefficient, principal components analysis (PCA) and cluster analysis (CA)were performed as applied in Hamzah *et al.*, (2016); and Ghesquière *et al.,* (2015). The physiochemical data of the groundwater and wetland samples used were first logged normally distributed using the Kolmogorov-Smirnov (K-S) statistics. According to the K-S test, all the variables were log normally distributed with 95% or higher confidence.

Prior to the extraction of the principal components, the dataset was subjected to normalization with the following formula:

$$N = \frac{CV - MC}{SD} \quad (6.2)$$

Where:

N= normalized data,

CV=concentration of each variable,

MC=mean concentration of each variable and

SD= standard deviation of the data variable.



### 6.3.1 Correlation matrix

The relationships between the physicochemical parameters were studied using correlation analysis matrix and the results are shown in Table 6.1. The correlation matrix in Table 6. emphasizes the relationship between the parameters directly related to salinity such as EC, $Na^+$, $K^+$, $Ca^{2+}$, $Mg^{2+}$, $Cl^-$ and $SO_4^{2-}$. Hence, the relationships between $Cl^-$ to EC and $Cl^-$ to $Na^+$ show relatively high correlation levels (0.94 and 0.98 respectively). Moderate correlation exists between $Cl^-$ and K (r=0.54). The results show that $Na^+$ and $Cl^-$ have a high correlation (r=0.98) with one another. The strong relationship between EC with $Na^+$ and EC with $Cl^-$ (0.92 and 0.94 respectively) is due to the relationship these two ions have with salinity (EC) in the waters, which is directly proportional.

A high to moderate relationship exist between EC and Na (r=0.92) and EC and $SO_4^{2-}$ (r=0.75). This suggests that EC is mostly controlled by these ions. EC had an inversely moderate to weak correlation with K (r=-0.51). In addition, $Ca^{2+}$ and $Mg^{2+}$ (r=0.92) are significant and attributable to seawater intrusion significantly raising the concentration of the ions in the water. The strong correlation between $Ca^{2+}$ and $Mg^{2+}$ (0.92) could be an indication of carbonate dissolution as a source of these ions. The correlation between $Na^{+}$ and $SO_4^{2-}$ (r=0.78) may indicate gypsum or anhydrite as another source of these ions in the water, but because the correlation is moderate, it shows that gypsum or anhydrite dissolution is not the main source. $Ca^{2+}$ and $Mg^{2+}$ show a moderate positive (r=0.76 and 0.64 respectively) relationship with temperature. This could be an indication of effect of temperature on the solubility of these ions.

### 6.3.2 Extraction of principal factors

Principal Component Analysis (PCA) was applied to the measure physicochemical variables in groundwater and wetland water samples. The Kaiser–Mayer–Olkin (KMO) method was executed before analyzing PCA and a KMO greater than 0.5 was found suitable for further analysis. The present study obtained a KMO value of 0.51. The rotated factor loadings, eigen values, percentages of variance and cumulative percentages of variance is given in Table 6.2. The highlighted variables have their absolute values greater than 0.67 showing a strong correlation. A high value (close to 1) generally indicates that principal component or factor analysis may be useful.

**Table 6.1: Correlation matrix of the groundwater and wetland water sample in the Sakumo basin**

| | T°C | pH | EC | Ca | Mg | Na | K | $HCO_3^-$ | Cl | SO4 | $PO_4^{3-}$ | $NO_3^-$ | Fe | Cu | Zn | Mn |
|---|---|---|---|---|---|---|---|---|---|---|---|---|---|---|---|---|
| T°C | 1 | | | | | | | | | | | | | | | |
| pH | .088 | 1 | | | | | | | | | | | | | | |
| EC | -.163 | .015 | 1 | | | | | | | | | | | | | |
| Ca | **.756**$^{**}$ | .063 | .080 | 1 | | | | | | | | | | | | |
| Mg | **.649**$^{**}$ | .005 | .115 | **.923**$^{**}$ | 1 | | | | | | | | | | | |
| Na | -.336$^{**}$ | .000 | **.918**$^{**}$ | -.146 | -.088 | 1 | | | | | | | | | | |
| K | -.237$^{*}$ | -.034 | **.505**$^{**}$ | -.154 | -.096 | **.552**$^{**}$ | 1 | | | | | | | | | |
| $HCO_3^-$ | -.055 | -.068 | .119 | .156 | .272$^{*}$ | .076 | .010 | 1 | | | | | | | | |
| $Cl^-$ | -.242$^{*}$ | .008 | **.940**$^{**}$ | -.006 | .039 | **.978**$^{**}$ | **.537**$^{**}$ | .031 | 1 | | | | | | | |
| $SO_4^{2-}$ | .081 | -.058 | **.747**$^{**}$ | .301$^{**}$ | .369$^{**}$ | **.758**$^{**}$ | .478$^{**}$ | -.085 | **.825**$^{**}$ | 1 | | | | | | |
| $PO_4^{3-}$ | **-.757**$^{**}$ | -.041 | .412$^{**}$ | **-.509**$^{**}$ | -.427$^{**}$ | **.518**$^{**}$ | .301$^{**}$ | .172 | .440$^{**}$ | .160 | 1 | | | | | |
| $NO_3^-$ | .464$^{**}$ | **.808**$^{**}$ | -.045 | .452$^{**}$ | .354$^{**}$ | -.137 | -.183 | -.072 | -.057 | .069 | -.319$^{**}$ | 1 | | | | |
| Fe | -.371$^{**}$ | -.050 | .382$^{**}$ | -.200 | -.199 | .431$^{**}$ | .139 | .142 | .404$^{**}$ | .222$^{*}$ | .478$^{**}$ | -.195 | 1 | | | |
| Cu | -.138 | -.006 | -.054 | -.107 | -.095 | -.044 | -.049 | .017 | -.067 | -.111 | .024 | -.063 | .039 | 1 | | |
| Zn | **-.529**$^{**}$ | -.033 | .282$^{**}$ | -.413$^{**}$ | -.385$^{**}$ | .397$^{**}$ | .198 | .074 | .333$^{**}$ | .106 | .327$^{**}$ | -.261 | .333$^{**}$ | .396$^{**}$ | 1 | |
| Mn | **-.588**$^{**}$ | -.042 | .049 | -.400$^{**}$ | -.279$^{**}$ | .114 | .140 | .191 | .049 | -.183 | .369$^{**}$ | -.249 | .258 | .338$^{**}$ | **.549**$^{**}$ | 1 |

**. Correlation is significant at the 0.01 level (2-tailed).

*. Correlation is significant at the 0.05 level (2-tailed).

**Table 6.2: Results of the extracted principal components of the physicochemical variables of the groundwater and wetland water samples**

| Variables | PC1 | PC2 | PC3 | PC4 | PC5 |
|---|---|---|---|---|---|
| T°C | **-0.72** | **0.55** | -0.08 | 0.03 | 0.16 |
| pH | -0.14 | 0.18 | **0.93** | -0.06 | -0.17 |
| EC | **0.73** | **0.60** | 0.02 | 0.02 | 0.01 |
| Ca | **-0.51** | **0.73** | -0.11 | 0.34 | 0.01 |
| Mg | -0.41 | **0.71** | -0.18 | 0.44 | -0.03 |
| Na | **0.85** | 0.47 | 0.04 | -0.07 | 0.03 |
| K | **0.57** | 0.27 | -0.06 | -0.17 | 0.13 |
| $HCO_3^-$ | 0.09 | 0.06 | -0.16 | **0.69** | **-0.55** |
| $Cl^-$ | **0.78** | **0.58** | 0.04 | -0.07 | 0.06 |
| $SO_4^{2-}$ | 0.48 | **0.78** | -0.09 | -0.08 | 0.20 |
| $PO_4^{3-}$ | **0.76** | -0.20 | 0.06 | -0.03 | -0.38 |
| $NO_3^-$ | -0.43 | 0.44 | **0.75** | 0.03 | -0.09 |
| Fe | 0.58 | 0.01 | 0.03 | 0.17 | -0.28 |
| Cu | 0.11 | -0.28 | 0.20 | 0.53 | **0.60** |
| Zn | **0.63** | -0.27 | 0.19 | 0.33 | 0.34 |
| Mn | 0.45 | -0.47 | 0.16 | 0.48 | 0.05 |
| Eigen value | 4.36 | 3.56 | 1.80 | 1.72 | 1.45 |
| Total variance (%) | 27.24 | 22.24 | 11.27 | 10.80 | 9.09 |
| Cumulative variance %) | 27.24 | 29.48 | 60.75 | 71.55 | 80.64 |
| Source | Industrial activities | Seawater intrusion | Farming activities | Farming activities | Farming activities |



The principal component analysis identified five factors influencing the groundwater and wetland water chemistry. However, following varimax rotation, two major principal components were used to interpret the data. The two factors account for 84.75% of the total variance. The two factors loading are shown in Figure 6.4. The first factor (PC1), which accounts for about 79.16% of the variance, has positive loadings for EC, $Cl^-$, $HCO_3^-$, $K^+$, $Ca^{2+}$, $Na^+$, $Mg^{2+}$, $PO_4^{3-}$ $SO_4^{2-}$, Cu, Fe, Mn and Zn. PC1 indicates salinity enhancement in the area due to sea water intrusion and the defect of industrial waste on the chemical loading of the waters. The high positive loadings of EC, $Cl^-$,

$Na^+$ and $Ca^{2+}$ connotes high salinity due to sea water intrusion whiles $SO_4^{2-}$ indicates possible redox reactions and land use practices. The high positive loadings of $K^+$, $NO_3^-$ and $PO_4^{3-}$ could be attributed to pollution from fertiliser application and wastes from farming activities in the area. Mn and Zn indicates industrial waste discharge.

The second factor (PC2) accounts for 6.59% of the variance is weighted with pH and $NO_3^-$. The parameters associated with factor 2 indicates salinity enhancement due to pollution from industrial wastes and dissolution of the rock mineral feldspars. The two main PC's are indicative of high salinity, water-rock interaction and pollution of the groundwater and wetland water. The high salinity in the groundwater further suggest little mobility of groundwater in the area hence little possibility of groundwater-wetland interaction.

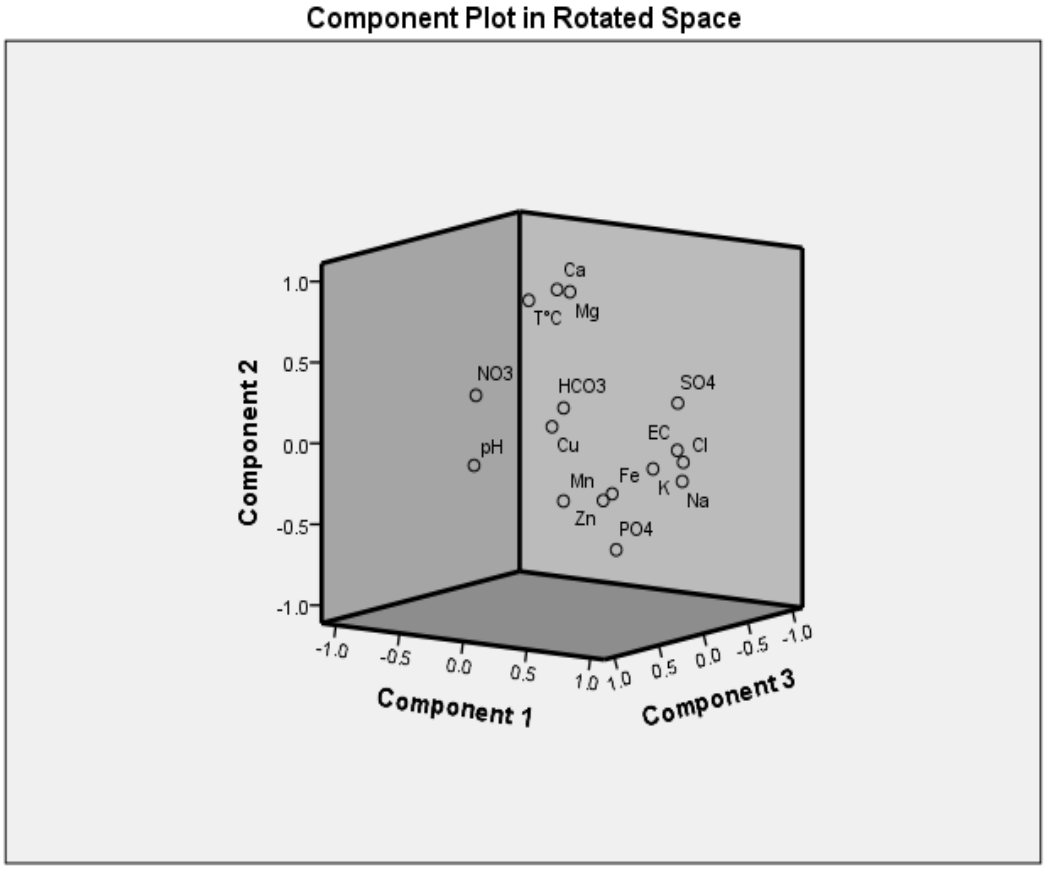


**Figure 6.4: Principal component analysis in rotated space of the groundwater and wetland physicochemical parameters**

### 6.3.3 Cluster analysis

Cluster analysis was applied to the physicochemical data from the groundwater and wetland water sampling sites in the Sakumo basin. The relationships among the sampling sites were obtained through Q-mode cluster analysis (CA). This information was used to identify sites with similar physicochemical parameters thus indicating the water exchange. The cluster analysis provided a graphical result, the dendrogram (Figure 6.5), which showed the groupings of the groundwater and wetland water samples in the basin. According to the clustering, three distinct groups were identified based on their hydrogeochemical characteristics.

Cluster 1 is mainly made up of water samples from the streams, river, dam and shallow piezometers in the Sakumo basin. The sites in cluster 1 include $O_3$, $O_4$, $O_1$, $O_2$, $OM_1$, $OM_3$, $Dz_2$, $Dz_3$, $Dz_4$, $Dz_5$, $Dz_1$, $M_1$, $M_4$, $M_2$, U. Dam, L. Dam, $DD_1$, $DD_2$, $OM_2$, $SP_9$, $SP_{10}$, $SP_{12}$, $SP_5$, $SP_2$, $SP_3$, $SP_1$, $SP_4$, $SP_6$, $SP_7$, $SP_8$, $SP_{11}$, BF, $M_3$. Cluster 1 accounted for about 40.25% of the total analysed water samples. The grouping of these sites in one cluster indicates that waters have a distinct hydrochemical characteristic. The sites of cluster 1 are mainly populated areas with human settlements and agricultural activities. The waters in this group are relatively fresh with EC, $HCO_3$, Cl, Na, K, as the dominant ions. The low degree of mineralization of these waters suggests that the contact time with rock and soil may be short.



Cluster 2 is mainly made up of the water samples from the wells mainly from the underlying groundwater in the basin. Cluster 2 constitute 46.34 % of the total analysed data set. The waters in this group are saline with high concentrations of Na, Cl, Ca, Ma, Na, K. The high ion concentrations indicate a long contact time with the soil and rock. Cluster 3 accounts for 13.41% of the analysed data set and consist of the wetland water samples. The water in this group is brackish with a mean EC value 18200 µS/cm and has sodium and chloride as the dominant ions. As dissolution of halite is a slow process, the increase in EC from cluster 1 to 3 (groundwater flowpath) may be as a result of the long residence time or contact time with the groundwater. This shows that, there is no or little interaction between the wetland and the underlying groundwater.

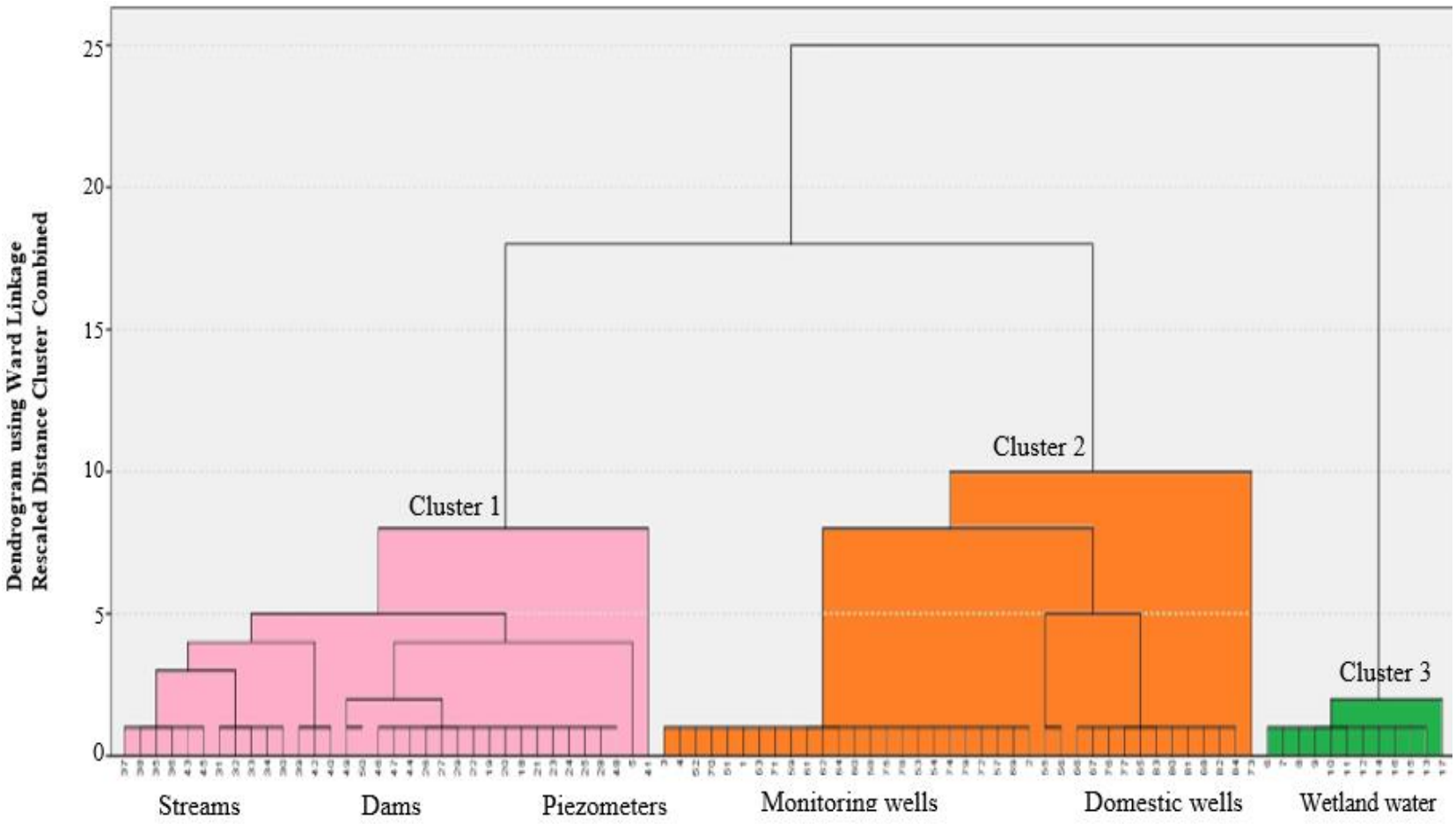


**Figure 6.5: Dendrogram of Q-mode and cluster analysis of the groundwater and wetland water in the Sakumo basin**

## 6.4 Temperature profiling

Groundwater–wetland connections are exists where an aquifer provides water to a wetland or vice versa (Winter, 1999). The use of hydrochemistry serves as a rapid and cost-effective means by which the interaction groundwater-wetland interaction can be identified using water quality data and temperature profiles. Among the field methods typically used to identify and quantify the groundwater-wetland interactions include the use of water temperature as an indicator of groundwater inflow to a wetland (Larocque *et al*., 2016; Middleton *et al.*, 2016). Time-series analyses of water levels and water temperature of the groundwater and wetland can be used to identify connections between wetland and the underlying aquifer (Larocque *et al*., 2016). When water flows from the aquifer to a wetland, it regulates temperature conditions which sustain the ecosystem (Hoffmann *et al.*, 2009). However, when water flows from a wetland to an aquifer, it contributes to the recharge of groundwater. Such interactions affect the stability of both the wetland water body and the underlying aquifer. Knowledge of this is important to establish a sustainable water resources management plan for wetlands.



Due to the shallow depth (rarely exceeding 2 m above sea level) of the wetland level, groundwater is found at shallow depths, about 5m. Hence, a water depth-temperature profile was used to establish the occurrence of groundwater–wetland interaction in the Sakumo basin. Temperature measurements were taken at regular intervals from the surface to the bottom of the wetland. Figure 6.6 shows the results of the monthly (August to November, 2016) temperature profiles taken at various depths of the wetland. The observation of monthly temperature profiles for water columns in wetland showed that, temperature profile exhibited similar trends in the various months. The monthly temperature profiles remained practically constant with depth (0-1.5 m) in most parts of the wetland and only decreased slightly with depth in few instances (Figure 6.6). This means that, no groundwater-wetland interaction occurred within the wetland basin. This also confirms that the main wetland water body (0-2 m) is homogenous.

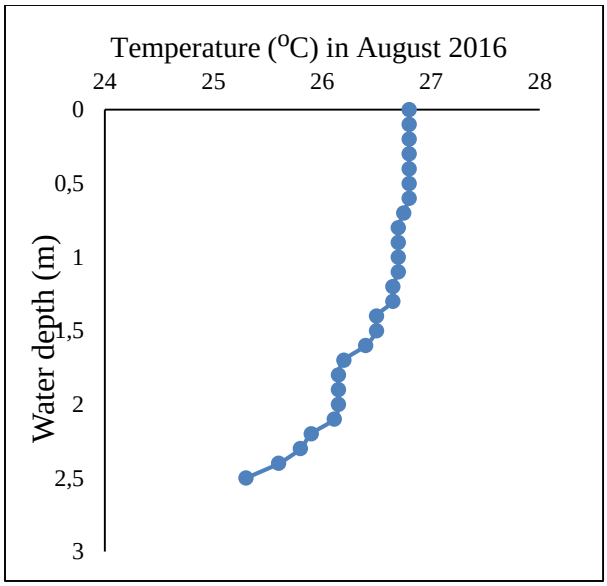


a) Temperature profiles recorded in August 2016

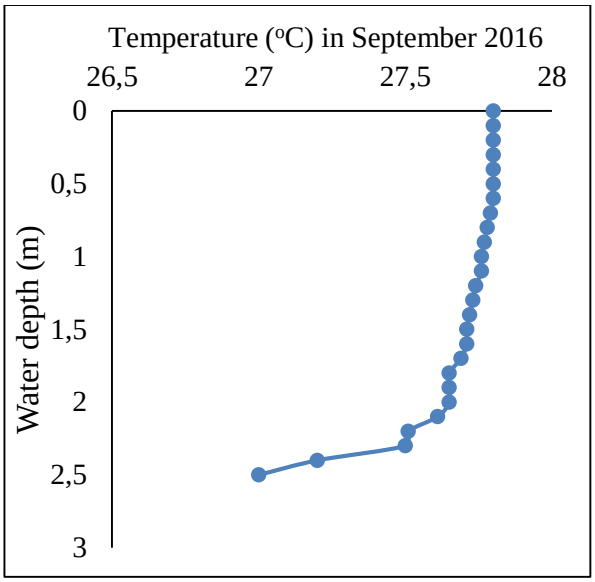


b) Temperature profiles recorded in September 2016

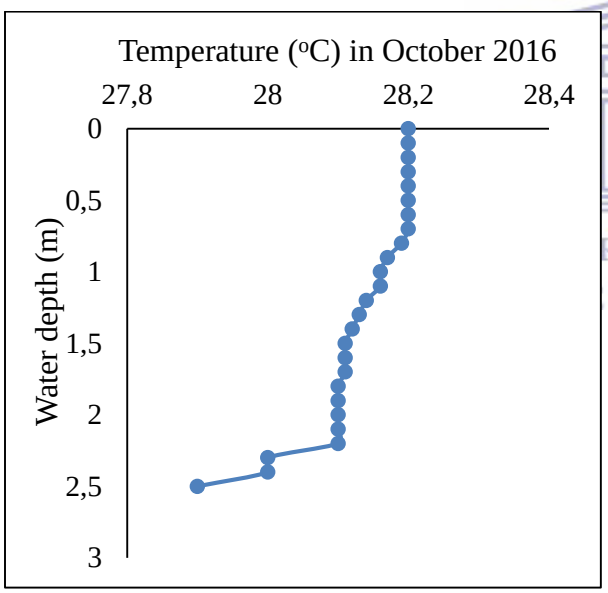


c) Temperature profiles recorded in October 2016

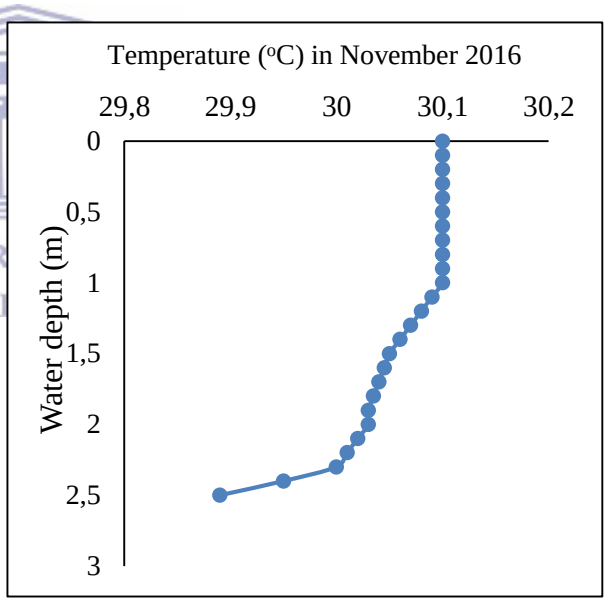


d) Temperature profiles recorded in November 2016

**Figure 6.6: Monthly variation between temperature (T°) and wetland water depth (m) in the Sakumo wetland**

The results of the temperature profiles taken at various transects of the wetland are presented in Figure 6.7. The results in Figure 6.7 showed similar temperature profiles taken from the various transects from the surface to the bottom of the wetland as no significant temperature stratification occurred within the wetland water body. This means that there is no observable interaction between

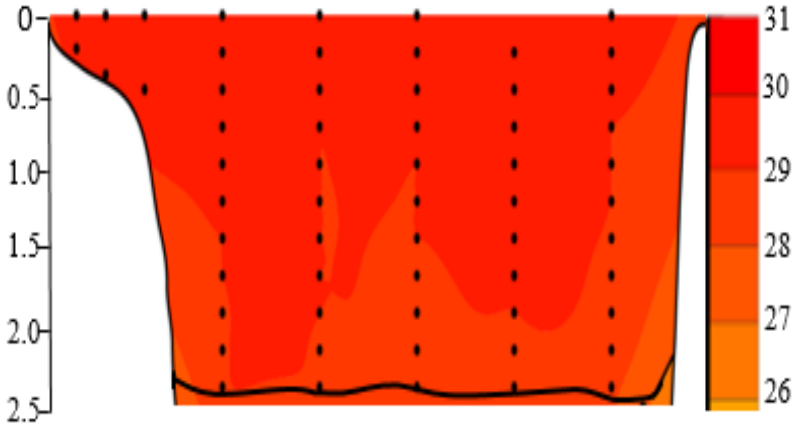


**Figure 6.7: A depth profile relationship between temperature (ºC) and wetland water depth (m) in November, 2016**

the wetland and the underlying aquifer at the specified sites of the basin. The results obtained from the temperature profile is key in the development of a water quality monitoring programme for the management and conservation of the wetland water resources as a single resource.

# CHAPTER 7: CONCLUSIONS AND RECOMMENDATIONS

## 7.1 Introduction

This study focused on quantifying the water fluxes contributing flows to the Sakumo wetland and characterized the groundwater and wetland water resources using numerical model, hydrochemical and environmental isotopes analysis models. The first part of the study focused on understanding the groundwater flow system in the Sakumo basin. The Sakumo wetland is characterized by shallow unconfined groundwater situated in the alluvial sediments. Physical, hydrological, hydrogeological data were used to conceptualise the groundwater flow system in the study area. A numerical flow model was then used to simulate the groundwater flow in the basin and the wetland water fluxes calculated from the water balance.

The second part of the study characterized the water quality in the wetland environment. This was achieved by collection and interpretation of hydrochemical and environmental isotope data (from wetland, streams, river, boreholes and piezometers). In addition, the main factors affecting groundwater-wetland interaction were identified from the dissimilarities in physicochemical characteristics of both groundwater and wetland. The key findings from the study are important in designing practical management strategies for maintaining the quantity and quality of the freshwater and saline water balance of the wetland.



## 7.2 Groundwater flow system in the Sakumo wetland

A local flow model was developed for the Sakumo wetland basin where the aquifer head over space and time was simulated. The conceptual model developed revealed that the Sakumo wetland is not hydraulically connected to the groundwater system. Hence, a change in one system does not affect the other. The general groundwater flow direction is from North West to South East towards the Gulf of Guinea. The simulated heads match reasonably with the observed heads with a difference of 0.8 m. Sensitivity analysis revealed that, the developed model was sensitive to hydraulic conductivity and to some extent recharge. The simulation results of the developed model therefore provided useful information for the development of practical strategies for managing the wetland water resource.

## 7.3 Water chemistry in the Sakumo wetland

Hydrogeochemical processes affecting the chemical composition of groundwater and wetland water in the Sakumo wetland basin indicate hydrochemical differences between the three hydrological units analysed. In rivers and streams, water is a low-salinity sodium bicarbonate type with a predominance of $CO_2$(g) dissolution, carbonate dissolution and ion exchange. In the underlying aquifer, water is saline sodium chloride type and its chemical characteristics are as a result of the dissolution of halite (NaCl) minerals in the soil zone and water-rock-interaction (silicate weathering). The wetland water is a sodium chloride type and the composition shows the incidence of seawater encroachment. Sea water does not seem to play a principal role in the salinization of groundwaters of the basin as postulated. Anthropogenic activities, evaporation and concentration, cation exchange and rock-water interaction are the factors of increasing major ions concentrations in the groundwater. Knowledge of these processes in determining the wetland hydrogeochemistry constitute an essential tool in the management and preservation of the wetland environmental characteristics.

Environmental isotopic ($\delta^{18}O$ and $\delta^{2}H$) data reveal infrequent participation of sea water in the groundwater samples and an evaporation trend in the wetland water. The relation between $\delta^{18}O$ and $\delta^{2}H$ with respect to the global meteoric water line (GMWL) and the local meteoric water line (LMWL) showed rainwater samples plotting between the GMWL and the LMWL whiles the wetland samples plotted away from the two lines. This suggests meteoric water as the main source of recharge to the groundwater. The rainwater samples also reflected partially evaporated waters with enriched isotopic signature. These groundwater samples plot close to the LMWL indicating meteoric origin. In contrast, the wetland waters showed highly evaporated waters with enriched isotopic signatures as a result of the large surface area exposed to evaporation. Rainfall recharge, evaporation and long residence times that defined the hydrochemical and isotopic features of the groundwater and wetland water samples showed no signs interaction between the wetland and the underlying aquifer.

## 7.4 Groundwater-wetland interaction

Hydrochemical data showed two hydrochemical facies. The wetland water is predominately Na-Cl type. The groundwater, deep and shallow systems have distinct hydrochemical characteristics. The shallow water from the piezometers is dominated Na-$HCO_3$-Cl facies indicating active recharge and a flushed system. While, the deep groundwater is mostly Na-Ca-Cl facies, indicating the dissolution of the calcium rich rock formation. Two principal components (PC's) were extracted in the factor analysis of groundwater and wetland physicochemical data. The two PC's were interpreted in terms of pollution due to farming activities in the area i.e. the use of fertilizers and agrochemicals and redox reactions as a result of industrial wastes discharges into the wetland.

## 7.5 Recommendations

The following are recommendations emanated from the present study:

1. Detailed aquifer characterisation is needed in the development of a realistic conceptual model for input into the numerical model
2. Drill holes to install piezometers around the wetland (within the saline water and in the fresh water) to record the stratigraphic logs of the area in order to improve the conceptual model.
3. It is essential to build flumes at the inlet and outlet to the wetland to monitor flow (and chemistry) of the water and install level loggers to measure pressure, temperature and electrical conductivity;
4. Install a tipping bucket rain gauge and a full weather station in the vicinity of the wetland to measure hydro-meteorological data to be used in numerical model;
5. Continuous groundwater and wetland water level measurements are needed to further understand the wetland water balance response and to improve the conceptual model.

# REFERENCES


Adomako, D., Maloszewski, P., Stumpp, C., Osae S. & Akiti, T.T. (2010). Estimating groundwater recharge from water isotope ($\delta^2H$, $\delta^{18}O$) depth profiles in the Densu River basin, Ghana. *Hydrological Sciences Journal,* 55(8),1405-1416

Agbevanu, K. (2015). Modelling and simulation of groundwater flow and radionuclide transport in groundwaters of Dahomeyan system of the Accra Plains in Ghana. *MPhil thesis.* University of Ghana. 168pp

Aggarwal, P. K., Dillon, M. A. and Tanweer A. (2004). Isotope fractionation at the soil atmosphere interface and the $^{18}O$ budget of atmospheric oxygen. *Geophys. Res. Lett.* 31, L14202. https://doi: 10.1029/2004GL019945

Agyepong, G.T., R. Asmah, & C.C. Amankwa. 1999. Coastal wetlands management project. Management plan for Sakumo Ramsar site prepared for department of Game and wildlife, government of Ghana. 45pp

Akiti, T. T. (1987). Environmental isotope study of groundwater in crystalline rocks of the Accra Plains, Ghana. Proceedings of the 4th Working Meeting, Isotopes in Nature, Leipzig, September 1986

Akiti, T.T. (1980). Etude geochimique et isotopique de quelques groundwatere du Ghana. Ph.D. thesis, Universite' de Paris-Sud

Alfa, Bob Atia (2010). Distributed numerical modelling of hydrological/hydrogeological processes in the Densu Basin. PhD thesis, University of Ghana.

Allen, R., Pereira, L.A., Raes, D. & Smith, M. (1998). Crop evapotranspiration. In FAO irrigation and drainage paper No. 56, FAO, Rome, Italy

Allison, G. B., C. Barnes, C. M. Hughes, & Leaney, F. (1984), Effect of climate and vegetation on oxygen-18 and deuterium profiles in soils, *in* Isotope Hydrology 1983, *edited by IAEA, pp.* 105–122, *Int. At. Energy Agency*, Vienna

Alvarez, M. P., Dapen˜a, C. Bouza P.J., Rı´os, I. & Herna´ndez, M.A. (2015). Groundwater salinization in arid coastal wetlands: a study case from Playa Fracasso, Patagonia, Argentina. *Environ Earth Sci*. 73,7983–7994. https://doi: 10.1007/s12665-014-3957-3

Alvarez, M del Pilar, Carol E. & Dapeña C. (2015). The role of evapotranspiration in the groundwater hydrochemistry of an arid coastal wetland (Península Valdés, Argentina). *Science of The Total Environment* 506, 299-307

Amankwah, C. C. (1998). Coastal Wetland Management Project, Wildlife Department.http:\\www.wetlands.org/RSIS/_COP9Directory/Directory/ris/1GH004en.pdf

Ameli, A. A. & Creed, I.F. (2017). Quantifying hydrologic connectivity of wetlands to surface water systems. *Hydrology and Earth System Sciences*, 21(3):1791-1808

America Publication Health Association (2012). Standard methods for the examination of water and wastewater 22nd edition, Parts 3111, 3500 & 2340

Amiri, V., Nakhaei M., Lak, R. & Kholghi, M. (2016). Assessment of seasonal groundwater quality and potential saltwater intrusion: a study case in Urmia coastal groundwater (NW Iran) using the groundwater quality index (GQI) and hydrochemical facies evolution diagram (HFE-D). *Stoch Environ Res Risk Assess* 30, 1473–1484. https://doi:10.1007/s00477-015-1108-3

Anderson, M. P. (2005). Heat as a ground water tracer. *Ground Water*, 43(6), 951–968, https://doi:10.1111/j.1745–6584.2005.00052

Anderson, M.P. & Woessner W.W. (1992). Applied groundwater modeling: simulation of flow and advective transport. Academic Press, Toronto, Ontario, Canada

Anderson, M.P. & Woessner, W.W. (2002). Applied groundwater modeling: simulation of flow and advective transport. New York: Academic Press Toronto, Ontario, Canada

Andriesse, W. (1986). Area and Distribution. In: Juo and Lowe (eds*)* The Wetlands and rice in Sub-Saharan Africa. Proceedings of an International Conference. Ibadan, November 1985. IITA, Ibadan, Nigeria. 15-30 pp

Antolino, D.J. (2011). Geochemical conditions and groundwater-surface water interactions within a municipal well field in Miami-Dade County, Florida. *MSc thesis*, Atlantic University Boca Raton, Florida

Akpabli, C.K. & Drah, G.K. (2001). Water quality of the main tributaries of the Densu river. *Ghana J. Sci*. 3 (2), 84-94

Appelo, C.A.J. & Postma, D. (2005). Geochemistry, Groundwater and Pollution. 2nd ed. AA Balkema, Rotterdam

Armah, A. K. (1991). Coastal erosion in Ghana: causes, patterns, research needs and possible solutions. *Coastal Zone*, 91, 2463-2473

Asmah, R., Dankwa, H., Biney, C. A., & Amankwah, C. C. (2008). Trend analysis relating to pollution in Sakumo lagoon, Ghana. *African Journal of Aquatic Science*, 33(1), 87–93

Atobra, K. (1983). Groundwater Flow in the crystalline rocks of the Accra Plains, West Africa. *PhD Thesis*, Princeton University, USA.

Aufdenkampe, A. K., Mayorga, E., Raymond, P. A., Melack, J. M., Doney, S. C., Alin, S. R., Aalto, R. E. & Yoo, K. (2011). Riverine coupling of biogeochemical cycles between land, oceans, and atmosphere, Front. *Ecol. Environ.*, 9(1), 53–60

Ayenew, T., Demlie, M. & Wohnlich, S. (2007) Application for numerical modeling for groundwater flow system analysis in the Akaki Catchment, Central Etihiopia. *Int Assoc Mathemat Geol*, 40, 887-906

Banks, E.W., Simmons, C.T., Love, A.J. & Shand, P. (2011). Assessing spatial and temporal connectivity between surface water and groundwater in a regional catchment: Implications for regional scale water quantity and quality. *J Hydrol.* 404, 30–49

Banoeng-Yakubo, B., Yidana S.M., Ajayi, J.O. and Daniel, A. (2010). Hydrogeology and groundwater resources of Ghana: A review of the hydrogeological zonation in ghana. Portable Water and Sanitation pp. 77-114

Baraer, M., McKenzie, J. M. Mark, B. G. Bury, J. Knox, S. & Fortner, S. (2009). Characterizing contributions of glacier melt and groundwater during the dry season in a poorly gauged catchment of the Cordillera Blanca (Peru), *Adv. Geosci*., 22, 41–49

Barakat, A., Baghdadi, M.E., Rais, J., Aghezzaf, B. & Slassi, M. (2016). Assessment of spatial and seasonal water quality variation of Oum Er Rbia River (Morocco) using multivariate statistical techniques. *International soil and water conservation research*, 2(4), 284–292

Bear, J. & Verruijt, A. (1987). Modeling groundwater flow and pollution theory and application of transport in porous media. D. Reidel Publishing company, Boston. 414 pp

Bedford, B.L. (1996). The need to define hydrologic equivalence at the Landscape scale for freshwater wetland mitigation. *Ecological Applications* 6,57-68

Beekman, H.E. & Xu, Y. (2003). Review of groundwater recharge estimation in arid and semi-arid southern Africa. In: Xu Y and Beekman HE (eds.) Groundwater Recharge Estimation in Southern Africa. UNESCO International Hydrological Programme, Paris

Belkhiri, L., Boudoukha, A., Mouni, L. & Baouz, T. (2010). Application of multivariate statistical methods and inverse geochemical modeling for characterization of groundwater a case study: Ain Azel plain (Algeria). *Geoderma*, 159(3–4),390–398

Beretta, G. P. & Terrenghi, J. (2016). Groundwater flow in the Venice lagoon and remediation of the Porto Marghera industrial area (Italy). *Hydrogeol J*., https://doi:10.1007/s10040-016-1517-5



Bertrand, G., Siergieiev, D., Ala-Aho, P. & Rossi, P.M. (2013). Environmental tracers and indicators bringing together groundwater, surface water and groundwater-dependent ecosystems: importance of scale in choosing relevant tools. *Environ Earth Sci,* 72, 813–827

Bhat, S.A., Meraj, G., Yaseen, S. & Pandit, A.K. (2014). Statistical Assessment of Water Quality Parameters for Pollution Source Identification in Sukhnag Stream: An Inflow Stream of Lake Wular (Ramsar Site), Kashmir Himalaya. *J Ecosyst.*, 1–18

Bhuiyan, M.A.H., Dampare, S.B., Islam, M.A. & Suzuki, S. (2015). Source apportionment and pollution evaluation of heavy metals in water and sediments of Buriganga River, Bangladesh, using multivariate analysis and pollution evaluation indices. *Environ. Monit. Assess*., 187, 4075

Bocanegra, E., Quiroz Londoño O., Martínez, D. & Romanelli, A. (2013). Quantification of the water balance and hydrogeological processes of groundwater–lake interactions in the Pampa Plain, Argentina. *Environ Earth Sci*. 68,2347–2357

Bradford, R.B. & Acreman, M.C. (2003) Applying MODFLOW to wet grassland in-field habitats: a case study from the Pevensey Levels, UK. *Hydro Earth Syst Sc* 7(1), 43–55

Bradley, C. (2002). Simulation of the annual water table dynamics of a floodplain wetland, Narborough Bog, UK. *Journal of Hydrology,* 261(1-4), 150-172

Brannen, R., Spence, C., & Ireson, A. (2015). Influence of shallow groundwater–surface water interactions on the hydrological connectivity and water budget of a wetland complex, *Hydrol. Process*., 29, 3862–3877

Brinson, M.M. (1993). A hydrogeomorphic classification for wetlands, Technical report WRP-DE-4, U.S. Army engineer waterways experiment station, Vicksburg, MS. NTIS No. AD A 270 053

Brodie, R., Sundaram, B., Tottenham, R., Hostetler, S. & Ransley, T. (2007). An overview of tools for assessing groundwater–surface water connectivity. Bureau of Rural Sciences, Canberra (October), 133 pp



Bullock, A. & Acreman, M. (2003). The role of wetlands in the hydrological cycle. *Hydrology and Earth System Sciences*, 7 (3), 358-389

Butler, C.A. (2009). A rapid method for measuring local groundwater-surface water interactions and identifying potential non-point source pollution inputs to rivers. *MSc thesis*, University of California

Cai, W.J., Hu, X., Huang, W.J., Murrell, M.C., Lehrter, J.C., Lohrenz, S.E., Chou, W. C., Zhai, W., Hollibaugh, J.T., Wang, Y., Zhao, P., Guo, X., Gundersen, K., Dai M. & Gong, G.C. (2011). Acidification of subsurface coastal waters enhanced by eutrophication. *Nature Geoscience*, 4, 766–770

Cappa, C. D., Hendricks, M. B. & DePaolo, D. J. (2003). Isotopic fractionation of water during evaporation. *Journal of Geophysical Research*, 108(D16), 4525. https://doi:10.1029/2003JD003597

Carol, E., Mas-Pla J. & Kruse, E. (2013). Interaction between continental and estuarine waters in the wetlands of the northern coastal plain of Samborombon Bay, Argentina. *Applied geochemistry*, 34, 152-163

Carol, E. & Kruse, E. (2012). Hydrochemical characterization of the water resources in the coastal environments of the outer Río de la Plata estuary, Argentina. *J S Am Earth Sc.i*, 37,113–121

Carol, E. Kruse, E. & Mas-Pla J. (2009). Hydrochemical and isotopical evidence of groundwater salinization processes on the coastal plain of Samborombo Bay, Argentina. *Journal of Hydrology*, 365 (3), 335-345

Carol, E., Kruse, E., Mancuso, M. & Melo, M. (2013). Local and regional water flow quantification in groundwater-dependent wetlands. *Water resources management*, 27 (3), 807-817

Cartwright, I., Hall, S., Tweed, S. & Leblanc, M. (2009). Geochemical and isotopic constraints on the interaction between saline lakes and groundwater in southeast Australia. *Hydrogeology Journal*, 17, 1991-2004

Cartwright, I. & Morgenstern, U. (2012). Constraining groundwater recharge and the rate of geochemical processes using environmental isotopes and major ion geochemistry: ovens catchment, southeast Australia. *Journal of Hydrology*, 475, 137–149

Chapman, J.B., Lewis, B. & Greg, L. (2003). Chemical and isotopic evaluation of water sources to the fens of South Park, Colorado. *Environmental Geology*, 43, 533–545. https://doi: 10.1007/s00254-002-0678-9

Chapman, D. (1992). Water Quality Assessment-A Guide to the Use of Biota, Sediments and Water in Environmental Monitoring. First Edn., Cambridge University Press, Cambridge, 585 pp

Chaturvedi, R.S. (1973). A note on the investigation of ground water resources in western districts of Uttar Pradesh. In Annual report; U.P. Irrigation Research Institute: Bahadrabad, India. 86–122 pp

Chen, J., Liu, X., Sun, X., Su, Z. and Yong, B. (2014). The origin of groundwater in Zhangye Basin, northwestern China, using isotopic signature. *Hydrogeol J*, 22(2),411–424

Chevoratev, II (1955). Metamorphism of natural water in the crust of weathering. *Geochim Cosmochim Acta*, 8,22–48

Choi, H. & Harvey J. W. (2000). Quantifying time-varying ground-water discharge and recharge in wetlands of the northern Florida Everglades. *Wetlands*, 20(3), 500–511

Cohen, M. J., Creed, I. F., Alexander, L., Basu, N. B., Calhoun, A. J., Craft, C., D'Amico, E., DeKeyser, E., Fowler, L. & Golden, H. E. (2016). Do geographically isolated wetlands influence landscape functions? *P. Natl. Acad. Sci. USA*, 113,1978–1986

Coplen, T.B. (2011). Guidelines and recommended terms for expression of stable isotope-ratio and gas-ratio measurement results. Rapid Commun. Mass Spectrom. 25:2538–2560

Coplen, T. B. & Hanshaw, B. B. (1973). Ultrafiltration by a compacted clay membrane, 1. Oxygen and hydrogen isotopic fractionation. *Geochim. Cosmochim. Acta, V.* 37, 2295-2310

Cook, P.G., Lamontagne, S., Berhane, D. & Clark, J.F. (2006). Quantifying groundwater discharge to Cockburn River, south-eastern Australia, using dissolved gas tracers 222Rn and SF6. *Water resource management*, 42(10), 1–12

Clark, I. & Fritz, P. (1997). Environmental isotopes in hydrogeology. Lewis Publisher, New York, 328 pp



Constantz, J. (2008). Heat as a tracer to determine streambed water exchanges. *Water Resour. Res.*, 44

Cowardin, L.M., Carter, V., Golet, F.C. & LaRoe, E.T. (1979). Classification of wetlands and deep-water habitats of the United States, U.S. Department of the Interior Fish and Wildlife Service Office of Biological Services, Washington DC

Craig, H. (1961). Isotopic variations in meteoric waters. *Sciences*, 133, 1702-1703

Craig, H. & L. I. Gordon. (1965). Deuterium and oxygen-18 variations in the ocean and marine atmosphere. Laboratory of Geology and Nuclear Science, Pisa, Italy. Stable isotopes in oceanographic studies and paleo temperatures. 9–130pp

Crowe, A. S. & Shikaze. S.G. (2004). Linkages between groundwater and coastal wetlands of Laurenthian Lakes. *Aquat. Eco.Health & Manage*. 7(2), 199-213

Dadson, J.A. (1995). Ghana Coastal Wetlands Management Project, Baseline Socio-economic studies (Sakumo site), Prepared for the Department of Game and Wildlife, Government of Ghana

Dansgaard, W. (1964). Stable isotopes in precipitation. Tellus XVI 4, 437-468

Darko, P.K., Barnes, E.A. & Sekpey. N.K. (1995). Groundwater assessment of the Accra plains, Water Resources Research Institute (CSIR), Accra, Ghana.

Dickson, K.A. & Benneh, G.A. (1995). A New Geography of Ghana. UK: Longman

Dinka, M.O., Loiskandl, W. & Ndambuki, J.M. (2015). Hydrochemical characterization of various surface water and groundwater resources available in Matahara areas, Fantalle Woreda of Oromiya Region, *J. Hydrol.: Regional Studies,* 3,444–456

Diserens, E. (1934). Beitrag zur Bestimmung der Durchlässigkeit des Bodens in natürlicher Bodenlagerung. *Schweiz. Landw. Monatstr*. 12

Drever, J. I. & Smrth, C. L. (1978). Cyclic wetting and drying of the soil zone as an influence on the chemistry of groundwater and terrains. *American Journal Science* 278, 1448-1454

Durov, S.A. (1948). Natural waters and graphic representation of their compositions. Dokl Akad Nauk SSSR 59, 87–90

El-Kadi, A.I. (1995). Groundwater models for water resources analysis and management. CRC Lewis Publishers, London. 367 pp

Elango, L. & Kannan, R. (2007). Rock–water interaction and its control on chemical composition of groundwater, *Developments in environmental science,* 5,229-243

Environmental Protection Agency (2006). U.S. Environmental Protection Act. Available online at http//www.epa.gov. (Accessed on 22/05/2016)

Environmental Protection Agency (EPA/ World Bank) (1997). Towards an integrated coastal zone management strategy for Ghana. 139 pp

Ernst, L., & Westerhof, J. (1950). A new formula for the calculation of the permeability factor with auger hole method, Translated from Dutch by H. Bouwer, Cornell University. Ithaca, NY: Cornell University

Faust, C.R. & Mercer, J.W. (1980). Groundwater modeling: numerical models. *Groundwater*, 18(4), 395-409

Ferrarin C., Ghezzo, M., Umgiesser, G., Tagliapietra, D., Camatti, E., Zaggia L. & Sarretta, A. (2013). Assessing hydrological effects of human interventions on coastal systems: numerical applications to the Venice Lagoon. *Hydrol Earth Syst Sci*, 17, 1733–1748

Fetter, C. (2001). Applied hydrogeology + Visual Modflow, Flow net and Aqtesolv student version software on CD-ROM: Prentice Hall, Upper Saddle River

Fitts, C. R. (2000). Groundwater Science, Academic Press, UK, 7-8 pp

Fonteh, M. L., Fonkou T., Fonteh M. F., Njoyim, E. B. T. & Lambi, C.M. (2017). Spatial variability and contamination levels of fresh water resources by saline intrusion in the coastal low-lying areas of the Douala Metropolis-Cameroon. *Journal of Water Resource and Protectio*n, 9, 215-237

Freeze, R.A. & Cherry, J.A. (1979). Groundwater. 2nd Edition, Prentice Hall, Eaglewood Cliff, 604 pp

Freeze, R.A. & Witherspoon P.A. (1968). Theoretical analysis of regional groundwater flow: 3. Quantitative interpretations. *Water Resources Research*, 4(3), 581-590

Ganyaglo, S. Y. (2014). Hydrogeochemical and isotopic studies of groundwater in coastal groundwaters of Ghana. *PhD Thesis*, University of Ghana

Garbish, E. W. (1994). Achieving the correct hydrology to support constructed wetlands. St. Micheals, MD: Environmental concern, Inc

Garrels, R.M. & Christ, C.L. (1965). Solutions, minerals and equilibria. Harper, New York, 450 pp

Gat, J.R. (1998). Modification of the isotopic composition of meteoric waters at the land-biosphere- atmosphere interface: In: Isotope Techniquesin the Study of Environmental Change, IAEA,Vienna, Austria, 153-164

Gbeckor – Kove, P.D. (2010). Land use / land cover changes in fast developing urban settlements: A case study of the Sakumo lagoon catchment and ramsar site. University of Ghana

GCLME/UNEP/UNEP-GPA/US-NOAA (2007). Draft Protocol to the Abidjan Convention Concerning Cooperation in the Protection of Marine and Coastal environment from Land-based Sources and Activities in the West and Central African region. 13pp

Gedeon, M. & Mallants, D. (2012). Sensitivity analysis of a combined groundwater flow and solute transport model using local-grid refinement: A case study. *Mathematical geosciences*, 44(7), 881-899

Ghesquière, O., Walter, J., Chesnaux, R. & Rouleau, A. (2015). Scenarios of groundwater chemical evolution in a region of the Canadian Shield based on multivariate statistical analysis. *Journal of Hydrology: Regional Studies* 4,246–266

Gibbs, R. J. (1970). Mechanism controlling world water chemistry. *Science*, 170, 1088-1090

Gibson, J., Edwards, T., Birks, S., St Amour, N., Buhay, W., McEachern, P., Wolfe, B. & Peters, D. (2005). Progress in isotope tracer hydrology in Canada. *Hydrol Process*. 19,303–327

Gibson, G.R., Barbour, M.T., Stribling, J., Gerritsen, J. & Karr, J. (1996). Biological criteria: technical guidance for streams and small rivers. Washington, DC: Environmental Protection Agency, Office of Water

Glynn, P.D. & Plummer, L.N. (2005). Geochemistry and the understanding of groundwater systems. *Hydrogeo J.* 13(1),263–287

Glover, E. T., Akiti, T. T. and Osae, O. (2013). Environmental stable isotope studies of groundwater in the in the Accra Plains. *Elixir Pollution*. *55*: 12813-12819

Glover, E. T., Akiti, T. T. & Osae, S. (2012). Major ion chemistry and identification of hydrogeochemical processes of groundwater in the Accra Plains. *Elixir Geosciences,* 50, 10279-10288.

Golden, H., Creed, I. F., Ali, G., Basu, N. B., Neff, B., Rains, M., McLaughlin, D., Alexander, L., Ameli, A. A., Christensen, J., Evenson, G., Jones, C., Lane, C. & Lang, M. (2017). Scientific tools for integrating geographically isolated wetlands into land management decisions. *Front. Ecol. Environ.*,

Grygoruk, M., Batelaan, O., Okruszko, T, Mirosław-Świątek, D., Chormański, J. & Rycharski, M. (2011). Groundwater modelling and hydrological system analysis of wetlands in the Middle

Biebrza Basin. Modelling of hydrological Processes in the Narew Catchment, Geoplanet: *Earth and Planetary Sciences Springer Verlag*, Berlin-Heidelberg

Guan, H., Zhang, X., Skrzypek, G., Sun, Z. & Xu, X. (2013). Deuterium excess variations of rainfall events in a coastal area of south Australia and its relationship with synoptic weather systems and atmospheric moisture sources. *Journal of geophysical research: atmospheres,* 118 (2),1-16

Guay, C., Nastev, M., Paniconi, C. & Sulis M. (2013). Comparison of two modeling approaches for groundwater–surface water interactions, *Hydrol. Processe*s, 27(16), 2258–2270

Guiguer, N.A. & Molson, J. (1996). Flonet/trans: Two dimensional steady-state and advective-dispersive contaminant transport model. Users guide, Waterloo Hydorlogic Software, Centre for Groundwater Research

Guler, C, Thyne, G. D, McCray, J. E. & Turner, A. K. (2002). Evaluation of graphical and multivariate statistical methods for classification of water chemistry data. *Hydrogeo J.* 10, 455-474

Gusyev, M.A. & Haitjema, H.M. (2011). Modelling flow in wetlands and underlying groundwaters using a discharge potential formulation. Journal of Hydrology 408, 91-99

Gwin, S.E., Kentula, M.E. & Shaffer, P.W. (1999). Evaluating the effects of wetland regulation through hydrogeomorphic classification and landscape profiles. *Wetlands* 19, 477–489

Ha, R.R. & Ha, J.C. (2011). Integrative statistics for the social and behavioral sciences, Sage

Hamzah, M., Jaafar O., Jani, W.N.F.A. & Sabdullah, M.S. (2016). Multivariate analysis of physical and chemical parameters of marine water quality in the Straits of Johor, Malaysia. *Journal of Environmental Science and Technology,* 9, 427-436

Harbaugh, A.W., Banta, E.R., Hill, H.C. & McDonald, M.G. (2000). MODFLOW-2000. The U.S. geological survey modular ground-water model-user guide to modularization concepts and the ground-water flow processes. United States Geological Survey Government Printing Office, Reston

Harbaugh, A. W. (2005). MODFLOW-2005 the U.S. geological survey modular groundwater model-the ground-water flow process, U.S. Geological Survey techniques and methods

Hargreaves, G.H. & Samani, Z.A. (1985). Reference crop evapotranspiration from temperature. *American Society of Agricultural Engeneering*, 1(2),96–99

Hayashi, M., van der Kamp, G. & Rosenberry, O. (2016). Hydrology of Prairie Wetlands: Understanding the integrated surface-water and groundwater processes. *Wetlands*, 1–18. https://doi: 10.1007/s13157-016-0797-9

Hayashi, M. & Van der Kamp, G. (2009). Progress in scientific studies of groundwater in the hydrologic cycle in Canada, 2003-2007. *Canadian Water Resources Journal*, 34 (2), 177-186

Hem, J. D. (1970). Study and interpretation of the chemical characteristics of natural water. U.S. Geological Survey Water-Supply Paper 1473, second edition, p. 363

Herczeg, A.L., Dogramaci, S.S. & Leaney, F.W.J. (2001). Origin of dissolved salts in a large, semi-arid groundwater system: Murray Basin, Australia. *Mar. Freshw. Res*., 52, 41-52

Helsel, D.R. & Hirsch, R.M. (1992). Statistical methods in water resources. Elsevier

Hinga, K.R. (2002). Effects of pH on coastal marine phytoplankton. *Marine Ecology Progress Series* 238, 281-300

Hodson, M. Tranter, A. Gurnell, M. Clark, & J. O. Hagen, (2002). The hydrochemistry of Bayelva, a high Arctic proglacial stream in Svalbard. *Journal of Hydrology*, 257 (1-4), 91–114

Hoefs, J. (2004). Stable isotope geochemistry. Berlin: *Springer,* 340 pp

Hoffmann, C. C., Kjaergaard, C. Uusi-Kämppä, J. Bruun Hansen, H. C. & Kronvang, B. (2009). Phosphorus retention in riparian buffers: Review of their efficiency. *Journal of Environmental Quality* 38(5): 1942–1955

Hopkins, B.G., Horneck, D. A., Stevens, R.G., Ellsworth, J.W. & Sullivan, M. (2007). Managing irrigation water quality for crops production in the Pacific Northwest, Pacific Northwest extension pub. 597pp

Hunt, R.J., Krabbenhoft, D.P. & Anderson, M.P. (1996). Groundwater inflow measurements in wetland systems. *Water Resour. Res*., 32: 495–507

Hunt, R.J., Bullen, T.D., Krabbenhoft, D.P. & Kendall, C. (1998). Using stable isotopes of water and strontium to investigate the hydrology of a natural and a constructed wetland. *Ground Water* 36, 434–443

International Atomic Energy Agency (2010). Global Network of isotopes in precipitation. The GNIP database

Jacob, C.E. (1944). Notes on determining permeability by pumping test under water table conditions. U.S.G. S Open File Report

Jankowski, J., & Acworth, R. I. (1997). Impact of debris flow deposits on hydrogeochemical process and the development of dry land salinity in the Yass River catchment, New South Wales, Australia. *Hydrogeology Journal,* 5, 71–88. https://doi:10.1007/s100400050119.

Jaros, A., Rossi, P., Ronkanen, A.K. & Kløve, B. (2016). Modelling wetland-groundwater interactions in the boreal Kälväsvaara esker, Northern Finland. EGU General Assembly, Vienna Austria. 12103 pp

Johnson, L.E. (2008). Geographic information systems in water resources engineering, CRC Press

Jessen, S., Holmslykke, H.D., Rasmussen K., Richardt N. and Holm, P. E. (2014). Hydrology and pore water chemistry in a permafrost wetland, Ilulissat, Greenland. *Water Resour. Res*., 50, 4760–4774

Jolly, I.D., McEwan, K.L. & Holland, K.L. (2008). A review of groundwater–surface water interactions in arid/semi-arid wetlands and the consequences of salinity for wetland ecology. *Ecohydrology* 1, 43–58

Junner, N.R. & Bates, D.A. (1945). Geol. Surv. Gold Coast memoir, 7

Kalbus, E., Reinstorf, F. & Schirmer, M., (2006). Measuring methods for groundwater – surface water interactions : a review. *Hydrol. Earth Syst. Sci*, 10, 873–887

Karunanithi, N., Grenney, W., Whitley, D., & Bovee, K. (1994). Neural networks for river flow prediction. *Journal of Computing in Civil Engineering*, 201-220

Kebede, S., Travi, Y., Alemayehu, T. & Marc, V. (2006). Water balance of Lake Tana and its sensitivity to fluctuations in rainfall, Blue Nile basin, Ethiopia. *J. Hydrol*. 316(1–4), 233–247

Kelbe, B. E., Grundling, A. T. & Price J. S. (2016). Modelling water-table depth in a primary groundwater to identify potential wetland hydrogeomorphic settings on the northern Maputaland Coastal Plain, KwaZulu-Natal, South Africa. *Hydrogeol J*. https://doi:10.1007/s10040-015-1350-2

Kendall, C. & McDonnell, J.J. (2012). Isotope tracers in catchment hydrology. Amsterdam: Elsevier

Kendall, C. & Coplen, T.B. (2001). Distribution of oxygen-18 and deuterium in river waters across the United States. *Hydrol Process*, 5,1363–1393

Ketchen, D.J. & Shook, C.L. (1996). The application of cluster analysis in strategic management research: An analysis and critique. *Strat. Manage. J*., 17, 441-458

Kim, H., Kim, H.R., Lee, T., Cheong, T.J., Yum, B.W. & Chang, H.W. (2005). Multivariate statistical analysis to identify the major factors governing groundwater quality in the coastal area of Kimje, South Korea. *Hydrological Processes*, 19 (6), 1261–1276

Kirkham, D. (1955). Measurement of the hydraulic conductivity of soil in place. Symposium on permeability of soil. Am. Soc. for Testing Materials. *Spec. Techn. Publ. No*. 163

Koranteng, K.A. (1995) Ghana coastal wetlands management project. Environmental baseline studies (Sakumo Ramsar Site). Fisheries GW/A.285/SF2/31

Koranteng, K. A., Ofori-Danson, P. K & Entsua-Mensah, M. (1998). Comparative study of the fish and fisheries of three coastal lagoons in West Africa. *Int. jour. of Eco. And Env.*, 24, 371-382

Kortatsi, B.K. & Jorgensen N. O. (2001). The origin of high salinity waters in the Accra Plains groundwaters, Conference proceedings - First international conference on saltwater intrusion and coastal groundwaters - monitoring, modelling, management, Morocco

Kránsý, J., 1(993). Classification of Transmissivity magnitude and variation. *Groundwater*, 1(2), 230–236

Krishna, M., Rao, B.M., Murty, G., Gantasala, G.P. & Rama, B. (2012). Cluster analysis in data mining. *Int.jour. of compt. tech and elec eneg.*, 2(5)

Kwei, E.A. (1977). Biological, chemical and hydrological characters of coastal lagoons of Ghana, West Africa. *Hydrobiologia,* 56(2), 157-174

Kyei-Baffour, N., Ofori, E., Mensah, E., Agyare W.A. & Atta-Darkwa T. (2013). Modelling groundwater flow of the besease inland valley Bottom in Ghana. *Global J. Energy Agric. Health Sci*. 2(1), 52-69

Laar, C., Akiti, T. T., Brimah, A. K., Fianko, J. R., Osae, S., & Osei, J. (2011). Hydrochemistry and isotopic composition of the Sakumo Ramsar site. *Research Journal of Environmental and Earth Sciences*, 3(2), 147–153

Larocque, M.P., Biron, M., Buffin-Bélanger, T., Needelman, M., Cloutier, C. A., McKenzie, J. M. (2016). Role of the geomorphic setting in controlling groundwater–surface water exchanges in riverine wetlands – A case study from two southern Québec rivers (Canada). *Canadian Water Resources Journal*

Lee, J.Y. & Song, S.H. (2007). Groundwater chemistry and ionic ratios in a western coastal groundwater of Buan, Korea: Implication for seawater intrusion. *Geosci. Journ. Hyd*., 3, 259-270

Lessels, J.S., Tetzlaff, D.J., Birkel, C., Dick, J. & Soulsby, C. (2015). Water sources and mixing in riparian wetlands revealed by tracers and geospatial analysis. *Water Resour. Res*., 52,456-470

Levin, S.A. (2001). Encyclopedia of Biodiversity. Academic press New York. 5 (R-Z),797-8000

Li, H., Shi, A., Li, M. & Zhang, X. (2013). Effect of pH, Temperature, Dissolved Oxygen, and Flow Rate of Overlying Water on Heavy Metals Release from Storm Sewer Sediments. *Journal of Chemistry,* 434012, 11

Liu, Q. & Mou, X. (2016). Interactions between surface water and groundwater: key processes in ecological restoration of degraded coastal wetlands caused by reclamation. *Wetland,* 36, 95. http://doi:10.1007/s13157-014-0582-6

Liu, Q., Li, F., Zhang, Q., Li, J., Zhang, Y., Tu, C. & Ouyang, Z. (2014). Impact of water diversion on the hydrogeochemical characterization of surface water and groundwater in the Yellow River Delta. *Applied Geochemistry,* 48, 83–92

Liu, C.W., Lin, K.H. & Kuo, Y.M. (2003). Application of factor analysis in the assessment of groundwater quality in a balckfoot diseases area in Taiwan. *Sci of the Total Environ,* 313,77–89

Lowry, C.S., Walker, J.F., Hunt R.J. & Anderson, M.P. (2007). Identifying spatial variability of groundwater discharge in a wetland stream using a distributed temperature sensor. *Journal of Water Resource Research,* 43, W10408. https://doi:10.1029/2007WR006145

Luoma, S.N. (1983). Bioavailability of trace metals to aquatic organisms - A review. *Sci of the Total Environment,* 28,1-22

Maclear, L. G. A. (1994). A groundwater hydrocensus and water quality investigation of the Swartkops River basin – Uitenhage. Technical Report Gh 3817, Directorate of Geohydrology, Department of Water Affairs and Forestry, Pretoria

Mahmoodinobar F., Ding, Y, & Hazen, R. (2013). Analyses of Groundwater Contribution to a Riverine Wetland. Annual Graduate Student Research Day, Newark, NJ

Martínez, D. E., Quiroz Londoño, O. M., Solomon, D. K., Dapeña, C., Massone, H. E., Benavente, M. A., & Panarello, H. O. *(*2017*).* Hydrogeochemistry, isotopic composition and water age in the hydrologic system of a large catchment within a plain humid environment (Argentine Pampas): Quequén Grande River, Argentina. *River Res. Applic.,* 33, 438–449

Mazor, E. (1991). Applied chemical and isotopic groundwater hydrology. USA Canada and Latin America: Halsted press

Mazor, E. (2004). Chemical and Isotopic Groundwater Hydrolysis, Third Edition, Marcel Dekker Inc. New York

Manno, E., Vassallo M., Varrica, D. & Dongarrà G. and Hauser, S. (2007). Hydrogeochemistry and water balance in the coastal wetland area of Biviere di Gela, Sicily, Italy. *Water, air soil pollut,* 178,179-193. https://doi:10.1007/s11270-0060-9189-8

McCallum, J. L., Engdahl, N. B., Ginn, T. R. & Cook. P.G. (2014). Nonparametric estimation of groundwater residence time distributions: What can environmental tracer data tell us about groundwater residence time? *Water Resour. Res.,* 50, 2022–2038. https://doi:10.1002/2013WR014974

Medina-Gómez, I. & Herrera-Silveira, J.A. (2003). Spatial characterization of water quality in a karstic coastal lagoon without anthropogenic disturbance: a multivariate approach. *Estuar. Coast. Shelf Sci.* 58,455–465. https://doi: 10.1016/S0272-7714(03)00112-4

Mendoza-Sanchez, I., Phanikumar, M. S. Niu, J., Masoner, J.R., Cozzarelli, I.M. & McGuire, J.T. (2013). Quantifying wetland–groundwater interactions in a humid subtropical climate region: An integrated approach. *Journal of Hydrology,* 498 (0), 237-253

Ministry of Lands and Forestry, (1999). Managing Ghana's Wetlands: A National Wetlands Conservation Strategy

Middleton, M. A., Allen, D. M. & Whitfield, P. H. (2016). Comparing the groundwater contribution in two groundwater-fed streams using a combination of methods. *Canadian Water Resources Journal*. doi:10.1080/07011784.2015.1068136

Misstear, B.D.R., Brown, L. & Daly, D. (2009). A methodology for making initial estimates of groundwater recharge from groundwater vulnerability mapping. *Hydrogeol. J.,* 17, 275–285

Molla, M.A., Saha, N., Salam, S.A. & Rakib-uz-Zaman, M. (2015). Surface and groundwater quality assessment based on multivariate statistical techniques in the vicinity of Mohanpur, Bangladesh. *Int. J. Environ. Health Eng.,* 4,18



Moseki, M. C. (2013). Surface–groundwater interaction: development of methodologies suitable for South African conditions. *PhD thesis,* University of the Free State, Bloemfontein, South Africa

Mosimane, K., Struyf E., Gondwe, M.J., Frings, P., Pelt D.V., Wolski P., Schoelynck J., Schaller J., Conley D.J. & Hudson, M. M. (2017). Variability in chemistry of surface and soil waters of an evapotranspiration-dominated flood-pulsed wetland: solute processing in the Okavango Delta, Botswana. *Water SA,* 43

Muteraja, K.N. (1986). Applied Hydrology. Tata MGraw-Hill: New Delhi, India

Nartey, V.K., Edor, K.A., Doamekpor, L.K. & Bobobee, L.H. (2011). Nutrient load of the Sakumo lagoon at the Sakumo Ramsar site Tema, Ghana. *West Africa Journal of Applied Ecology* 19.

Nayaka, S.B., Ramakrishna, M., Jayaprakash, S. and Delvi, M.R. (2009). Impact of heavy metals on water, fish (Cyprinus carpio) and sediments from a water tank at Tumkur, India. *Oceanol. Hydrobiol. Stud*., 38(2), 17-28

Négrel, P., Petelet-Giraud, E., Barbier, J. & Gautier, E. (2003). Surface water-groundwater interactions in an alluvial plain: Chemical and isotopic systematics, *Journal of Hydrology*, 277, 248-267

Négrel, P. & Lachassagne, P. (2000). Geochemistry of the Maroni River (French Guyana) during low water stage: Implications for water rock interaction and groundwater characteristics. *J of Hydrol* 237, 212-233

Nesbitt, H. W., Markovics, G. & Price, R.C. (1980). Chemical processes affecting alkalis and alkalme earths during continental weathering. *Geochimica et Cosmochimica Acta*. 44,1659-1666

Nonterah, C., Xu, Y., Osae, S., Akiti, T. T. & Dampare, S.B. (2015). A review of the ecohydrology of the Sakumo wetland in Ghana. *Environ Monit Assess*. 187: 671 DOI 10.1007/s10661-015-4872-0

Ntiamoa-Baidu, Y. (1991b). Conservation of coastal lagoons in Ghana. The traditional approach. Elsevier Science Publishers B.V., Amsterdam. Landscape and urban planning 20,41-46

Nur, A., Ishaku, J. M. & Yusuf, S. N. (2012). Groundwater flow patterns and Hydrochemical facies distribution using Geographical Information System (GIS) in Damaturu, Northeast Nigeria, 1096–1106

Nyarko, B. K. (2007). Floodplain wetland-river flow synergy in the White Volta River basin, Ghana. *Ecology and Development Series Bd*. 53

Nyende, J., van Tonder G. & Danie Vermeulen, D. (2014). Hydrochemical Characteristics of Ground and Surface water under the influence of Climate variability in Pallisa District, eastern Uganda. *International Journal of Environmental Science and Toxicology*, 2(4), 90-107

Odokuma-Alonge, O. & Adekoya, J.A. (2013). Factor analysis of stream sediment geochemical data from onyami drainage system, southwestern Nigeria, *International Journal of Geosciences*, 4, 03656

Park, S.C., Yun, S.T., Chae, G.T., Yoo, I.S., Shin, K.S., Heo, C.H. & Lee, S.K. (2005). Regional hydrochemical study on salinization of coastal groundwaters, western coastal area of South Korea. *J Hydrol*, 313, 182–194

Phillips, P. J. & Shedlock, R. J. (1993). Hydrology and chemistry of groundwater and seasonal ponds in the Atlantic Coastal Plain in Delaware, USA, *Journal of Hydrology*, 141, 157-178

Piper, A.M. (1944). A graphic procedure in the geochemical interpretation of water analyses. Transactions of the American Geophysical Union 25, Plenum Press, Boca Raton: 914–928

Qian, H., Wu, J., Zhou, Y. & Li, P. (2014). Stable oxygen and hydrogen isotopes as indicators of lake water recharge and evaporation in the lakes of the Yinchuan Plain. *Hydrol Process* 28(10), 3554–3562

Ramsar Convention Secretariat. (2014). Country Profile: Ghana. Retrieved from http://www.ramsar.org/wetland/ghana.

Ramsar Convention (1971). Convention on Wetlands of International Importance Especially as Waterfowl Habitat, Feb 2, 1971, II. I.L.M.969

Reardon, I.S. & Harrell, R. M. (1990). Acute toxicity of formalin and copper sulfate to striped bass fingerlings held in varying salinities. *Aquaculture,* 87, 255-270

Reghunath, R., Murthy, T.R.S. & Raghavan, B.R. (2002). The utility of multivariate statistical techniques in hydrogeochemical studies: an example from Karnataka, India. *Water Research,* 36 (10), 2437–2442

Reynolds, D.A. & Marimuthu, S. (2007). Deuterium composition and flow path analysis as additional calibration targets to calibrate groundwater flow simulation in a coastal wetlands system. *Hydrogeol J*, 15(3), 515-535. https:// doi:10.1007/s10040-006-0113-5

Revelle, R. (1941). Criteria for recognition of sea water in groundwater. *Transactions of American Geophysical Union*, 22, 593–597.

Romanelli, A. (2011). Integrated Hydrogeological Study of Surface & Ground Water Resources in the Southeastern Buenos Aires Province, Argentina. *Int. J. Environ. Res.*, 5(4), 1053-1064

Rosenberry, D.O., Lewandowski, J., Meinikmann, K. & Nützmann, G. (2015). Groundwater-the disregarded component in lake water and nutrient budgets. Part 1: Effects of groundwater on hydrology. *Hydrol. Process*., 29, 2895–2921

Rosenberry, D.O. & LaBaugh. J.W. (2008). Field techniques for estimating water fluxes between surface water and groundwater: U.S. Geological Survey Techniques and Methods 4-D2. Reston, Virginia: USGS

Rozanski, K., Araguas-Araguas, L. & Gonfiantini, R. (1993). Isotopic patterns in modern global precipitation. In Climate Change in Continental Isotopic Records, Geophysical Monograph 78, Swart PK, Lohman KC, McKenzie J, Savin S (eds). American Geophysical Union: Washington, DC, 1–36.

Rudnick, S. Lewanski J. & Nützmann. G. (2014). Investigating groundwater–lake interactions by hydraulic heads and a water balance. *Ground Water* 53(2), 227–237

Sakai, H & Matsubaya, O (1977). Stable isotopic studies of Japanese geothermal system. Geothermics 5:97–124

Salvendy, G. (2012). Handbook of human factors and ergonomics. John Wiley & Sons

Sami, K. (1992). Recharge mechanisms and geochemical processes in a semi-arid sedimentary basin, Eastern Cape, South Africa. *Journal of Hydrology* (Amsterdam), *139*, 27–48. https://doi:10.1016/ 0022-1694(92)90193-Y

Sarkar, S. & Bhattacharya, B.D. (2010). Water quality analysis of the coastal Regions of Sundarban Mangrove wetland, India using multivariate statistical techniques. Environmental management, Santosh Sarkar (Ed.), InTech, https://doi: 10.5772/10105

Schot, P. P., Dekker, S. C. & Poot, A. (2004). The dynamic form of rainwater lenses in drained fens. *Journal of Hydrology* 293, 74-84

Stets, E.G. Kelly, V.J. & Crawford, C.G. (2014). Long-term trends in alkalinity in large rivers of the conterminous US in relation to acidification, agriculture, and hydrologic modification. *Science of the total environment*, 488–489, 280–289

Shan, V., Singh, S.K. & Haritash, A.K. (2017). Major ions chemistry of surface water in Bhindawas wetland. *International Journal of Advance Research and Innovation*, 5(1), 117-121

Shaw, G.D., Mitchell, K.L. & Gammons, C.H. (2017). Estimating groundwater inflow and leakage outflow for an intermontane lake with a structurally complex geology: Georgetown Lake in Montana, USA. *Hydrogeol J*., 25, 135

Sheela, A.M., Letha J., Joseph, S., Chacko, M., Sanal kumar S.P. & Thomas, J. (2012). Water quality assessment of a tropical coastal lake system using multivariate cluster, principal component and factor analysis. *Lakes & Reservoirs*: *Research and Management*, 17, 143-159

Shrestha, S. & Kazama, F. (2007). Assessment of surface water quality using multivariate statistical techniques: A case study of the Fuji river basin, Japan. *Environmental Modelling & Software*, 22 (4), 464-475

Skrzypek, A., Dogramaci, S. & Grierson, P.F. (2013). Geochemical and hydrological processes controlling groundwater salinity of a large inland wetland of northwest Australia. *Chem. Geol.,* 357, 164-177

Smith, S.D., Lamontagne, S., Taylor, A.R. & Cook, P.G. (2015). Evaluation of groundwater – surface water interactions at Bool lagoon and Lake Robe using environmental tracers, Goyder Institute for Water Research Technical Report Series No. 15/14



Sola, F., Vallejos, A., Daniele, L. & Pulido-Bosch, A. (2014). Identification of a Holocene groundwater–lagoon system using hydrogeochemical data. *Quat. Res.*, 82, 121-131

Somay, M.A. & Filiz, S. (2003). Hydrology, hydrogeology and hydrochemistry of wetlands: a case study in Izmir Bird Paradise, Turkey. *Env Geol* 43, 825 https:// doi:10.1007/s00254-002-0697-6

Sophocleous, M. & Perry, C. A. (1985). Experimental studies in natural groundwater – recharge dynamics: the analysis of observed recharge events. *J. Hydrol.,* 8, 297–332

Soulsby, C., Tetzlaff, D., van den Bedem, N., Malcolm, I.a., Bacon, P.G. & Youngson, F.a. (2007). Inferring groundwater influences on surface water in montane catchments from hydrochemical surveys of springs and stream waters. *J. Hydrol.*, 333, 199–213

Spellman, F.R. & Drinan, J. (2000). The drinking water handbook. Technomic Publishing Company Inc., Lancaster, 260 pp

Spitz, K. & Moreno, J. (1996). A practical guide to groundwater and solute transport modeling 3rd ed., New York: John Wiley & Sons.Inc.

Sprecher, S. (2008). Installing monitoring wells in soils (Version 1.0). National soil survey center, NRCS, USDA, Lincoln, NE

Sun, X., Xu, Y., Jovanovic, N.Z., Kapangaziwiri, E., Brendonck, L. & Bugan, R.D.H. (2013). Application of the rainfall infiltration breakthrough (RIB) model for groundwater recharge estimation in west coastal South Africa. *water SA,* 39(2), 221–230

Sundaray, S.K. (2010). Application of multivariate statistical techniques in hydrogeochemical studies-a case study: Brahmani–Koel River (India). *Environ Monit Assess*., 164, 297. https:// doi:10.1007/s10661-009-0893-x

Taak, J.K. & Singh, K.P. (2014). Hydrochemical Investigations of Sukhna Wetland and Adjoining Groundwater Regime. *International Journal of Environmental Science and Toxicology Research*, 2(5), 108-118.

Templ, M., Filzmoser, P. & Reimann, C. (2008). Cluster analysis applied to regional geochemical data: problems and possibilities. *Applied Geochemistry*, 23 (8), 2198- 2213



Theis, C.V. (1935). The relation between the lowering of the piezometric surface and the rate and duration of discharge of a well using groundwater storage. Trans Am Geophys Union 16:519–524.

Tiner, R.W. (2003). Geographically isolated wetlands of the United States. *Wetlands* 23,494–516

Tóth, J. (1963). A theoretical analysis of groundwater flow in small drainage basins. *J Geophys Res* 68(16), 4795–4812

Turnadge, C.J. & Lamontagne, S. (2015). A MODFLOW-based approach to simulating wetland–groundwater interactions in the Lower Limestone Coast Prescribed Wells Area, Goyder Institute for Water Research Technical Report Series No. 15/12, Adelaide, South Australia

Turner, K. W., Wolfe, B. B. & Edwards, T. W. D. (2010). Characterizing the role of hydrological processes on lake water balances in the Old Crow Flats, Yukon Territory, Canada, using water isotope tracers. *Journal of Hydrology,* 386, 103–117

U. S. Army Corps of Engineers (1999). Groundwater Hydrology: Engineering and Design, Engineer Manual, 1110-2-1421

Venkatramanan, S., Chung, S.Y., Ramkumar, T., Gnanachandrasamy G. & Vasudevan, S. (2013). Multivariate statistical approaches on physicochemical characteristics of ground water in and around Nagapattinam district, Cauvery deltaic region of Tamil Nadu, India. *Earth Sci. Res. J*., 17, 97-103

Vieira, J.S., Pires, J.C.M., Martins, F.G., Vilar, V.J.P., Boaventura, R.A.R. & Botelho, C.M.S. (2012). Surface water quality assessment of Lis River using multivariate statistical methods. *Water Air Soil Pollut.* https:// doi:10.1007/s11270-012-1267-5

Viessman, W., Jr. & Lewis, G.L. (1996). Introduction to Hydrology, ed 4. New York: Harper Collins College Publishers

Wang, J.Z., Jiang, X.W., Wan, L., Wang, X.S. & Li, H. (2014). An analytical study on groundwater flow in drainage basins with horizontal wells. *Hydrogeol J.,* 22(7), 1625–1638

Watson, K.A., Mayer, A.S. & Reeves, H.W. (2014). Groundwater availability as constrained by hydrogeology and environmental flows. *Ground Water,* 52(2), 225-238

Weitz, J. & Demlie, M. (2014). Conceptual modelling of groundwater-surface water interactions in the Lake Sibayi Catchment, Eastern South Africa. *J. of Afric. Earth Science*, 99, 613-624

Weitz, J. & Demlie, M. (2015). Hydrogeological system analyses of the Lake Sibayi catchment, North-Eastern South Africa. *South African Journal of Geology*, 118 (1), 91-106

Weissmann, G. S., Zhang, Y. LaBolle, E. M. & Fogg, G. E. (2002). Dispersion of groundwater age in an alluvial groundwater system, *Water Resour. Res*., 38(10), 1198. https:// doi:10.1029/2001WR000907

World Health Organization (2011). Guidelines for drinking water quality. WHO Library Cataloguing-in-Publication Data, fourth Edition, Vol.1, Geneva

Williams, M. (1991). Wetlands: a threatened Landscape. B. Blackwell, Oxford

Williams, L.K & Langely, R.L. (2001). Environmental Health Secrets. Hanley and Belfus ,Inc. Press,Philadelphia

Winston, R.B. (2009). ModelMuse-a graphical user interface for MODFLOW-2005 and PHAST. Techniques and methods 6-A29 USGS, Reston

Winter, T. C. (1999). Relation of streams, lakes, and wetlands to groundwater flow systems. *Hydrogeology Journal* 7 (1): 28–45

Winter, T.C. & Rosenberry, D.O. (1998). Hydrology of prairie pothole wetlands during drought and deluge: A 17-year study of the Cottonwood Lake wetland complex in North Dakota in the perspective of longer term measured and proxy hydrological records. *Climatic Change* 40, 189–209

Winter, T.C., Harvey, J.W., Franke, O.L. & Alley, W.M. (1998). Groundwater and surface water-A single resource. U.S. Geological Survey Circular No. 1139. Reston, Virginia: USGS

Winter, T.C. (1978). Numerical simulation of steady-state three-dimensional groundwater flow near lakes. *Water Resour Res*, 14, 245–254

Woldemariyam, F. & Ayenew, T. (2016). Identification of hydrogeochemical processes in groundwater of Dawa River basin, southern Ethiopia. *Environ Monit Assess.,* 188, 481. https://:10.1007/s10661-016-5480-3



Wood, W.W. (1976). Guidelines for collection and field analysis of groundwater samples for selected unstable constituents. Techniques of Water Resources Investigations of the United States Geological Survey, Book 1, chapter D2, 24 pp

World Bank/EPA (World Bank/ EPA) (1996). Towards an Integrated Coastal Zone Management Strategy for Ghana. The World Bank Washington D.C. USA /Environmental Protection Agency, Accra

Wotany, E.R., Ayonghe, S.N., Fantong, W.Y., Wirmvem, M.J. & Ohba, T. (2013). Hydrogeochemical and anthropogenic influence on the quality of water sources in the Rio del Rey basin, South Western, Cameroon, Gulf of Guinea. *African Journal of Environmental Science and Technology,* 7, 1053-1069

Water Resources Commission (2003). Ghana Raw Water Criteria and Guidelines, Vol. 1. Domestic Water. CSIR-Water Research Institute, Accra, Ghana

Xu, Y., Colvin, C., Van Tonder, G.J., Hughes, S., le Maitre, D., Zhang, J., Mafanya, T., & Braune, E. (2002). Towards the resource directed measures: groundwater component (Version 1.1). WRC Report No. 1090-2/1/03. Pretoria: Water Research Commission

Yang, Q., Zhang J., Wang Y., Fang Y. & Delgado M.J. (2015). Multivariate statistical analysis of hydrochemical data for shallow groundwater quality factor identification in a coastal groundwater. *Pol. J. Environ. Stud*. 24(2), 769-776

Yang, L., Song, X., Zhang, Y., Han, D., Zhang, B. & Long, D. (2012). Characterizing interactions between surface water and groundwater in the Jialu River basin using major ion chemistry and stable isotopes. *Hydrol. Earth Syst. Sci*., 16, 4265–4277

Yawson, S.K. (2003). Gender, environmental management and water quality in the Sakumo catchment. *MPhil. Thesis* University of Ghana. 210 pp

Yidana, S. M., Banoeng-yakubo, B. & Akabzaa, T. M. (2010). Analysis of groundwater quality using multivariate and spatial analyses in the Keta basin, Ghana. *Journal of African Earth Sciences*, 220–234

Yihdego, Y., Webb, J.A. & Vaheddoost, B. (2017). Highlighting the Role of Groundwater in Lake–Groundwater Interaction to Reduce Vulnerability and Enhance Resilience to Climate Change. *Hydrology*, 4,10

Younger, P. (2007). Groundwater in the environment: an introduction. Blackwell Publishing, UK.

Yuan, Li-R., Xin, P., Kong, J., Li, L. & Lockington, D. (2011). A coupled model for simulating surface water and groundwater interactions in coastal wetlands. *Hydrol. Process.*, 25, 3533–3546

Yuan, R., Song, X., Zhang, Y., Han, D., Wang, S. & Tang, C. (2011). Using major ions and stable isotopes to characterize recharge regime of a fault-influenced groundwater in Beiyishui River Watershed, North China Plain. *J. Hydrol.* 405, 512-521

Zabala, M., Manzano, M. & Vives, L. (2015). The origin of groundwater composition in the Pampeano Groundwater underlying the Del Azul Creek basin, Argentina. *Science of The Total Environment,* 518, 168-188

Zech, A., Zehner, B., Kolditz, O. & Attinger, S. (2016). Impact of heterogeneous permeability distribution on the groundwater flow systems of a small sedimentary basin. *J. Hydrol*, 532, 90–101

Zeng, C., Wang, L., Huang, W. & Wang, W. (2012). Research on influencing factors of water environment in the typical western of Taihu Lake based on the principal component analysis. *Adv. Mat. Res.*, 356-360, 924-92

Zghibi, A. Merzougui A., Zouhri, L. & Tarhouni, J. (2014). Interaction between groundwater and seawater in the coastal groundwater of Cap-Bon in the semi-arid systems (north-east of Tunisia). *Carbonates Evaporites* 29, 309–326. https:// doi:10.1007/s13146-013-0181-2

Zhou, Y. & Li, W. (2011). A review of regional groundwater flow modelling. *Geoscience Frontiers*, 2(2), 205–214

## APPENDICE

Appendix 4.1: Hydraulic properties on the x-axis

| Well ID | Hydraulic gradient in x-axis | Average T on the x-axis | Average K on the x-axis | Apparent flow rate Vx ($m^2$/day) | Apparent flow velocity Vx (m/day) | Flow direction |
|---|---|---|---|---|---|---|
| MW 2 | 0.026 | 1.940 | | 0.050 | | 166 N |
| MW 6 | 0.003 | 0.645 | 0.035 | 0.002 | 0.0001 | 80 N |
| MW 15 | 0.007 | 8.081 | 0.288 | 0.057 | 0.0020 | 355 |
| MW 8 | 0.023 | 7.924 | 0.008 | 0.181 | 0.0002 | 20 N |
| MW 4 | 0.022 | 3.133 | | 0.069 | | 155 N |

Appendix 4.2: Hydraulic properties on the y-axis

| Well ID | Hydraulic gradient in x-axis | Average T on the x-axis | Average K on the x-axis | Apparent flow rate Vx ($m^2$/day) | Apparent flow velocity Vx (m/day) | Flow direction |
|---|---|---|---|---|---|---|
| MW 2 | 0.057 | 2.840 | - | 0.016 | - | 76 N |
| MW 6 | 0.071 | 8.080 | 0.288 | 0.056 | 0.0021 | -10 N |
| MW 15 | 0.015 | 10.572 | 0.288 | 0.167 | - | 235 N |
| MW 8 | 0.048 | 2.294 | 0.150 | 0.010 | 0.0007 | -70 N |
| MW 4 | 0.088 | 2.830 | - | 0.024 | - | 65 N |



Appendix 4.3: Hydraulic parameter properties of the Sakumo basin

| Property | Values | SI units |
|---|---|---|
| Thickness | 12.5 | m |
| Transmissivity in x-direction (Tx) | 4.3E-05 | $m^2$/s |
| Transmissivity in y-direction (Ty) | 4.64E-05 | $m^2$/s |
| Hydraulic conductivity in the x-direction (Kx) | 1.77E-06 | m/s |
| Hydraulic conductivity in the y-direction (Ky) | 1.77E-06 | m/s |
| Hydraulic gradient in x direction (Ix) | 0.11 | |
| Hydraulic gradient in y direction (Iy) | 0.0066 | |
| Apparent flow rate in the x-direction | 8.47E-07 | $m^2$/s |
| Apparent flow rate in the y-direction | 4.25E-07 | $m^2$/s |
| Apparent velocity in the x-direction | 3.43E-08 | m/s |
| Apparent velocity in the y-direction | 1.07E-08 | m/s |

Appendix 5.1a: Chemical and environmental isotope composition of wetland water samples in the Sakumo basin ($mgL^{-1}$)

| Sample ID | | pH | EC | Temp. | $HCO_3^-$ | $Cl^-$ | $Na^+$ | $K^+$ | $Ca^{2+}$ | $Mg^{2+}$ | $SO_4^{2-}$ | $NO_3^-$ | $\delta^{18}O‰$ | $\delta^2H‰$ | d-excess |
|---|---|---|---|---|---|---|---|---|---|---|---|---|---|---|---|
| NL1 | Wetland | 8.45 | 12700 | 28.2 | 410.00 | 5895.17 | 3750.00 | 78.00 | 34.01 | 40.72 | 285.00 | 1.10 | 2.14 | 14.54 | -2.58 |
| NL2 | Wetland | 8.50 | 12200 | 24.7 | 440.00 | 5998.61 | 3800.00 | 83.00 | 39.76 | 49.70 | 280.00 | 1.01 | 2.09 | 14.09 | -2.63 |
| NL3 | Wetland | 7.42 | 13700 | 24.8 | 310.00 | 5998.76 | 3850.00 | 80.00 | 44.61 | 50.80 | 280.00 | 0.96 | 2.12 | 14.33 | -2.63 |
| NL4 | Wetland | 8.34 | 13750 | 25.1 | 310.00 | 5795.12 | 4270.00 | 80.60 | 45.70 | 42.45 | 475.2 | 1.20 | 2.10 | 14.20 | -2.60 |
| ML1 | Wetland | 8.03 | 19400 | 25.6 | 43000 | 7575.95 | 4767.00 | 105.00 | 50.14 | 55.80 | 455.00 | 1.16 | 1.94 | 9.22 | -6.30 |
| ML2 | Wetland | 8.00 | 19500 | 25.8 | 400.00 | 7198.08 | 5145.00 | 110.00 | 50.95 | 60.54 | 450.00 | 1.91 | 1.90 | 8.80 | -6.40 |
| ML3 | Wetland | 8.56 | 19800 | 25.0 | 410.00 | 7975.36 | 5600.00 | 100.00 | 53.98 | 60.86 | 465.00 | 0.85 | 1.92 | 9.20 | -6.16 |
| ML4 | Wetland | 8.66 | 21006 | 25.2 | 430.00 | 7995.45 | 5515.70 | 98.50 | 51.80 | 60.46 | 488.75 | 2.36 | 1.94 | 9.21 | -6.31 |
| SL1 | Wetland | 8.48 | 16500 | 25.1 | 450.00 | 8055.8 | 5840.00 | 120.00 | 51.96 | 60.56 | 490.00 | 1.88 | 1.23 | 6.64 | -3.20 |
| SL2 | Wetland | 8.07 | 16750 | 25.6 | 410.00 | 8095.01 | 5495.00 | 118.00 | 51.94 | 61.13 | 475.0 | 0.77 | 1.22 | 6.64 | -3.12 |
| SL3 | Wetland | 8.11 | 16540 | 25.8 | 410.00 | 8185.93 | 5560.00 | 120.00 | 52.10 | 60.38 | 453.00 | 0.80 | 1.22 | 6.60 | -3.16 |
| SL4 | Wetland | 8.26 | 17110 | 26.0 | 380.00 | 7906.35 | 5145.11 | 112.50 | 46.76 | 54.70 | 482.60 | 0.65 | 1.23 | 6.45 | -3.39 |
| SP1 | Piezometer | 7.75 | 1458 | 25.2 | 280.00 | 1357.54 | 1015.00 | 85.00 | 20.33 | 36.90 | 186.04 | 1.67 | -0.51 | -9.30 | -5.22 |
| SP2 | Piezometer | 7.74 | 1655 | 25.6 | 230.00 | 1405.35 | 1005.70 | 72.45 | 19.10 | 38.20 | 175.60 | 0.35 | -0.53 | -8.29 | -4.05 |
| SP3 | Piezometer | 7.43 | 1845 | 25.8 | 210.00 | 1408.20 | 990.00 | 66.84 | 18.00 | 25.50 | 155.90 | 0.27 | -0.55 | -8.30 | -3.90 |
| SP4 | Piezometer | 8.04 | 1564 | 26.0 | 230.00 | 1404.64 | 1087.00 | 84.60 | 14.09 | 20.35 | 195.90 | 0.16 | -0.44 | -9.17 | -5.65 |
| SP5 | Piezometer | 8.23 | 1770 | 25.6 | 280.00 | 2996.76 | 2145.35 | 50.80 | 15.70 | 22.00 | 262.30 | 1.23 | -0.40 | -9.16 | -5.96 |
| SP6 | Piezometer | 7.84 | 1670 | 25.8 | 110.00 | 1250.00 | 806.00 | 50.00 | 12.65 | 10.33 | 155.30 | 1.01 | -0.41 | -9.15 | -5.87 |

Appendix 5.1b: Physicochemical and environmental isotope composition of wetland water samples in the Sakumo basin

| Sample ID | | pH | EC | Temp. | $HCO_3^-$ | $Cl^-$ | $Na^+$ | $K^+$ | $Ca^{2+}$ | $Mg^{2+}$ | $SO_4^{2-}$ | $NO_3^-$ | $\delta^{18}O‰$ | $\delta^2H‰$ | d-excess |
|---|---|---|---|---|---|---|---|---|---|---|---|---|---|---|---|
| SP7 | Piezometer | 7.73 | 1750 | 26.0 | 110.00 | 1195.50 | 850.00 | 49.00 | 15.00 | 20.35 | 158.90 | 1.10 | -0.23 | -.91 | -8.07 |
| SP8 | Piezometer | 7.89 | 2050 | 25.2 | 160.00 | 1250.35 | 875.70 | 54.00 | 18.50 | 25.14 | 160.33 | 1.79 | -0.25 | -9.65 | -7.65 |
| SP9 | Piezometer | 7.57 | 1520 | 25.6 | 280.00 | 2199.65 | 1450.00 | 46.00 | 15.90 | 22.65 | 224.00 | 0.55 | -1.22 | -10.55 | -0.79 |
| SP10 | Piezometer | 7.82 | 1667 | 25.8 | 210.00 | 2215.11 | 1429.00 | 42.00 | 12.45 | 20.28 | 255.32 | 0.85 | -1.23 | -10.55 | -0.71 |
| SP11 | Piezometer | 7.84 | 1705 | 26.0 | 210.00 | 1950.98 | 1249.10 | 41.60 | 11.74 | 20.65 | 163.00 | 0.69 | -1.22 | -10.53 | -0.77 |
| SP12 | Piezometer | 7.88 | 1685 | 25.6 | 210.00 | 2033.81 | 1515.00 | 44.60 | 12.45 | 20.06 | 250.41 | 1.30 | -1.25 | -10.60 | -0.60 |
| MW2 | Monitoring well | 7.15 | 3320 | 27.8 | 329.00 | 540.00 | 446.00 | 21.00 | 99.00 | 81.00 | 110.00 | 0.05 | -2.51 | -12.73 | 7.35 |
| MW4 | Monitoring well | 7.40 | 565 | 26.0 | 520.00 | 1600.00 | 1850.00 | 35.00 | 145.000 | 185.00 | 260.00 | 0.03 | -3.32 | -13.23 | 13.33 |
| MW6 | Monitoring well | 7.50 | 4220 | 27.2 | 277.00 | 1350.00 | 180.00 | 23.00 | 44.60 | 45.10 | 44.60 | 0.02 | -2.44 | -11.54 | 7.98 |
| MW8 | Monitoring well | 6.90 | 2650 | 27.0 | 159.00 | 1080.00 | 108.00 | 16.00 | 50.06 | 50.40 | 50.60 | 0.03 | -3.50 | -14.70 | 13.30 |
| MW15 | Monitoring well | 7.20 | 2850 | 28.7 | 245.00 | 540.00 | 208.00 | 316.00 | 68.00 | 55.25 | 25.05 | 0.05 | -3.25 | -15.30 | 10.70 |
| DD1 | Leachate | 8.10 | 4580 | 27.8 | 470.0 | 1350.98 | 1005.00 | 58.00 | 12.78 | 7.86 | 33.75 | 0.39 | -0.59 | -4.62 | 0.10 |
| DD2 | Leachate | 8.11 | 4570 | 27.1 | 490.00 | 1445.06 | 1167.00 | 56.00 | 12.50 | 7.65 | 34.05 | 0.42 | -0.57 | -4.58 | -0.02 |
| UD | Dam | 7.65 | 195.8 | 28.0 | 230.00 | 40.48 | 51.00 | 23.00 | 14.39 | 18.30 | 27.39 | 0.40 | 2.53 | 14.12 | -6.12 |
| L.D | Dam | 7.89 | 186.7 | 27.9 | 180.00 | 31.99 | 47.80 | 25.71 | 14.16 | 18.91 | 41.57 | 0.37 | 1.75 | 10.30 | -3.70 |

Appendix 5.1c: Physicochemical and environmental isotope composition of wetland water samples in the Sakumo basin *Contd.*

| Sample ID | | pH | EC | Temp. | $HCO_3^-$ | $Cl^-$ | $Na^+$ | $K^+$ | $Ca^{2+}$ | $Mg^{2+}$ | $SO_4^{2-}$ | $NO_3^-$ | $\delta^{18}O‰$ | $\delta^{2}H‰$ | d-excess |
|---|---|---|---|---|---|---|---|---|---|---|---|---|---|---|---|
| Dz1 | River | 7.77 | 2020 | 27.1 | 560 | 230.63 | 307.00 | 13.00 | 19.89 | 33.20 | 31.75 | 0.49 | -1.07 | 0.67 | 9.23 |
| Dz2 | River | 7.86 | 2025 | 27.0 | 560 | 227.10 | 310.00 | 13.50 | 15.20 | 34.10 | 30.09 | 0.52 | -1.12 | -2.09 | 6.87 |
| Dz3 | River | 7.85 | 2010 | 27.1 | 580 | 210.08 | 312.00 | 10.80 | 11.11 | 30.40 | 32.10 | 0.50 | 0.81 | 6.25 | -0.23 |
| Dz4 | River | 7.79 | 2100 | 27.1 | 550 | 188.12 | 305.00 | 11.70 | 14.77 | 22.80 | 32.00 | 0.44 | -0.87 | -0.57 | 6.39 |
| Dz5 | River | 7.80 | 2009 | 27.5 | 560 | 165.09 | 310.00 | 12.10 | 14.95 | 13.10 | 31.70 | 0.50 | -0.99 | -0.78 | 7.14 |
| O1 | Stream | 7.86 | 1920 | 28.0 | 470 | 585.10 | 355.00 | 65.00 | 52,48 | 76.55 | 39.00 | 1.10 | -2.40 | -10.46 | 8.74 |
| O2 | Stream | 7.72 | 1866 | 28.1 | 430 | 555.75 | 352.00 | 69.00 | 55.5 | 75.19 | 47.38 | 1.10 | -2.08 | -7.55 | 9.09 |
| O3 | Stream | 7.79 | 1900 | 28.5 | 400 | 550.73 | 338.00 | 65.00 | 55.22 | 78.60 | 45.97 | 1.40 | -0.36 | -3.50 | -0.62 |
| O4 | Stream | 7.82 | 1890 | 28.2 | 430 | 553.84 | 340.00 | 65.00 | 6.05 | 78.95 | 46.10 | 1.30 | -0.35 | -3.30 | -0.5 |
| O5 | Stream | 7.80 | 1910 | 27.5 | 410 | 555.02 | 350.00 | 73.00 | 6.22 | 85.50 | 47.15 | 1.20 | -0.36 | -3.50 | -0.62 |
| M1 | Stream | 7.73 | 2550 | 27.5 | 450 | 750.05 | 624.00 | 28.00 | 8.21 | 25.88 | 48.38 | 0.44 | -0.33 | -3.30 | -0.66 |
| M2 | Stream | 7.79 | 2540 | 28.8 | 400 | 762.75 | 655.00 | 35.00 | 8.05 | 26.07 | 52.06 | 0.45 | -0.35 | -3.30 | -0.50 |
| M3 | Stream | 7.80 | 2555 | 28.5 | 330 | 770.10 | 630.00 | 38.00 | 8.16 | 26.45 | 50.11 | 0.39 | 0.05 | -1.61 | -2.01 |
| M4 | Stream | 7.65 | 2550 | 27.6 | 470 | 710.65 | 650.00 | 29.00 | 8.20 | 25.90 | 45.23 | 0.42 | 0.05 | -1.60 | -2.00 |
| OM1 | Stream | 7.27 | 1954 | 28.5 | 410 | 755.45 | 605.00 | 35.00 | 10.99 | 31.06 | 57.38 | 0.50 | 0.05 | -1.60 | -2.00 |
| OM.2 | Stream | 7.30 | 1930 | 27.8 | 540 | 747.62 | 610.00 | 49.00 | 16.04 | 40.50 | 38.25 | 0.48 | 0.03 | -1.60 | -1.84 |
| OM3 | Stream | 7.29 | 1955 | 27.9 | 530 | 760.48 | 635.00 | 50.00 | 16.43 | 42.70 | 35.70 | 0.52 | 0.04 | -1.61 | -1.93 |

Appendix 5.2a: Physicochemical and environmental isotope composition of the groundwater in the Sakumo basin

| ID | pH | EC | Temp. | $HCO_3^-$ | $Cl^-$ | $Na^+$ | $K^+$ | $Ca^{2+}$ | $Mg^{2+}$ | $SO_4^{2-}$ | $NO_3^-$ | $\delta^{18}O‰$ | $\delta^{2}H‰$ | d-excess |
|---|---|---|---|---|---|---|---|---|---|---|---|---|---|---|
| BH 1 | 6.5 | 2900 | 26.40 | 227.2 | 493.80 | 198.6 | 19.70 | 104.05 | 64.90 | 138.7 | 4.35 | -2.44 | -11.54 | 7.98 |
| BH 2 | 6.7 | 2060 | 28.40 | 226.0 | 517.98 | 198.15 | 20.50 | 122.82 | 81.60 | 145.00 | 3.55 | -2.01 | -11.35 | 4.73 |
| BH 3 | 6.7 | 2200 | 30.25 | 240.00 | 532.00 | 197.35 | 21.70 | 94.50 | 72.70 | 130.00 | 5.80 | -2.75 | -10.51 | 11.65 |
| BH 4 | 6.6 | 3420 | 31.50 | 272.85 | 519.30 | 198.78 | 19.35 | 93.22 | 75.40 | 113.50 | 4.10 | -2.90 | -14.68 | 8.52 |
| BH 5 | 6.8 | 480 | 30.20 | 1430.0 | 330.25 | 275.20 | 27.50 | 152.45 | 65.70 | 54.10 | 4.10 | -2.76 | -14.07 | 7.97 |
| BH 6 | 6.7 | 6030 | 30.45 | 1850.0 | 350.40 | 245.10 | 32.79 | 180.80 | 24.70 | 61.80 | 1.90 | -2.53 | -12.99 | 7.22 |
| BH 7 | 7.1 | 2080 | 27.20 | 240.50 | 1190.35 | 208.27 | 45.50 | 140.24 | 67.50 | 47.00 | 4.30 | -2.51 | -12.73 | 7.36 |
| BH 8 | 7.2 | 1260 | 28.80 | 445.45 | 1275.95 | 164.42 | 32.45 | 48.90 | 37.68 | 12.85 | 10.10 | -3.32 | -13.23 | 13.35 |
| BH 9 | 7.1 | 1318 | 29.60 | 169.20 | 270.10 | 173.3 | 14.90 | 40.25 | 36.10 | 75.10 | 2.80 | -3.10 | -12.60 | 12.20 |
| BH 10 | 6.9 | 640 | 30.50 | 56.15 | 178.15 | 118.45 | 16.20 | 30.09 | 21.70 | 93.80 | 1.20 | -3.03 | -13.16 | 11.11 |
| BH 11 | 6.7 | 1110 | 29.00 | 145.10 | 285.20 | 138.45 | 18.90 | 45.00 | 38.00 | 64.50 | 1.32 | -2.94 | -13.32 | 10.21 |
| BH 12 | 6.8 | 1160 | 28.40 | 168.45 | 195.10 | 105.25 | 10.30 | 56.54 | 39.60 | 78.20 | 3.00 | -2.68 | -10.69 | 10.72 |
| BH 13 | 6.9 | 1190 | 25.10 | 172.80 | 200.85 | 114.8 | 10.90 | 53.72 | 35.12 | 69.85 | 7.20 | -2.89 | -10.47 | 12.65 |
| BH 14 | 6.8 | 1030 | 28.20 | 143.00 | 235.85 | 89.50 | 16.30 | 60.05 | 43.05 | 59.85 | 1.15 | -3.60 | -16.20 | 12.60 |
| BH 15 | 6.4 | 8590 | 30.24 | 310.00 | 2985.0 | 155.10 | 48.75 | 41.50 | 30.20 | 75.5 | 4.22 | -3.80 | -16.90 | 13.50 |
| BH 16 | 7.1 | 4400 | 30.50 | 360.00 | 1820.0 | 660.25 | 21.20 | 232.60 | 165.85 | 24.1 | 2.55 | -3.45 | -16.10 | 11.50 |
| BH 17 | 7.2 | 6070 | 29.28 | 312.00 | 1925.0 | 845.65 | 31.74 | 285.20 | 185.00 | 35.50 | 2.80 | -2.55 | -13.40 | 7.00 |
| BH 18 | 7.3 | 6410 | 30.07 | 360.00 | 1910.0 | 850.30 | 38.15 | 300.15 | 213.00 | 37.05 | 2.47 | -3.20 | -16.00 | 9.60 |
| BH 19 | 7.2 | 4200 | 28.01 | 435.00 | 1270.0 | 720.28 | 21.20 | 170.25 | 130.00 | 34.70 | 3.68 | -3.50 | -17.00 | 11.00 |

Appendix 5.2b: Physicochemical and environmental isotopes composition of the groundwater in the Sakumo basin *Contd.*

| ID | pH | EC | Temp. | $HCO_3^-$ | $Cl^-$ | $Na^+$ | $K^+$ | $Ca^{2+}$ | $Mg^{2+}$ | $SO_4^{2-}$ | $NO_3^-$ | $\delta^{18}O‰$ | $\delta^{2}H‰$ | d-excess |
|---|---|---|---|---|---|---|---|---|---|---|---|---|---|---|
| BH 20 | 7.0 | 2740 | 28.5 | 170.05 | 1455.20 | 180.20 | 20.00 | 95.02 | 70.03 | 95.10 | 2.50 | -2.45 | -13.5 | 6.10 |
| BH 21 | 7.2 | 1680 | 29.4 | 155.95 | 1300.30 | 115.75 | 12.00 | 51.34 | 37.75 | 48.67 | 5.44 | -2.95 | -13.98 | 9.62 |
| BH 22 | 7.4 | 3420 | 29.2 | 220.51 | 1140.20 | 430.82 | 25.00 | 183.63 | 140.95 | 125.06 | 4.61 | -3.48 | -15.50 | 12.50 |
| BH 23 | 7.4 | 3980 | 30.0 | 190.58 | 1302.39 | 573.85 | 24.58 | 195.25 | 102.56 | 73.13 | 4.20 | -3.49 | -14.70 | 13.30 |
| BH 24 | 7.5 | 3450 | 30.1 | 165.25 | 1080.10 | 447.68 | 36.12 | 185.45 | 95.85 | 112.50 | 6.20 | -3.25 | -15.30 | 10.70 |
| BH 25 | 7.4 | 3220 | 29.7 | 145.20 | 1035.20 | 400.65 | 28.00 | 209.02 | 78.50 | 126.03 | 1.01 | -3.20 | -15.50 | 10.10 |
| BH 26 | 7.5 | 5270 | 28.8 | 240.55 | 1650.15 | 485.60 | 32.80 | 362.50 | 126.40 | 115.04 | 7.10 | -3.56 | -15.00 | 13.48 |
| BH 27 | 7.4 | 6760 | 30.0 | 230.10 | 2344.00 | 955.97 | 37.00 | 310.50 | 160.35 | 257.00 | 8.21 | -3.26 | -13.00 | 13.08 |
| BH 28 | 7.5 | 4520 | 29.1 | 180.20 | 1465.00 | 685.00 | 43.05 | 198.00 | 68.29 | 21.01 | 1.75 | -3.20 | -14.70 | 10.90 |
| BH 29 | 7.3 | 3350 | 29.2 | 315.25 | 1020.70 | 380.05 | 26.98 | 178.25 | 85.99 | 78.00 | 5.10 | -3.50 | -15.50 | 12.50 |
| BH 30 | 7.1 | 6610 | 30.2 | 347.00 | 1350.00 | 850.05 | 33.00 | 360.00 | 250.35 | 264.00 | 4.20 | -3.50 | -14.70 | 13.30 |
| BH 31 | 7.1 | 6250 | 30.1 | 345.00 | 1770.00 | 880.00 | 31.25 | 280.00 | 175.70 | 372.00 | 9.00 | -2.55 | -13.40 | 7.00 |
| BH 32 | 7.4 | 6690 | 30.2 | 310.00 | 2020.00 | 898.11 | 34.95 | 345.00 | 225.30 | 350.00 | 11.22 | -2.94 | -17.61 | 5.91 |
| BH 33 | 7.3 | 6200 | 29.7 | 350.00 | 1895.20 | 750.15 | 34.90 | 335.07 | 235.05 | 250.00 | 5.30 | -2.78 | -12.38 | 9.86 |
| BH 34 | 7.4 | 6940 | 27.8 | 350.00 | 2135.00 | 867.06 | 57.45 | 395.02 | 266.50 | 393.00 | 6.90 | -2.63 | -11.31 | 9.73 |
| BH 35 | 7.1 | 580 | 27.4 | 445.00 | 3285.00 | 705.05 | 20.00 | 370.03 | 245.25 | 510.00 | 16.45 | -2.18 | -7.60 | 9.84 |
| BH 36 | 7.2 | 1150 | 29.6 | 370.00 | 3045.00 | 420.0 | 55.00 | 495.00 | 380.07 | 363.00 | 16.50 | -1.95 | -11.58 | 4.02 |
| BH 37 | 7.3 | 9370 | 29.8 | 560.00 | 4232.00 | 448.05 | 48.15 | 395.50 | 260.20 | 586.00 | 10.03 | -1.88 | -1.75 | 13.29 |

Appendix 5.3a: Physicochemical and environmental isotope composition of rainwater samples in the Sakumo basin

| DATE | Rainfall Amount | pH | EC | Temp. | $HCO_3^-$ | $Cl^-$ | $Na^+$ | $K^+$ | $Ca^{2+}$ | $Mg^{2+}$ | $SO_4^{2-}$ | $NO_3^-$ | $\delta^{18}O‰$ | $\delta^{2}H‰$ | d-excess |
|---|---|---|---|---|---|---|---|---|---|---|---|---|---|---|---|
| 08/02/2013 | 19.0 | 5.98 | 31.70 | 27.8 | 12.19 | 16.99 | 6.00 | 2.4 | 2.88 | 0.80 | 73.1 | 0.80 | -2.24 | -10.45 | 7.47 |
| 16/03/2013 | 10.0 | 6.57 | 32.20 | 26.9 | 73.15 | 16.49 | 10.20 | 5.9 | 19.84 | 0.88 | 58.22 | 0.60 | -0.96 | 4.18 | 11.86 |
| 28/04/2013 | 13.9 | 5.74 | 13.99 | 26.9 | 24.28 | 17.49 | 4.10 | 1.00 | 0.64 | 1.10 | 49.10 | 0.57 | -2.22 | -12.89 | 4.87 |
| 08/05/2013 | 6.0 | 5.55 | 8.74 | 27.8 | 24.28 | 18.49 | 3.50 | 0.50 | 1.92 | 0.89 | 45.62 | 0.89 | -2.34 | -11.40 | 7.32 |
| 14/05/2013 | 11.8 | 5.62 | 12.93 | 26.9 | 24.28 | 19.49 | 3.60 | 0.30 | 1.92 | 0.80 | 55.15 | 0.76 | -2.22 | -10.45 | 7.31 |
| 20/05/2013 | 21.8 | 5.61 | 11.91 | 25.8 | 24.28 | 15.49 | 4.40 | 0.60 | 1.28 | 1.03 | 58.45 | 0.43 | -2.75 | -30.16 | -8.16 |
| 25/05/2013 | 22.0 | 6.05 | 21.3 | 26.6 | 24.28 | 20.49 | 5.80 | 2.50 | 2.24 | 0.67 | 52.92 | 0.48 | -1.31 | -4.10 | 6.38 |
| 03/06/2013 | 68.4 | 6.85 | 50.5 | 25.7 | 97.53 | 95.97 | 13.05 | 8.9 | 9.60 | 0.52 | 51.58 | 0.36 | -2.37 | -14.68 | 4.28 |
| 07/06/2013 | 81.6 | 5.40 | 20.97 | 25.8 | 29.26 | 25.99 | 2.30 | 1.20 | 2.40 | 0.44 | 17.06 | 0.39 | -2.79 | -9.97 | 12.35 |
| 12/06/2013 | 40.2 | 6.20 | 40.01 | 26.9 | 29.26 | 62.39 | 2.84 | 1.60 | 1.60 | 0.91 | 54.37 | 0.01 | -1.23 | -1.15 | 8.69 |
| 20/06/2013 | 23.6 | 6.50 | 70.39 | 26.8 | 58.52 | 45.09 | 7.09 | 3.30 | 4.81 | 0.65 | 34.95 | 0.16 | -0.29 | 3.80 | 6.12 |
| 05/07/2013 | 23.8 | 6.60 | 40.76 | 25.6 | 29.26 | 21.69 | 7.11 | 4.90 | 1.60 | 0.28 | 10.68 | 0.25 | -1.87 | -7.66 | 7.30 |
| 12/07/2013 | 22.6 | 6.40 | 90.80 | 26.4 | 58.52 | 17.99 | 15.20 | 11.2 | 2.40 | 0.42 | 41.25 | 0.16 | 0.26 | 7.12 | 5.04 |
| 13/07/2013 | 21.4 | 6.52 | 73.65 | 26.6 | 126.79 | 20.69 | 17.59 | 13.6 | 2.89 | 0.26 | 24.22 | 0.07 | -0.94 | 5.18 | 12.70 |
| 16/07/2013 | 17.6 | 6.74 | 57.85 | 26.2 | 39.01 | 17.89 | 8.70 | 6.50 | 1.60 | 0.66 | 40.30 | 0.16 | -0.76 | 6.69 | 12.77 |
| 20/07/2013 | 14.2 | 6.49 | 58.10 | 25.5 | 39.01 | 19.37 | 12.6 | 7.10 | 2.40 | 1.05 | 15.34 | 0.162 | -0.70 | 4.58 | 10.18 |
| 17/08/2013 | 2.6 | 6.20 | 46.38 | 24.4 | 19.51 | 23.19 | 3.5 | 2.20 | 2.40 | 0.58 | 15.50 | 0.31 | -3.65 | -22.92 | 6.28 |
| 20/08/2013 | 3.0 | 6.10 | 54.05 | 24.1 | 39.01 | 53.19 | 7.8 | 6.40 | 1.60 | 0.95 | 11.65 | 0.52 | -3.28 | -21.14 | 5.10 |
| 04/09/2013 | 8.0 | 6.40 | 35.50 | 27.0 | 29.26 | 18.89 | 4.2 | 2.70 | 1.60 | 0.75 | 33.10 | 0.09 | -0.25 | 4.55 | 6.55 |

Appendix 5.3b: Chemical and environmental isotope composition of rainwater samples in the Sakumo basin *Contd.*

| DATE | Rainfall Amount | pH | EC | Temp. | $HCO_3^-$ | $Cl^-$ | $Na^+$ | $K^+$ | $Ca^{2+}$ | $Mg^{2+}$ | $SO_4^{2-}$ | $NO_3^-$ | $\delta^{18}O‰$ | $\delta^{2}H‰$ | d-excess |
|---|---|---|---|---|---|---|---|---|---|---|---|---|---|---|---|
| 05/10/2013 | 8.10 | 6.40 | 34.08 | 25.5 | 48.77 | 25.99 | 4.20 | 3.6 | 1.60 | 0.53 | 8.92 | 0.58 | -0.43 | 3.57 | 7.01 |
| 07/10/2013 | 7.60 | 6.30 | 38.13 | 25.2 | 48.77 | 17.99 | 2.80 | 0.5 | 1.60 | 0.45 | 4.24 | 0.99 | -1.64 | -5.49 | 7.63 |
| 10/10/2013 | 8.50 | 6.37 | 38.74 | 25.3 | 39.01 | 45.09 | 4.30 | 1.30 | 1.60 | 0.97 | 7.51 | 0.52 | -1.50 | -4.23 | 7.77 |
| 22/10/2013 | 5.60 | 6.15 | 20.24 | 25.4 | 29.26 | 19.29 | 3.40 | 0.80 | 1.60 | 0.65 | 4.63 | 0.49 | -1.19 | 1.39 | 10.91 |
| 26/02/2014 | 6.00 | 5.60 | 34.90 | 25.4 | 21.95 | 7.70 | 7.70 | 0.18 | 1.92 | 1.01 | 6.22 | 1.51 | -2.58 | -9.46 | -10.64 |
| 13/03/2014 | 11.40 | 5.26 | 47.25 | 24.5 | 14.63 | 21.94 | 7.10 | 0.29 | 1.85 | 1.20 | 8.70 | 1.35 | 0.55 | 10.29 | 14.37 |
| 26/03/2014 | 17.80 | 4.93 | 89.30 | 25.1 | 29.26 | 13.25 | 9.20 | 2.00 | 1.80 | 1.10 | 10.65 | 8.84 | -1.13 | 7.06 | 0.97 |
| 27/04/2014 | 24.60 | 5.09 | 72.30 | 25.6 | 17.07 | 11.30 | 8.30 | 0.70 | 1.93 | 0.81 | 6.24 | 2.24 | -3.63 | -12.77 | -19.04 |
| 06/05/2014 | 23.60 | 5.10 | 48.70 | 25.7 | 19.51 | 10.72 | 9.55 | 0.66 | 1.94 | 0.82 | 7.78 | 9.68 | -2.08 | -1.47 | -6.64 |
| 04/06/2014 | 52.20 | 5.37 | 36.70 | 25.1 | 19.51 | 6.90 | 9.10 | 0.90 | 1.78 | 1.10 | 8.65 | 4.12 | -1.36 | -9.8 | 1.08 |
| 07/06/2014 | 69.60 | 5.30 | 43.15 | 25.4 | 17.07 | 10.14 | 5.25 | 0.70 | 1.56 | 0.85 | 4.19 | 8.70 | -0.70 | -3.85 | 1.75 |
| 08/06/2014 | 39.40 | 6.13 | 28.60 | 26.0 | 73.15 | 19.26 | 3.13 | 16.3 | 2.14 | 1.80 | 9.87 | <0.001 | 1.50 | 5.88 | -6.12 |
| 12/06/2014 | 38.40 | 4.53 | 91.90 | 25.7 | 24.45 | 20.92 | 11.80 | 2.15 | 1.90 | 0.60 | 5.78 | <0.001 | -0.58 | -0.06 | 4.58 |
| 16/06/2014 | 34.00 | 5.13 | 102.6 | 27.2 | 53.64 | 24.31 | 28.40 | 4.90 | 1.67 | 0.80 | 9.50 | <0.001 | -0.64 | 3.59 | 8.71 |
| 21/06/2014 | 27.10 | 5.7 | 271.0 | 27.3 | 73.50 | 25.40 | 21.35 | 3.10 | 1.30 | 0.90 | 3.67 | <0.001 | -1.04 | -2.69 | 5.63 |
| 27/06/2014 | 41.20 | 5.75 | 265.0 | 27.2 | 63.37 | 18.33 | 13.29 | 7.29 | 1.95 | 1.08 | 8.49 | <0.001 | -5.03 | -35.21 | 5.03 |
| 28/06/2014 | 30.20 | 6.08 | 249.0 | 26.9 | 24.84 | 25.50 | 18.30 | 4.70 | 1.00 | 0.40 | 2.80 | <0.036 | -0.70 | -1.02 | 4.58 |
| 29/06/2014 | 49.60 | 6.85 | 219 | 26.9 | 65.09 | 26.92 | 15.70 | 10.8 | 1.00 | 0.40 | 6.06 | <0.001 | -1.62 | -7.02 | 5.94 |

Appendix 5.3c: Physicochemical and environmental isotope composition of rainwater samples in the Sakumo basin *contd.*

| DATE | Rainfall Amount | pH | EC | Temp. | $HCO_3^-$ | $Cl^-$ | $Na^+$ | $K^+$ | $Ca^{2+}$ | $Mg^{2+}$ | $SO_4^{2-}$ | $NO_3^-$ | $\delta^{18}O‰$ | $\delta^2H‰$ | d-excess |
|---|---|---|---|---|---|---|---|---|---|---|---|---|---|---|---|
| 03/07/2014 | 32.0 | 6.25 | 210 | 27.2 | 36.01 | 10.04 | 8.40 | 2.0 | 0.89 | 0.243 | 1.36 | 0.001 | -2.85 | -17.18 | 5.62 |
| 08/07/2014 | 20.0 | 6.00 | 75 | 27 | 38.14 | 12.54 | 11.0 | 1.9 | 0.70 | 0.10 | 1.69 | 0.001 | -0.15 | 0.82 | 2.02 |
| 10/07/2014 | 12.6 | 6.15 | 75.6 | 25.5 | 17.07 | 9.399 | 7.82 | 4.6 | 0.84 | 0.18 | 1.98 | 0.001 | -5.33 | -33.67 | 8.97 |
| 20/07/2014 | 17.2 | 5.5 | 46.5 | 26.7 | 43.89 | 13.87 | 14.45 | 3.2 | 1.25 | 0.42 | 10.48 | 12.98 | -3.79 | -23.40 | 6.92 |
| 23/07/2014 | 9.2 | 6.10 | 91.6 | 26.7 | 50.41 | 43.28 | 44.23 | 15.8 | 0.79 | 0.20 | 5.12 | 17.68 | -1.42 | 0.58 | 11.94 |
| 27/07/2014 | 7.4 | 6.45 | 235 | 26.8 | 9.53 | 14.90 | 8.59 | 6.I6 | 2.88 | 0.08 | 2.56 | <0.001 | -0.46 | 4.17 | 7.85 |
| 28/07/2014 | 5.8 | 7.27 | 370 | 24.7 | 14.94 | 24.80 | 13.19 | 8.0 | 1.28 | 0.08 | 2.84 | <0.001 | 0.57 | 8.82 | 4.26 |
| 05/08/2014 | 3.4 | 5.20 | 20.1 | 24.1 | 10.65 | 19.92 | 13.50 | 3.40 | 1.67 | 0.98 | 9.24 | <0.001 | -0.38 | 7.28 | 10.32 |
| 10/08/2014 | 2.6 | 5.40 | 25.7 | 24.2 | 5.70 | 19.90 | 10.60 | 5.90 | 0.96 | 0.87 | 1.13 | <0.001 | -1.88 | -1.75 | 13.29 |
| 07/10/2014 | 6.6 | 6.74 | 25.5 | 89.5 | 7.26 | 14.49 | 11.30 | 3.63 | 2.24 | 0.13 | 3.67 | <0.001 | -0.25 | 8.85 | 10.85 |
| 14/10/2014 | 14.5 | 6.05 | 25.3 | 58.7 | 10.34 | 14.49 | 11.00 | 4.40 | 1.60 | 0.23 | 4.92 | <0.001 | -0.62 | 2.68 | 7.64 |
| 17/10/2014 | 7.5 | 5.96 | 26.7 | 17.58 | 7.63 | 15.98 | 4.28 | 3.30 | 1.42 | 0.14 | 1.24 | <0.001 | -0.07 | 3.54 | 4.10 |
| 04/04/2015 | 10.5 | 5.89 | 26.2 | 88.8 | 7.47 | 12.98 | 4.40 | 3.10 | 1.50 | 0.06 | 1.02 | 0.76 | -0.50 | 4.45 | 8.45 |
| 25/04/2015 | 14.6 | 6.79 | 29.10 | 38.7 | 15.50 | 14.45 | 19.50 | 10.1 | 1.60 | 0.08 | 1.13 | 1.02 | -0.54 | 5.29 | 9.61 |
| 04/05/2015 | 42.8 | 6.40 | 27.90 | 123.6 | 8.52 | 19.98 | 3.17 | 9.20 | 1.92 | 0.08 | 1.11 | 0.83 | -2.22 | -3.28 | 14.48 |
| 21/05/2015 | 30.0 | 6.24 | 26.4 | 74.80 | 7.02 | 12.98 | 9.30 | 25.5 | 2.24 | 0.38 | 0.75 | 0.85 | -0.16 | 8.44 | 9.72 |

Appendix 5.3d: Physicochemical and environmental isotope composition of rainwater samples in the Sakumo basin C*ontd.*

| DATE | Rainfall Amount | pH | EC | Temp. | $HCO_3^-$ | $Cl^-$ | $Na^+$ | $K^+$ | $Ca^{2+}$ | $Mg^{2+}$ | $SO_4^{2-}$ | $NO_3^-$ | $\delta^{18}O‰$ | $\delta^2H‰$ | d-excess |
|---|---|---|---|---|---|---|---|---|---|---|---|---|---|---|---|
| 30/05/2015 | 20.20 | 6.59 | 19.5 | 25.5 | 9.24 | 12.98 | 13.33 | 13.0 | 1.92 | 0.09 | 0.889 | 0.54 | -1.61 | 1.39 | 14.27 |
| 03/06/2015 | 68.90 | 6.0 | 5.85 | 25.7 | 1.09 | 12.98 | 11.30 | 6.42 | 1.92 | 0.09 | 0.46 | 0.49 | 0.14 | 9.30 | 8.18 |
| 05/06/2015 | 45.70 | 6.27 | 10.5 | 27.8 | 11.46 | 12.98 | 17.12 | 5.80 | 1.92 | 0.07 | 1.45 | 0.78 | 0.32 | 10.03 | 7.47 |
| 07/06/2015 | 30.20 | 6.12 | 5.74 | 25.9 | 10.21 | 10.72 | 3.55 | 4.47 | 1.28 | 0.12 | 4.10 | 0.25 | -0.41 | 3.07 | 6.35 |
| 12/06/2015 | 22.60 | 5.55 | 35.20 | 25.30 | 14.33 | 16.98 | 12.60 | 4.53 | 0.96 | 0.10 | 3.83 | 0.78 | -1.56 | -5.04 | 7.44 |
| 02/07/2015 | 18.10 | 5.81 | 11.37 | 26.10 | 12.63 | 20.74 | 10.60 | 5.40 | 1.92 | 0.12 | 2.67 | 0.15 | -2.78 | -12.92 | 9.32 |
| 09/07/2015 | 12.50 | 4.98 | 18.95 | 28.00 | 14.49 | 17.55 | 8.80 | 11.71 | 2.56 | 0.09 | 2.05 | 0.37 | -1.57 | -9.50 | 3.06 |
| 21/08/2015 | 2.80 | 5.06 | 20.60 | 25.20 | 1.74 | 7.99 | 8.52 | 3.90 | 3.52 | 0.33 | 1.528 | 0.33 | -0.70 | -3.85 | 1.75 |
| 26/08/2015 | 3.50 | 5.09 | 91.42 | 24.70 | 12.01 | 12.98 | 24.81 | 16.38 | 1.60 | 0.45 | 5.73 | 0.50 | 1.50 | 5.88 | -6.12 |
| 05/09/2015 | 6.40 | 7.47 | 16.36 | 27.20 | 7.25 | 10.40 | 41.46 | 15.91 | 2.88 | 0.34 | 1.77 | 0.01 | -0.58 | -0.06 | 4.58 |
| 15/10/2015 | 6.20 | 4.62 | 11.20 | 26.20 | 1.45 | 12.98 | 18.80 | 11.20 | 1.28 | 0.22 | 0.58 | 0.15 | -0.64 | 3.59 | 8.71 |
| 01/11/2015 | 2.00 | 5.50 | 10.18 | 26.80 | 7.69 | 8.99 | 7.22 | 4.11 | 1.60 | 0.29 | 3.47 | 0.48 | -1.04 | -2.69 | 5.63 |